UNIVERSITÀ DEGLI STUDI DI MILANO

DIPARTIMENTO DI CHIMICA

CORSO DI DOTTORATO IN CHIMICA

XXXI CICLO

One-pot synthesis of thio-glycomimetics through ring opening reactions

Settore Scientifico Disciplinare CHIM/06

Dottorando: Alice TAMBURRINI

Tutor: Prof. Anna BERNARDI

Coordinatore: Prof. Emanuela LICANDRO

A.A. 2018/2019

Table of contents

CHAPTER ONE: glycomimetics

Sugars are the most abundant class of organic molecules on Earth. They are essential components of life and are some of the most complex natural oligomeric structures present in Nature. Glycans can be found as monosaccharides, that are the principal source of energy for cellular metabolism, and as polysaccharides or glycoconjugates (with proteins or lipids), that are involved in many other important biological processes.[1-2] They coat the cell surface of every organism, creating a nanolayer (called glycocalix) that plays a crucial role in the interaction with the surrounding biological environment. [3-4]

Although the structures of the monosaccharidic units were first elucidated by Fischer in the mid-1880s, it took nearly a century before scientists began to appreciate the complex roles of carbohydrates.[5] Maybe this delay was due to the high density of functional groups, the large variety of glycans and their structural and synthetic complexity that made the comprehension of their biological functions an incredible challenge, certainly more complicated compared to proteins and nucleic acids.

Nowadays, it is well known that glycans play an essential role in many biological events including cellular adhesion and migration, organism development, disease progression and the modulation of immunological responses.[6-8] Recently, an increased understanding of the glycans ability to encode a large number of biochemical information, in both physiological and pathological conditions, has inspired numerous efforts towards an intensive investigation about glycobiological and glycochemical processes. In particular, it was recognized the crucial role played by carbohydrates in recognition events involved in a large number of normal cell functions which are found to be decisive in the first stages of inflammation, cancer proliferation and infection processes. This is the main reason why glycosidic and pseudo-glycosidic molecules are being increasingly involved in drug discovery for the treatment of diverse pathologies.[9] Furthermore, the recent development of new tools and techniques to study and produce structurally defined carbohydrates has spurred renewed interest in the therapeutic applications of glycans.

The often insufficient metabolic stability of carbohydrate-based drugs, which compromises both their bioavailability and potency, have pushed the development of chemically modified analogues designed as potential alternative therapeutic agents. Recently, the meaning of *carbohydrate mimetics* has been reformulated by the scientific community and now it is mainly used to refer to any compounds that have been demonstrated to truly mimic the structural and functional aspects of the corresponding natural carbohydrates. These glycomimetics potentially show enhanced enzymatic stability and, at the same time, a better selectivity towards the desired protein-target.

In the list of the main objectives pursued by synthetic chemists that modify the natural structure of carbohydrates, we can include:

- increasing the metabolic and chemical stability of the compounds

- improving the interaction with receptors/enzymes through the insertion of proper functionalities in the molecule
- providing functionalities for chemoselective ligation to other chemical entities, such as proteins, lipids, solid supports or nanoparticles.

The main goal of using glycomimetics, *e.g.* as therapeutic agents, is the manipulation of the chemical information encoded by sugars, controlling and altering the flow of information they direct. Thus, sugar mimics can become fundamental tools for the investigation of biological processes and interesting candidates for the development of new drugs.

Although these structures still remain challenging from a synthetic point of view, the noteworthy development of carbohydrate chemistry has led to a wide variety of structural modifications to generate glycomimetics with improved drug-like characteristics and *in vivo* stability. Generally speaking, two major groups of sugar mimics have been devised by replacement of either the *endo*-or *exo*-cyclic oxygen atom with another atom (*e.g.* carbon, sulphur, nitrogen), effectively disrupting the reactivity of the anomeric position. These modifications therefore induce a change in the chemical and enzymatic stability, polarity, charge, conformation, ring flexibility, and hydrogen-bonding pattern of the molecule, influencing at the same time their affinity for the target protein.[10]

In the next chapters (1.1-1.3), some of these glycomimetics will be introduced and discussed mainly from a synthetic point of view.

1.1 Endocyclic oxygen replacement

Some examples of glycomimetics obtained through the replacement of the endocyclic oxygen are reported below (**Fig. 1.1**).

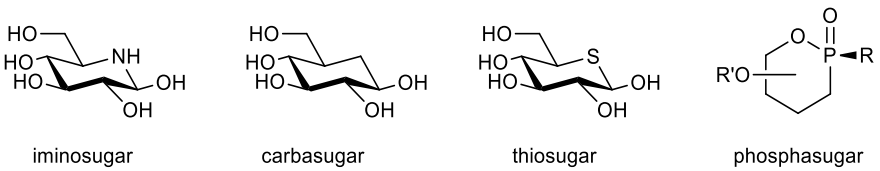

Fig. 1.1 Examples of glycomimetics obtained through the replacement of the endocyclic oxygen atom

1.1.1 Iminosugars

Iminosugars (called also azasugars or iminosaccharides) are obtained through the substitution of the endocyclic oxygen atom with a nitrogen.[11] Without any doubt, they are the most outstanding class reported so far in the field of glycomimetics. One of the reasons is their application as candidates for the treatment of various diseases, including cancer, diabetes, viral infections and lysosomal storage disorders, such as Gaucher and Fabry diseases.[12]

Iminosugars have been reported as potent inhibitors of carbohydrate processing enzymes such as glycoside hydrolases, glycosyltransferases or glycogen phosphorylases.[13-14] Their inhibitory potency against glycosidases was demonstrated to depend on the structural and electronic similarity to the transition state

of the natural substrate, preventing the normal hydrolysis/glycosylation process: at phisiological pH, the ammonium cation shows close resemblance to the typical carbocation/oxocarbenium ion.[15]

These glycomimetics can be classified into two major groups: monocyclic (pyrrolidines, piperidines or seven membered azepanes) and bicylic iminosugars (pyrrolizidines, indolizidines or nortropanes), both classes have been recently exstensively reviewed.[13, 15] Here I will highlight some of the more recent and innovative results in this field.

In 2014, in the Crich's laboratory a set of hydroxylamine-linked di- and trimeric polyhydroxypiperidines were synthetized, with the aim of creating mimetics of β-(1→3)-glucans (**Fig. 1.2**).[16]

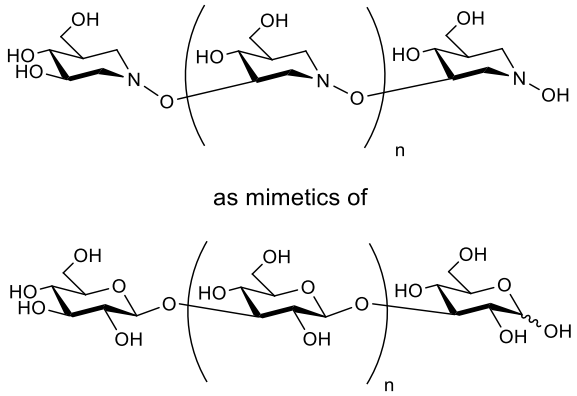

Fig. 1.2 Hydroxylamine-linked di- and trimeric polyhydroxypiperidines as mimetics of β-(1->3)-glucans

β-(1→3)-glucans are well-known immunomodulating agents that occur widely in nature. However, the difficulties in the isolation of pure oligomers have stimulated considerable interest in the chemical synthesis of their mimetics. The corresponding hydroxylamine-based structures, in particular, were found to inhibit binding of anti-CR3 and anti-dectin-1 fluorescent antibodies to their respective binding sites and to stimulate phagocytosis.

Recently it was reported that multivalent iminosugars (obtained through a number of different conjugation chemistry to a variety of scaffolds) allowed a significant enhancement of inhibitory activity per ligand unit and a remarkable selectivity against a panel of glycosidases when compared to their monovalent derivatives.[17-18]

Recently, also fluoro–containing iminosugar *C*-glycosides have gained the attention of the scientific community for their promising inhibitory activity against various glycosidases. The impact of fluorine atoms on the glycosidases inhibition potencies of iminosugars still remains not predictable, because this modification might deeply influence the hydrophobicity or the electron density of the molecule, as well as the pKa of the amine function.[19] Behr and his team have recently reported the synthesis of iminosugars that bear a perfluoroalkyl chain at the pseudo-anomeric position, where the key synthetic step is the stereoselective nucleophilic addition of fluorinated Grignard reagents onto a cyclic nitrone (**Fig. 1.3**).[20]

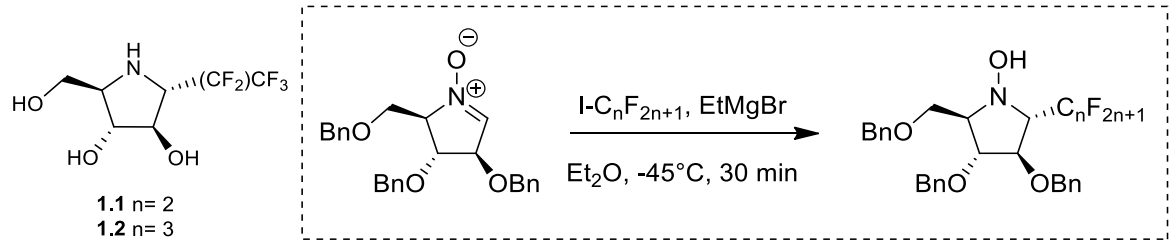

Fig. 1.3 Structure of iminosugars bearing a perfluoroalkyl chain at the pseudo-anomeric position (on the left); the key step of stereoselective nucleophilic addition of Grignard reagent onto a cyclic nitrene (on the right)

These two fluorinated iminosugars with a perfluoropropyl or a perfluorobutyl chain were tested against a panel of glycosidases: while the introduction of a C_4F_9 group (**Fig. 1.3**, compound **1.2**) proved to be deleterious for enzyme binding, the presence of C_3F_7 (**Fig. 1.3**, compound **1.1**) moiety afforded potent and selective inhibition of α-fucosidase and α-glucosidase from yeast.

1.1.2 Carbasugars

The substitution of the ring oxygen in carbohydrates by a methylene group leads to a group of glycomimetics called carbasugars. This substitution abolishes the anomeric effects, modifies the intramolecular hydrogen-bond pattern, modulates the amphiphilicity of the sugar ring and results in changes of the flexibility and conformation population distributions.[21] Furthermore, the lack of anomeric reactivity implies an increased metabolic stability towards glycosidases and glycosyltrasferases.

The term *carbasugar* was first proposed by McCasland et al. in 1966.[22] Since then, carbasugars have been extensively studied and some of the synthetized compounds were later found in Nature, such as *myo*-inositol, validamycin (antibiotic) and acarbose (commercialized by Bayer to treat obesity and Type 2 diabetes mellitus, **Fig.1.4**).[23] Some of these compounds revealed high therapeutic potential, a condition that has led to a growing interest in the development and identification of new carbasugars.[24-25]

An authorative review article about the synthetic methodologies and the conformational and the biological aspects of carbasugars was published by Plumet et al. in 2007[26] and has been recently updated and extended to include both carbapyranoses and carbafuranoses.[27]

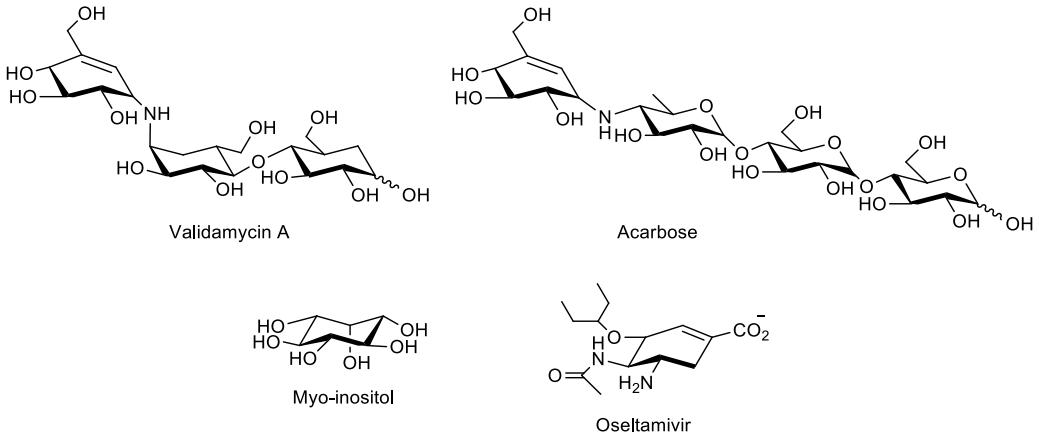

Fig. 1.4 Examples of bioactive carbasugars

Most of the synthetic procedures to generate carbasugars, that have found wide application, are based on Ferrier rearrangement, the Hg^{2+} promoted process shown in **Fig. 1.5**.[28]

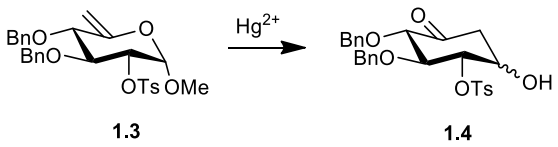

1.3 **1.4**

Fig. 1.5 Ferrier rearrangement

The proposed mechanism for the rearrangement of compound **1.3** is described below (**Fig. 1.6**) and it goes through the hydroxymercuriation of the terminal olefin **1.3** producing an hemiacetalic species **1.3a** as the first intermediate. Loss of MeOH from **1.3a** generates an aldehyde and a mercury enolate that cyclize by intramolecular aldol condensation to form the carbocycle **1.4** as the product.

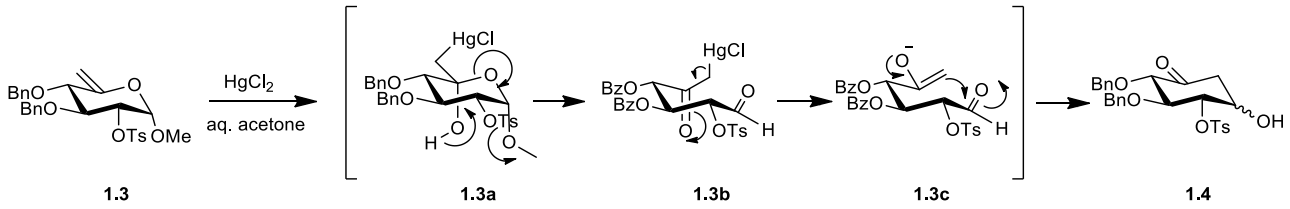

1.3 **1.3a** **1.3b** **1.3c** **1.4**

Fig. 1.6 Proposed mechanism for Ferrier rearrangement of **1.3**

The method has been strongly improved replacing $HgCl_2$ with $AlBu_3$ (TIBAL) or $Ti(OiPr)Cl_3$ which, upon coordination of the anomeric and the C-2 oxygens, allows the rearrangement to proceed while maintaining the glycosidic bond. Interestingly, this protocol can be applied to disaccharides (*e.g.* **1.5**, **Fig. 1.7**) generating disaccharidic cyclitols.[29]

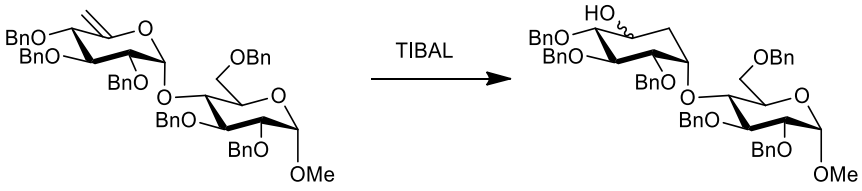

1.5 **1.6**

Fig. 1.7 Generation of disaccharidic cyclitols

In 2009, a tandem isomerisation lactonization pathway has been proposed for the construction of carbasugars (**Fig. 1.8**).[30] In this pathway methylenation of the non-reducing end of the sugar generates an allyl ether (**1.7**, **Fig. 1.8**) which, in a photochemical reaction catalyzed by $Fe(CO)_5$, isomerises into a vinyl ether that spontaneously undergoes the aldol cyclisation, forming the carbasugar core (**1.8**).

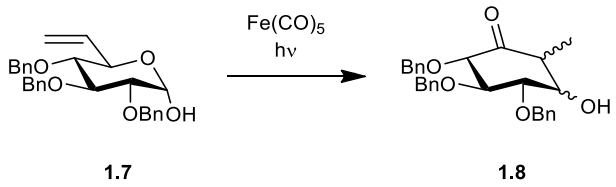

Figure 1.8 Synthesis of cyclitols exploiting a photochemical protocol

Also the ring-closing metathesis reaction has been used to generate carbasugars from the corresponding sugars.[31] The general strategy, reported in **Fig. 1.9**, involves the insertion of two double bonds in the sugar skeleton, one at the reducing end and the other at the non-reducing end. Finally, the carbasugar is obtained using Grubb's catalyst.[32]

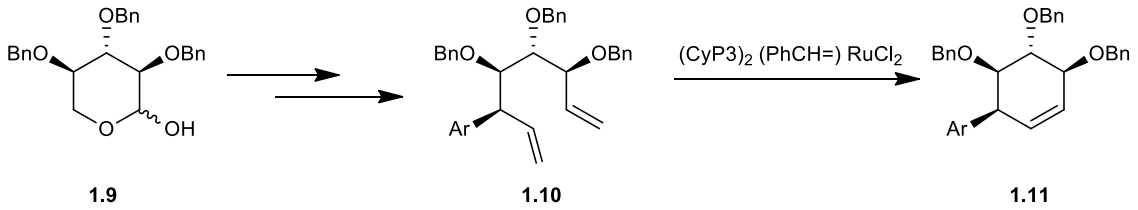

Figure 1.9 Synthesis of cyclitols exploiting a ring-closing metathesis reaction

In 2017, Mayer and co-workers proposed the synthesis of mono-fluoro-modified carba variants of α-D-glucosamine and β-L-idosamine as synthetic mimics of the natural glmS ribozyme ligands (see chapter 1.2 for all the synthetic details).[33] In particular, for the construction of the carbocyclic moiety of compound **1.15**, they also exploited the Ferrier reaction. In particular, the Ferrier carbocyclization of **1.14** (**Fig. 1.10**) was performed under catalytic conditions to generate the carbocyclic compound **1.15** as a mixture of diastereoisomers.[34]

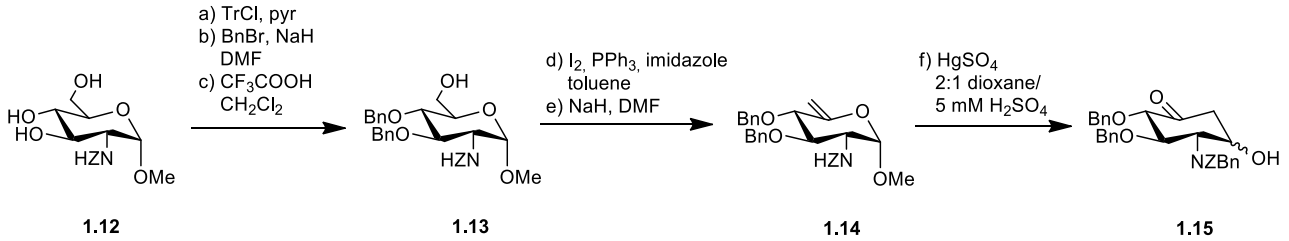

Figure 1.10 Synthesis of the carbacyclic compound **1.15** through Ferrier carbocyclization of **1.14**

In 2016 the synthesis of aminocyclitols, an amino-carbasugar structural motif found in a variety of aminoglycoside antibiotics,[35] was proposed (**Fig. 1.11**).

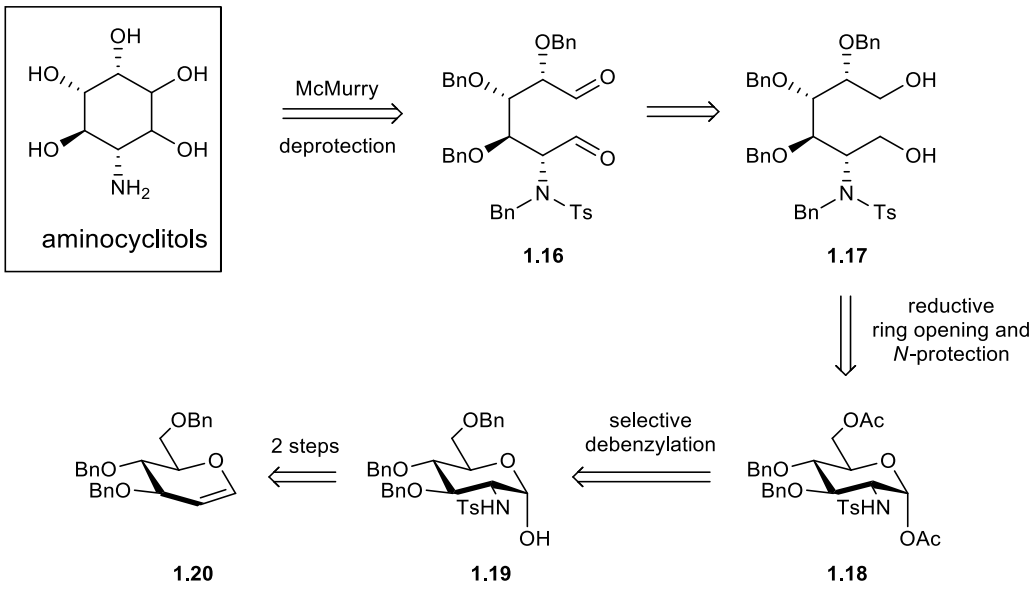

Figure 1.11 Synthesis of aminocyclitols

The synthesis started with the conversion of the tri-*O*-benzyl-D-glucal **1.20** to 2-deoxy-2-sulfonamido-D-glucose **1.19**, following a modified procedure of the Danishefsky reaction.[36] Selective debenzylation of the primary benzyl ether of **1.19** and bis-acetylation afforded compound **1.18**, that was reduced (using $LiAlH_4$) and at the same time opened to give a diol as intermediate. This intermediate underwent protection (silylation), benzylation of the amino group and deprotection (desilylation) to obtain diol **1.17**, that was oxidized to aldehyde **1.16** under Swern conditions (DMSO and oxalyl chloride) in order to generate a suitable substrate for McMurry coupling.[37]

Carba-cyclophellitols **1.24** (**Fig. 1.12**) were originally reported by Hashimoto and co-workers[38] via Simmons-Smith cyclopropanation of cyclohexene **1.23**. The class was recently expanded by Overkleeft and his team that prepared the corresponding cyclophellitol **1.21** and cyclophellitol aziridine **1.22** (**Fig. 1.12**),[39] using Ethyl DiAzoacetate (EDA) as the cyclopropanating agent.[40-41] Their optimized synthetic pathway allowed the construction of gluco- and galacto-pyranose-configured cyclophellitol cyclopropanes, as potential enzyme inhibitors (**1.25**, **1.40**; **Fig. 1.14**)

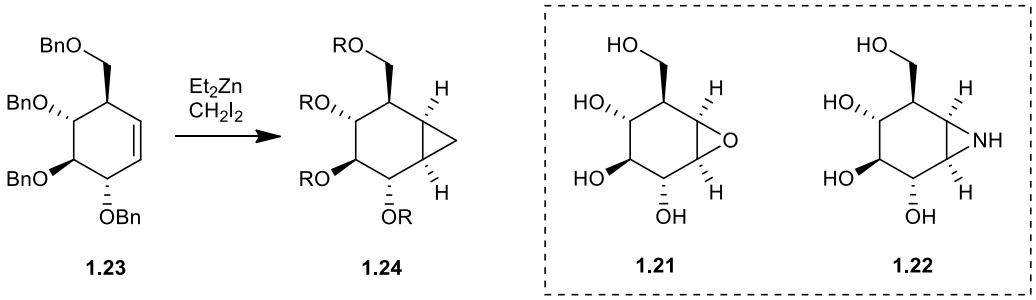

Fig. 1.12 Simmons-Smith cyclopropanation reaction of cyclohexene **1.23** (on the left); cyclophellitol **1.21** and cyclophellitol aziridine **1.22** proposed as carbohydrate mimics by Overkleeft[39]

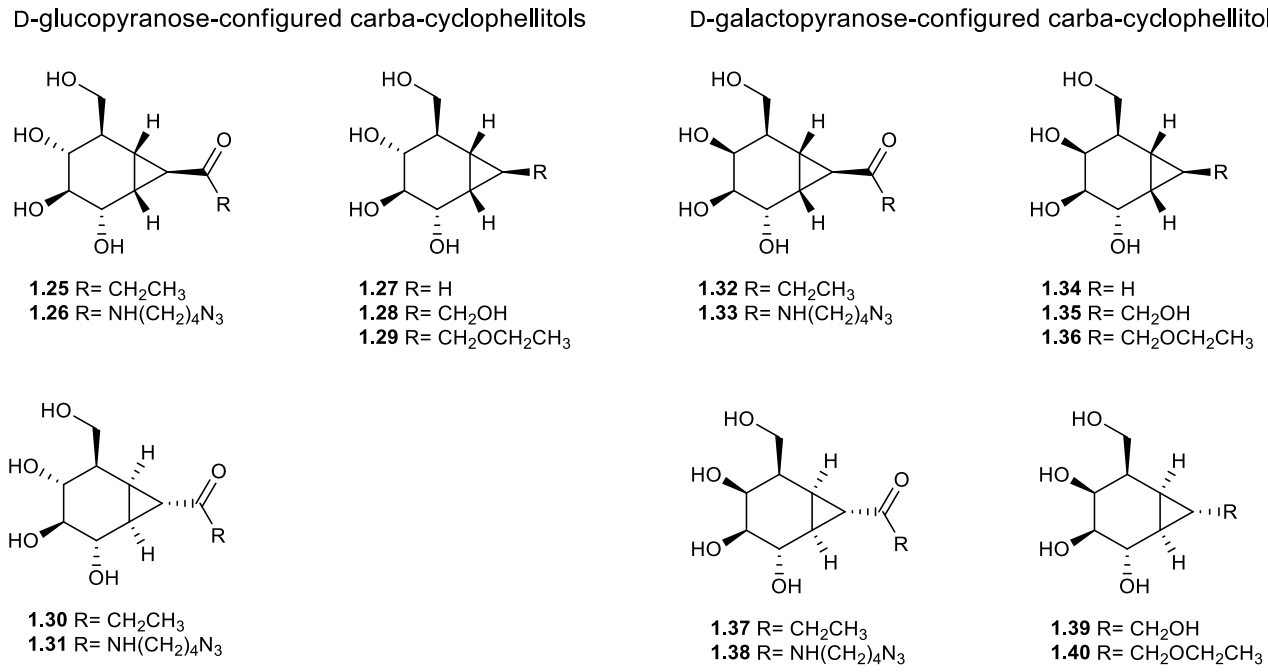

Fig. 1.13 Gluco- and galacto-pyranose-configured cyclophellitol cyclopropanes

The rise of drug-resistant influenza A virus strains led to great efforts in the development of new antiviral drugs, with different structural motifs and functionalities. Recently, a bicyclic (bicyclo[3.1.0]hexane, with general structure of **1.41** reported in **Fig. 1.14**) analogue of sialic acid was designed to mimic the conformation adopted during enzymatic cleavage within the neuraminidase (NA; sialidase) active site. [42]

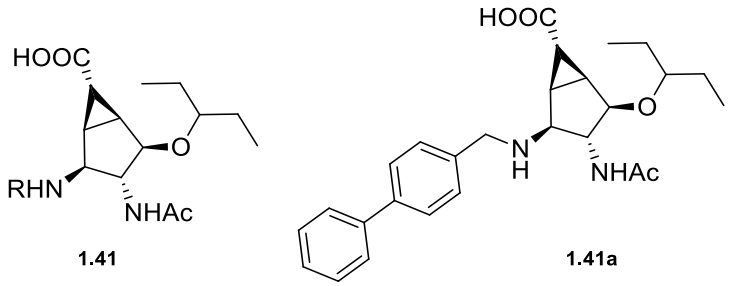

Fig. 1.14 Bicyclo[3.1.0]hexane scaffolds as analogues of sialic acid

Retrosynthetically, these derivatives were synthetized through a Johnson-Corey-Chaykovsky cyclopropanation (that allowed systematic variation of the relative stereochemistry of the scaffold's stereocenters) that followed a photochemical pyridine ring contraction.

The compounds displayed 'slow-binding' time-dependent inhibition of N1 and N2 sialidases with IC_{50} values in the micromolar range. The strongest inhibition exhibited by these compounds (IC_{50}= 10 μM) was observed with compound **1.41a** (R = 4-phenylbenzyl).

To further develop the structure activity relationship of this new scaffold, a second set of compounds was synthesized in order to analyze the effect of replacing the amino group of **1.41** with a larger guanidium moiety and to probe the role of the ether side chain (compounds of general formula of **1.42**, **Fig. 1.15**).[43]

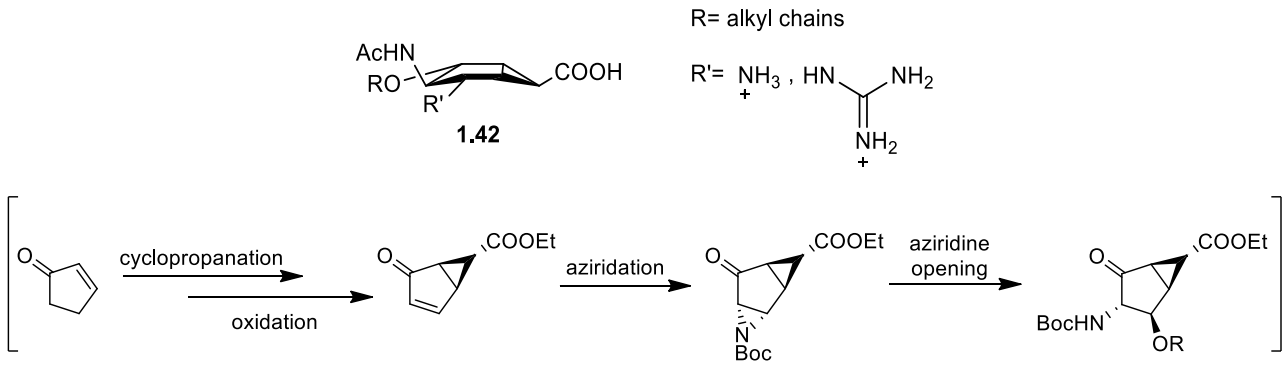

Fig. 1.15 General structure of new sialidase inhibitors bearing a guanidium moiety (on the top); general synthetic strategy (on the bottom)

The introduction of a guanidium group as a substituent took inspiration from the example of Zanamivir, where the presence of this motif is crucial for the antiviral activity.[44] In this work, a new, much simplified synthetic route for the bicyclo[3.1.0]hexane framework was adopted, starting from cyclopropanation of cyclopentenone followed by aziridination and further functionalization of the five membered ring. This strategy allowed the efficient preparation of a small library of 10 bicyclic ligands (**Fig. 1.15**), densely functionalized, designed with the aid of molecular modelling to engage in additional interactions within the NA binding site. However, these compounds were tested against various influenza A neuraminidases and none of the new structural variants displayed activity at concentrations less than 2 mM.

Another class of antiviral molecules, where the carbasugar moiety was introduce in order to both mimic the natural ligand conformation and improve the metabolic stability, has the lectin DC-SIGN as protein target. DC-SIGN (see Chapter 2.1) is known to be involved in the recognition of viruses and pathogens at the mucosal level and it contains a binding site selective for mannose- and fucose-based carbohydrates. In 2016, the synthesis of the pseudo-disaccharide **1.43** (**Fig. 1.16**), containing a mannose connected with a D-carbamannose unit, was reported: these structures were designed to mimic the minimal natural epitope Manα(1,2)Man **1.44** of DC-SIGN.[45]

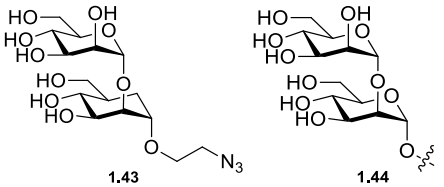

Fig. 1.16 Chemical structures of pseudo-disaccharide **1.43** as carba-analogue of epitope **1.44**.

The stereoselective synthesis of pseudo-disaccharides **1.43** proceeded through the construction of the precursor **1.47** by glycosylation of the carbamannose glycosyl acceptor **1.46** with tetrabenzoyl mannose trichloroacetimidate **1.45** as typical glycosyl donor (**Fig 1.17**).

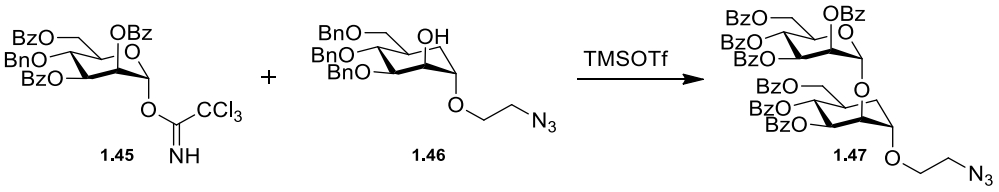

Fig. 1.17 Glycosylation reaction between donor **1.45** and acceptor **1.46** to obtain the pseudo-disaccharide **1.47**

The synthesis of **1.46** started from the construction of the carbocyclic system **1.49** through a Claisen rearrangement developed by Sudha and Nagarajan[46] to the glycal substrate **1.48** (**Fig. 1.18**).

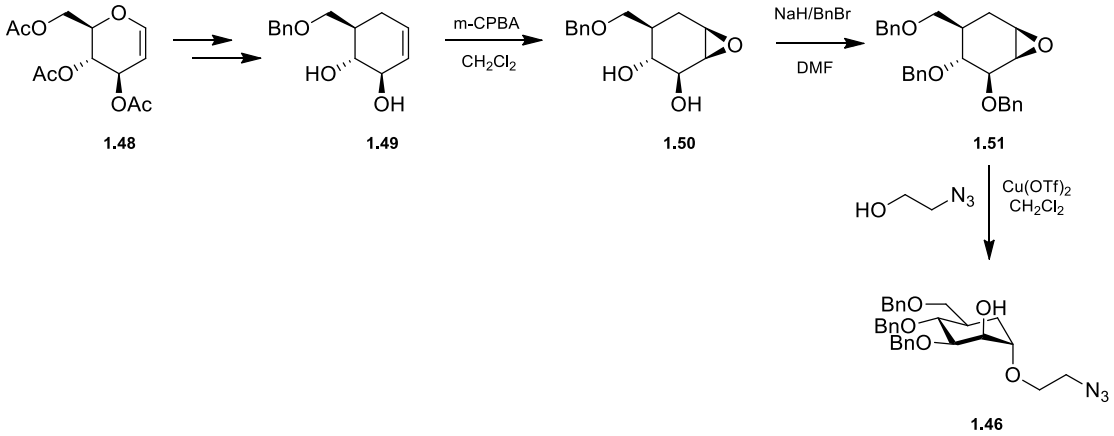

Fig. 1.18 Synthesis of the acceptor **1.46** starting from the glycal substrate **1.48**

Allyl alcohol **1.49** is stereoselectively epoxidized by m-CPBA, which reacts with the double bond face *syn* to the allyl hydroxy group affording epoxide **1.50** as the only reaction product. Followed the ring opening with azido-ethanol in a copper catalysed process in the presence of a Lewis Acid to give the cyclohexanol derivative **1.46**.

1.1.3 Thio sugars

Thio-sugars are carbohydrate mimics obtained by replacement of the endocyclic oxygen atom with a sulphur atom, in both furanose and pyranose structures.[47-48] Due to the unique conformational and electronic properties imparted by the sulphur atom, these compounds have found widespread applications as glycosidase inhibitors, demonstrating potent biological activity as antiviral, antidiabetic or anticancer compounds. [49-50]

Recently, it was demonstrated that the introduction of the endocyclic sulphur atom can be achieved via thiyl radical mediated cyclization. This process has been extensively investigated for the preparation of carbohydrate derivatives, due to the mild reaction conditions, the high yields and the tolerance to a wide range of functional groups. The Scanlan group has recently reported the application of the intramolecular thiol-ene and thiol-yne cyclisation reaction for the preparation of both thiosugars and thioglycals.[51] This approach allows the construction of both thiofuranoses and thiopyranoses from a single acyclic starting material, usually obtained from commercially available *O*-benzyl protected sugars (see compound **1.52** in **Fig. 1.19**), subsequently modified into the corresponding alkene-glycosyl thiol derivatives through a multistep

process that involves a Witting olefination and an S_N2 displacement of the triflate group by KSAc and finally the hydrolysis of the thioester to the corresponding thiol.

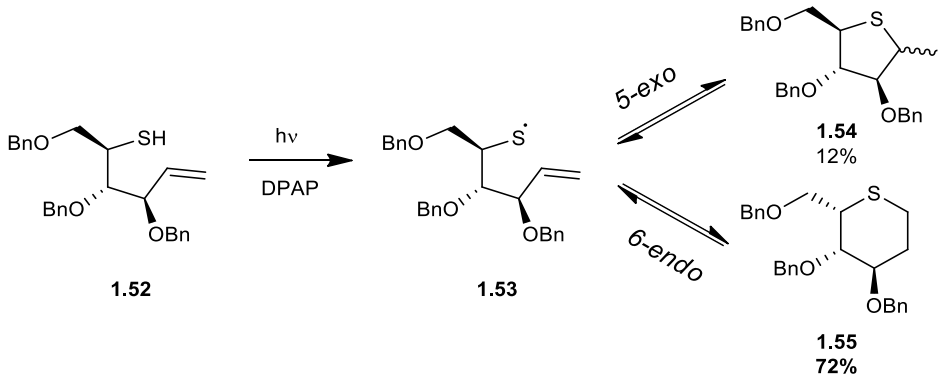

Figure 1.19 Example of intramolecular thiol-ene cyclisation reaction for the preparation of thiosugars

In **Fig. 1.19** the main strategy of this work is described. It involves the formation of the thiyl radical **1.53** (upon photochemical irradiation and using 2,2-Dimethoxy-2-phenylacetophenone (DPAP) as photoinitiator) followed by intramolecular thiol-ene cyclisation that leads to both the 5-*exo* and the 6-*endo* products.[52] The free-radical version of the intramolecular thiol-yne cyclisation reaction was investigated again by Scanlan and co-workers.[53]

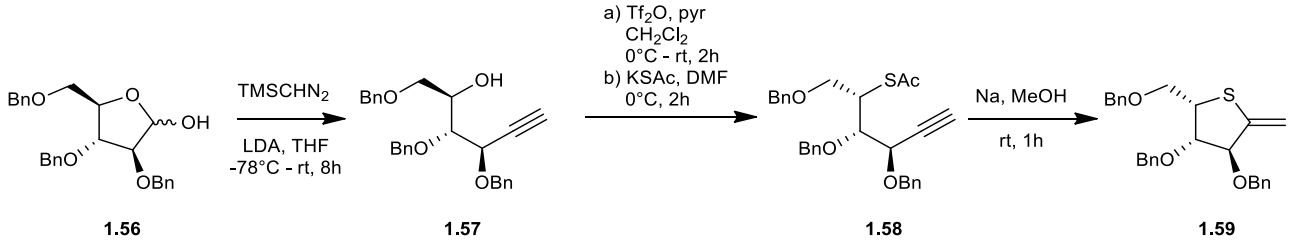

Fig. 1.20 The free-radical version of the intramolecular thiol-yne cyclisation reaction proposed by Scanlan et al.[53]

The introduction of the alkyne function onto 2,3,5-tri-*O*-benzyl arabinose **1.56** was perfomed through Colvin rearrangement, *via* a lithiated trimethylsilyl diazomethane intermediate (**Fig. 1.20**). Afterwards, the thioester **1.58** was obtained by treatment of alchol **1.57** with triflic anhydride followed by nucleophilic displacement with KSAc. Finally, the Zemplén conditions (Na, MeOH) promoted spontaneous formation of the 5-*exo*-glycal product **1.59**.

1.1.4 Oxaphosphinanes

Another class of carbohydrate mimetic structures obtained through an endocyclic modification is represented by phosphorus-based sugars, where the ring oxygen or the anomeric carbon are replaced by a P=O group. These compounds have received continuous attention in the past 20 years as sugar analogues because of considerable interest in their physiochemical properties and potential biological activity. Depending on how the phosphorous atom is inserted into the cycle, three main classes of compounds can be

obtained: phospha-sugars, phosphono-sugars (or phostones) and phosphino-sugars (or phostines), schematically reported below (**Fig. 1.21**).

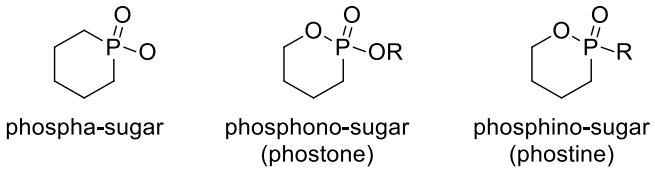

Fig. 1.21 General classification of phosphorous containing glycomimetics

Generally, these compounds, containing a phosphoryl bond (P=O), show high Lewis/Brønsted basicity.[54] As observed with glycopyranoside derivatives, phosphorus six-membered rings show also stereoelectronic-dependent interactions with phosphorus atoms that are closely related to the anomeric effect.[55] Another important feature of oxaphosphinanes is that such phosphorus heterocycles are considerably more resistant to the ring-opening/closure processes occurring between the open-chain and the cyclic pyranose forms.[56-57]

1.1.4.1 Phospha-sugars

The compounds obtained through the replacement of the ring oxygen with a phosphorous atom are called phospha-sugars. Hanaya with his team have dedicated an intense activity to the investigation and the development of new methods for the introduction of a phosphinyl group into the sugar skeleton. In 2002, they published a procedure for the preparation of D-mannopyranose analogues (with general structure of **1.60**, **Fig. 1.22**).[58]

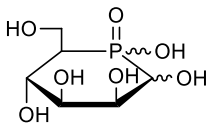

1.60

Fig. 1.22 D-mannopyranose phospha-sugar analogue

In details, the synthetic pathway started from the α-D-mannofuranoside **1.61** that underwent epoxidation under Mitsonobu conditions affording derivative **1.62** (**Fig. 1.23**). Epoxide opening by treatment with BnONa led to the 6-*O*-benzyl compound **1.63**, which after a Swern oxidation led to the key intermediate **1.64** where the phosphonyl group was introduced as dimethyl-phosphonate, in the presence of DBU as a base. This reaction generated two epimers in C(5): the major product **1.65a** was converted in methoxalyl ester **1.66a** and then reduced with Bu_3SnH to afford a mixture of the 5-deoxy products.

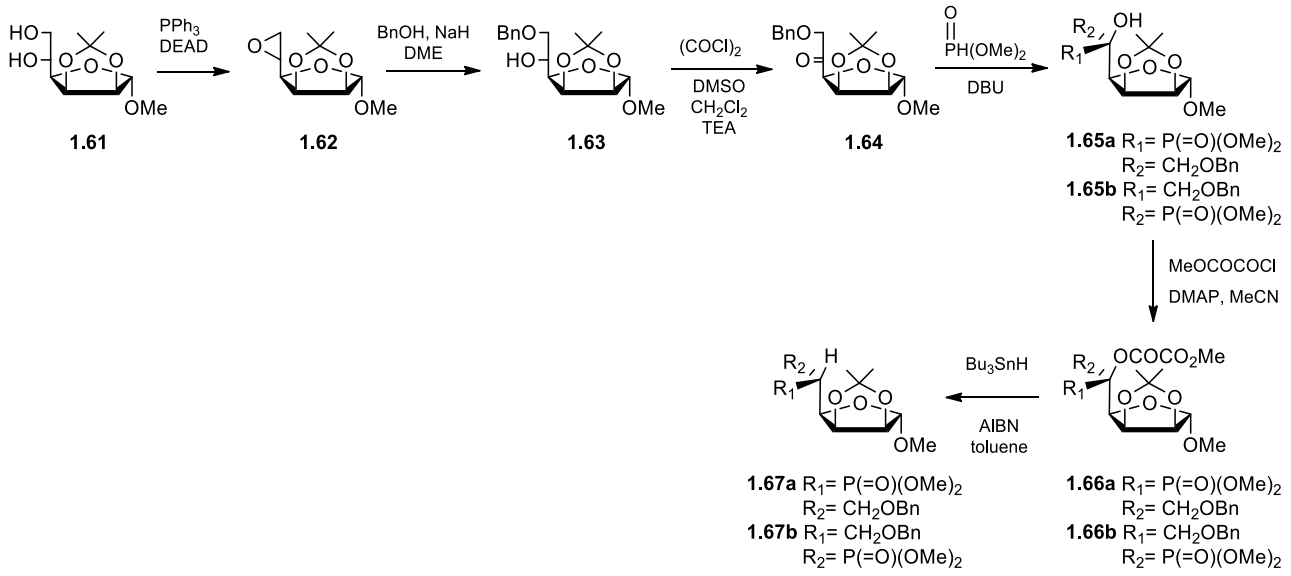

Fig. 1.23 Synthetic pathway of phospha-sugars proposed by Hanaya et al.[58]

The desired mannofuranoside derivative (**1.67a**) was obtained in minor quantity respect to the gulofuranoside isomer (**1.67b**). However, **1.67a** was then reduced to generate the 5-phopshino derivative **1.68**, which after acetal ring opening in acidic conditions and oxidation with H_2O_2 afforded the phospha-mannopyranose **1.69** (or **1.70**, by treatment with Ac_2O/pyridine and then ethereal CH_2N_2) (**Fig. 1.24**).

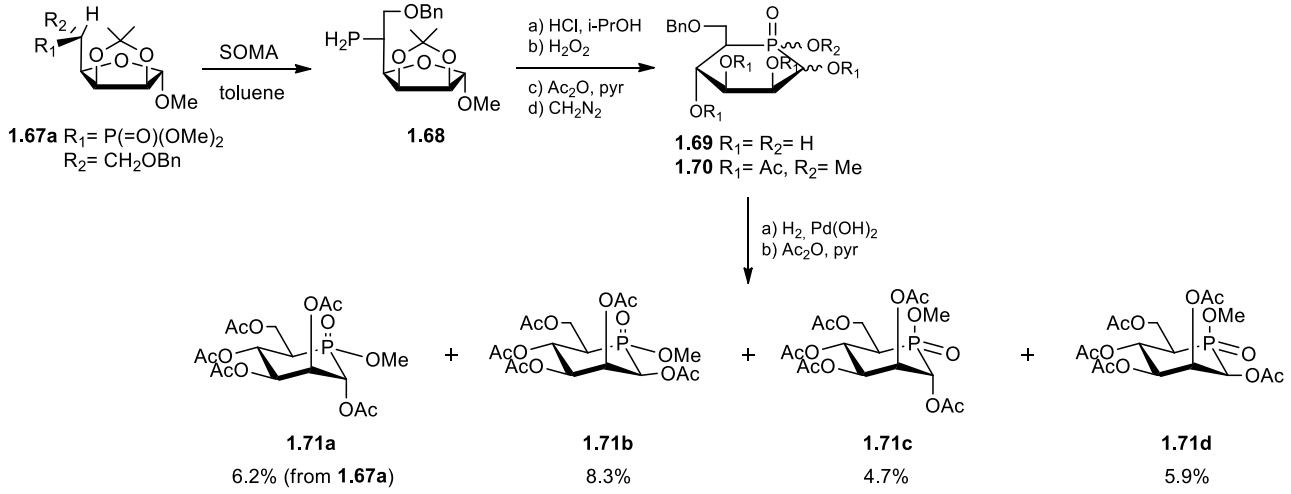

Fig. 1.24 Synthetic pathway of phospha-sugars **1.71a-d** proposed by Hanaya et al.[58]

To allow the separation of the diastereomeric mixture through chromatographic column, compound **1.70** was converted into the corresponding penta-acetates **1.71a-d**.

The same strategy was then employed and optimized for the synthesis of other phospha-sugars.[59-60]

1.1.4.2 Phosphono-sugars (phostones)

Phosphono-sugars (or phostones) are obtained replacing the anomeric carbon with a phosphonate group. Their similarity to natural carbohydrates suggested that they should have interesting and potentially useful biological properties.

One of the first example reported in literature for the synthesis of phosphono-sugars (phostones) was reported by Hanessian in 1999.[61] The target molecule **1.73** (**Fig. 1.25**) was an analogue of phosphoramidon **1.72**, a compound derived from cultures of Streptomyces tanashiensis with activity as inhibitor of the enzyme thermolysin,[62] as membrane metallo-endopeptidase inhibitor[63] and as endothelin converting enzyme inhibitor.

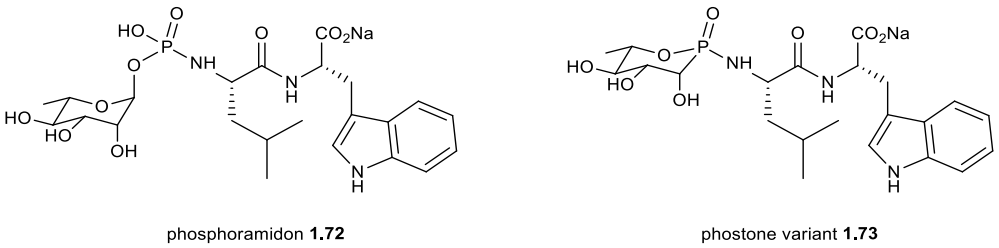

Fig. 1.25 Phosphoramidon **1.72** and its phostone analog **1.73**

The synthetic pathway is reported below (**Fig. 1.26**).

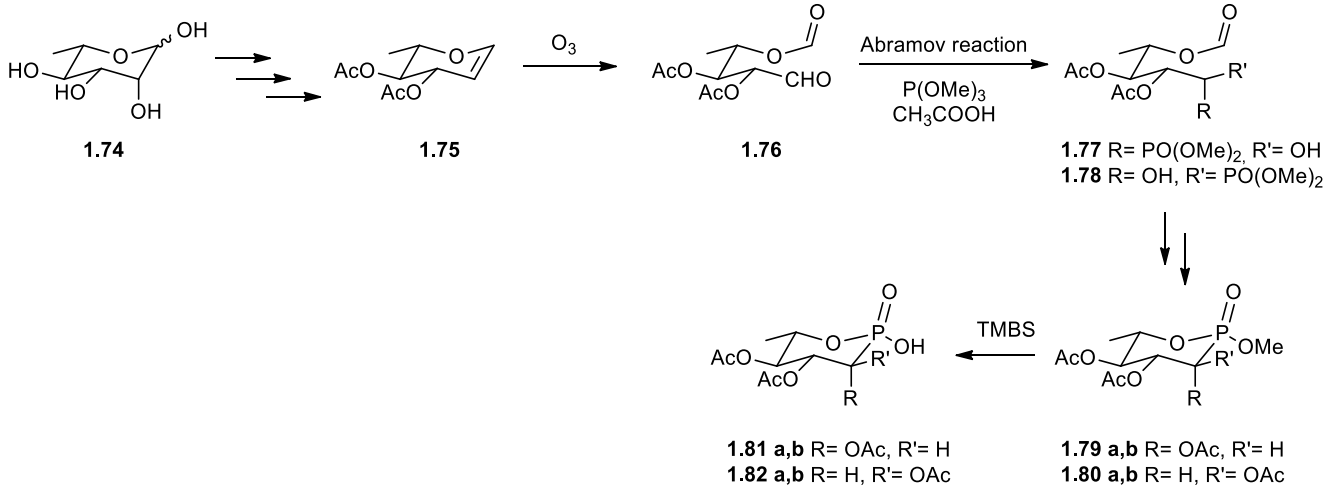

Fig. 1.26 Synthetic pathway for the preparation of phosphonic acids **1.81** and **1.82**

Natural L-rhamnose underwent modification to afford rhamnal derivative **1.75**[64] that was cleaved by ozonolysis to produce the corresponding lyxose ester **1.76** (**Fig. 1.26**). Introduction of the phosphonate group occurred through Abramov reaction,[65] in the presence of trimethylphosphite in glacial acetic acid led to a mixture of two epimers (**1.77** and **1.78**). [66] The subsequent ring closure afforded the corresponding cyclic phosphonate esters **1.79** and **1.80** which were finally treated with trimethylsilyl bromide to give phosphonic acids **1.81** and **1.82**, as an inseparable mixture. The final coupling with the L-Leu-Trp-OMe unit required to obtain the target mimetic **1.73** was performed with the corresponding phosphonyl chlorides of **1.81** and **1.82** in the presence of trimethylamine. [67-68]

More recently, Hanson and co-workers published an efficient strategy for the diastereoselective generation of a number of novel phosphono-sugars.[69]

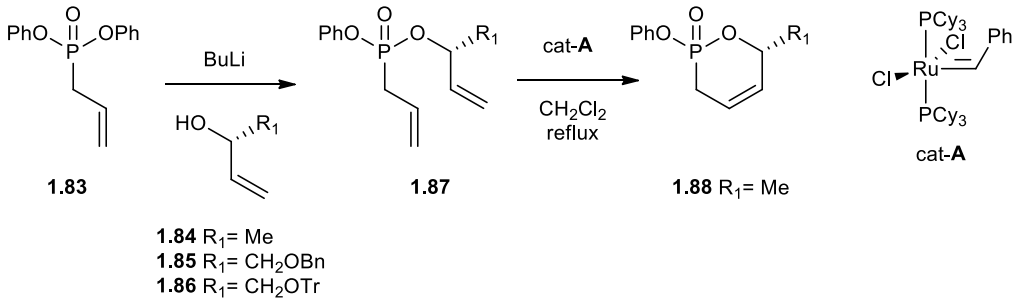

Fig. 1.27 Synthetic pathway proposed by Hanson et al.[69] for the preparation of allyl phostone **1.88** through RCM

The stereoselective alkoxide addition of allylic alcohols (**1.84**, **1.85** or **1.86**) to the allyl diphenyl phosphonate **1.83** afforded diene **1.87** as intermediate (**Fig. 1.27**). The acyclic precursor was closed through a Ring Closing Metathesis (RCM) catalysed by a 1st generation Grubbs catalyst to give allyl phostone **1.88**.

Dihydroxylation of **1.88** provided diol **1.89** with high stereoselectivity (**Fig. 1.28**). Subsequent eliminative opening of the corresponding carbonate or mesylate of **1.89** afforded vinyl phostones **1.90** (R_1= H) and **1.91** (R_1= Ms).

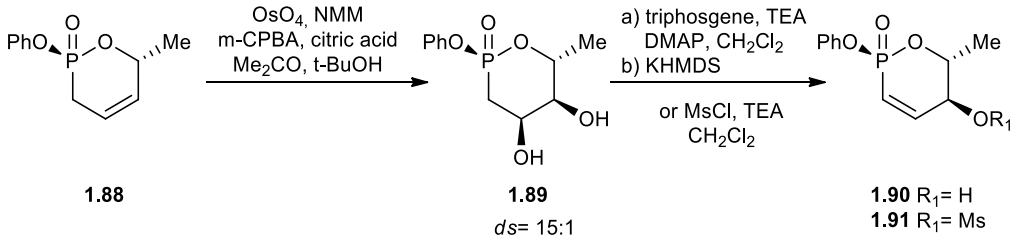

Fig. 1.28 Hanson's synthesis of vinyl phostones **1.90** and **1.91**[69]

Directed dihydroxylation of **1.90** using the Donohoe protocol with stoichiometric amounts of OsO_4/TMEDA provided the C(3)-C(5) all *syn*-triol **1.92** with excellent selectivity (**Fig. 1.29**).

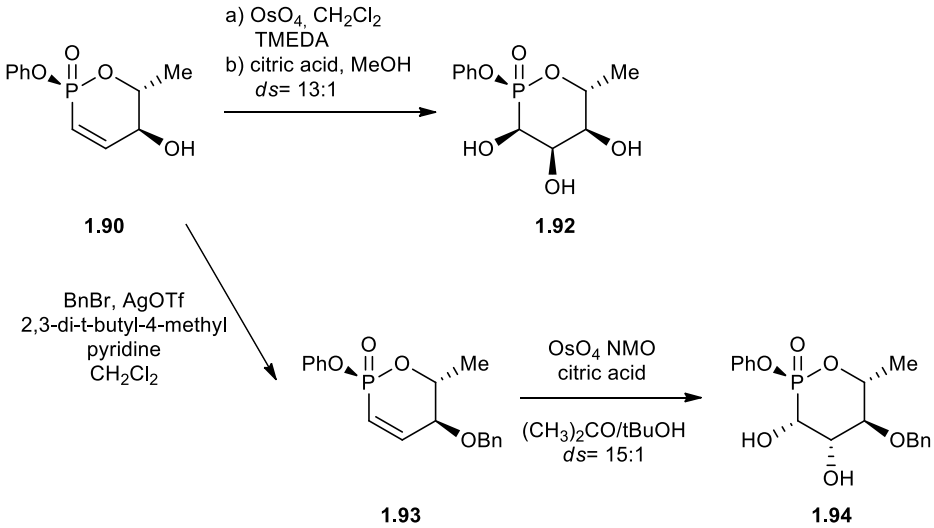

Fig. 1.29 Final steps for the preparation of phosphono-sugars **1.92** and **1.94**

The authors further improved this selectivity by protecting the hydroxyl-group of **1.90** as benzyl ether (**Fig. 1.29**). The subsequent dihydroxylation of compound **1.93** generated triol **1.94** in excellent yield and selectivity.

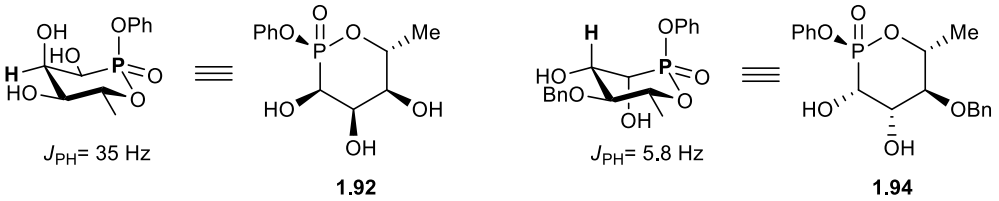

1.92 **1.94**

Fig. 1.30 Configuration of **1.92** and **1.94**

The configurations of compounds **1.92** and **1.94** was finally confirmed by the NMR analysis of the coupling constants between C(4) protons and P(1) atoms (**Fig. 1.30**).

1.1.4.3 Phosphino-sugars (phostines)

Phosphino-sugars (or phostines) are those compounds that present an 1,2-oxaphosphinane heterocyclic core. They are still considered glycomimetics since the phosphinolactone group represents an isoster (*i.e.* a group with similar shape and electronic properties) of the corresponding lactol. Furthermore, since the phosphinolactone is an hydrogen bond acceptor and a metal-complexing agent, the compounds containing this motif become very attractive structures for drug discovery.

Similar modifications of lactol groups have already been exploited in *C*-glycosides and aza- or thio-sugars, leading to compounds of therapeutic interests. However, these compounds are different from the phostone family because of the exocyclic P−C bond, which confers to the molecules a higher stability.

No example of synthesis of phostines was described before 2005, when Pirat and his group published the first synthesis of 2-phenyl-1,2-oxaphosphinane under base-catalyzed transesterification conditions.[70] They combined *C*-arylglycosides and phosphonosugars in the same molecule to obtain a cyclic polyhydroxylated phosphino-sugar (**Fig. 1.31**).

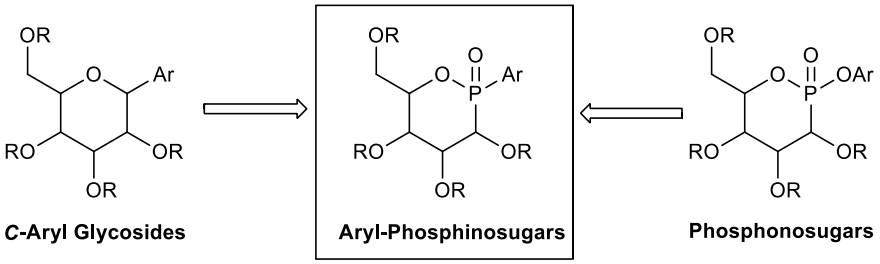

Fig. 1.31 Combination of *C*-arylglycosides and phosphonosugars proposed by Pirat et al.[70] to obtain aryl-phosphinosugars

In **Fig. 1.32** the general strategy for the synthesis of these compounds is reported.

Methylphenylphosphinate **1.96** was prepared following the procedure described by Afarikna and Yu, using phenylphopshinic acid and methyl chloroformate.[71] Compound **1.96** reacted with the protected mannofuranose **1.95** under basic conditions to give a mixture of three cyclic *P*-phenyl-oxaphosphinanes **1.98**. Potassium tert-butoxide allows not only the activation of **1.96** by removing its acidic proton and enhancing

its nucleophilicity, but it is also responsible for the deprotonation of the intermediate **1.97** allowing the spontaneous transesterification.

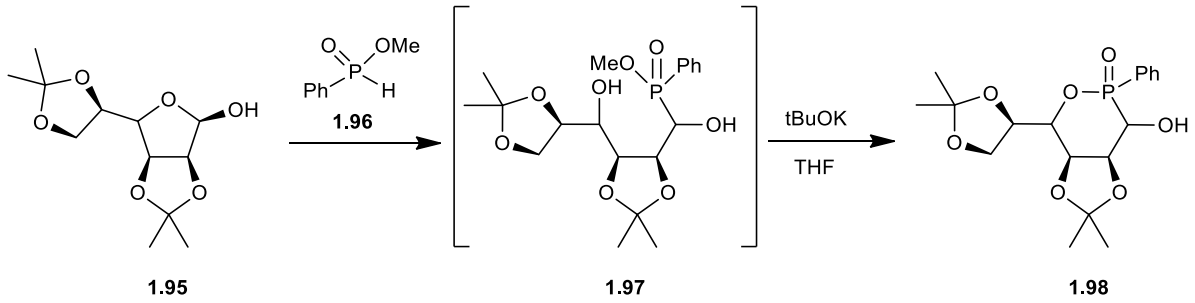

Fig. 1.32 General strategy proposed for the synthesis of aryl-phosphinosugar **1.98**[70]

This procedure allowed the synthesis on large scale of *P*-phenyl-phopshinosugars and for this reason was employed later on for the preparation of other phosphinosugars.[72]

In 2017, phostines were employed as glycomimetic compounds in drug design to interfere with glycosylation processes in cancer cells.[73] In particular, the glucose-like phostine **1.99** (reported in **Fig. 1.33**) was selected for its ability to inhibit the Mannoside acetyl GlucosAminylTransferase-5 (MGAT5), whose overexpression is associated to malignancies and correlates with cell migration, invasion, and epithelial–mesenchymal transition.

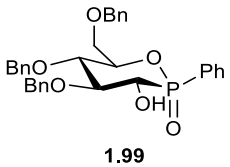

Fig. 1.33 Glucose-like phostine **1.99**

There are also example of pseudo-disaccharides containing the oxaphosphinane core (**Fig. 1.34**). This kind of compounds are obtained by replacing the glycosidic linkage with a phosphalactone (phosphino- or phosphono-lactone) in order to create more stable pseudoglycans, avoiding all the drawbacks related to the anomeric position.

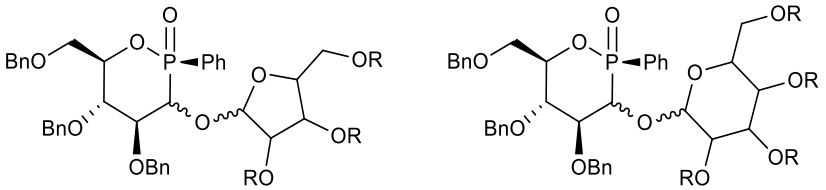

Fig. 1.34 General structures of pseudo-disaccharides containing the oxaphosphinane core

Very recently, Pirat and co-workers[74] proposed a synthetic pathway for these structures, starting from oxaphosphinanes **1.100** and **1.101** (cyclic phosphinates, **Fig. 1.35**) that can be compared to *C*-aryl hexopyranoses which were found to have potent anti-proliferative, anti-migration and anti-invasion activities.[72, 75-76]

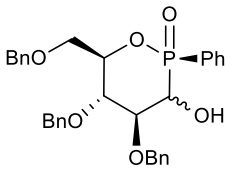

1.100
1.101

Fig. 1.35 Oxaphosphinanes **1.100** and **1.101**

Pseudo-disaccharides were synthesized by introducing a furanosyl or pyranosyl sugar unit on oxaphosphinane moiety, creating a glycosidic bond at the free hydroxyl group in position 2. In this way, the phostines were used as glycosyl acceptors: due to the presence of the phosphoryl group in adjacent position, the –OH in that position becomes more acidic (pKa≈ 13.5) than a typical sugar alcohol (pKa usually between 16 and 19),[77] thus improving the glycosidation results.

The starting oxaphosphinanes **1.100** and **1.101** were prepared following a previously published procedure (**Fig. 1.36**).[72, 78]

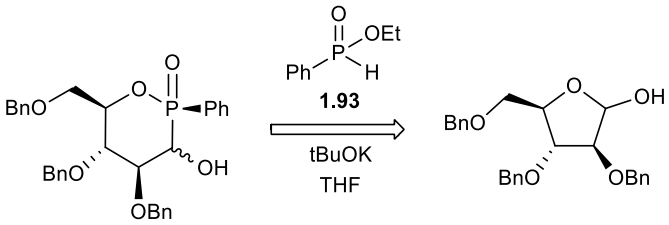

1.100
1.101

1.102

Fig. 1.36 Synthesis of phosphinosugars **1.100** and **1.101**

For the coupling reaction, a series of glycosyl donors were prepared as trichloroacetimidates (**1.104a-c**; **Fig. 1.37**).

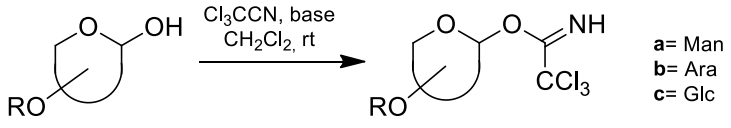

1.103a-d

1.104a-c

Fig. 1.37 Synthesis of glycosyl donors **1.104a-c**

Afterwards, the first coupling reaction occurred between the α-mannosyl donor **1.104a** and the glucose-like oxaphosphinane **1.100**, in the presence of a Lewis acid at 0°C (**Fig. 1.38**).

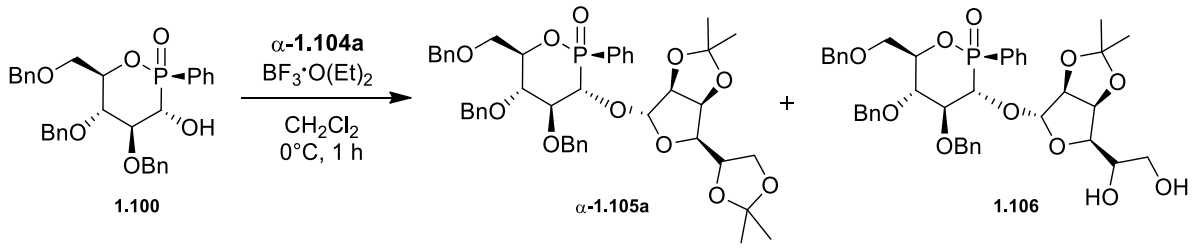

Fig. 1.38 Coupling reaction between α-mannosyl donor **1.104a** and oxaphosphinane **1.100**

In these conditions, the authors observed a partial deketalisation that led to the formation of the side product **1.106**.

Since with the arabinofuranosyl donor **1.104b** in these conditions no reaction occurred, the glycosylation reaction in this case was performed by using a palladium/silver catalytic system (**Fig. 1.39**).[79]

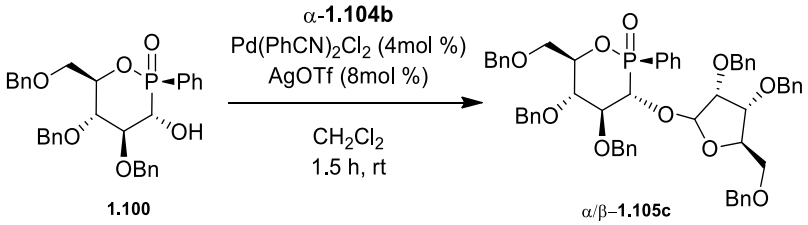

Fig. 1.39 Pd-catalysed coupling reaction between α-mannosyl donor **1.104b** and oxaphosphinane **1.100**

The cationic specie generated *in situ* by the palladium catalyst is known to generally direct the β-selectivity. However, the selectivity seemed to be very sensitive to the oxaphosphinane acceptor when the reaction occurred at room temperature. Indeed, the reaction between **1.100** and the glucopyranosyl acetimidate **1.104c** afforded **1.107** as a mixture, where the major diastereoisomer had the unexpected α-configuration (**Fig. 1.40**).

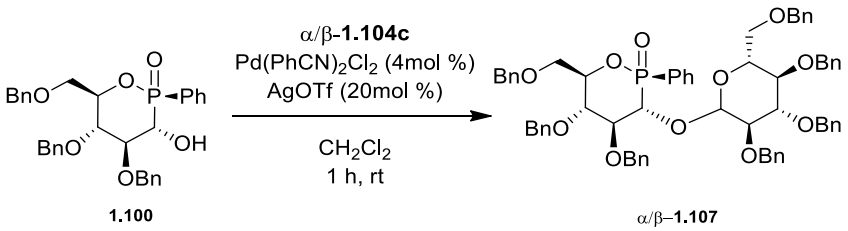

Fig. 1.40 Pd-catalysed coupling reaction between α-mannosyl donor **1.104c** and oxaphosphinane **1.100**

Another method to create pseudo-disaccharides with the oxaphosphinane core was proposed by again Pirat and his group in 2015.[76] Their strategy relied in the use of α-halogenated oxaphosphinane (with general structure of **Fig. 1.41**).

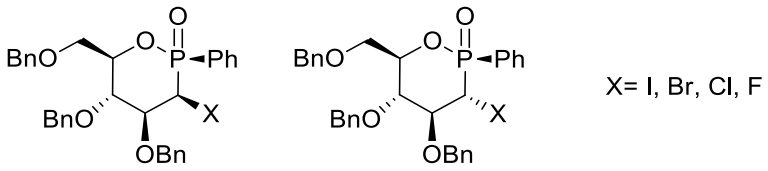

Fig. 1.41 α-halogenated oxaphosphinanes

In this case, the phosphino sugar would represent the donor in the glycosylation process.

1.2 Fluorosugars

The incorporation of fluorine atoms into bioactive molecules is a general strategy in medicinal chemistry to improve their pharmacokinetics properties and to modulate their biological properties.[80] From the perspective of steric effects, fluorine is the smallest substituent that can be used as replacement of the C-H bond, with a van der Waals radius of 1.47 Å, close to the 1.20 Å value for hydrogen. However, the high electronegativity of fluorine (3.98 on the Pauling electronegativity scale compared to 2.20 for H, 3.44 for O, and 2.55 for C) results in a highly polarized C–F bond, which presents a strong dipole moment. This feature has been exploited in many ways for the development of enzyme inhibitors or to render molecule resistant to chemical degradation. Furthermore, it was demonstrated that fluorination can influence the molecular conformation and can change the lipophilicity profile of drug molecules, influencing solubility, permeability and protein binding.

Fluorinated glycomimetics have been explored as well. Some examples of fluoro-containing carbohydrate mimetics are reported in **Fig. 1.42**.

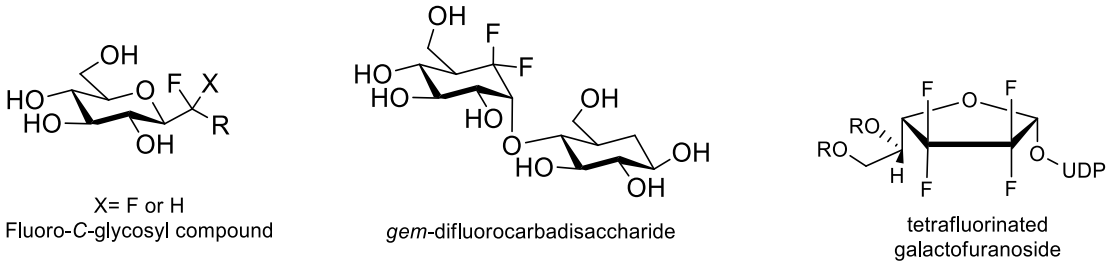

Fig. 1.42 Examples of fluorinated glycomimetics

Depending on the substituted position, the fluorine substituent can have remarkable effects upon the physical and chemical properties of the molecule. As already mentioned, it could induce increase of lipophilicity, decrease in pKa values of certain groups by OH–F electrostatic interaction, modulate the hydrogen-bond acceptor/donor ability or foster the presence of a particular ring conformation.[81]

The strategic fluorination of antigenic glycans has also emerged as an interesting approach for glycoconjugates vaccine development: selectively fluorinated carbohydrate antigens have shown improved metabolic stability, as well as comparable or even enhanced immunogenicity.[82]

More recently, carbasugars were combined with fluorination strategies to increase their stability, lipophilicity or to modulate the acidity and basicity (see chapter 1.1.2 of carbasugars).[33] Moreover, fluoro-carbasugars revealed to be advantageous in mimicking the natural sugar conformations.[83]

Recently, in two different papers Jiménez-Barbero and co-workers highlighted the importance of fluorination, preparing and investigating the behaviour of a new generation of fluorine-containing glycomimetics.[83-84] They proposed a synthetic route for the preparation of *gem*-difluorocarbadisaccharides and *gem*-difluorocarbasugar analogues of β-L-idose (**1.110** and **1.109a**, while **1.109b** is the Glc analogue; **Fig. 1.43**). The presence of fluorine atoms emulates, to a certain degree, the properties of the endocyclic oxygen.

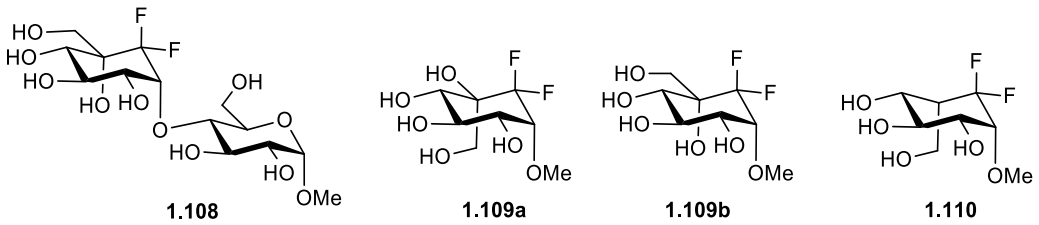

Fig. 1.43 Examples of *gem*-difluorocarbadisaccharide and *gem*-difluorocarbasugar analogues of β-L-idose

The synthesis of compounds **1.109a**, **1.109b** and **1.108** building block followed similar strategy and involved a firstly modified Pummerer reaction using diethylaminosulphur trifluoride (DAST) as fluoride source in combination with the *N*-iodosuccinimide (NIS) for the synthesis of α-fluoro-sulphide derivatives.[85] The mechanism of this process is similar to the usual Pummerer reaction and proceeds through a selective iodination of the sulphur atom, followed by HI elimination triggered by succinimide to give the sulfonium ion, which is attacked by fluoride to give the final α-fluoro-sulphide product.

The second fluorination process was performed using Selectfluor in the presence of DAST (see reaction from **1.113** to **1.114** in **Fig. 1.44**). Afterwards, m-CPBA oxidation generated the corresponding sulphoxide that underwent thermolysis using Bn_3N in Ph_2O at 190°C for 120 hours to give the difluorovinyl compound **1.16**. This alkene was then treated with triisobutylaluminium (TIBAL) giving the desired carbacycle that was oxidized into ketone **1.117** with Dess-Martin periodinane. The reaction using Tamao's reagent provided β-hydroxysilanes which were subjected to oxidative cleavage of the Si-C bond by basic hydrogen peroxide giving diols **1.118** and **1.119** which were separated.

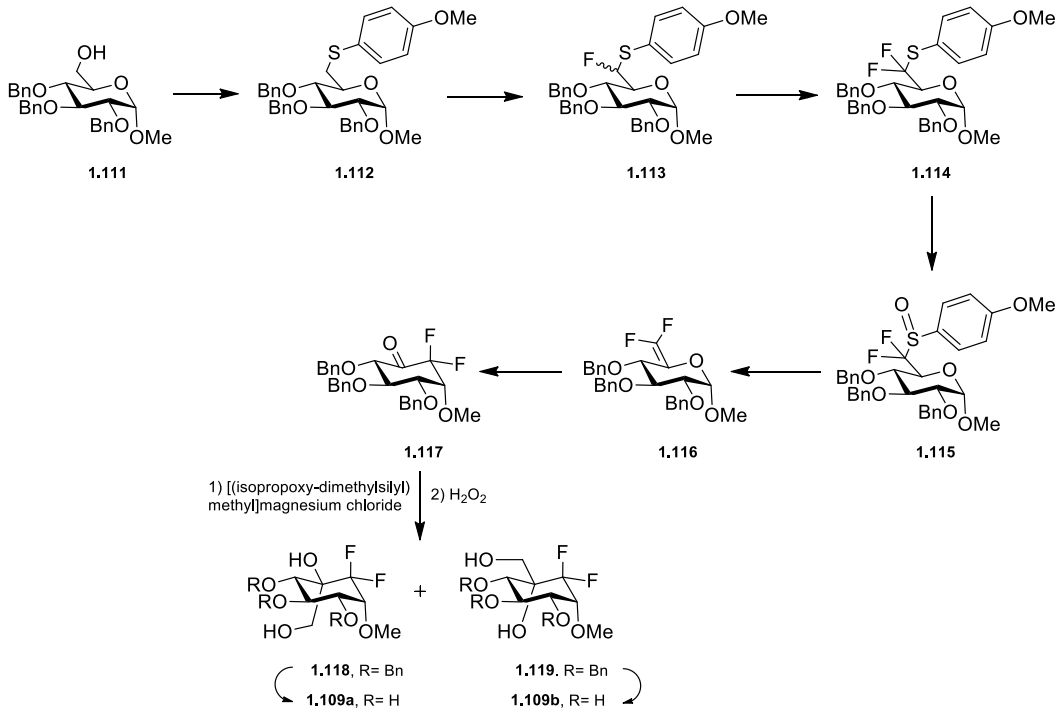

Fig. 1.44 Synthesis of *gem*-difluorocarbasugars **1.109a** and **1.109b**

Final deprotection of both **1.118** and **1.119** through hydrogenolysis using Pd/C gave the target *gem*-difluorocarbasugars **1.109a** and **1.109b** in quantitative yields.

For the synthesis of compound **1.110**, the authors followed a different strategy, in which the fluorine atoms are introduced after carbocyclisation of the sugar by difluorination of a ketone.[84]

Since for ido-like sugars, flexibility is intrinsically related to biological activity, ^{19}F and ^{1}H homo- and heteronuclear NMR spectroscopic experiments (performed in water and dimethyl sulfoxide solutions), supported by computational methods were carried out to determine the intrinsic conformational and structural properties of **1.109a**, **1.109b** and **1.110** and in particular to investigate the conformational effects of the difluoromethylene function.[84] It is, well known that for L-idopyranoses the theoretically more favourable $^{1}C_4$ chair displays three axially oriented hydroxyl groups, with the corresponding steric consequences. The alternative $^{4}C_1$ chair places the bulky hydroxymethyl group at the axial orientation, with the corresponding collapse. Therefore, alternative skew-boat conformers are also present in the conformational equilibrium, depending on the hydroxyl substitution, chemical environment, and solvent.[86-88] Ido-like carbasugars, with a CH_2 group mimicking the endocyclic oxygen atom, did not show any conformational plasticity.[89] In contrast, the β-L-idose analogues **1.109a**, **1.109b** and **1.110**, with CF_2 moieties replacing the endocyclic O, show important conformational plasticity. The dynamic process has been quantified in terms of energy barriers and free-energy differences. Compound **1.109b** (Glc-like) displays a unique $^{4}C_1$ chair conformer with a very well defined geometry, as in the natural compound. Compound **1.110** displays significant conformational distortions. ^{19}F-based variable temperature experiments demonstrated the existence of a conformational equilibrium between two forms between the canonical $^{4}C_1$ (minor) and $^{1}C_4$

(major) chair forms. In contrast, compound **1.109a** shows a unique conformational behaviour: the chemical shift and coupling constant values drastically changed upon temperature variation indicating that its conformational distributions depend on the temperature. This observation strongly suggests that the conformational entropy of the contributing geometries is different. The major and enthalpy-favoured conformer is the $^4C_1$ chair, while the other participating conformers display a skew boat geometry. In conclusion, only in the presence of a CF_2 group replacing the endocyclic oxygen atom, the ido-like six-membered ring recovers its required flexibility, absent in regular CH_2-Ido-carbasugars,[90] while the presence of a bulky substituent at position C5 strongly reduces the ring flexibility and introduces important steric clashes.

In 2017, Mayer and co-workers have focused their attention on the development of new artificial cofactors of the glmS ribozyme (a bacterial gene-regulating riboswitch that controls cell wall synthesis, present in several human pathogen bacteria).[91-92] The natural glmS cofactor is the glucosamine-6-phosphate (GlcN6P) (**Fig. 1.45**).

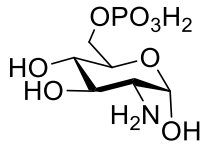

α-**D-Glucosamine-6-phosphate**

Fig. 1.45 α-D-glucosamine-6-phosphate: the natural glmS cofactor

Mayer and his team proposed the synthesis of mono-fluoro-modified carba variants of α-D-glucosamine and β-L-idosamine as synthetic mimics of the natural glmS ribozyme ligands in order to interfere with the cell wall synthesis and thereby inhibit bacterial cell growth.

With this aim, carbocyclic mimics of GlcN6P and IdoN6P that bear fluorine at the carba-position were synthesized (**Fig. 1.46**).

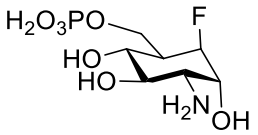

Fluoro-carba-α-**D-Glucosamine-6-phosphate**

1.120

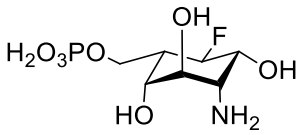

Fluoro-carba-β-**L-Idosamine-6-phosphate**

1.121

Fig. 1.46 Carbocyclic **1.120** and **1.121** mimics of GlcN6P and IdoN6P that bear fluorine at the carba-position

Compound **1.122** (**Fig. 1.47**) was obtained following the procedure already discussed before (see chapter 1.1.2 Carbasugars).[33] The synthesis then proceeded with compound **1.123** that was converted to the corresponding enolate by treatment with lithium diisopropylamide (LDA) and finally fluorinated using *N*-fluoro-benzenesulfonimide (NFSI) as fluorinating agent (**Fig. 1.47**).[93]

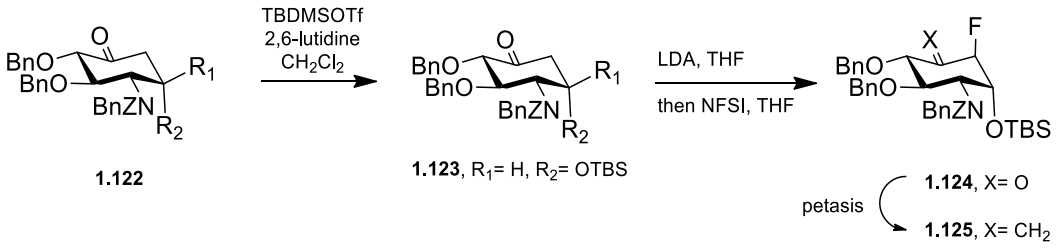

Fig. 1.47 Synthesis of compound **1.125**

In this way, the mono-fluorinated cyclohexanone **1.124** was isolated in moderate yield (46%) as a single diastereoisomer. Finally, exposure of **1.124** to Petasis reagent ($(C_5H_5)_2Ti(CH_3)_2$) provided olefin **1.125** that underwent hydroboration and subsequently oxidation to afford the fluoro-carba idopyranose compound **1.126** in a stereoselective way (**Fig. 1.48**).

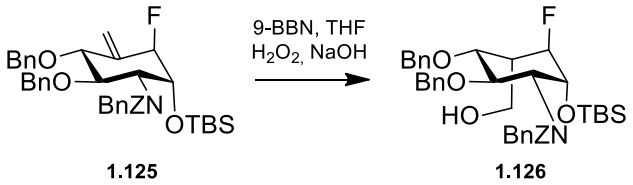

Fig. 1.48 Hydroboration of **1.125** to obtain the fluoro-carba idopyranose **1.126**

The corresponding isomer **1.128**, where the configuration at C(5) should be inverted, was not accessible directly from **1.126** through simple isomerization. The alternative route developed to obtain **1.128** required a first epoxidation of the double bond (that needed 14 days to form compound **1.127** in 59% yield) and a subsequent regioselective epoxide opening (**Fig. 1.49**).

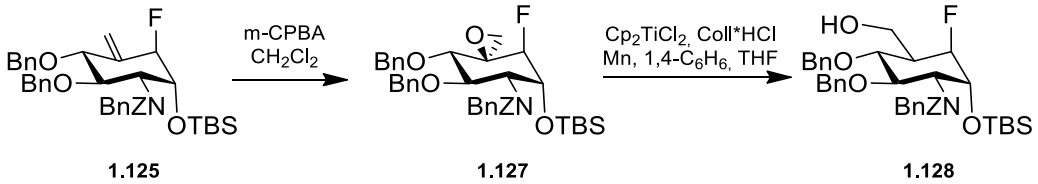

Fig. 1.49 Synthesis of the corresponding isomer of **1.126**

However, this latter process represented a not trivial step: indeed, all the attempts reported in literature regarding ring opening in the presence of a fluorine in the same molecule (but in particular in the adjacent position) have failed. The authors in this case developed a catalytic approach using $TiCp_2Cl$ and collidine hydrochloride that, protonating the titanocene, had the role to regenerate the titanium specie. However, even if this procedure allowed the isolation of the desired product with high diastereoselectivity, compound **1.128** was obtained in only 33% yield.

The deprotection of compounds **1.126** and **1.128** was achieved through removal of the TBS protecting group (using the tris(dimethylamino)sulfonium difluorotrimethylsilicate TASF) followed by hydrogenolysis with Pd/C that afforded compounds **1.129** (in 34% yield) and **1.130** (53%) (**Fig. 1.50**).

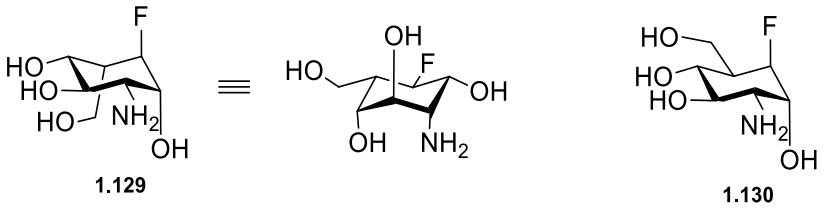

Fig. 1.50 Final compounds **1.129** and **1.130** obtained through hydrogenolysis of **1.126** and **1.128**

Finally, the corresponding 6-phoshorylated compounds were synthesized starting from **1.126** and **1.128** giving the corresponding α-D-glucosamine-6-phosphate **1.120** and β-L-idosamine-6-phosphate **1.121** that were analysed to test their capability to induce glmS ribozyme self-cleavage in vitro.

1.3 Exocyclic oxygen replacement

Sugar mimics have also been created by replacement of the exocyclic oxygen atom. One must be aware that the conformational behaviour of these mimetics can drastically change compared to their natural counterparts: for example a greater flexibility around the interglycosidic linkage can be observed as well as the presence of conformations that are not available to the native compound.[83] These changes are often detrimental to the efficient interaction of such molecules with target proteins. On the other hand, they may become instrumental when the bound conformation of an oligosaccharide ligand differs from the most abundant in water solution. The change in conformational behaviour has been attributed to the absence of the anomeric effects, especially the *exo*-anomeric one.[94] The *exo*-anomeric effect plausibly finds its origin in the favourable interaction between a lone pair of electrons on the exocyclic anomeric oxygen atom with the parallel s* orbital of the adjacent C1–O5 bond.

In the figure below (**Fig. 1.51**), some example of glycomimetics obtained through replacement of the exocyclic oxygen are reported.

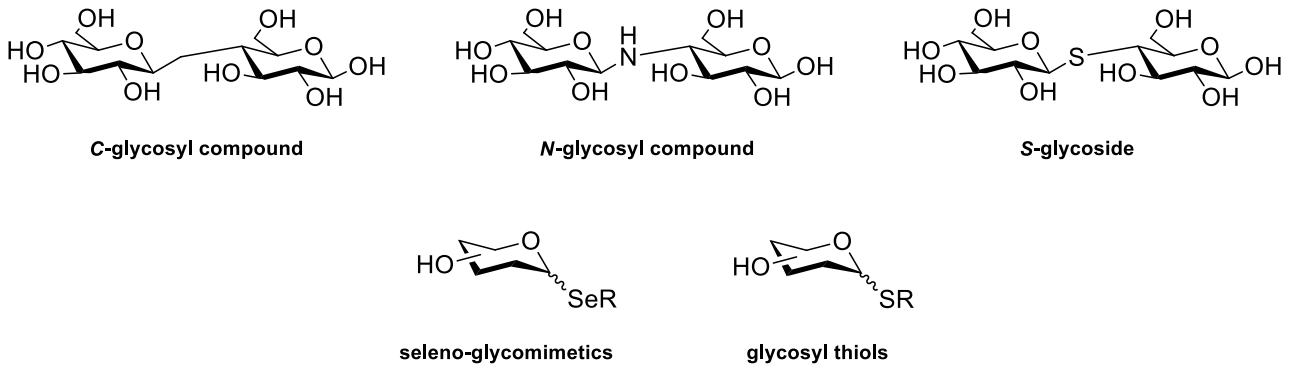

Fig. 1.51 Examples of glycomimetics obtained through the replacement of the exoocyclic oxygen atom

1.3.1 C-glycosyl compounds

The replacement of the exocyclic anomeric C–O bond with a C–C bond is a good strategy to provide hydrolytically stable derivatives, called *C*-glycosides. These carbohydrate mimetics have received considerable attention due to their diverse and valuable properties. Since the nature of the anomeric centre

is electrophilic, the most obvious way to generate a *C*-glycoside is to exploit a nucleophilic carbon atom.[23] However, there are many examples in the literature describing the efforts made to generate an anomeric nucleophile (as carbo- or organometallic-anion) that, through the reaction with an electrophilic carbon atom or an anomeric radical, can generate the *C*-glycoside.

The general approaches to synthesize *C*-glycosides are reported in **Fig. 1.52**.

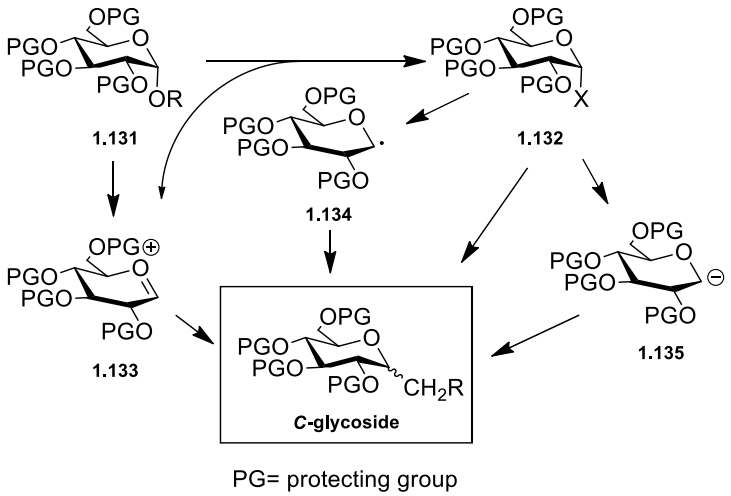

Figure 1.52 General approaches to obtain *C*-glycosides

Glycoside **1.131** can be converted into an activated glycosyl donor **1.132** (where X is typically an halide) that, undergoing nucleophilic substitution by treatment with a carbon nucleophile (such as a Grignard reagent or a malonate anion), gives a *C*-glycoside. The glycosyl halide **1.132** can also give rise to a glycosyl radical **1.134** or a glycosyl anion **1.135**. Alternatively, treatment of the glycoside **1.131** (or even the activated glycosyl donor **1.132**) with a Lewis acid affords the oxacarbenium ion **1.133**, which is able to react with an electron-rich carbon atom.

For all the details regarding recent synthetic advances for the preparation of *C*-glycosides, the review of Yu and Yang summarizes all the methodologies developed between 2000 and 2016.[95]

Various strategies have been also devised to introduce acyl groups at the anomeric carbon in glycosides. *C*-acyl glycosides are a subfamily of *C*-glycosides that display interesting biological activity, [96-97] such as inhibition of reactive oxygen species (ROS, involved in oxidative stress cell-signaling) and glutamate-induced cell death. From a synthetic point of view, they are generally prepared either by nucleophilic addition of organometallic reagents to *C*-glycosyl aldehydes followed by oxidation,[98] addition of aldehydes[99] or electrophilic acylating agents[100] to glycosyl-based lithium, tin or samarium reagents (**Fig. 1.53**, A), or the addition of Grignard reagents to glyconitriles[101] or glycosyl benzothiazoles.[102] However, all these methodologies rely on harsh conditions and require the use of organometallic reagents, limiting their applicability in drug development with sensitive protecting groups, generally used in carbohydrate chemistry. In 2014, Gong *et al.* proposed a nickel-catalyzed reductive coupling of aliphatic carboxylic acids with glycosyl bromides under milder conditions (**Fig. 1.53**, B).[103]

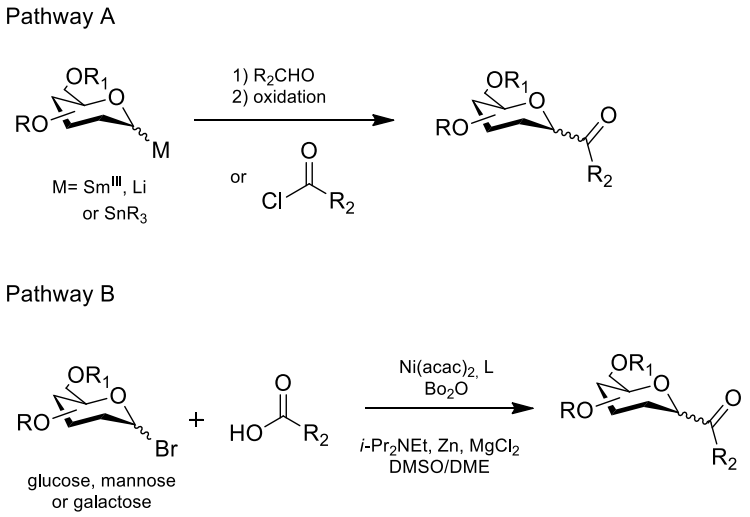

Fig. 1.53 Pathway A: addition of aldehydes or acylating agents to C1 glycosyl nucleophiles. Pathway B: Ni-catalysed reductive coupling of aliphatic acids with glycosyl bromides proposed by Gong et al.[103]

Very recently, Molander and co-workers have published a report proposing a practical and versatile route towards the acylation of highly functionalized *C*-acyl glycosides.[104] By utilizing a dual-catalytic Ni/photoredox system, they were able to employ a vast array of glycosyl based radicals that preserve the anomeric carbon up to the final stage of the synthesis (**Fig. 1.54**).

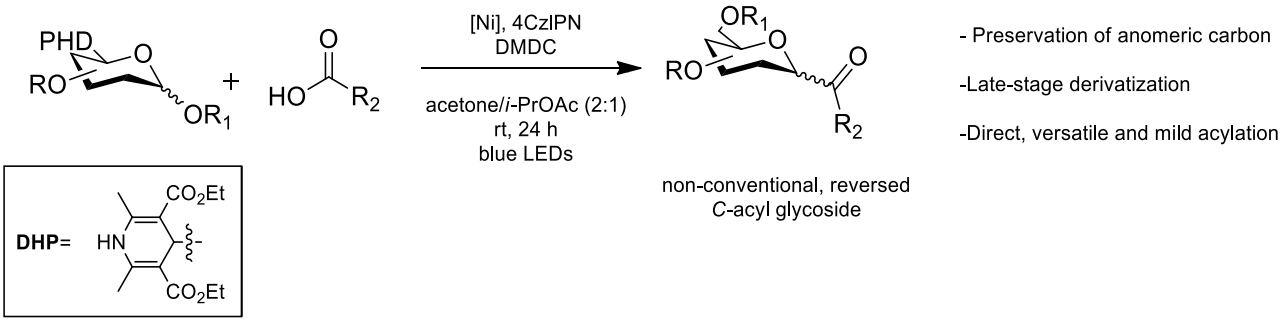

Fig. 1.54 Dual-catalytic Ni/photoredox system proposed by Molander et al.[104] for the acylation of highly functionalized non-anomeric *C*-acyl glycosides

Another type of *C*-glycosyl compounds of interest are the so called aryl *C*-glycosides: these molecules have been found as common structural motif in many bioactive natural products, imaging agents and glycoproteins.[105-106] Walczak and co-workers proposed a stereospecific cross-coupling reaction using a diaryliodonium triflate with glycosyl stannanes (**Fig. 1.55**).[107] This process, promoted by a palladium catalyst in the presence of a bulky phosphine ligand (JackiePhos), proceeds with an exclusive transfer of the anomeric configuration from the substrate to the product, thanks to the prerogative of configurationally stable C1 stannanes that promote a stereoretentive reaction.

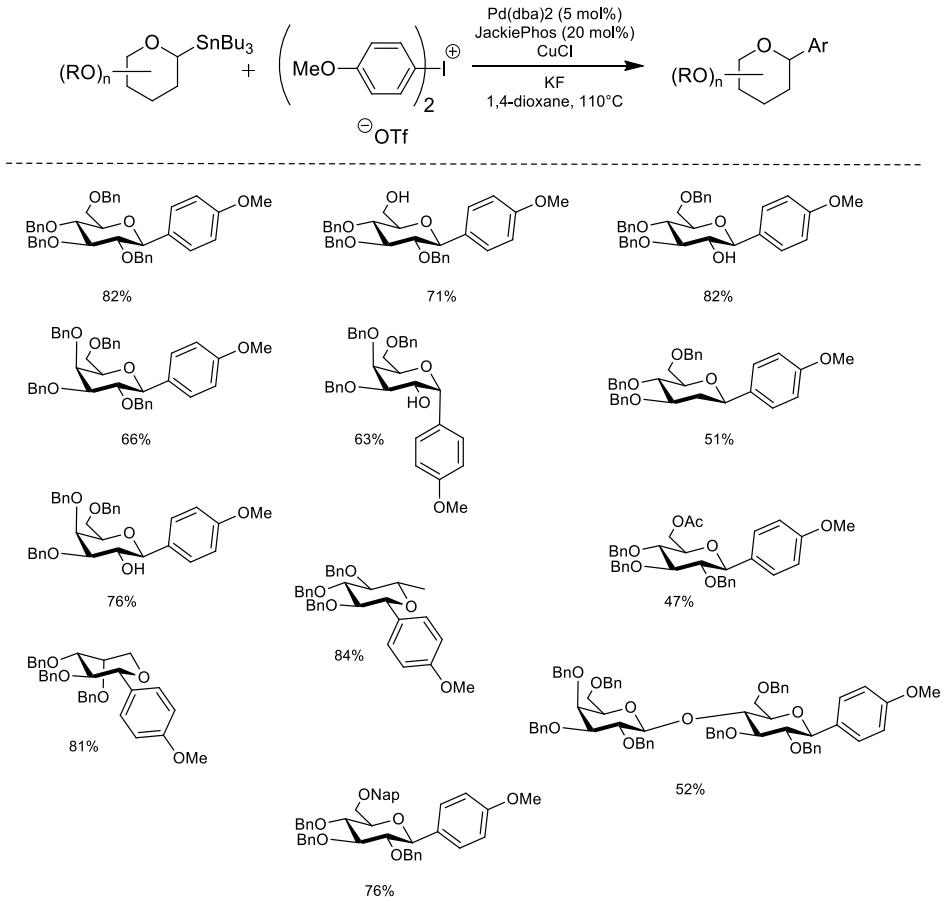

Fig. 1.55 The stereospecific cross-coupling reaction using a diaryliodonium triflate with glycosyl stannanes proposed by Walczak et al.[107] and the substrate scope

This methodology was then employed to examine a substrate scope (**Fig. 1.55**), where all the aryl *C*-glycosidic compounds were obtained in moderate to excellent yields with complete retention of the anomeric configuration.

1.3.2 *N*-glycosyl compounds

N-glycosides are a class of carbohydrate mimetics in which the anomeric oxygen is replaced by a nitrogen atom. Although such compounds are of great pharmaceutical interest, for example as anti-cancer agents,[108-109] almost all the reports present in the literature are about *N*-glycosidic linkages created between a sugar and an aglycon (often a peptide),[110-112] while synthetic methods for the synthesis of *N*-glycosidic bonds between two monosaccharide units remain scarce.

One of the most important contribution in this field came from the work of Renaudet and Dumy who developed in 2002 a stereoselective synthesis of β-*N*(OMe)-linked disaccharides using the Koenigs-Knorr method;[113] in the same year Pinto and colleagues described the preparation of *N*-linked disaccharides with a 4-thiogalactofuranosyl moiety.[114] Chemoselective ligation with oxime bond formation by *N*,*O*-disubstituted hydroxylamine reagents has also been used extensively.[115] This approach allows to connect the hydroxylamine directly to the aldehydic carbon of the sugar (generally unprotected), but it does not always allow to fully control the anomeric configuration of the product. More recently, glycosyl azides have been

used for the synthesis of *N*-glycosyl amides[116-117] and *N*-glycosyl triazoles.[118-119] *N*-glycosyl amides have also been obtained by direct glycosylation of carboxyamides.[120-121]

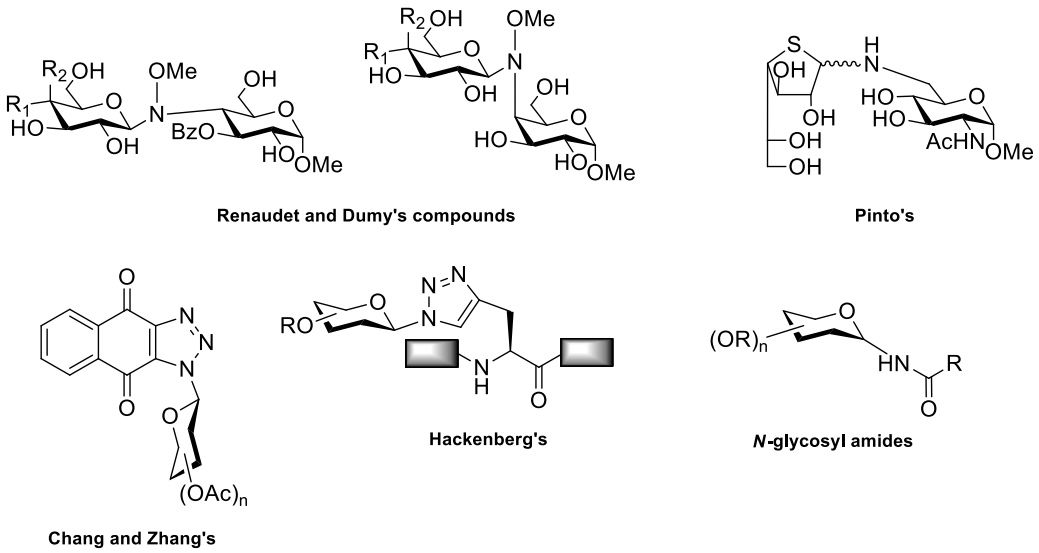

Fig. 1.56 Examples of *N*-glycosyl compounds

1.3.3 Selenoglycomimetics

Recently, another class of glycomimetics have raised great interest in the scientific community: selenoglycosides. They are known to possess various useful biological activities and thus they have been employed in the development of new carbohydrate-based drugs for anti-metastatic, anti-tumor[122-123] and immunostimulatory[124] therapeutic treatments (an example in **Fig. 1.57**).

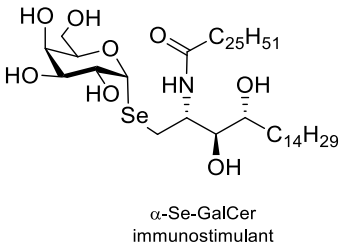

Fig. 1.57 An example of selenoglycomimetic used as immunostimulant

These compounds can be used also as tools for the investigation of sugar-protein interactions.[125-127]

From a synthetic point of view, selenoglycosides show a unique reactivity as glycosyl donors:[128] indeed, the C-Se bond can be readily ionized under photo-[129-131] and electro-chemical[132] conditions, generating very reactive cationic and radical-cationic species. However, the preparation of selenoglycosides involves major limitations, related to restricted substrate scope (e.g. unprotected sugars are not tolerated under the reaction conditions) and to the limited access to only one anomer.

Walczak and co-workers in 2018 proposed a stereoretentive preparation of *Se*-glycomimetics, through a stereospecific cross coupling process between anomeric stannanes and symmetrical diselenides that allow to obtain both the anomeric products (**Fig. 1.58**).[133]

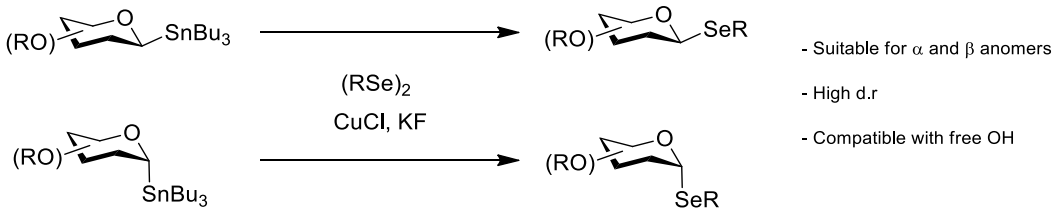

Fig. 1.58 Stereoretentive glycosyl cross-coupling proposed by Walczak and co-workers for the synthesis of *Se*-glycosides[133]

Anomeric stannanes represent configurationally stable nucleophiles that can be stored and manipulated under ambient conditions without loss of stereochemical integrity, even after extended periods of time (six months at room temperature or one year at -20°C). They can be easily prepared starting from the corresponding glycals, affording either 1,2-*cis* or 1,2-*trans,* thus allowing the formation of both the C(1) anomers.[107, 134-135]

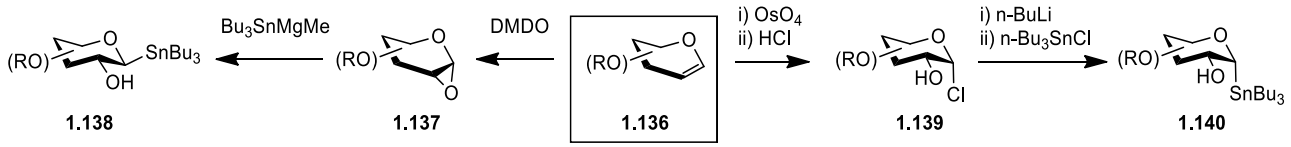

Fig. 1.59 Synthesis of configurationally stable anomeric stannanes

The preparation of the 1,2-*trans* anomer **1.138** (**Fig. 1.59**)**,** for example, starts from the epoxidation with dimethyldioxirane (DMDO) of the protected glycal **1.136** followed by ring opening by $Bu_3SnMgMe$. For the synthesis of the 1,2-*cis* stannane **1.140**, glycal **1.136** has to be converted into the α-chloride **1.139**, using HCl, and then exposed to a strong base (such as n-BuLi) to deprotonate the free hydroxyl group. Afterwards the resultant lithium alkoxide is treated at -100°C with lithium naphthalenide and finally quenched with Bu_3SnCl. This procedure allows the transfer of the configurational information from the α-chloride **1.139** to the corresponding anomeric stannane **1.140**.

At this point, glycosyl stannanes can be employed as nucleophilic species in the cross-coupling with symmetrical diselenides for the preparation of selenoglycosides. The proposed mechanism of this copper-catalysed process is reported below (**Fig. 1.60**):

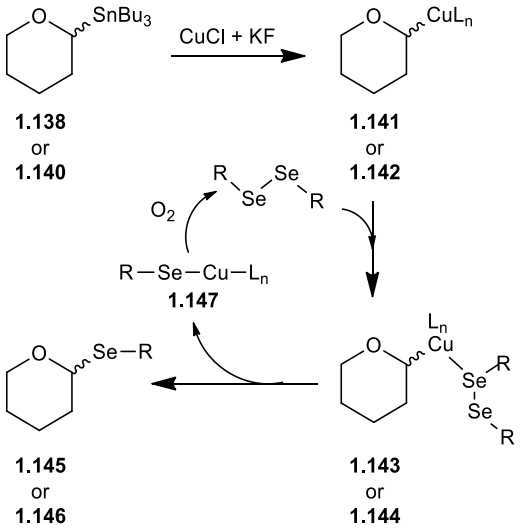

Fig. 1.60 Proposed mechanism for the cross-coupling between anomeric stannanes with symmetrical diselenides

Copper replaces the Sn-substituent generating the intermediate **1.41**/**1.42** that is configurationally stable at the C(1); it undergoes nucleophilic reaction with the diselenide, giving **1.43**/**1.44** and subsequently the seleno-copper by-product **1.147**. Under oxidative conditions **1.147** can be reconverted into the original diselenide $(RSe)_2$ which can enter again in the cycle. In this reaction, the presence of fluoride ions seem to facilitate the stereoretentive transmetalation from the nucleophile **1.138**/**1.140** to the copper, possibly the activation of the anomeric stannane that results in the formation of an insoluble Bu_3SnF by-product.

When the symmetric diselenide bears two sugar units, the cross-coupling reaction with the anomeric stannane generates an 1,1-selenodisaccharide. In particular, the retention of the configuration along all the process allows a perfect stereocontrol of the final product by the proper selection of the corresponding coupling partners. In **Fig. 1.61** are reported some examples as the proof of the concept.

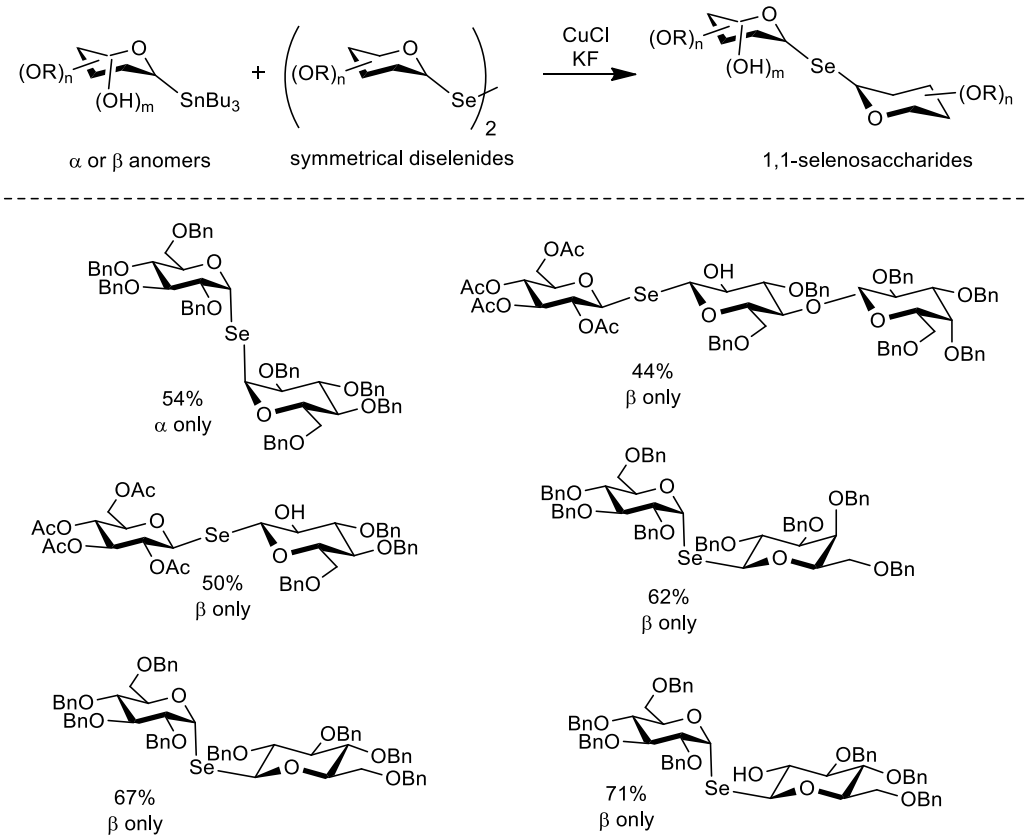

Fig. 1.61 Cross-coupling reaction between symmetric diselenides and anomeric stannanes to generate 1,1-selenosaccharides

Finally, the authors applied the same method to the synthesis of selenium-containing peptides. Below it is reported the cross-coupling between seleno-L-cysteine **1.148** and protected glycosyl stannanes that produced the corresponding selenocysteine glyconjugates in good yields (**Fig. 1.62**).

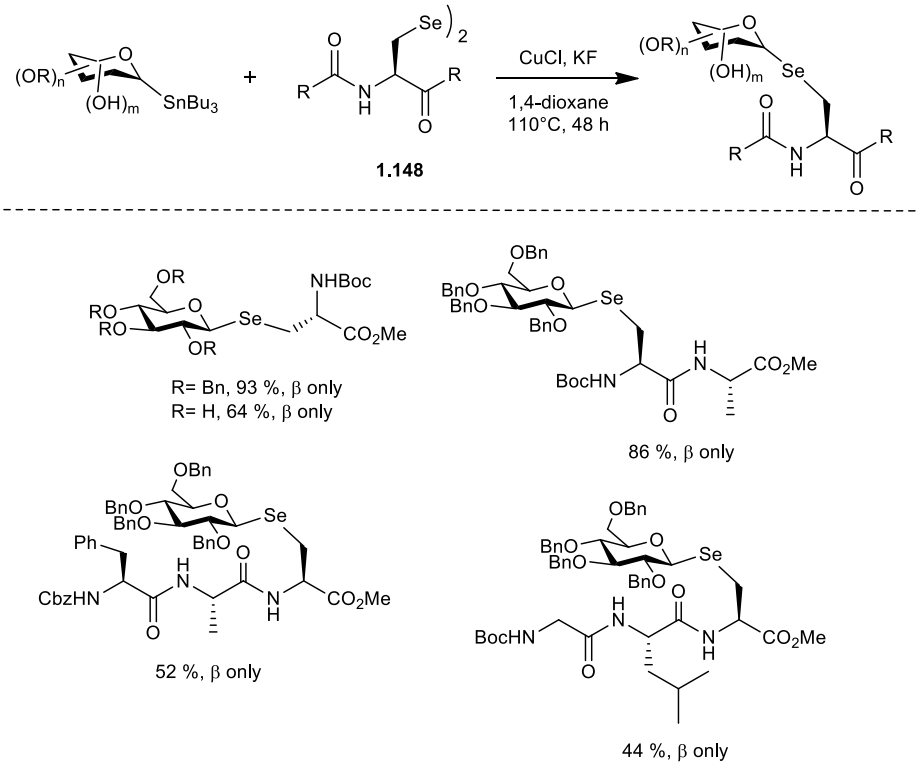

Fig. 1.62 Examples of stereospecific synthesis of selenoglycopeptides

These results represent the first example of stereospecific glycodiversification of selenopeptides with exclusive control of anomeric configuration and unprecedented functional-group tolerance.

1.3.4 Thioglycosides

The acidic and enzymatic sensitivity of *O*-glycosidic bonds stimulated the development of more stable glycosides, such as thio-linked oligosaccharides.

Belonging to the same group in the periodic table, oxygen and sulphur share similar bonding and geometries: indeed, although the C-S bond is longer than the corresponding C-O bond by about 0.4 Å, the C-S-C bond angle is smaller than the C-O-C angle, which renders thioglycosides conformationally similar to the corresponding *O*-glycosides, with a very small difference in the positions of the atoms along the glycosidic linkage. However, since sulphur is less basic than oxygen, the *S*-glycosidic linkage is typically more resistant toward both acid-catalyzed and enzymatic hydrolysis and thus thioglycosides are often competitive inhibitors of glycosidases and are considered promising molecules for the development of new therapeutics.[136] The higher stability of thioglycosides could be ascribed to the lower proton affinity of sulphur in comparison to *O*-glycosides. According to the Hard−Soft Acid−Base (HSAB) theory, sulphur behaves more like soft base while oxygen is a hard base; a hard acid like proton is thus prone to attack the hard base *O*-glycosides, not the soft base thioglycosides.[137]

Furthermore, sulphur is more nucleophilic than oxygen and thus it can allow simpler synthetic approaches for the construction of more complex systems.

Another property of thiodisaccharides, due again to the larger bond distance between carbon and sulphur, is their often enhanced conformational flexibility. Thus, thioglycosides can adapt their conformation to enable a better fit into the catalytic site of a receptor.[138-140] Indeed, their different conformational preferences compared to *O*-glycosides could influence their biological properties and often lead to more potent biological activity.

Thioglycosides can also be employed as donors in glycosylation reactions. Indeed, they can be activated under extremely mild conditions: numerous promoters have been developed and tested for the activation of alkyl/phenyl 1-thioglycosides for the construction of glycosidic linkages.[141] The promoters are molecules capable of generating thiophilic species and they can be classified as metal salts, halonium reagents, organosulphur reagents, single-electron-transfer reagents. Under classical glycosylation conditions, thioglycosides can also be employed as glycosylation acceptors when the alkyl/aryl-thio group serves as an anomeric group.

Another important advantage of this class of compounds is their easy accessibility: thioglycosides can be prepared from readily available starting materials, such as free sugars via peracetylation and subsequent treatment with thiols in a Lewis acid catalysed process. Moreover, unlike *O*-glycoside formation, the synthesis of *S*-linked glycosides can be achieved through S_N2 displacement of sugar halides by sugar thiolates.[142]

Another important property of these molecules concerns their configurational stability: anomeric thiolates, once formed, often retain their anomeric configuration in subsequent reactions.[143] Glycosyl thiols do not mutarotate easily, unless they are exposed to harsh conditions. However, although their compatibility with numerous protection/deprotection steps and with biological systems, it was demonstrated that 1-thioaldopyranoses undergo mutarotation in aqueous media in a pH dependent way.[144] In particular, this process proceeds at lower and neutral pH, while is slower or even blocked under basic conditions.

Working under controlled and mild conditions, their stability allows to perform stereoselective *S*-alkylation and thiol-ene or thiol-yne coupling processes, thanks to the retention of the anomeric configuration during synthetic transformations.

Despite all these valid reasons to promote the use of thioglycosides, they implicate an inevitable disadvantage: the very unpleasant odor of the starting thiols and of the resulting wastes. This point makes thioglycosides unfavourable alternatives in the large scale synthesis, especially in industrial applications.

As already mentioned above, most of these thioglycosides are prepared from glycosyl thiols (or 1-thio sugars) by alkylation,[145-150] conjugate-addition[151-152] or thiol-ene coupling reactions.[153-155]

1.3.4.1 Glycosyl thiols

The great utility and potential that glycosyl thiols have exhibited in carbohydrate chemistry brought great impetus to the development of procedures for their stereoselective preparation. In recent years, glycosyl thiols have become key building blocks for the construction of thio-oligosaccharides and *S*-glycoconjugates that often show increased chemo- and enzymatic stability and are tolerated by most biological systems. The

good affinity of glycosyl thiols towards gold also stimulated interest in their application as drugs (like auranofin).[156-157]

There are various methods available in literature for the preparation of glycosyl thiols.

The first methods have involved either the treatment of glycosyl halides with sulphur nucleophiles (such as thiourea[158-159] or potassium thioacetate) followed by hydrolysis,[160-162] or the conversion of the same halide **1.149** into a thioacetate group that finally underwent deacetylation by NaSMe[163] to give the thiol function at the anomeric position (**Fig. 1.63**).

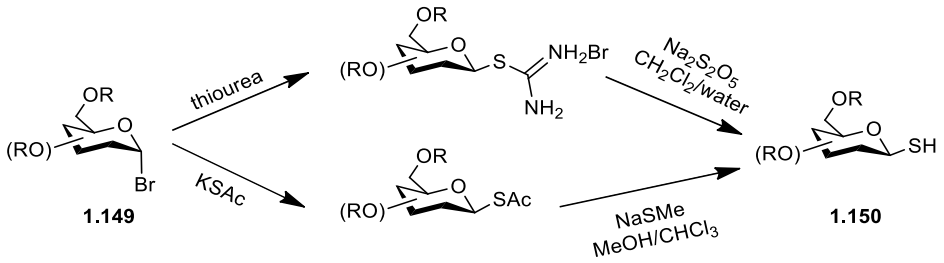

Fig. 1.63 Methods for the preparation of glycosyl thiols

In 2006, Davis *et al.* proposed a new procedure for the preparation glycosyl thiols where Lawesson reagent was employed.[164] In this process, considering how Lawesson's reagent (LR) works,[165-166] it was reasonable for the authors to believe that it could act as both oxaphilic electrophile and sulphur source. Previously, this reagent had found application in the conversion of benzylic alcohols into the corresponding thiols trough an S_N1 or S_N1-like pathway.[167-168] Taking into account the high reactivity of anomeric hydroxyl groups in S_N1-like processes, Davis and co-workers applied the same methodology for the preparation of anomeric thiols (**Fig. 1.64**).

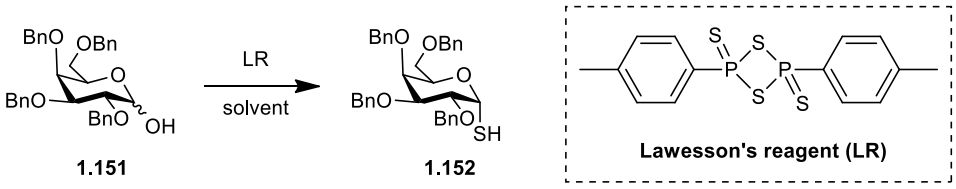

Fig. 1.64 Preparation of glycosyl thiol **1.152** by using Lawesson's reagent

The substrate scope was also investigated and it was demonstrated that this procedure is applicable for the preparation of a variety of differently protected 1-thiosugars, in good yields (>70 % in all the cases).

The same process was then investigated for unprotected sugars (**Fig. 1.65**): 1-thio-glucose, -mannose and -galactose were synthetized in moderate yields (60-70%). However, in these cases the purification and the subsequent isolation of the resulting thiols turned out to be very complex.

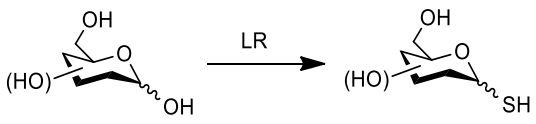

Fig. 1.65 Synthesis of glycosyl thiols using Lawesson's reagent, starting from unprotected sugars

Although this method allowed the direct formation of glycosyl thiols in a single step and in acceptable yields, it led to anomeric mixtures. Furthermore, besides the formation of the desired thiol, in almost all the cases also the generation of the corresponding disulphide side-products was observed as well. This and the presence of LR decomposition products in the reaction crude made the chromatographic purification step very complicated.

In 2011, Wang and co-workers reported the first direct stereospecific procedure for the preparation of α-glycosyl thiols starting from 1,6-anhydrosugars.[137] Their aim was to develop a method to selectively introduce a sulfhydryl group in the anomeric position with a specific configuration. The Wang's method consists in a ring opening reaction of the previously synthesized 1,6-anhydrosugars[169] using bis(trimethylsilyl)sulphide as a nucleophilic specie that, attacking from the less hindered side, and generating only α-thiols, since the β-face is blocked by the intramolecular dioxolane ring (**Fig. 1.66**).

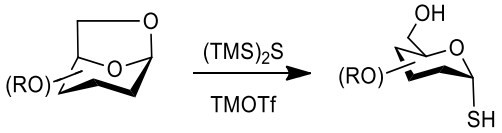

Fig. 1.66 Ring-opening reaction of 1,6-anhydrosugars proposed by Wang et al.[137] for the synthesis of α-glycosyl thiols

Finally, the trimethylsilyl group is cleaved *in situ* under glycosylation conditions (*e.g.* using TMSOTf).

The same procedure was then applied for the preparation of differently protected and even partially unprotected anhydrosugars, generating the corresponding α-thiols in good/excellent yields without observing the formation of the corresponding β-product.

A few years later (in 2015), a series of thio-α/β-D-mannose derivatives (**Fig. 1.67**) were synthesized by Wu and his team in order to investigate the role of the thiol group in different positions of the mannopyranose ring in binding affinity towards lectin Concavalin A (Con A).[170] These compounds were obtained using the strategy of protection/deprotection pattern and inversion (an example is reported below, **Fig. 1.67**, for the synthesis of the β-thio-mannopyranose **1.159**), while compound **1.158** can be readily obtained following the already known procedure. [171]

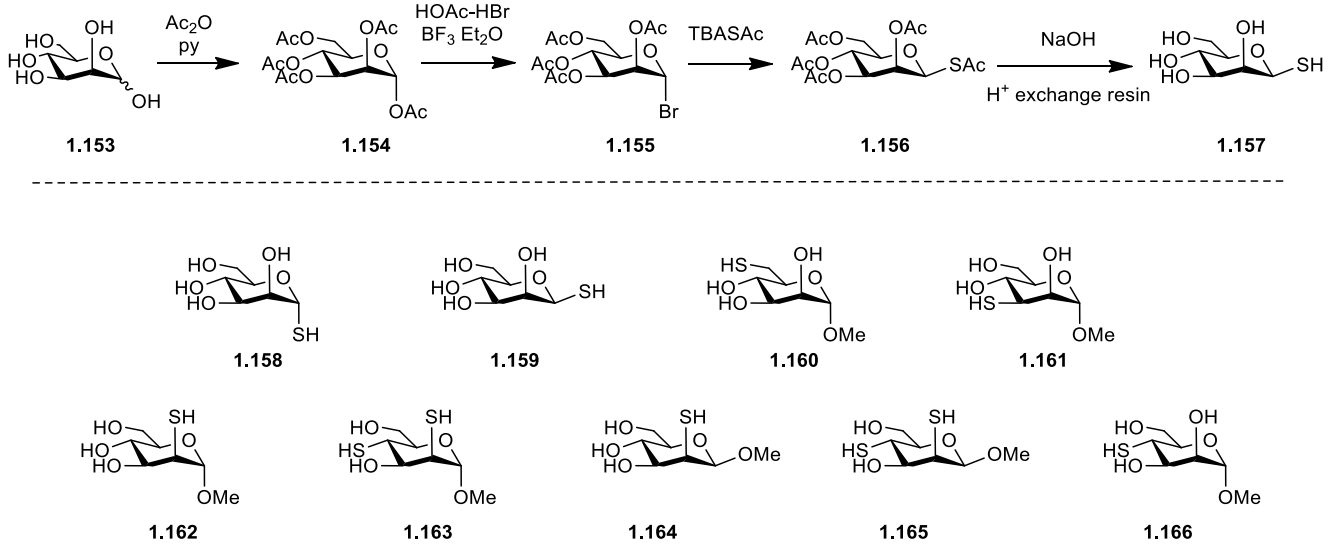

Fig. 1.67 Synthesis of 1-thio-α/β-D-mannopyranose **1.157**; the positional thio-α/β-D-mannose derivatives **1.158**-**1.166**

In the same year (2015), also the work of Shu and co-workers was published that reported a practical strategy toward the synthesis of glycosyl thiols by selective *S*-deacetylation reactions.[172] A few years ago, Misra's group also developed an expedient one-step pathway to β-glycosyl thiols by reaction of glycosyl bromides with CS_2 and $Na_2S_9{\cdot}H_2O$,[173-174] although some of the thioglycosides, contamined with impurities, resulted difficult to purify. Shu and his team instead proposed a method inspired by Native Chemical Ligation (NCL) to selective deacetylate anomeric thioacetates with absolute control of the anomeric configuration. The classical NCL involves a reversible trans-thio-esterification between a *C*-terminal peptidyl thioester and another peptide that presents an N-terminal cysteine residue (see **Fig. 1.68a**). This step is then followed by the irreversible shift of the acyl group from the sulphur to the nitrogen atom of cysteine, which generates a new peptide bond released at the same time the free thiol. The authors of this work applied the same strategy to the selective *S*-deacetylation of glycosyl thioacetates to produce glycosyl thiols.

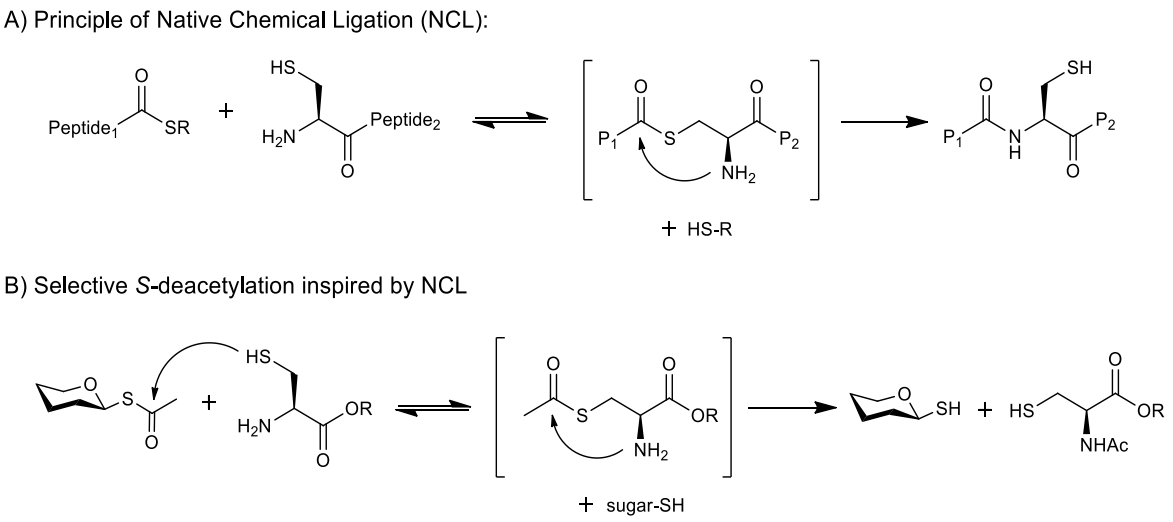

Fig. 1.68 Selective *S*-deacetylation reaction inspired by NCL proposed by Shu et al.

The precedure was optimized on the peracetylated thio-glycoside **1.167** (**Fig. 1.69**). In the presence of the cysteine methyl ester hydrochloride **III** (quenched by $NaHCO_3$), the reaction proceeded fast and the desired product was isolated in 95% yield together with N-acetyl cysteine.

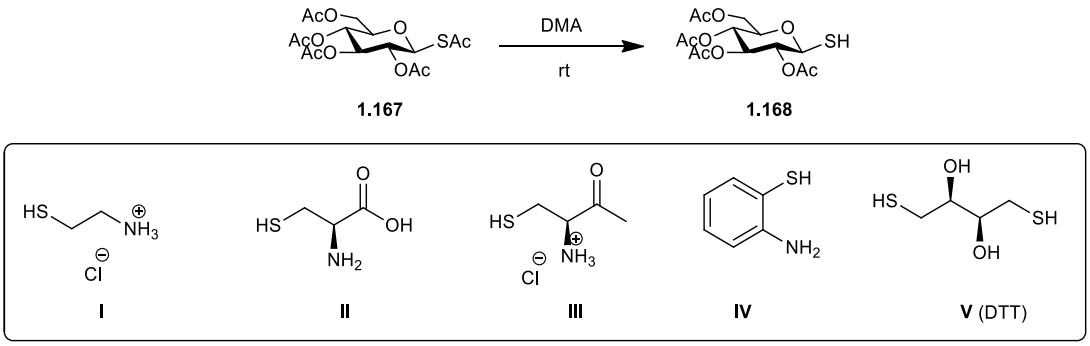

Fig. 1.69 Optimization of selective deacetylation reaction conditions

Considering that 1,4-dithiothreitol **V** (DTT) is often used as a scavenger in these reactions to limit the formation of the disulphide side product,[175-179] it was also tested in this reaction. DTT mediated the *S*-deacetylation through a *trans*-thio-esterification pathway that led the anomeric *S*-acetyl group to the sulphur atom of the DTT. Surprisingly, when DTT in stoichiometric amount was used in combination with $NaHCO_3$ the reaction still proceeded smoothly giving the desired deacetylated compound in 90% yield. Since the *trans*-thio-esterification step is reversible, in the optimized procedure DTT is used in excess. Furthermore, this process is favoured in a weak base environment: a catalytic amount of the base ($NaHCO_3$ or TEA) was proved crucial for the performance of the reaction. Dimethylacetamide (DMA) was the best solvent for this transformation, because it simplified the purification step (by a simple extraction with toluene the product is isolated without needing further purification). The authors described also a protocol to recover and regenerate DTT by simply another extraction followed by hydrolysis with K_2CO_3-MeOH. This procedure can facilitate the large-scale synthesis of glycosyl thiols (for an industrial application).

Finally, the reaction scope was investigated and various *S*-acetylated glycosides were employed to create a library of differently protected sugars bearing conformationally defined anomeric thiols (**Fig. 1.70**).

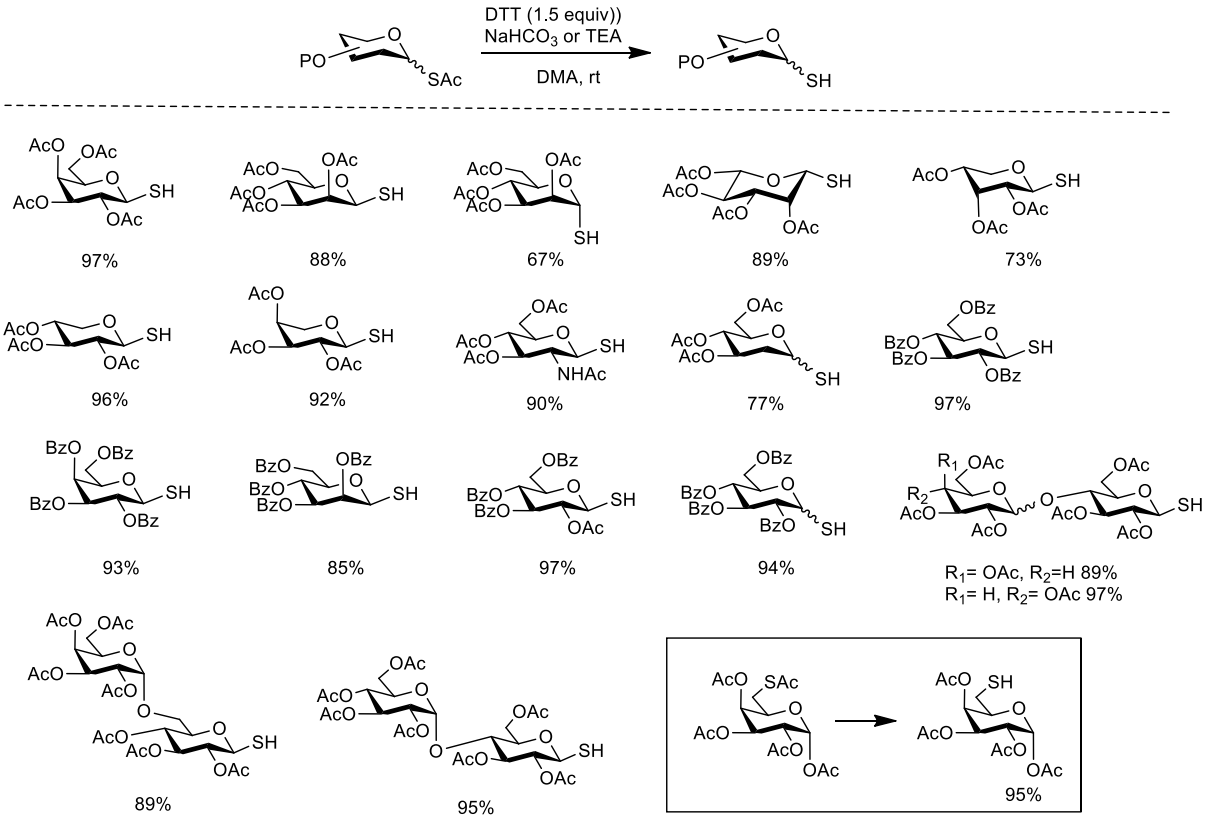

Fig. 1.70 Library of differently protected sugars bearing anomeric thiols synthesized starting from various *S*-acetylated glycosides

The configurations of the anomeric C-S bond was not altered during the process (β-*S*-acetylated sugars gave β-glycosyl thiols while the α-anomers gave the corresponding α-products).

This method was finally employed for the preparation of the building blocks necessary for the construction of the *S*-linked-trisaccharide **1.175** (**Fig. 1.71**).

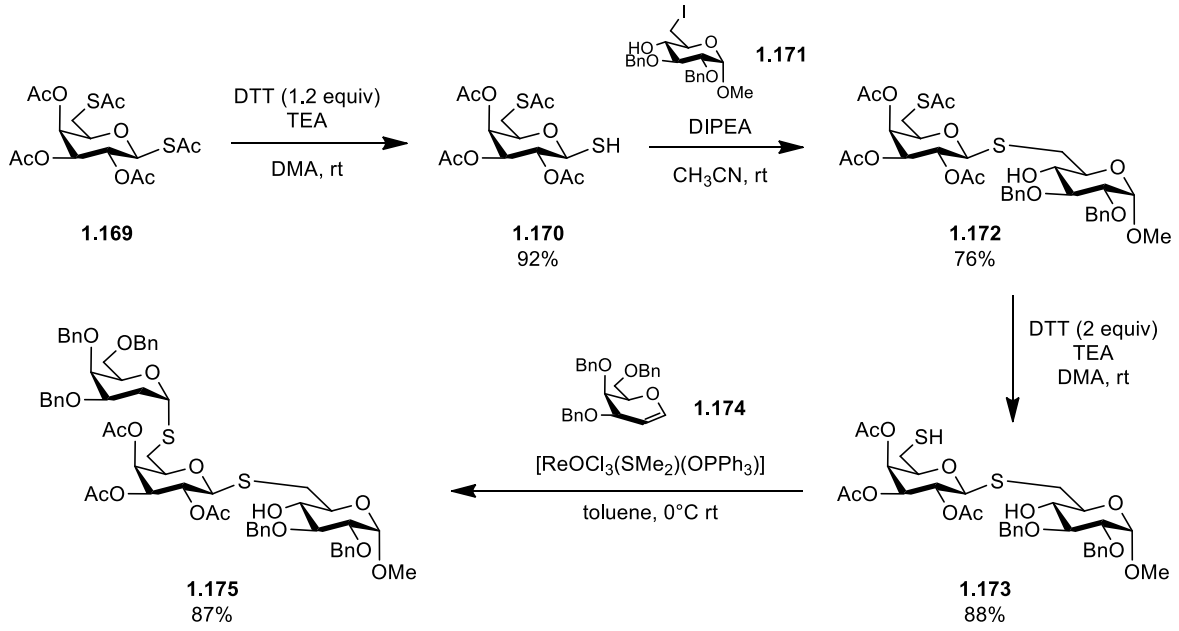

Fig. 1.71 Preparation of the *S*-linked-trisaccharide **1.175**

If on one hand 1-thiosugars are being extensively used in the construction of specific thiooligosaccharides and thiopeptides, on the other little attention has been devoted to their use for the preparation of (hetero)arylthioglycosides. Indeed, thioglycosides could be used as nucleophiles combined with transition metal-catalysts (**Fig. 1.72**), an approach that has been recently reviewed.[180]

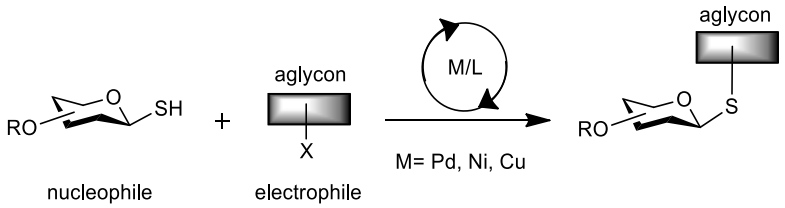

Fig. 1.72 Metal- catalyzed cross-coupling for the construction of functiolized thioglycosides

Among different examples reported, the Pd catalysed approach of Messaoudi and co-workers stands out as an efficient and stereoselective coupling of various unprotected and protected glycosyl thiols with aglycon halides in mild conditions, achieved employing G3-XantPhos as the precatalyst (**Fig. 1.73**).[181]

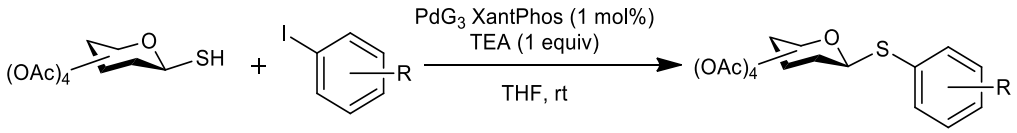

Fig. 1.73 Coupling of glycosyl thiols with aglycon halides by using G3-XantPhos as precatalyst

The reaction is versatile (various aryl, akenyl and alkynyl halides can be used), tolerates several functional groups (e.g. –Br, -OTs, -OH, -CN, -CO_2Me, -$CONR_2$, C(Me)=NNHTs) and it is reproducible up to a multigram-scale. The scope was then expanded to (1→2)-*S*-linked saccharides and *S*-linked glycoconjugates.[182] The same method was also applied to heteroaryl bis-glycosides, where *N*-glycosyl quinolin-2-ones (general structure reported in **Fig. 1.74**) in which a glycosyl unit is attached to a quinolin-2-one core (one of the most important heterocycle in medicinal chemistry).[183]

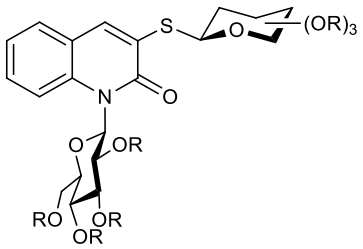

Fig. 1.74 General structure of *N*-glycosyl *S*-galactosyl quinoli-2-ones

In addition, the first use of PdG3-WantPhos in a tandem process for the synthesis of unsymmetrical biaryles thioglycosides was recently described by the same group.[184] The procedure consists of using a single Pd-catalyst which promotes under the same catalytic cycle, the catalysis of two individual steps: the first is a selective coupling reaction between β-thiosugars and di-halogenated arenes (iodo-bromoarenes); the

second is based on C-C bond formation between the mono-halogenated thioglycoside intermediate and diverse aryl boronic acids (**Fig. 1.75**).

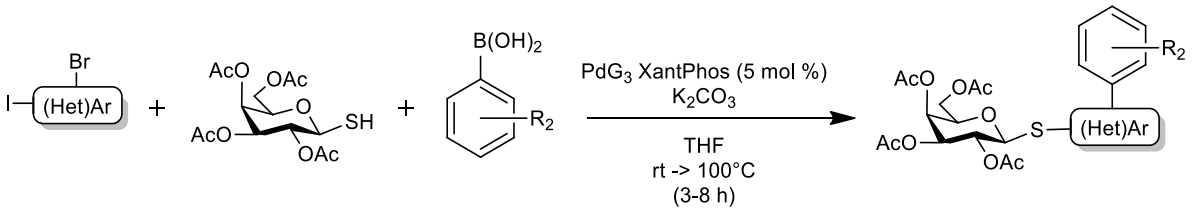

Fig. 1.75 First use of PdG3-WantPhos for the synthesis of unsymmetrical biaryles thioglycosides

This procedure showed for the first time the use of PdG3-XantPhos in a multicomponent process under mild conditions and it represented one of the most robust methods developed so far in the thioglycoconjugation chemistry that could be further explored for range of medicinal chemistry screening programmes.

1.3.4.2 S-linked oligosaccharides

As mentioned before, glycosyl thiols represent the main building blocks used for the construction of *S*-linked saccharides.

In 2012, Marra and Dondoni exploited the thiol-ene coupling reaction for the synthesis of *S*-disaccharides.[155] The figure below (**Fig. 1.76**) shows the reaction between tetra-*O*-acetyl 1-thio-β-*D*-glucose **1.168** and sugar alkenes **1.176**, **1.78** and **1.180**: these reactions occurr at room temperature under UV irradiation at λ_{max} 365 nm, using 2,2-dimethoxy-2-phenylacetophenone (DPAP) as initiator, affording **1.177**, **1.179** and **1.181** that are the corresponding isosteres of 1,6- and 1,5-linked natural *O*-disaccharides, respectively.

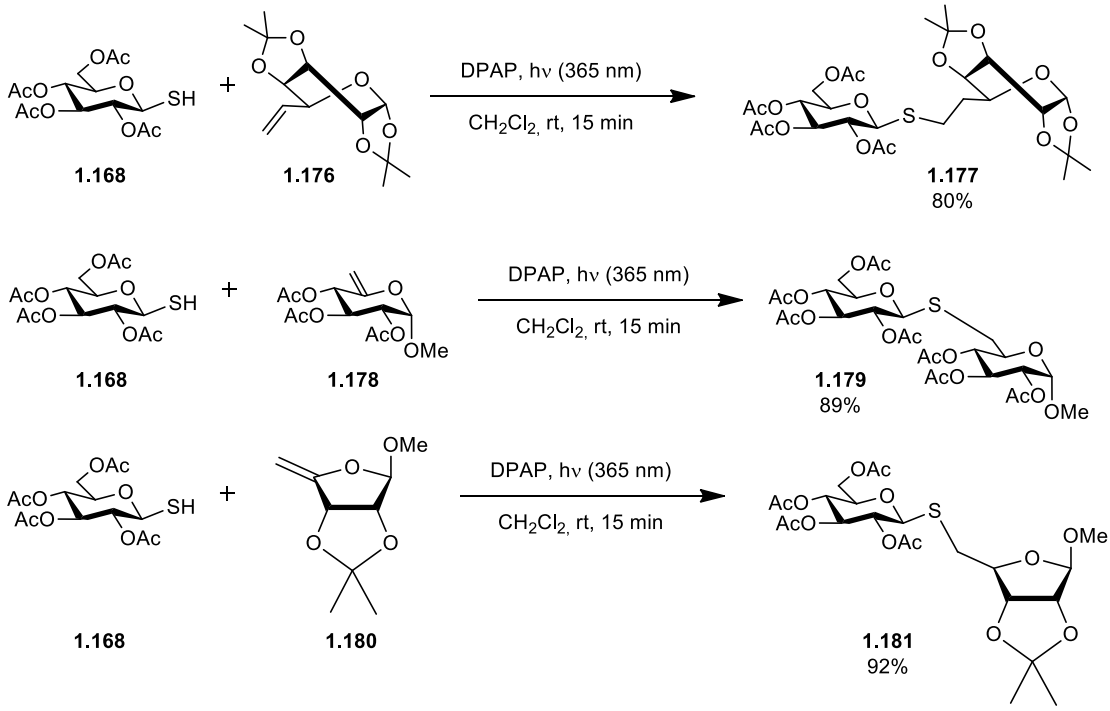

Fig. 1.76 Examples of thiol-ene coupling between sugar thiols and sugar alkenes

The same process was then applied for the construction of *S*-linked glycopeptides (**Fig. 1.77**).

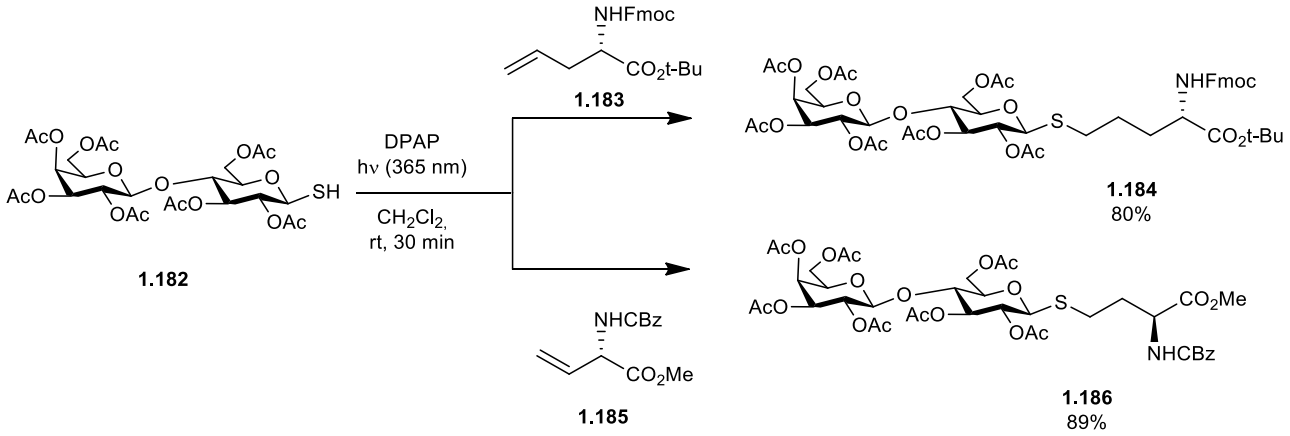

Fig. 1.77 Synthesis of alkyl-tethered *S*-lactosyl glycosides

In 2016 Belz and co-workers proposed a practical synthesis of *S*-linked glycosides achieved through S_N2 displacement of sugar halides by sugar thiolates.[185] This procedure allowed to avoid the isolation of the often unstable corresponding thiol compound.

Two different approaches were proposed by Belz's group for this process: the first requires an initial insertion of the mercapto group into the glycosyl acceptor, with the leaving group on the glycosyl donor (or viceversa) and it is for sure the most convenient for the synthesis of β-linked compounds (as α-glycosyl halides can be readily prepared). The second one is based on the configurational stability of anomeric thiolates. This strategy is applied for α-linked *S*-glycosides, installing the sulphur atom into the glycosyl donor with stereochemical control at the building block stage.

Belz's work focused in particular on the preparation of *S*-linked α-1,6-oligomannosides. Disaccharide **1.189** is obtained thorugh the coupling of iodide **1.187** and thioacetate **1.188** (**Fig. 1.78**) in the presence of diethylamine in dimethylformamide.

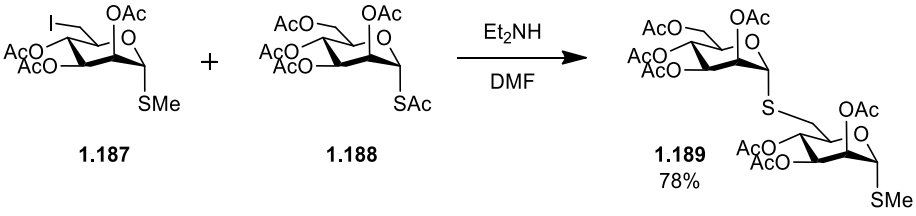

Fig. 1.78 Preparation of *S*-linked α-1,6-oligomannoside **1.189**

The α-mercapto precursor of **1.187** is the isothiouronium bromide **1.188**[186] that was treated with MeI/Et_3N in acetonitrile to afford the corresponding thiomethyl glycoside **1.189** (**Fig. 1.79**). Finally, the deacetylation under Zemplén conditions, followed by iodination using I_2, PPh_3, imidazole and acetylation gave the iodide **1.187**.

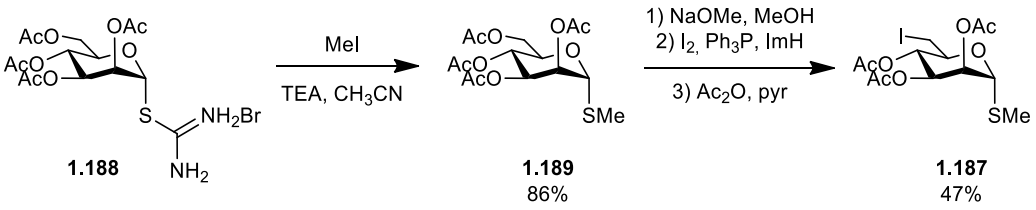

Fig. 1.79 Synthesis of the iodide α-mercapto compound **1.187**

The temporary protection of the anomeric sulphur allowed the nucleophilic S-glycoside formation. Afterwards the latent thiolate precursor can be release to perform the subsequent coupling reaction.

In summary...

This overview about the state of the art of glycomimetics highlights the strong interest that these structures have raised in the last decades. Although the efforts of the scientific community spent to develope and propose increasingly innovative synthetic procedures for the preparation of sugar mimics, the majority of them still require multiple steps, complicate reaction conditions that must to be under careful control, sometimes expensive and also sensitive reagents. Furthermore, most of the procedures reported so far describe the synthesis of mono-saccharide mimics, while, for the preparation of oligosaccharide structures, the standard glycosylation protocol is still applied, with all its drawbacks and difficulties.

My PhD project takes place in this scenario with the aim to design a new class of glycomimetic compounds, accessible through a simple and straightforward synthesis involving few steps. With this goal, we started from a specific model: the Manα(1,2)Man disaccharide, a natural ligand for DC-SIGN.

1.4 References

1) R. Apweiler; H. Hermjakob; N. Sharon, *Biochimica et Biophysica Acta (BBA) - General Subjects* **1999**, *1473*, 4-8.
2) T. Wennekes; R. J. van den Berg; R. G. Boot; G. A. van der Marel; H. S. Overkleeft; J. M. Aerts, *Angew Chem Int Ed Engl* **2009**, *48*, 8848-69.
3) J. W. VanTeeffelen; J. Brands; E. S. Stroes; H. Vink, *Trends in Cardiovascular Medicine* **2007**, *17*, 101-105.
4) M. Nieuwdorp; M. C. Meuwese; H. L. Mooij; C. Ince; L. N. Broekhuizen; J. J. Kastelein; E. S. Stroes; H. Vink, *J Appl Physiol (1985)* **2008**, *104*, 845-52.
5) C. R. Bertozzi; L. L. Kiessling, *Science* **2001**, *291*, 2357-64.
6) R. S. Haltiwanger; J. B. Lowe, *Annu Rev Biochem* **2004**, *73*, 491-537.
7) K. Ohtsubo; J. D. Marth, *Cell* **2006**, *126*, 855-867.
8) Y. van Kooyk; G. A. Rabinovich, *Nature Immunology* **2008**, *9*, 593.
9) J. E. Hudak; C. R. Bertozzi, *Chem Biol* **2014**, *21*, 16-37.
10) A. García-Herrero; E. Montero; J. L. Muñoz; J. F. Espinosa; A. Vián; J. L. García; J. L. Asensio; F. J. Cañada; J. Jiménez-Barbero, *Journal of the American Chemical Society* **2002**, *124*, 4804-4810.
11) G. Horne; F. X. Wilson; J. Tinsley; D. H. Williams; R. Storer, *Drug Discovery Today* **2011**, *16*, 107-118.
12) A. Naoki, *Current Topics in Medicinal Chemistry* **2003**, *3*, 471-484.
13) A. E. Stütz; T. M. Wrodnigg, *Chapter 4 - Imino sugars and glycosyl hydrolases: Historical context, current aspects, emerging trends*, Horton, D., Ed. Academic Press: **2011**; *66*, 187-298.
14) P. Compain; O. R. Martin *Iminosugars: From Synthesis to Therapeutic Applications*, Wiley, New York: **2007**.
15) R. Lahiri; A. A. Ansari; Y. D. Vankar, *Chemical Society Reviews* **2013**, *42*, 5102-5118.
16) A. Ferry; G. Malik; X. Guinchard; V. Vetvicka; D. Crich, *J Am Chem Soc* **2014**, *136*, 14852-7.
17) R. Zelli; J.-F. Longevial; P. Dumy; A. Marra, *New Journal of Chemistry* **2015**, *39*, 5050-5074.

18) S. Sattin; A. Bernardi, *Design and synthesis of glycomimetics*, **2015**; 1-25.
19) J. Paszkowska; O. N. Fernandez; I. Wandzik; S. Boudesoque; L. Dupont; R. Plantier-Royon; J.-B. Behr, *Eur. J. Org. Chem.* **2015**, *2015*, 1198-1202.
20) F. Massicot; R. Plantier-Royon; J. L. Vasse; J. B. Behr, *Carbohydr Res* **2018**, *464*, 2-7.
21) B. Lopez-Mendez; C. Jia; Y. Zhang; L. H. Zhang; P. Sinay; J. Jimenez-Barbero; M. Sollogoub, *Chem Asian J* **2008**, *3*, 51-8.
22) G. E. McCasland; M. O. Naumann; L. J. Durham, *The Journal of Organic Chemistry* **1966**, *31*, 3079-3089.
23) L. Cipolla; B. La Ferla; C. Airoldi; C. Zona; A. Orsato; N. Shaikh; L. Russo; F. Nicotra, *Future Med Chem* **2010**, *2*, 587-99.
24) S. Ogawa; N. Chida; T. Suami, *Chemistry Letters* **1980**, *9*, 1559-1562.
25) S. Ogawa; H. Shibata; T. Nose; t. Suami, *Bull Chem Soc Jpn* **1985**, *58*, 3387.
26) Odon Arjona; Ana M. Gomez; J. Cristobal Lopez; J. Plumet, *Chem. Rev.* **2007**, *107*, 1919-2036.
27) S. Roscales; J. Plumet, *International Journal of Carbohydrate Chemistry* **2016**, *2016*, 1-42.
28) R. J. Ferrier; S. Middleton, *Chemical Reviews* **1993**, *93*, 2779-2831.
29) A. J. Pearce; M. Sollogoub; J.-M. Mallet; P. Sinaÿ, *Eur. J. Org. Chem.* **1999**, *1999*, 2103-2117.
30) D. H. Mac; R. Samineni; J. Petrignet; P. Srihari; S. Chandrasekhar; J. S. Yadav; R. Grée, *Chemical Communications* **2009**, 4717-4719.
31) P. Joaquin; M. G. Ana; J. C. Lopez, *Mini-Reviews in Organic Chemistry* **2007**, *4*, 201-216.
32) Y. J. Lee; K. Lee; S. I. Jung; H. B. Jeon; K. S. Kim, *Tetrahedron* **2005**, *61*, 1987-2001.
33) D. Matzner; A. Schuller; T. Seitz; V. Wittmann; G. Mayer, *Chemistry* **2017**, *23*, 12604-12612.
34) R. J. Ferrier, *Journal of the Chemical Society, Perkin Transactions 1* **1979**, 1455-1458.
35) V. K. Harit; N. G. Ramesh, *J Org Chem* **2016**, *81*, 11574-11586.
36) R. V. Salunke; N. G. Ramesh, *Eur. J. Org. Chem.* **2016**, *2016*, 654-657.
37) J. E. McMurry; N. O. Siemers, *Tetrahedron Letters* **1993**, *34*, 7891-7894.
38) N. Akiyama; S. Noguchi; M. Hashimoto, *Bioscience, Biotechnology, and Biochemistry* **2011**, *75*, 1380-1382.
39) T. J. M. Beenakker; D. P. A. Wander; J. D. C. Codée; J. M. F. G. Aerts; G. A. van der Marel; H. S. Overkleeft, *European Journal of Organic Chemistry* **2018**, *2018*, 2504-2517.
40) T. Ye; M. A. McKervey, *Chemical Reviews* **1994**, *94*, 1091-1160.
41) A. Caballero; A. Prieto; M. M. Díaz-Requejo; P. J. Pérez, *Eur. J. Inorg. Chem.* **2009**, *2009*, 1137-1144.
42) C. Colombo; B. M. Pinto; A. Bernardi; A. J. Bennet, *Organic & Biomolecular Chemistry* **2016**, *14*, 6539-6553.
43) C. Colombo; C. Podlipnik; L. Lo Presti; M. Niikura; A. J. Bennet; A. Bernardi, *PLoS One* **2018**, *13*, e0193623.
44) M. von Itzstein; W.-Y. Wu; G. B. Kok; M. S. Pegg; J. C. Dyason; B. Jin; T. Van Phan; M. L. Smythe; H. F. White; S. W. Oliver; P. M. Colman; J. N. Varghese; D. M. Ryan; J. M. Woods; R. C. Bethell; V. J. Hotham; J. M. Cameron; C. R. Penn, *Nature* **1993**, *363*, 418.
45) V. Bordoni; V. Porkolab; S. Sattin; M. Thépaut; I. Frau; L. Favero; P. Crotti; A. Bernardi; F. Fieschi; V. Di Bussolo, *RSC Advances* **2016**, *6*, 89578-89584.
46) A. V. R. L. Sudha; M. Nagarajan, *Chemical Communications* **1998**, 925-926.
47) I. Robina; P. Vogel; Z. J. Witczak, *Current Organic Chemistry* **2001**, *5*, 1177-1214.
48) Z. J. Witczak, *Curr Med Chem* **1999**, *6*, 165-178.
49) P. Greimel; J. Spreitz; F. K. Sprenger; A. E. Stutz; T. M. Wrodnigg, *Org. Chem. Sugars* **2006**, 383.
50) Z. J. Witczak; J. M. Culhane, *Applied Microbiology and Biotechnology* **2005**, *69*, 237-244.
51) E. Scanlan; V. Corcé; A. Malone, *Molecules* **2014**, *19*, 19137.
52) L. McSweeney; F. Dénès; E. M. Scanlan, *European Journal of Organic Chemistry* **2016**, *2016*, 2080-2095.
53) V. Corce; L. McSweeney; A. Malone; E. M. Scanlan, *Chem Commun (Camb)* **2015**, *51*, 8672-4.
54) R. S. Edmundson, *Chemical Properties and Reactions of Phosphine Chalcogenides*, **1992**; 287-407.
55) J. Hernández; R. Ramos; N. Sastre; R. Meza; H. Hommer; M. Salas; B. Gordillo, *Tetrahedron* **2004**, *60*, 10927-10941.
56) W. S. Wadsworth; W. D. Emmons, *Journal of the American Chemical Society* **1962**, *84*, 610-617.
57) J.-N. Volle; D. Virieux; M. Starck; J. Monbrun; L. Clarion; J.-L. Pirat, *Tetrahedron: Asymmetry* **2006**, *17*, 1402-1408.
58) H. Y. T. Hanaya, *Helvetica Chimica Acta* **2002**, *82*, 2608-2618.

59) T. Hanaya; K.-i. Sugiyama; H. Kawamoto; H. Yamamoto, *Carbohydrate Research* **2003**, *338*, 1641-1650.
60) M. K. Tadashi Hanaya, Masakazu Sumi, Kazuo Makino,; H. Y. Keiko Tsukada, *Heterocycles* **2012**, *82*, 1147-1165.
61) O. R. Stephen Hanessian, *Bioorganic & Medicinal Chemistry Letters* **1999**, *9*, 2441-2446.
62) K. Kitagishi; K. Hiromi, *The Journal of Biochemistry* **1984**, *95*, 529-534.
63) K. Matsumaru; H. Kashimura; M. Hassan; A. Nakahara; K. Goto; H. Fukutomi; H. Muto; N. Tanaka, *Life Sciences* **1998**, *62*, PL79-PL84.
64) H. S. El Khadem; D. L. Swartz; J. K. Nelson; L. A. Berry, *Carbohydrate Research* **1977**, *58*, 230-234.
65) V. S. Abramov, *Zh. Obshch. Khim* **1957**, *22*, 647.
66) D. B. Berkowitz; M. Eggen; Q. Shen; R. K. Shoemaker, *The Journal of Organic Chemistry* **1996**, *61*, 4666-4675.
67) R. Hirschmann; K. M. Yager; C. M. Taylor; J. Witherington; P. A. Sprengeler; B. W. Phillips; W. Moore; A. B. Smith, *Journal of the American Chemical Society* **1997**, *119*, 8177-8190.
68) R. Hirschmann; K. M. Yager; C. M. Taylor; W. Moore; P. A. Sprengeler; J. Witherington; B. W. Phillips; A. B. Smith, III, *Journal of the American Chemical Society* **1995**, *117*, 6370-6371.
69) A. W. Diana S. Stoianova, and Paul R. Hanson, *J. Org. Chem.* **2005**, *70*, 5880-5889.
70) H.-J. Cristau; J. Monbrun; J. Schleiss; D. Virieux; J.-L. Pirat, *Tetrahedron Letters* **2005**, *46*, 3741-3744.
71) K. Afarinkia; H.-w. Yu, *Tetrahedron Letters* **2003**, *44*, 781-783.
72) L. Clarion; C. Jacquard; O. Sainte-Catherine; S. Loiseau; D. Filippini; M. H. Hirlemann; J. N. Volle; D. Virieux; M. Lecouvey; J. L. Pirat; N. Bakalara, *J Med Chem* **2012**, *55*, 2196-211.
73) Z. Hassani; A. Saleh; S. Turpault; S. Khiati; W. Morelle; J. Vignon; J. P. Hugnot; E. Uro-Coste; P. Legrand; M. Delaforge; S. Loiseau; L. Clarion; M. Lecouvey; J. N. Volle; D. Virieux; J. L. Pirat; H. Duffau; N. Bakalara, *Mol Cancer Res* **2017**, *15*, 1376-1387.
74) R. Babouri; L. Clarion; M. Rolland; A. Van der Lee; Z. Kabouche; J.-N. Volle; D. Virieux; J.-L. Pirat, *European Journal of Organic Chemistry* **2017**, *2017*, 5357-5369.
75) L. Clarion; C. Jacquard; O. Sainte-Catherine; M. Decoux; S. Loiseau; M. Rolland; M. Lecouvey; J.-P. Hugnot; J.-N. Volle; D. Virieux; J.-L. Pirat; N. Bakalara, *Journal of Medicinal Chemistry* **2014**, *57*, 8293-8306.
76) R. Babouri; M. Rolland; O. Sainte-Catherine; Z. Kabouche; M. Lecouvey; N. Bakalara; J.-N. Volle; D. Virieux; J.-L. Pirat, *European Journal of Medicinal Chemistry* **2015**, *104*, 33-41.
77) S. Feng; C. Bagia; G. Mpourmpakis, *J Phys Chem A* **2013**, *117*, 5211-9.
78) D. Filippini; S. Loiseau; N. Bakalara; Z. A. Dziuganowska; A. Van der Lee; J.-N. Volle; D. Virieux; J.-L. Pirat, *RSC Adv.* **2012**, *2*, 816-818.
79) E. A. Mensah; J. M. Azzarelli; H. M. Nguyen, *The Journal of Organic Chemistry* **2009**, *74*, 1650-1657.
80) K. L. Kirk, *Journal of Fluorine Chemistry* **2006**, *127*, 1013-1029.
81) E. Prchalová; O. Štěpánek; S. Smrček; M. Kotora, *Future Med Chem* **2014**, *6*, 1201-1229.
82) A. Baumann; S. Marchner; M. Daum; A. Hoffmann-Röder, *European Journal of Organic Chemistry* **2018**, *2018*, 3803-3815.
83) B. Xu; L. Unione; J. Sardinha; S. Wu; M. Etheve-Quelquejeu; A. Pilar Rauter; Y. Bleriot; Y. Zhang; S. Martin-Santamaria; D. Diaz; J. Jimenez-Barbero; M. Sollogoub, *Angew Chem Int Ed Engl* **2014**, *53*, 9597-602.
84) L. Unione; B. Xu; D. Diaz; S. Martin-Santamaria; A. Poveda; J. Sardinha; A. P. Rauter; Y. Bleriot; Y. Zhang; F. J. Canada; M. Sollogoub; J. Jimenez-Barbero, *Chemistry* **2015**, *21*, 10513-21.
85) H. Chen; Z. Hu; J. Zhang; G. Liang; B. Xu, *Tetrahedron* **2015**, *71*, 2089-2094.
86) A. Ardèvol; X. Biarnés; A. Planas; C. Rovira, *Journal of the American Chemical Society* **2010**, *132*, 16058-16065.
87) J. Angulo; P. M. Nieto; M. Martín-Lomas, *Chemical Communications* **2003**, 1512-1513.
88) X. Biarnés; A. Ardèvol; A. Planas; C. Rovira; A. Laio; M. Parrinello, *Journal of the American Chemical Society* **2007**, *129*, 10686-10693.
89) E. Säwén; M. U. Roslund; I. Cumpstey; G. Widmalm, *Carbohydrate Research* **2010**, *345*, 984-993.
90) B. M. Sattelle; B. Bose-Basu; M. Tessier; R. J. Woods; A. S. Serianni; A. Almond, *The Journal of Physical Chemistry B* **2012**, *116*, 6380-6386.
91) W. C. Winkler; A. Nahvi; A. Roth; J. A. Collins; R. R. Breaker, *Nature* **2004**, *428*, 281.

92) A. Schuller; D. Matzner; C. E. Lunse; V. Wittmann; C. Schumacher; S. Unsleber; H. Brotz-Oesterhelt; C. Mayer; G. Bierbaum; G. Mayer, *Chembiochem* **2017**, *18*, 435-440.
93) D. Enders; S. Faure; M. Potthoff; J. Runsink, *Synthesis* **2001**, *2001*, 2307-2319.
94) I. Tvaroška; T. Bleha, *Anomeric and Exo-Anomeric Effects in Carbohydrate Chemistry*, Tipson, R. S.; Horton, D., Eds. Academic Press: **1989**; *47*, 45-123.
95) Y. Yang; B. Yu, *Chem Rev* **2017**, *117*, 12281-12356.
96) Q. Wu; J.-G. Cho; D.-S. Lee; D.-Y. Lee; N.-Y. Song; Y.-C. Kim; K.-T. Lee; H.-G. Chung; M.-S. Choi; T.-S. Jeong; E.-M. Ahn; G.-S. Kim; N.-I. Baek, *Carbohydrate Research* **2013**, *372*, 9-14.
97) W. Disadee; C. Mahidol; P. Sahakitpichan; S. Sitthimonchai; S. Ruchirawat; T. Kanchanapoom, *Phytochemistry* **2012**, *74*, 115-122.
98) Y. Geng; A. Kumar; H. M. Faidallah; H. A. Albar; I. A. Mhkalid; R. R. Schmidt, *Bioorganic & Medicinal Chemistry* **2013**, *21*, 4793-4802.
99) D. Mazéas; T. Skrydstrup; J.-M. Beau, *Angew Chem Int Ed* **1995**, *34*, 909-912.
100) Y. Y. Belosludtsev; R. K. Bhatt; J. R. Falck, *Tetrahedron Letters* **1995**, *36*, 5881-5882.
101) N. E. S. Guisot; I. Ella Obame; P. Ireddy; A. Nourry; C. Saluzzo; G. Dujardin; D. Dubreuil; M. Pipelier; S. Guillarme, *The Journal of Organic Chemistry* **2016**, *81*, 2364-2371.
102) A. Dondoni; N. Catozzi; A. Marra, *The Journal of Organic Chemistry* **2005**, *70*, 9257-9268.
103) C. Zhao; X. Jia; X. Wang; H. Gong, *Journal of the American Chemical Society* **2014**, *136*, 17645-17651.
104) S. O. Badir; A. Dumoulin; J. K. Matsui; G. A. Molander, *Angew Chem Int Ed Engl* **2018**, *57*, 6610-6613.
105) T. Bililign; B. R. Griffith; J. S. Thorson, *Natural Product Reports* **2005**, *22*, 742-760.
106) S. Singh; A. Aggarwal; N. V. S. D. K. Bhupathiraju; G. Arianna; K. Tiwari; C. M. Drain, *Chemical Reviews* **2015**, *115*, 10261-10306.
107) D. Yi; F. Zhu; M. A. Walczak, *Org Lett* **2018**, *20*, 1936-1940.
108) Y. He; R. J. Hinklin; J. Chang; L. L. Kiessling, *Organic Letters* **2004**, *6*, 4479-4482.
109) S. Lian; H. Su; B.-X. Zhao; W.-Y. Liu; L.-W. Zheng; J.-Y. Miao, *Bioorganic & Medicinal Chemistry* **2009**, *17*, 7085-7092.
110) S. Libnow; M. Hein; P. Langer, *Synlett* **2009**, *2009*, 221-224.
111) K. M. Driller; S. Libnow; M. Hein; M. Harms; K. Wende; M. Lalk; D. Michalik; H. Reinke; P. Langer, *Organic & Biomolecular Chemistry* **2008**, *6*, 4218-4223.
112) W. Wang; P. Rattananakin; P. G. Goekjian, *Journal of Carbohydrate Chemistry* **2003**, *22*, 743-751.
113) O. Renaudet; P. Dumy, *Tetrahedron* **2002**, *58*, 2127-2135.
114) K. D. Randell; B. D. Johnston; B. M. Pinto, *Carbohydrate Research* **2000**, *326*, 145-150.
115) F. Peri; F. Nicotra, *Chem Commun (Camb)* **2004**, 623-7.
116) A. Bianchi; A. Bernardi, *Journal of Organic Chemistry* **2006**, *71*, 4565-4577.
117) F. Nisic; G. Speciale; A. Bernardi, *Chemistry* **2012**, *18*, 6895-906.
118) P. Cheshev; A. Marra; A. Dondoni, *Org Biomol Chem* **2006**, *4*, 3225-7.
119) D. Lim; M. A. Brimble; R. Kowalczyk; A. J. Watson; A. J. Fairbanks, *Angew Chem Int Ed Engl* **2014**, *53*, 11907-11.
120) H. A. V. Kistemaker; G. J. V. van Noort; H. S. Overkleeft; G. A. van der Marel; D. V. Filippov, *Organic Letters* **2013**, *15*, 2306-2309.
121) Y. Kobayashi; Y. Nakatsuji; S. Li; S. Tsuzuki; Y. Takemoto, *Angew Chem Int Ed Engl* **2018**, *57*, 3646-3650.
122) K. Bijian; Z. Zhang; B. Xu; S. Jie; B. Chen; S. Wan; J. Wu; T. Jiang; M. A. Alaoui-Jamali, *European Journal of Medicinal Chemistry* **2012**, *48*, 143-152.
123) K. Sidoryk; L. Rárová; J. Oklešťková; Z. Pakulski; M. Strnad; P. Cmoch; R. Luboradzki, *Organic & Biomolecular Chemistry* **2016**, *14*, 10238-10248.
124) A. W. McDonagh; M. F. Mahon; P. V. Murphy, *Organic Letters* **2016**, *18*, 552-555.
125) T. Suzuki; H. Makyio; H. Ando; N. Komura; M. Menjo; Y. Yamada; A. Imamura; H. Ishida; S. Wakatsuki; R. Kato; M. Kiso, *Bioorganic & Medicinal Chemistry* **2014**, *22*, 2090-2101.
126) I. Pérez-Victoria; O. Boutureira; T. D. W. Claridge; B. G. Davis, *Chemical Communications* **2015**, *51*, 12208-12211.
127) S. André; K. E. Kövér; H.-J. Gabius; L. Szilágyi, *Bioorganic & Medicinal Chemistry Letters* **2015**, *25*, 931-935.

128) A. V. Demchenko, *General Aspects of the Glycosidic Bond Formation*, Wiley: **2008**; 1-27.
129) T. Furuta; K. Takeuchi; M. Iwamura, *Chemical Communications* **1996**, 157-158.
130) I. Cumpstey; D. Crich, *Journal of Carbohydrate Chemistry* **2011**, *30*, 469-485.
131) M. Spell; X. Wang; A. E. Wahba; E. Conner; J. Ragains, *Carbohydrate Research* **2013**, *369*, 42-47.
132) S. Yamago; K. Kokubo; O. Hara; S. Masuda; J.-i. Yoshida, *The Journal of Organic Chemistry* **2002**, *67*, 8584-8592.
133) F. Zhu; S. O'Neill; J. Rodriguez; M. A. Walczak, *Angew Chem Int Ed Engl* **2018**, *57*, 7091-7095.
134) M. Walczak; F. Zhu; T. Yang, *Synlett* **2017**, *28*, 1510-1516.
135) F. Zhu; J. Rodriguez; T. Yang; I. Kevlishvili; E. Miller; D. Yi; S. O'Neill; M. J. Rourke; P. Liu; M. A. Walczak, *J Am Chem Soc* **2017**, *139*, 17908-17922.
136) H. Driguez, *Chem Bio Chem* **2001**, *2*, 311-318.
137) X. Zhu; R. T. Dere; J. Jiang; L. Zhang; X. Wang, *J Org Chem* **2011**, *76*, 10187-97.
138) E. Montero; A. García-Herrero; Juan L. Asensio; K. Hirai; S. Ogawa; F. Santoyo-González; F. J. Cañada; J. Jiménez-Barbero, *European Journal of Organic Chemistry* **2000**, *2000*, 1945-1952.
139) K. Bock; J. Ø. Duus; S. Refn, *Carbohydrate Research* **1994**, *253*, 51-67.
140) E. Montero; M. Vallmitjana; J. A. Pérez-Pons; E. Querol; J. Jiménez-Barbero; F. J. Cañada, *FEBS Letters* **1998**, *421*, 243-248.
141) G. Lian; X. Zhang; B. Yu, *Carbohydr Res* **2015**, *403*, 13-22.
142) K. Pachamuthu; R. R. Schmidt, *Chemical Reviews* **2006**, *106*, 160-187.
143) M. Blanc-Muesser; J. Defaye; H. Driguez; G. Marchis-Mouren; C. Seigner, *Journal of the Chemical Society, Perkin Transactions 1* **1984**, 1885-1889.
144) R. Caraballo; L. Deng; L. Amorim; T. Brinck; O. Ramstrom, *J Org Chem* **2010**, *75*, 6115-21.
145) S. Knapp; D. S. Myers, *The Journal of Organic Chemistry* **2002**, *67*, 2995-2999.
146) X. Zhu; K. Pachamuthu; R. R. Schmidt, *The Journal of Organic Chemistry* **2003**, *68*, 5641-5651.
147) X. Zhu; R. R. Schmidt, *Chemistry- A European Journal* **2004**, *10*, 875-887.
148) D. A. Thayer; H. N. Yu; M. C. Galan; C.-H. Wong, *Angew Chem Int Ed Engl* **2005**, *44*, 4596-4599.
149) N. Floyd; B. Vijayakrishnan; J. R. Koeppe; B. G. Davis, *Angew Chem Int Ed* **2009**, *48*, 7798-7802.
150) H. Wang; X. Zhu, *Organic & Biomolecular Chemistry* **2014**, *12*, 7119-7126.
151) Y. Zhu; W. A. van der Donk, *Organic Letters* **2001**, *3*, 1189-1192.
152) Y. Zhu; M. D. Gieselman; H. Zhou; O. Averin; W. A. van der Donk, *Organic & Biomolecular Chemistry* **2003**, *1*, 3304-3315.
153) M. Fiore; A. Marra; A. Dondoni, *The Journal of Organic Chemistry* **2009**, *74*, 4422-4425.
154) M. Lo Conte; M. J. Robb; Y. Hed; A. Marra; M. Malkoch; C. J. Hawker; A. Dondoni, *J Polym Sci A Polym Chem* **2011**, *49*, 4468-4475.
155) A. Dondoni; A. Marra, *Chem Soc Rev* **2012**, *41*, 573-86.
156) C. Gaujoux-Viala; J. S. Smolen; R. Landewé; M. Dougados; T. K. Kvien; E. M. Mola; M. Scholte-Voshaar; P. van Riel; L. Gossec, *Annals of the Rheumatic Diseases* **2010**, *69*, 1004.
157) C. F. Shaw, *Chemical Reviews* **1999**, *99*, 2589-2600.
158) Y. C. Lee; C. P. Stowell; M. J. Krantz, *Biochemistry* **1976**, *15*, 3956-3963.
159) C. P. Stowell; Y. C. Lee, *Preparation of neoglycoproteins using 2-imino-2-methoxyethyl 1-thioglycosides*, Academic Press: **1982**; *83*, 278-288.
160) B. D. Johnston; B. M. Pinto, *The Journal of Organic Chemistry* **2000**, *65*, 4607-4617.
161) O. B. Wallace; D. M. Springer, *Tetrahedron Letters* **1998**, *39*, 2693-2694.
162) W. Koenigs; E. Knorr, *Ber. Dtsch. Chem. Ges.* **1901**, *34*, 957-981.
163) S. A. Holick; L. Anderson, *Carbohydrate Research* **1974**, *34*, 208-213.
164) G. J. Bernardes; D. P. Gamblin; B. G. Davis, *Angew Chem Int Ed Engl* **2006**, *45*, 4007-11.
165) T. B. Rauchfuss; G. A. Zank, *Tetrahedron Letters* **1986**, *27*, 3445-3448.
166) B. S. Pedersen; S. Scheibye; W. H. Nilson; S. O. Lawesson, *Bull. Soc. Chim. Belg.* **1978**, *87*, 223-228.
167) T. Nishio, *Journal of the Chemical Society, Chemical Communications* **1989**, 205-206.
168) T. Nishio, *Journal of the Chemical Society, Perkin Transactions 1* **1993**, 1113-1117.
169) P. M. Aberg; B. Ernst, *Acta Chem Scand* **1994**, *48*, 228-233.
170) B. Wu; J. Ge; B. Ren; Z. Pei; H. Dong, *Tetrahedron* **2015**, *71*, 4023-4030.

171) Z. Pei; R. Larsson; T. Aastrup; H. Anderson; J. M. Lehn; O. Ramstrom, *Biosens Bioelectron* **2006**, *22*, 42-8.
172) P. Shu; J. Zeng; J. Tao; Y. Zhao; G. Yao; Q. Wan, *Green Chemistry* **2015**, *17*, 2545-2551.
173) M. Jana; A. K. Misra, *The Journal of Organic Chemistry* **2013**, *78*, 2680-2686.
174) T. Ghosh; A. Santra; A. K. Misra, *Beilstein journal of organic chemistry* **2013**, *9*, 974-982.
175) W. W. Cleland, *Biochemistry* **1964**, *3*, 480-482.
176) M. Carmack; C. J. Kelley, *The Journal of Organic Chemistry* **1968**, *33*, 2171-2173.
177) U. T. Rüegg; J. Rudinger, *Reductive cleavage of cystine disulfides with tributylphosphine*, Academic Press: **1977**; *47*, 111-116.
178) M. Narisada; Y. Terui; M. Yamakawa; F. Watanabe; M. Ohtani; H. Miyazaki, *The Journal of Organic Chemistry* **1985**, *50*, 2794-2796.
179) C. A. Evans; L. Bernier; J. Dugas; T. S. Mansour, *Tetrahedron Letters* **1997**, *38*, 7657-7660.
180) N. Ibrahim; M. Alami; S. Messaoudi, *Asian Journal of Organic Chemistry* **2018**.
181) A. Bruneau; M. Roche; A. Hamze; J.-D. Brion; M. Alami; S. Messaoudi, **2015**, *21*, 8375-8379.
182) R. A. A. Al-Shuaeeb; D. Montoir; M. Alami; S. Messaoudi, *The Journal of Organic Chemistry* **2017**, *82*, 6720-6728.
183) W. Redjdal; N. Ibrahim; B. Benmerad; M. Alami; S. Messaoudi, *Molecules* **2018**, *23*, 519.
184) S. Benmahdjoub; N. Ibrahim; B. Benmerad; M. Alami; S. Messaoudi, *Organic Letters* **2018**, *20*, 4067-4071.
185) T. Belz; S. J. Williams, *Carbohydr Res* **2016**, *429*, 38-47.
186) K. L. Matta; R. N. Girotra; J. J. Barlow, *Carbohydrate Research* **1975**, *43*, 101-109.

CHAPTER TWO: carbohydrate binding proteins

Carbohydrate-protein interactions are involved in many biological recognition phenomena, including fertilization, cell–cell recognition, immunological responses and pathogen–host cell attachment processes. In order to control these events, significant effort has been focused toward the development of high-affinity ligands for various carbohydrate-binding proteins. However, this is a challenging task, also because carbohydrate-protein interactions are usually weak, typically in the millimolar to micromolar range. Furthermore, the availability of saccharide ligands for carbohydrate-binding proteins is often limited by the tedious synthetic protocols required for their preparation. The knowledge on molecular recognition of sugars by carbohydrate-binding proteins has been employed for the development of new biomedical strategies. Glycans are selectively recognized by certain proteins, called lectins which can be either secreted or expressed on cell surface. Lectins, present at the surface of host cells, often recognize pathogen-specific sugar moieties, mediating attachment. They typically present binding sites shallow and exposed to the solvent, which makes recognition of oligosaccharides an intrinsically low-affinity process.

Depending on the composition of the binding site and thus of the target sugar specifically recognized, mammalian lectins are called galectins (binding pocket specific for the disaccharide lactose or *N*-acetylactosamine), SIGLECs (that bind preferentially sialic acid residues) and C-type lectins (which show a certain selectivity for mannose- and fucose-containing carbohydrates).[1] Despite the huge diversity among lectins, they share the presence of a Carbohydrate Recognition Domain (CRD), usually formed by less than 200 amino acids.

C-type lectin receptors (CLRs) represent the most abundant class and they are so called because of the presence of a calcium ion (Ca^{2+}) into their binding site. They are largely expressed by animals, viruses and parasites. In particular, these proteins play a crucial role in the immune system where they belong to the family of receptors expressed by Antigen Presenting Cells (APCs).

The main function of C-type lectins expressed by Dendritic Cells (DCs) is to interact with certain molecular patterns featured by non-self-cells, in order to start the internalization process of pathogens for processing and antigen presentation, thereby triggering the information cascade that lead to the immune responses against a diversity of microorganisms.

One of these C-type lectin is DC-SIGN.

2.1 DC-SIGN: structure and functionality

DC-SIGN (Dendritic Cell-Specific ICAM-3-Grabbing Non-integrin) is a C-type lectin whose important role in the human body was clarified in 2000 by van Kooyk and co-workers.[2] It is mainly expressed and displayed on their surface by immature DCs located on dermal and mucosal tissues (**Fig. 2.1**).

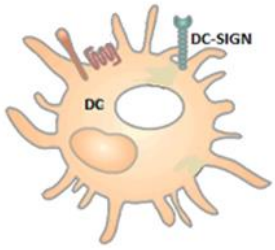

Fig. 2.1 Picture of a dendritic cell expressing DC-SIGN on its surface

DC-SIGN is a tetrameric transmembrane protein, composed by an N-terminal cytoplasmic domain, a transmembrane domain from which it departs a neck repeat domain formed by hydrophobic amino-acid residues (responsible for the tetramerization) that is connected with the CRD exposed in the extracellular environment (**Fig. 2.2**).

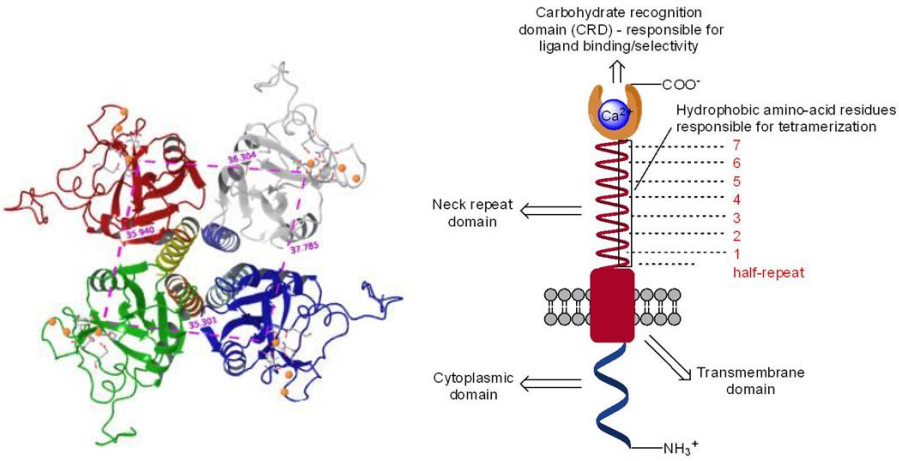

Fig. 2.2 Tetrameric and monomeric structure of DC-SIGN

The CRD of DC-SIGN is selective for mannose- and fucose-containing carbohydrates and includes the calcium ion responsible for both sugar binding and structural maintenance (**Fig. 2.3**).

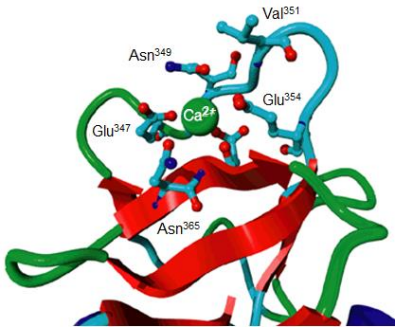

Fig. 2.3 Binding site of DC-SIGN

DC-SIGN plays a key role in the immune system. Indeed, it binds self glycoproteins InterCellular Adhesion Molecules 2 (ICAM-2) and ICAM-3 and thus mediates the interaction between dendritic cells and T-cells.[3] Furthermore, DC-SIGN is able to recognize several pathogens, like viruses (Hepatitis C, Ebola, Dengue, SARS), bacteria (*Mycobacterium tuberculosis*, *Klebsiella pneumonae*), yeasts (*Candida albicans*) and parasites

(*Leishmania spp*, *Schistosoma mansoni*) by specifically recognizing the glycosylated structures displayed at their surface.

However, several pathogens, such as Human Immunodeficiency Virus type-1 (HIV-1), hijack DCs to disseminate the infection in the human body. In particular, DC-SIGN represents the primary target recognized by all those pathogens that, as HIV-1, exploit mucosal entry pathways.[4] This explains why DC-SIGN has become an interesting target for the design of anti-infective agents.

DC-SIGN interaction with the HIV virus involves the highly mannosylated envelope protein of HIV called gp120 (**Fig. 2.4**).[5]

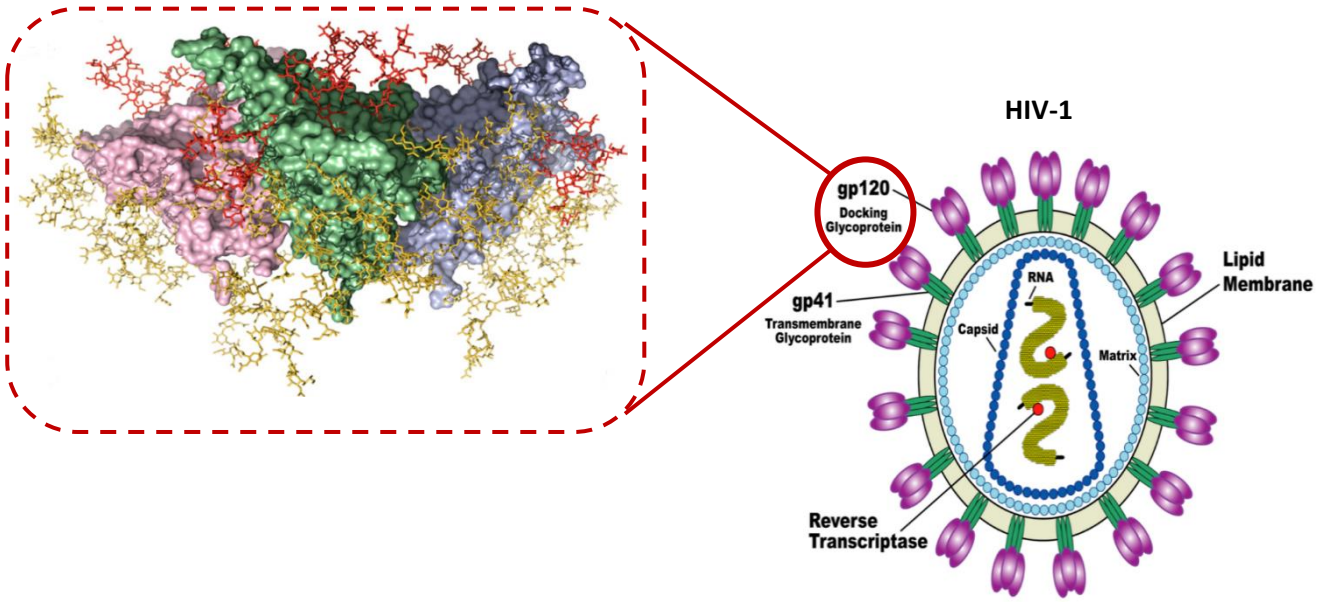

Fig. 2.4 Highly mannosylated gp120 envelope protein of HIV[6]

In particular, the main natural ligand recognized by the CRD of DC-SIGN is the high-mannose glycan $(Man)_9(GlcNAc)_2$, also known as Man_9, that is conjugated to the envelope protein and exposed on the viral surface (**Fig. 2.5**).[7]

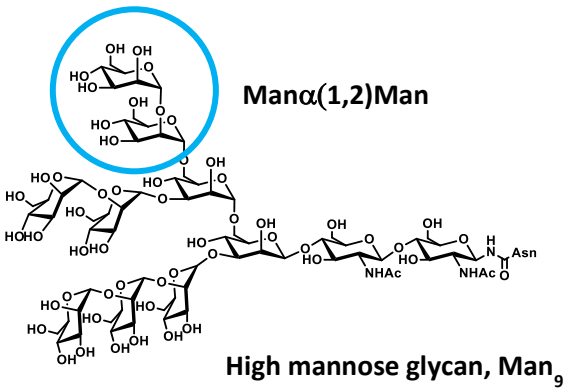

Fig. 2.5 High mannose glycan $(Man)_9(GlcNAc)_2$

2.1.1 DC-SIGN ligands

Binding assays revealed that a particular portion of Man_9 (the Manα(1,2)Man terminal epitope) is directly involved in the binding event with the receptor and, when presented on a glycoarray, it is sufficient to reach similar affinity value than the entire molecule.[8] Therefore, the artificial compounds designed as DC-SIGN pathogen antagonists should mimic this framework in order to achieve high activity. With this aim, the Bernardi's group has already developed some mannose-based DC-SIGN monovalent ligands, among which the pseudo-dimannoside (**2.1**) and the so-called Man030 (**2.2**) have shown interesting affinity towards the receptor (with IC_{50} values of 0.9 mM and 0.3 mM respectively, as measured by SPR inhibition assay) (**Fig. 2.6**).[8-9]

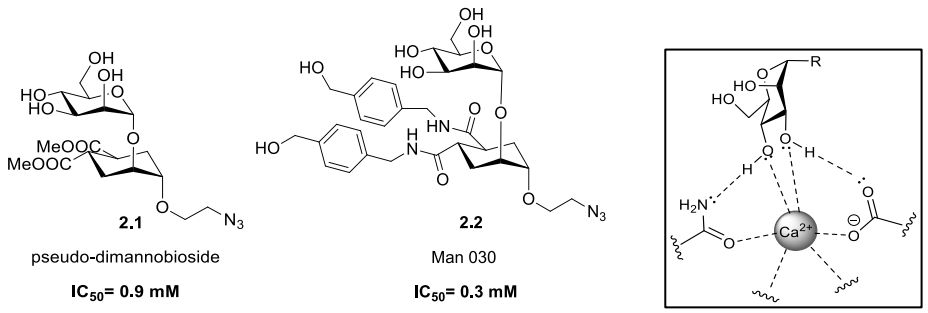

Fig. 2.6 Mannose-based DC-SIGN monovalent ligands **2.1** and **2.2**; interaction between –OH in position 3 and 4 of **2.1** and **2.2** and the calcium ion of the CRD

These two compounds contain a mannose ring, whose hydroxyl groups in position 3 and 4 are involved in the interaction with the calcium ion in the CRD (**Fig. 2.6**),[10] and a conformationally stable 1,2-*trans*-diaxial cyclohexanediol moiety, which is able to establish additional Van der Waals interactions with residues

present in the binding site. This latter moiety replaces the non-pharmacophoric part of the natural ligand mimics, the reducing end mannose residue and confers enzymatic stability to the molecule.[11]

Below, the synthetic pathways proposed for the preparation of the pseudo-dimannoside **2.1** (**Fig.2.7**) and the Man030 **2.2** (**Fig. 2.8**) are reported.

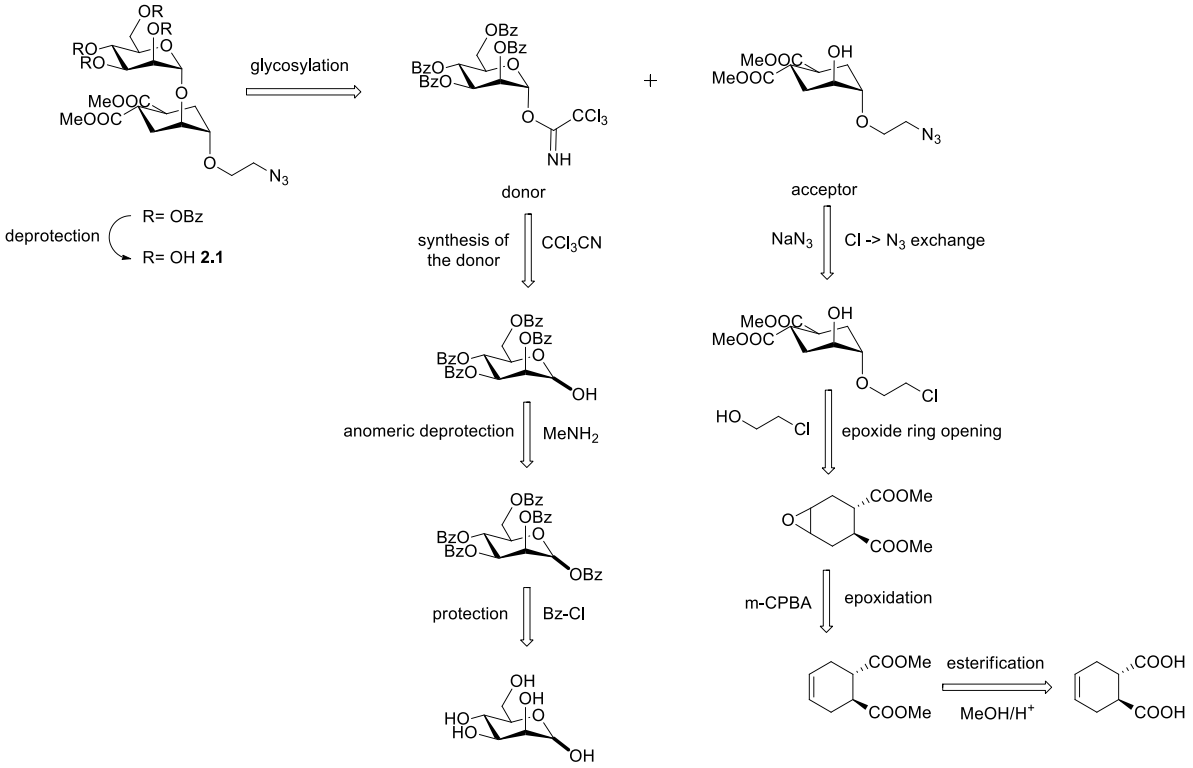

Fig. 2.7 Retroynthesis of the pseudo-dimannoside **2.1**

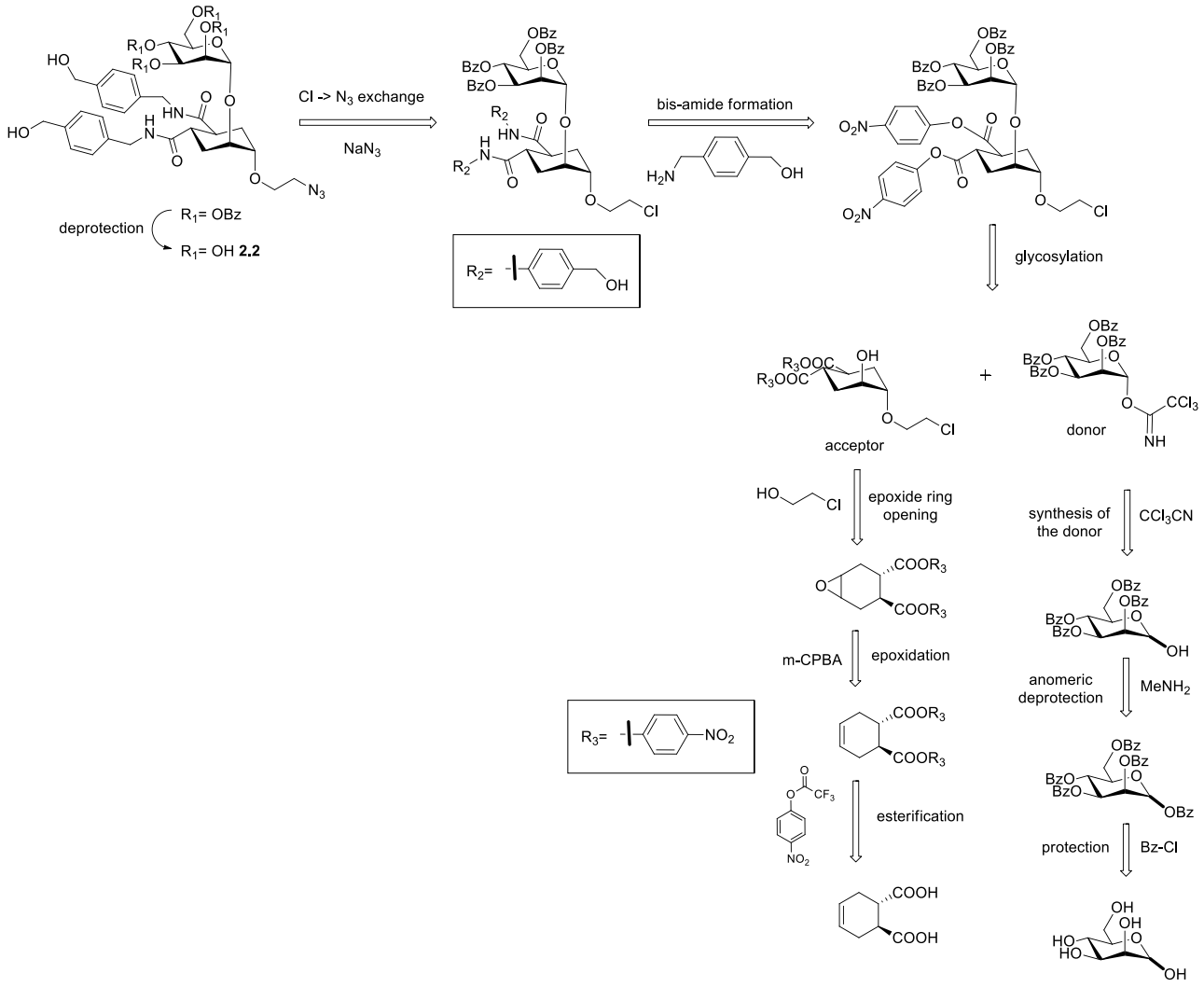

Fig. 2.8 Retroynthesis of the Man030 **2.2**

As mentioned before, carbohydrate-protein interactions typically show low affinity, usually in the millimolar range. This weak interaction is overcome both in Nature and in the development of new ligands by exploiting multivalency. In this way, high affinity is achieved through multiple glycan presentations towards the lectin protein. This concept has been exploited also for the development of DC-SIGN antagonists. Four main factors are fundamental in the design of such multivalent systems: number of copies of the monovalent ligand, overall dimension of the polyvalent construct relative to the size of the polymeric protein and to the separation of its binding sites, right balance between flexibility/rigidity, solubility.

The main strategy followed in our group for the preparation of multivalent systems consists in coupling the monovalent ligand, that has to bear at least one azido group, to a polyalkyne dendrimeric core through a 'click' reaction, obtaining dendrimers that show a certain flexibility. In the figure below, two examples of dendrimeric scaffolds which have DC-SIGN as target protein are reported:[9]

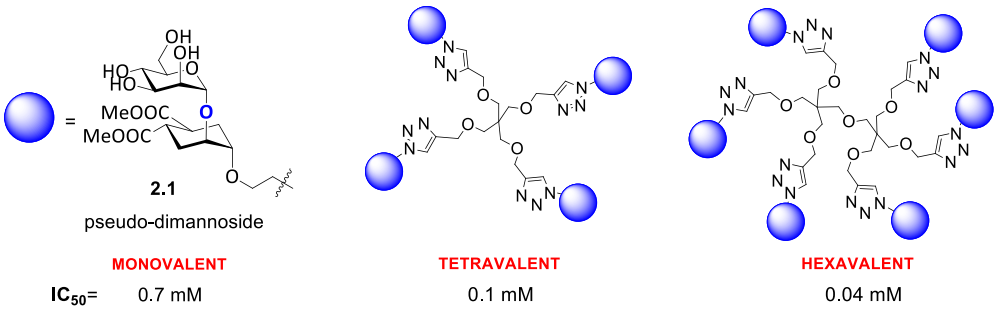

Fig. 2.9 Tetravalent and hexavalent dendrimeric scaffolds decorated with **2.1**

Comparing the IC_{50} values (obtained through an SPR inhibition assay) of the monovalent with the tetra- and the hexavalent systems, it is evident how the multiple presentation of the ligand towards the receptor helps the affinity (**Fig. 2.9**).

More recently, another strategy was developed in the design of these systems in order to further increase their activity. This approach rely on a linear rigid central spacer with a proper length, designed to efficiently exploit the chelation mechanism. ROD3 was shown to span the required distance (about 4 nm) to chelate two DC-SIGN biding sites at the same time (**Fig. 2.10**).[12]

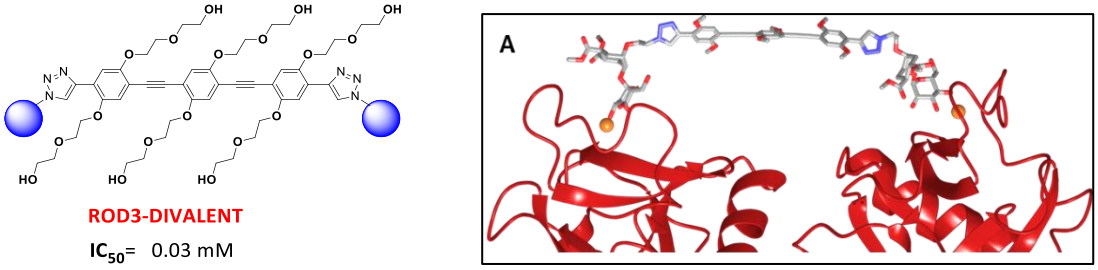

Fig. 2.10 ROD-3-divalent structure (on the left); ROD3-divalent/DC-SIGN complex in dynamic simulations performed using an implicit GB/SA water model (25 ns) (on the right)

In this case, the ROD3-divalent system, bearing two copies of pseudo-dimannoside **2.1**, was sufficient to reach a similar affinity towards DC-SIGN than the hexavalent dendrimer reported in **Fig. 2.9**.

2.2 References

1) H. Lis; N. Sharon, *Chemical Reviews* **1998**, *98*, 637-674.
2) T. B. H. Geijtenbeek; R. Torensma; S. J. van Vliet; G. C. F. van Duijnhoven; G. J. Adema; Y. van Kooyk; C. G. Figdor, *Cell* **2000**, *100*, 575-585.
3) D. A. Mitchell; A. J. Fadden; K. Drickamer, *J Biol Chem* **2001**, *276*, 28939-28945.
4) R. C. J. R. Gallo, *Retrovirology* **2006**, *3*, 72.
5) E. W. Adams; D. M. Ratner; H. R. Bokesch; J. B. McMahon; B. R. O'Keefe; P. H. Seeberger, *Chem Biol* **2004**, *11*, 875-81.
6) K. J. Doores; Z. Fulton; V. Hong; M. K. Patel; C. N. Scanlan; M. R. Wormald; M. G. Finn; D. R. Burton; I. A. Wilson; B. G. Davis, **2010**, *107*, 17107-17112.
7) E. van Liempt; C. M. C. Bank; P. Mehta; J. J. Garcı´a-Vallejo; Z. S. Kawar; R. Geyer; R. A. Alvarez; R. D. Cummings; Y. v. Kooyk; I. van Die, *FEBS Letters* **2006**, *580*, 6123-6131.
8) J. J. Reina; S. Sattin; D. Invernizzi; S. Mari; L. Martinez-Prats; G. Tabarani; F. Fieschi; R. Delgado; P. M. Nieto; J. Rojo; A. Bernardi, *ChemMedChem* **2007**, *2*, 1030-6.
9) N. Varga; I. Sutkeviciute; R. Ribeiro-Viana; A. Berzi; R. Ramdasi; A. Daghetti; G. Vettoretti; A. Amara; M. Clerici; J. Rojo; F. Fieschi; A. Bernardi, *Biomaterials* **2014**, *35*, 4175-84.

10) G. Tabarani; M. Thépaut; D. Stroebel; C. Ebel; C. Vivès; P. Vachette; D. Durand; F. Fieschi, *The Journal of biological chemistry* **2009**, *284*, 21229-21240.
11) S. Mari; H. Posteri; G. Marcou; D. Potenza; F. Micheli; F. J. Cañada; J. Jimenez-Barbero; A. Bernardi, *European Journal of Organic Chemistry* **2004**, *2004*, 5119-5225.
12) S. Ordanini; N. Varga; V. Porkolab; M. Thepaut; L. Belvisi; A. Bertaglia; A. Palmioli; A. Berzi; D. Trabattoni; M. Clerici; F. Fieschi; A. Bernardi, *Chem Commun (Camb)* **2015**, *51*, 3816-9.

CHAPTER THREE: aim of the work

Although the pseudo-dimannoside **2.1** and its bis-amide derivative **2.2** represented very promising candidates in this field, their structure and preparation still show some drawbacks: the first critical point of the synthesis is certainly the glycosylation reaction that requires extremely anhydrous conditions and low temperatures; additionally, there are some restrictions about the insertion of the azido linker that has to be introduced at a specific point in the synthesis and whose length cannot be easily modified. Finally, although **2.1** is composed of a sugar moiety connected to an unnatural aglycon through a pseudo-glycosidic bond, the pseudo-dimannoside was found to be a substrate of glycosidases, albeit as a low reacting one.[1]

The aim of this PhD project was to create a new class of glycomimetic DC-SIGN ligands, starting from all the know-how already gathered for compound **2.1**. The strategy that we have devised consisted in the replacement of the glycosidic oxygen atom of compounds **2.1** and **2.2** with a sulphur atom, in order to further improve the metabolic stability of these molecules,[2] while maintaining the affinity towards the receptor.

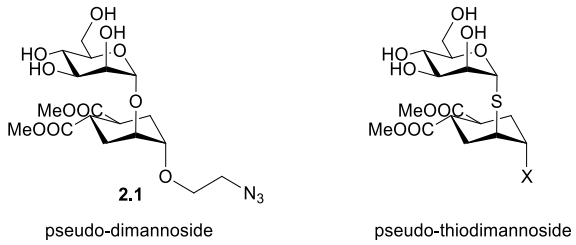

Fig. 3.1 The pseudo-dimannoside **2.1** (on the left) and the corresponding pseudo-thiodimannoside (on the right)

Furthermore, the presence of the carbon-sulphur bond should help to simplify the synthetic strategy, exploiting the lower basicity and the better nucleophilicity of the sulphur atom compared to oxygen: indeed, these structures (as already mentioned in the Chapter 1.3.4 of Thioglycosides) are usually prepared from sugar-thiolates, which can easily react by an S_N2-like mechanism with different substrates.[2-3] In addition, some examples in literature show that, since the C-S bond is longer than the corresponding C-O bond, these structures benefit of an increased conformational flexibility that can allow them to adapt their conformation and enable a better fit into a binding pocket, leading sometimes to a better affinity towards the receptor.

During this thesis, I have developed two novel strategies for the synthesis of pseudo-thiodimannosides, leading to either *O*-linked (X= OCOR) or *N*-linked (X= NHCOR) products. Both approaches rely on nucleophile opening of a 3-membered electrophile ring, either an epoxide or an aziridine of appropriate symmetry derived from the cyclohexene diester **4.4**, by the α-thioacetyl-tetra-*O*-acetylmannoside **4.8** (**Fig. 3.2**).

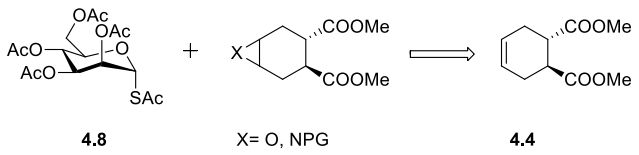

Fig. 3.2 General approach for the preparation of pseudo-thiodimannosides through nucleophile opening of an epoxide or an aziridine ring

1) S. Mari; H. Posteri; G. Marcou; D. Potenza; F. Micheli; F. J. Cañada; J. Jimenez-Barbero; A. Bernardi, *European Journal of Organic Chemistry* **2004**, *2004*, 5119-5225.
2) T. Belz; S. J. Williams, *Carbohydr Res* **2016**, *429*, 38-47.
3) K. Pachamuthu; R. R. Schmidt, *Chemical Reviews* **2006**, *106*, 160-187.

CHAPTER FOUR: synthesis of *O*-linked pseudo-thiodisaccharides

4.1 Results and discussion

As mentioned in the previous chapter, retrosynthetically, the *S*-analog of **2.1** (**4.9**) could be obtained through nucleophilic opening of the epoxide **4.5** (**Fig. 4.1**) by an α-glycosyl thiolate.

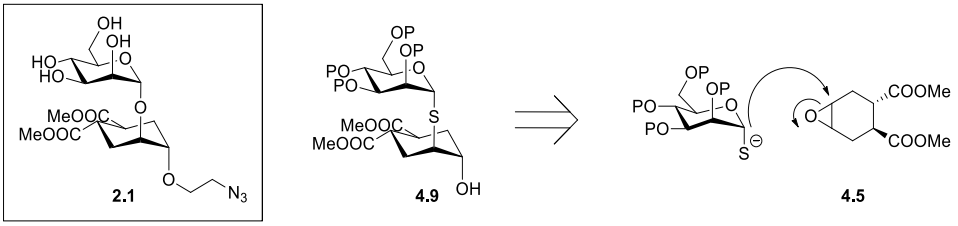

Fig. 4.1 The pseudo-dimannoside **2-1** (on the left); retrosynthetic approach to obtain the corresponding pseudo-thiodimannoside **4.9**

Indeed, the symmetry properties of **4.5** and **4.9**, coupled to the stereoelectronic requirements for *trans*-diaxial opening of epoxycyclohexanes, allow the formation of a single isomer during this reaction, which has the same configuration as **2.1**. Precedent literature on thiol alkylation suggests that this reaction could actually be performe one-pot, starting from the α-thioacetyl mannopyranose **4.8**.[1] This has the advantage of both streamlining the synthesis of **4.9** and reducing the risk for disulphide formation from the free thiol.

In this chapter, we show how we set up and optimised the synthesis of **4.9**, using the approach described above, as well as the properties of this molecule and its use for the synthesis of polyvalent DC-SIGN ligands.

4.1.1 Synthesis of the epoxide 4.5

For the synthesis of the epoxide **4.5** the already well-known procedure was followed:[2] starting from the enantiomerically pure dicarboxylic acid **4.3** ([α_D]= +169, custom-made by Alchemy) we performed a Fischer esterification with MeOH in standard conditions, followed by epoxidation of the double bond using *m*-chloroperbenzoic acid (m-CPBA) in dichloromethane (**Scheme 4.1**).[2] Both these steps gave the product almost in quantitative yield, and no chromatographic purification of the crude reaction mixture was required.

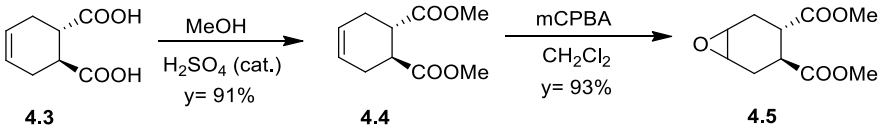

Scheme 4.1 Synthesis of epoxide **4.5**

4.1.2 Synthesis of the 1-*S*-acetyl-α-mannopyranose 4.8

The synthesis of the glycosyl donor **4.8** started from peracetylation of mannose **4.6**, used as a mixture of α and β anomers. Since this reaction was performed in a large scale (on 5 g of the natural sugar), to avoid the use of large quantities of pyridine, employed as solvent in standard protocols, an alternative method was applied that involved a catalytic amount of a Lewis acid (lanthanum(III) triflate) and acetic anhydride as both acylating agent and the solvent (**Scheme 4.2**).[3]

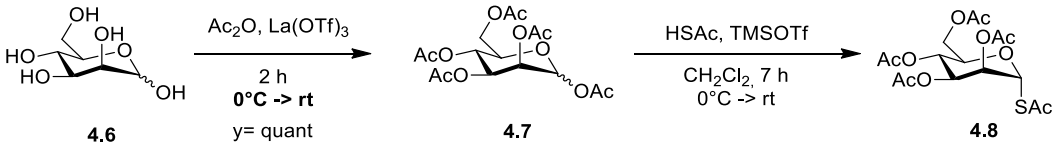

Scheme 4.2 Synthesis of the α-thioacetate **4.8**

The 1-*S*-acetyl-2,3,4,6-tetra-*O*-acetyl-α-mannopyranose **4.8** is a known compound.[4-5] It was prepared by treating the peracetylated mannose **4.7** with thioacetic acid in the presence of a Lewis acid. However, although the α-product is certainly the most favoured one, because of the strong anomeric effect of mannose and of the neighbouring group participation of the 2-*O*-acetyl protecting group, the formation of variable amounts of the β-product was observed in our first experiments. Although these amounts remained under 25% of the mixture, the separation by flash chromatography of the two stereoisomers was difficult and led to low yields of the isolated desired α-compound. For this reason, the thio-acetylation reaction was optimized and in the table below (**Table 4.1**) all the experiments carried out with this aim are reported. The critical elements necessary to guarantee reproducibility of the process were found to be the quality of the thioacetic acid batch, which needs to be freshly distilled before use, and the quality of the Lewis acids employed as promoters.

Table 4.1. Optimization of the synthesis of **4.8**. All reactions were performed at room temperature.

Entry	Solvent	time	LA	[4.7]	β anomer[a]	y	Eluent[b]
1	CH_2Cl_2	24 h	$BF_3 \cdot Et_2O$	0.25 M	19%	35% (α/β)	6:4 Hex:AcOEt
2	CH_2Cl_2	15 h	TMSOTf	1.5 M	11%	36% (α only)	8:2 iPr_2O:CH_2Cl_2
3	CH_2Cl_2 : Et_2O (1 : 1)	24 h	TMSOTf	1.5 M	17 %	/	/
4	Et_2O (and 5 drops of CH_2Cl_2)	50 h	TMSOTf	1.5 M	21 %	/	/
5	CH_2Cl_2	15 h	TMSOTf	1.5 M	11%	68% (α only)	8:2 iPr_2O:CH_2Cl_2[c]

[a] measured on the ^{1}H-NMR spectrum of the crude as the ratio of the anomeric proton signals ($CDCl_3$, α-anomer 5.97 ppm; β-anomer 5.51 ppm)
[b] used for the purification by chromatographic column
[c] product isolated through automated chromatography (Biotage, ULTRA column, HP samplet)

In the first experiment, even if the amount of the β anomer measured from the ^{1}H-NMR spectrum of the crude was lower than 20%, flash chromatography using 6:4 Hex:EtOAc afforded the thioacetate product as a mixture of the two anomers, moreover in low yield (**Table 4.1**, entry 1; **Fig. 4.2**). Indeed, this eluent provided scant separation of the two isomers also on TLC (6:4 Hex:EtOAc, cerium ammonium molibdate stain) and the

two spots of the starting α/β mixture and of the α/β mixture of the product were very close to each other's. Additionally, hydrolysis products were visible at the bottom of the plate.

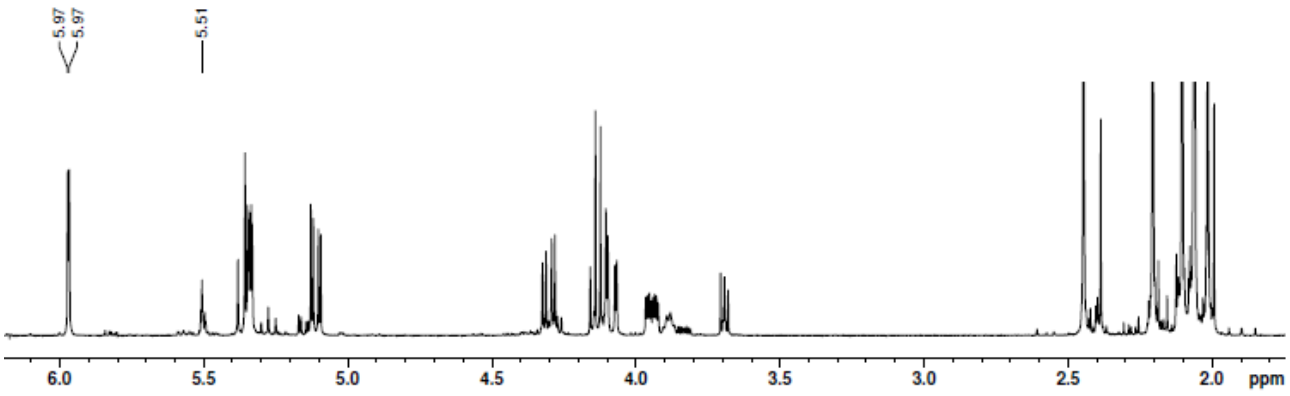

Fig. 4.2 ^{1}H-NMR spectrum of the α/β mixture of compound **4.8** of entry 1 (the anomeric proton signals are $H_{1\alpha}$ at 5.97 ppm, and $H_{1\beta}$ at 5.51 ppm)

In the next trial, the Lewis acid was replaced with trimehtylsilyl trifluoromethanesulfonate (TMSOTf) and the concentration of the substrate was increased to 1.5 M (**Table 4.1**, entry 2). In this case, after only 15 h at room temperature TLC (6:4 Hex:EtOAc) showed complete conversion of the starting sugar **4.7**. The concentration increase allowed to reduce the reaction time; furthermore the ^{1}H-NMR of the crude in this case was cleaner than the previous one. Although the amount of the β-product found in the crude was lower (11%) and the flash chromatography with 8:2 iPr_2O:CH_2Cl_2 as eluent allowed the isolation of the pure α-anomer in 36% yield, the separation efficiency was still modest and much of the desired product remained contaminated by the β-isomer.

Since the process follows presumably an S_N1-type mechanism (through the formation of the oxocarbenium ion intermediate under acidic catalysis conditions), we considered that the solvent could play an active role in this reaction. In particular, it is well described in the literature that the participation of ethers in these transformations could lead to the generation of an equatorial oxonium ion, which should favour the formation of the thermodynamically more stable axial α-product.[6] Taking this into account, the thio-acetylation was performed in a 1:1 mixture of CH_2Cl_2:Et_2O (**Table 4.1**, entry 3) and in only Et_2O (with some drops of CH_2Cl_2 necessary to dissolve completely the starting sugar, entry 4): in both these experiments the amount of the β-anomer found in the crude was comparable with the previous results. Moreover, the low solubility of the peracetylated compound **4.7** in ether led to an important increment of the reaction time (50 h for entry 4). In the last attempt, the same conditions of entry 2 were reproduced (CH_2Cl_2, TMSOTf), but the crude purification was performed by automated flash chromatography using 8:2 iPr_2O:CH_2Cl_2 and a high-performance column (Biotage, ULTRA column, HP samplet): only in this case starting from 1 g of crude (where 11% of the β was present) 680 mg of the only α-product were isolated, corresponding to 68% yield and thus to an increment of more than 30% compared to entry 2 (**Table 4.1**, entry 5).

4.1.3 Synthesis of the pseudo-thiodisaccharide 4.9

The pseudo-thiodisaccharide **4.9** was obtained through a one-pot ring opening reaction between the α-thioacetate **4.8** and the epoxide **4.5** (**Scheme 4.3**).

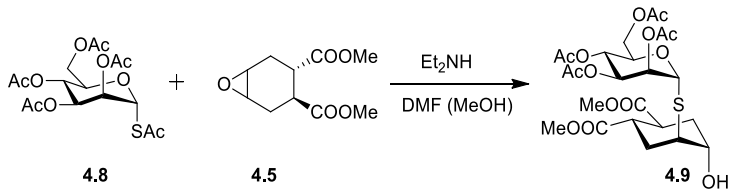

Scheme 4.3 Ring-opening reaction of epoxide **4.5** by **4.8** to generate the speudo-thiodisaccharide **4.9**

A one-pot procedure implies several advantages: first of all, it allows to improve the efficiency of the process whereby the reactants are subjected to successive transformations in the same reaction vessel, circumventing purification steps. In this way, a one-pot procedure can minimize chemical waste, save time, and simplify practical aspects. Recently, Hayashi gave an accurate definition of "one-pot process", summarizing all the characteristics and the limitations of this synthetic approach, presenting also the concept of "pot economy".[7] Furthermore, in the case in our hands, the procedure allowed to avoid the strict requirements of the standard glycosylation, such as anhydrous conditions and the low temperatures.

For the conditions of this process we were inspired by the procedure reported by Belz and co-workers two years ago (see chapter 1.3.4 of Thioglycosides), where diethylamine was used to deacetylate *in situ* the anomeric sulphur, generating a thiolate able to displace a sugar halide.[1] We decided to adopt their conditions to open the epoxide **4.5**, but added methanol (7-10 mol equiv) as a supplementary proton source. Below all the experiments performed in order to optimize this transformation are summarized and discussed (**Table 4.2**).

Table 4.2 Optimization of the one-pot ring opening reaction conditions. All the experiments were performed at room temperature

Entry	4.8 (eq)	4.5 (eq)	C_f[a] (M)	MeOH	t	Conv[b]	y[c]	Scale[d]	notes
1	1	1.5	0.2	7 eq	4h	56%	42%	30 mg	/
2	1.2	1	0.2	7 eq	3h	78%	48%	20 mg	monitored by ESI-MS
3	1	1	0.2	7 eq	3 days	69%	32%	30 mg	monitored by NMR
4	1+0.5	1	0.35[e]	7 eq	24 h	71%	30%	24 mg	/
5	1.15	1	0.6	/	< 2h	≈100%	61%	12 mg	increased epoxide concentration
6	1.3	1	0.6	/	7 h	≈100%	77%	scale up to 200 mg	Et_2NH 1.9 eq

[a] final concentration of the limiting reagent.
[b] measured on the ^{1}H-NMR spectrum of the crude by the integration of the signals associated to the starting epoxide (2xOMe singlets at 3.68 and 3.67 ppm) and the product (2xOMe singlets at 3.70 and 3.71 ppm); see **Fig. 4.4**.
[c] of the isolated product.
[d] referred to the limiting reagent.
[e] after the second addition of **4.8** (initial concentration= 0.4 M).

Although the epoxide was certainly the most precious reactant, since the starting material is custom made, in the first experiment (**Table 4.2**, entry 1) it was added in excess relative to **4.8** because of all the difficulties faced with the synthesis and the purification of the thio-acetyl compound. The reaction was performed in anhydrous *N,N*-dimethylformamide (DMF, 0.2 M concentration of the limiting agent), stirring under nitrogen atmosphere for 4 h at room temperature. Even after only 2 h, the TLC (6:4 Hex:EtOAc, cerium ammonium molibdate stain) showed the almost complete disappearance of the thio-sugar spot. The NMR of the crude showed, besides the unreacted epoxide, the presence of another species that was confirmed to be the expected product **4.9** by ESI-MS (m/z= 601, [**4.9** + Na]$^+$). Column chromatography (eluent 4:6 Hex:EtOAc) allowed to recover unreacted **4.5** (39%) and the pseudo-thiodisaccharide **4.9** in 42% yield. Beside affording the product and providing proof of principle for the synthetic concept, this experiment revealed that monitoring the reaction by TLC is inefficient, because detection of the epoxide becomes difficult at low concentration. For this reason, in the second attempt (**Table 4.2**, entry 2), the reaction course was followed by ESI-MS (**Fig. 4.3**). In this case, the limiting reagent was the epoxide **4.5.** Analysis by ESI-MS of a sample collected after 30 min of reaction at room temperature showed the presence of both the epoxide (peak at 237, [**4.5** + Na]$^+$) and the product (peak at 601, [**4.9** + Na]$^+$; **Fig. 4.3**, left panel). After 2 h the epoxide peak was no longer visible (**Fig. 4.3**, right panel) and the reaction was quenched (after 3 h).

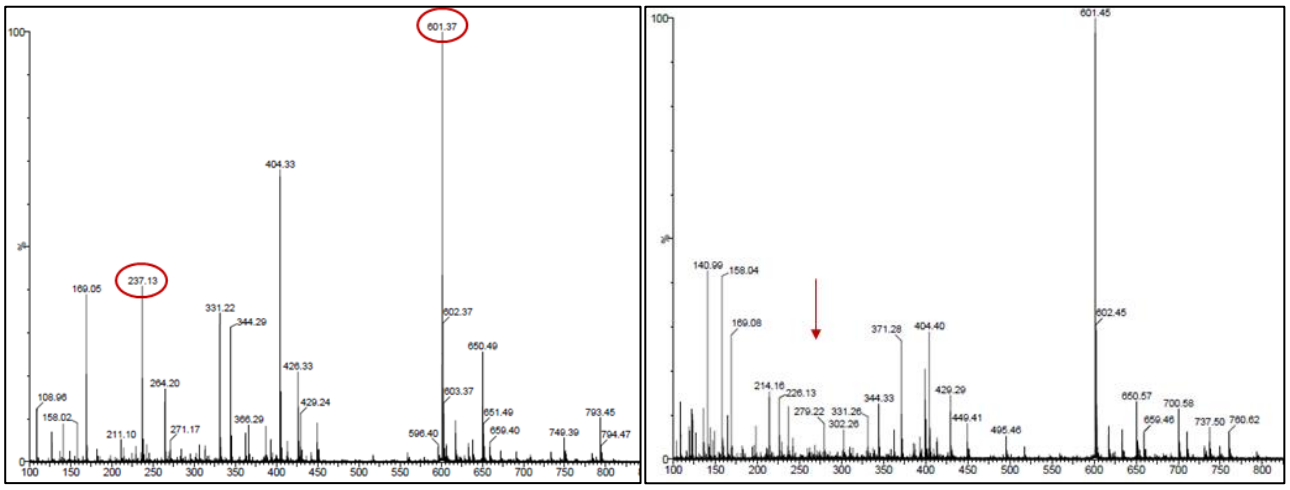

Fig. 4.3 Sample analysed by ESI-MS after 30' (left) and after 2h (right); peak at 601, [**4.9** + Na]$^+$, peak at 237, [**4.5** + Na]$^+$

However, in the NMR spectrum of the crude reaction mixture, some unreacted epoxide was still found (22%, **Fig. 4.4**). This implied that compound **4.5** does not fly well in the mass-spectrometer, compared to the reaction product, suggesting to select a different monitoring tool. Anyway, product **4.9** was isolated in moderate yield (48% with a conversion of 78%), better than in the previous experiment (42% with a conversion of 56%).

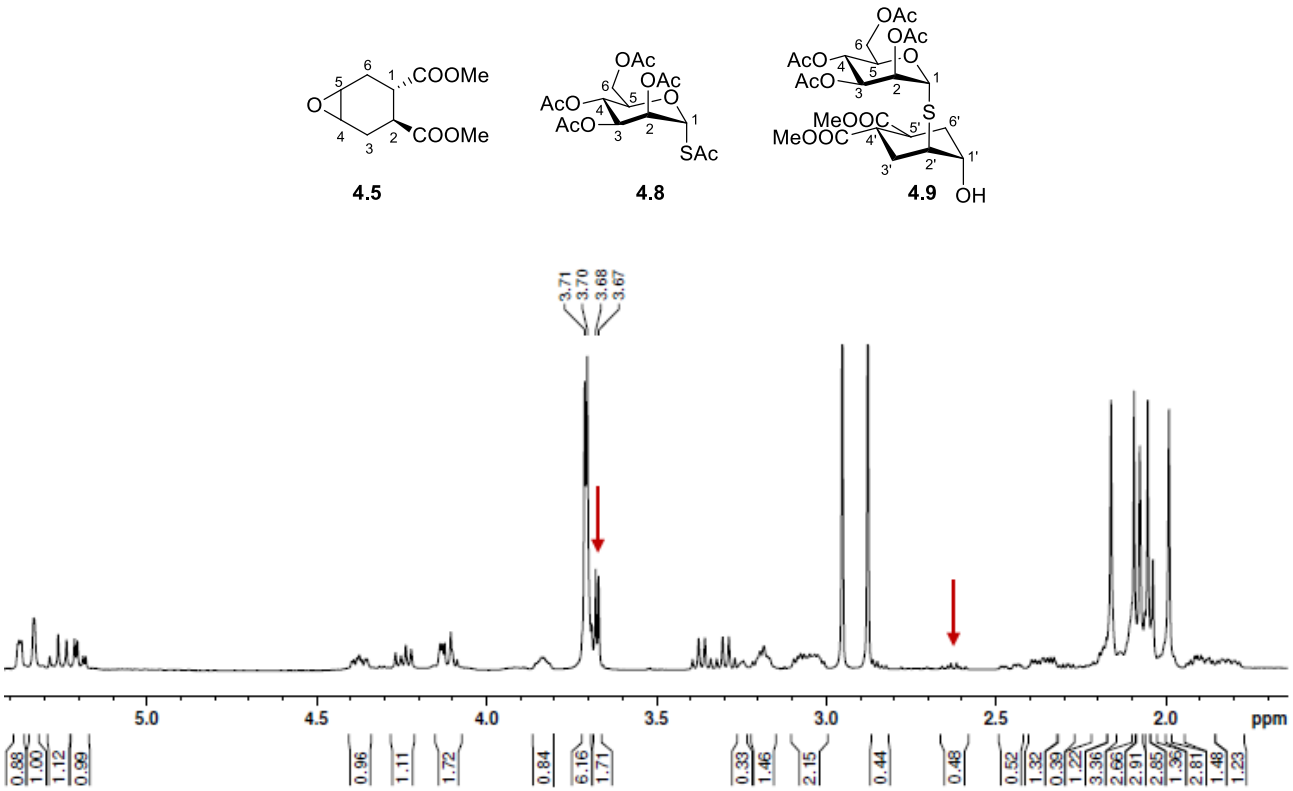

Fig. 4.4 ^{1}H-NMR of the crude where is still visible the unreacted epoxide (pointed by the red arrows, 2xOMe singlets at 3.67 and 3.68 ppm, and the multiplet of the H_2 at 2.62 ppm; NB the ppm values were affected by the presence of still DMF and $EtNH_2$ in the mixture)

The subsequent reaction (**Table 4.2**, entry 3) was then performed inside an NMR tube, using DMF-d^7 as solvent. The following signals were used to monitor the concentration of the different species, as the reaction proceeded: for the epoxide **4.5** the multiplet at 2.62 ppm of H_2, for the thioacetate **4.8** the anomeric proton H_1 at 5.82 ppm and for the reaction product **4.9** the multiplet at 3.8-3.88 ppm of $H_{1'}$. In particular, we followed the consumption of the H_1 of the thioacetate, the disappearance of the epoxide and the appearance of the diagnostic signals of the product. Plotting the relative integrations of these signals as a function of time, we obtained the graph reported below (**Fig. 4.5**) following the typical trend of a second order reaction, confirming the S_N2 pathway. The reaction was very fast at the beginning (see the curve slopes in the first 20 min), but after 100 min the rate decreased reaching a plateaux. In particular, it seemed that when the epoxide has reached a certain (low) concentration, it did not react anymore, while the thioacetate continued to be consumed, possibly by formation of the corresponding dithioether.

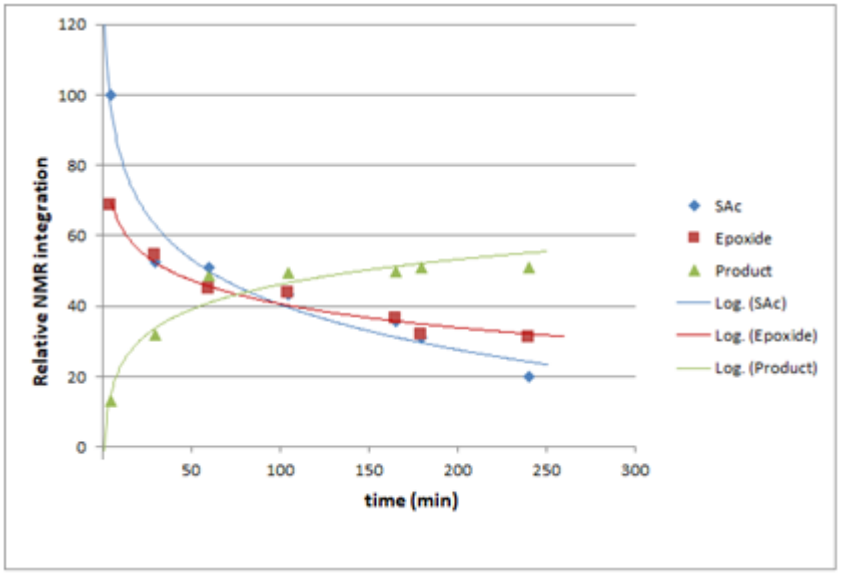

Fig. 4.5 Graph of the one-pot ring opening monitored by NMR spectroscopy, obtained plotting the relative NMR integrations of diagnostic signals associated to the reagents (**4.5** and **4.8**) and the product (**4.9**) in function of time

To force the conditions towards a better conversion of epoxide **4.5**, the thio-sugar **4.8** was added in two portions, starting with a stoichiometric ratio of the reagents. Addition of the second portion of **4.8** (0.5 mol equiv) was done after 2 h, when **4.8** was not revealed anymore by TLC, working in a more concentrated solution (0.35 M instead of 0.2 M, **Table 4.2**, entry 4). However, after 4 h, the reaction mixture was analysed by NMR spectroscopy revealing again the presence of the epoxide (30%). The work-up was performed after 24 h; the unreacted epoxide was recovered (25%) after the chromatographic column and the product **4.9** was isolated in only 30% yield. Better results were obtained by starting with an excess of thioacetate **4.8** (1.2 mol equiv) and 1.9 equivalents of Et_2NH at higher concentration (0.6 M, **Table 4.2** entry 5): under these conditions yields increased to over 60% after only 2 h. Furthermore, this experiment revealed that the additional MeOH was not required and that the epoxide could be reprotonated directly by the ammonium salt generated from Et_2NH (see **Fig. 4.6**). Finally, the best conditions were found by further increasing both the concentration of the thio-sugar (1.3 mol equiv added) and the reaction time (7 h) (**Table 4.2** entry 6). Under these conditions, scale up of the process to 200-300 mg of epoxide was allowed with reproducible yields.

Collecting all the information obtained during the optimization phase, we hypothesized a mechanism for the one-pot epoxide opening sequence (**Fig. 4.6**).

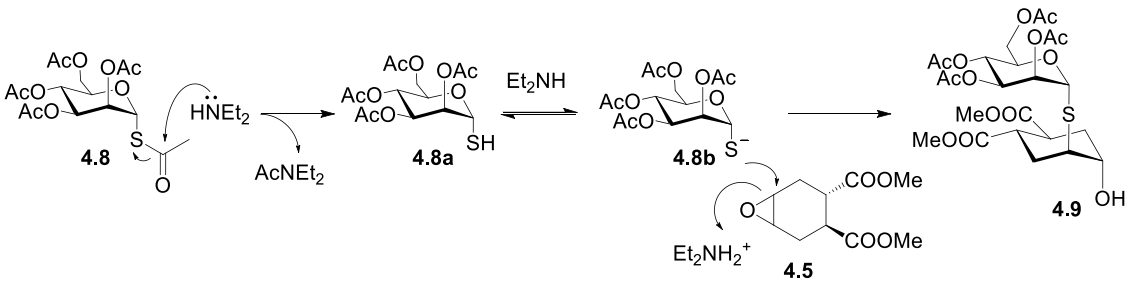

Fig. 4.6 Proposed mechanism for the one-pot ring opening reaction of **4.5** by **4.8**

The first equivalent of diethylamine acts as a nucleophile, selectively deacetylating the sulphur in the anomeric position, affording thiol **4.8a** that reacts with excess Et_2NH in an acid/base equilibrium. The thiolate **4.8b** thus generated can react with **4.5**, forming an alkoxide which is protonated by the Et_2NH^+ salt (or by the thiol itself) thus shifting the equilibrium towards the product. The pseudo-thiodisaccharide **4.9** is obtained as a single isomer as the product of an exclusively *trans*-diaxial opening of epoxide **4.5**. The tendency of epoxides to open *trans*-diaxially is well known and described in literature.[8] Furthermore, starting from an enantiomerically pure cyclohexene dicarboxylic acid (compound **4.3**) and considering the real conformation assumed by the epoxide **4.5** (reported in **Fig. 4.7**),[9] only one isomer can be actually obtained, regardless of the carbon that undergoes nucleophilic attack.

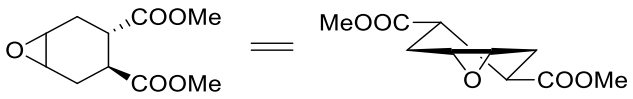

Fig. 4.7 Conformation of the epoxide **4.5**

The structure of product **4.9** and the conformation of the cyclohexane ring were confirmed from coupling constant analysis of the cyclohexane protons in the ^{1}H-NMR spectrum of the isolated compound: while in deuterated chloroform ($CDCl_3$, **Fig. 4.8**, left panel) the coupling constants could not be accurately measured, the spectrum in CD_3OD showed a large 11 Hz vicinal spin–spin coupling constant for protons H_4' and H_5' (**Fig. 4.8**, right panel) indicating a *trans*-diaxial orientation.

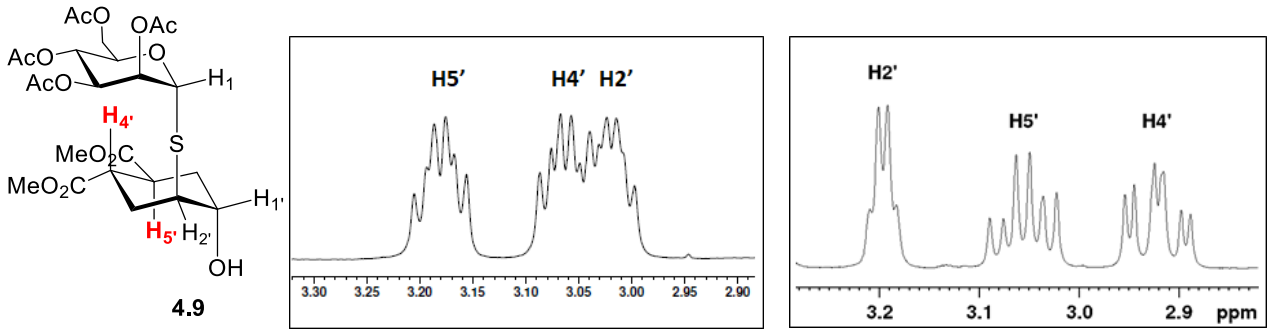

Fig. 4.8 ^{1}H-NMR spectrum of **4.9** in in $CDCl_3$ (left panel) and in CD_3OD (right panel); numbering of the ring is unconventional and used to simplify comparison with the natural Manα(1,2)Man disaccharide

The locked conformation (populated by ≥90%) of the cyclohexane moiety is due to the presence of the carbomethoxy groups, which preferentially assume the equatorial position: this feature is characteristic of vicinal *trans*-cyclohexanedicarboxylic acid derivatives, including the pseudo-dimannoside **2.1**, and it allows the distal substituents in **4.9** to occupy the axial position, thus mimicking the 3D features of an α-mannopyranose residue.[10]

Once the ring opening reaction was optimized and the mechanism of the process was rationally defined, we tried to further improve the reaction conditions by employing different techniques. The same process was

initially performed in a flow micro-reactor. At the beginning, we were inspired by all the potential advantages of this technology, compared to batch vessels. Some of them are reported below:

- improved **heat transfer** and **mixing** processes (that means a better control on the reaction parameters)
- the possibility to change the reaction conditions while the reactor is operational (that means fast optimization)
- the possibility to rapidly obtain several chemical information from **mg quantities** of starting material
- the opportunity to transfer the process to a large scale production by exploiting an automated flow process (interesting for an industrial application, for example)

In particular, we used the kit supplied by Chemtrix, reported in **Fig. 4.9**, that is composed by:

- gas-tight syringes, where the reactants are charged, dissolved in the reaction solvent
- a thermal controller, that allow to set the required reactor temperature
- a micro-reactor within a thermostated reaction platform
- a back-pressure regulator (optional), that prevents boiling of reactants or solvent when the reaction temperature is above their boiling points

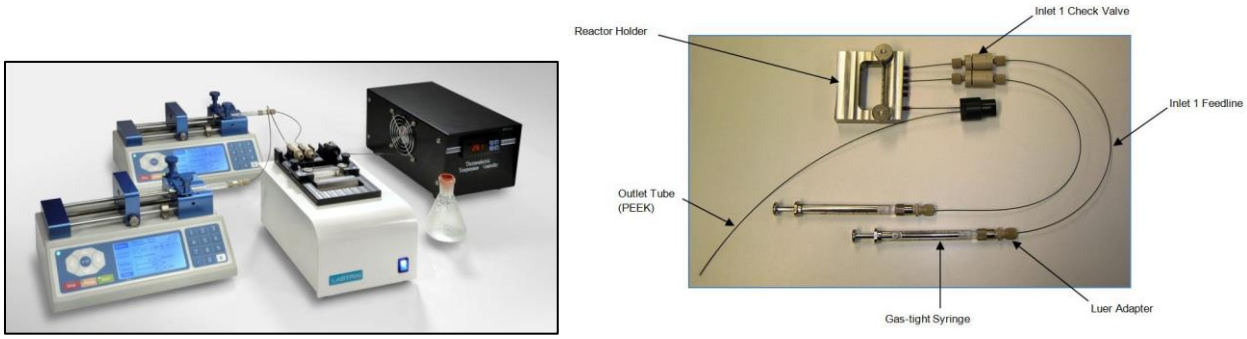

Fig. 4.9 Kit supplied by Chemtrix for flow-processes

In particular, the micro-reactor is a glass device containing channels in which reagent solutions can first be brought to the reaction temperature before they are mixed and allowed to react. The main components of a micro-reactor are listed below:

- **Mixer**: where reactants are combined
- **Residence time unit**: a thermally regulated micro channel in which the reaction takes place
- **Quench inlet**: where the reaction products are mixed with a quench agent before collection
- **Outlet**: where reaction products are collected

There are different micro-reactors specifically designed for various processes. In **Fig. 4.10** some of them are reported and the reaction type for which they are used is indicated.

Reactor ID	Reactor Image	Reactor Volume (µl)	Reaction Type
3221	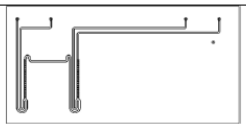	1.0	A + B = P1+Q = P
3222	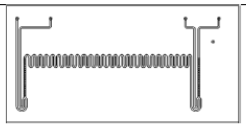	5.0	A + B = P1+Q = P
3223	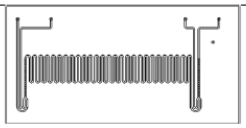	10.0	A + B = P1+Q = P
3224	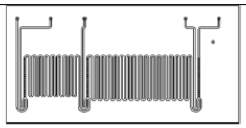	(5 + 10)	A+B = P1 + C = P2 + Q = P
3225	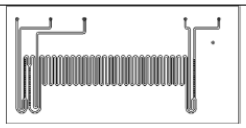	10.0 0.1 (A+B), 10 (+C)	A+B = P1 + C = P2 + Q = P
3227(*)		19.5	A + B = P1+Q = P

Fig. 4.10 Examples of micro-reactors (supplied by Chemtrix)

Flow reactions are performed by pumping reagent solutions into the reactor (via capillary tubing) where they are mixed and reacted. At the µm length scale, high viscous forces dominate and the flow is laminar. As a result, diffusion processes dominate and determine the mixing time, which is typically in the sec range. Compared to batch processes, the reaction time in a flow reactor is dependent on the reactant flow rate and the reactor volume, through the equation reported below:

$$\textbf{Residence Time} = \frac{\text{Reactor Volume (µl)}}{\text{Overall Flow Rate (µl min}^{-1}\text{)}}$$

Keeping in mind the mechanism of the one-pot ring opening (illustrated and discussed before, see **Fig. 4.6**), for the first trial we selected the set-up depicted below (**Fig. 4.11**).

Table 4.3 Conditions used for the first trial, in terms of final concentration of **4.5** (into the reactor) and equivalents of the other reagents

$[4.5]_f$	4.8	Et_2NH
0.3 M	1.3 eq	1.9 eq

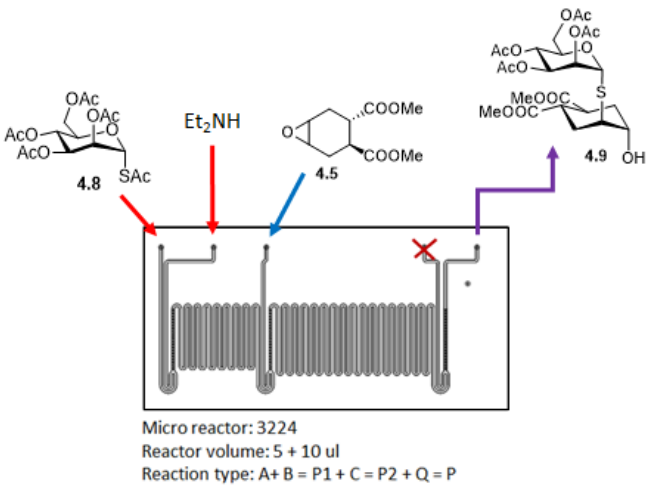

Micro reactor: 3224
Reactor volume: 5 + 10 ul
Reaction type: A+ B = P1 + C = P2 + Q = P

Fig. 4.11 Micro-reactor used for the first trials (on the right); the reaction conditions (**Table 4.3** on the left)

This reactor was designed for a reaction like A+B= P1+C= P2+Q= P, where A+B were thioacetate **4.8** and diethylamine (pushed through the first two inlet channels, dissolved in anhydrous DMF) that had to form the thiolate *in situ* (P1). At this point, the epoxide was charged into the third inlet channel (C) to be opened by the thiolate and give the final product **4.9** (P), which left the system through the output channel (keeping close the quench inlet, Q). For the first experiments, we decided to fix the flow rate, varying the temperature. The final concentration of the epoxide was 0.3 M and the molar equivalents of each reactant the same as in the optimized batch conditions (**Table 4.3**, N.B: a concentration of 0.3 in the reactor means that the reactants were previously charged into the syringe pumps as 0.6 M solutions). Finally, the crude collected outside the reactor was analysed by ^{1}H-NMR spectroscopy to measure the conversion of the epoxide **4.8** into the product, using the same signals mentioned above. The preliminary results are reported in the table below (**Table 4.4**).

Table 4.4 Results obtained (in terms of conversion) performing the one-pot reaction in the micro-reactor 3224 with different flow rates of the reactants at different temperatures

Entry	Flow	T	Residence time	Conversion
1	7.5 µl/min	60°C	2 min	13%
2	7.5 µl/min	70°C	2 min	17%
3	7.5 µl/min	80°C	2 min	13%

In these conditions, the conversions were always below 20% and the sugar appeared degraded in the crude's spectrum, whereas the unreacted epoxide was found still intact (**Fig. 4.12**).

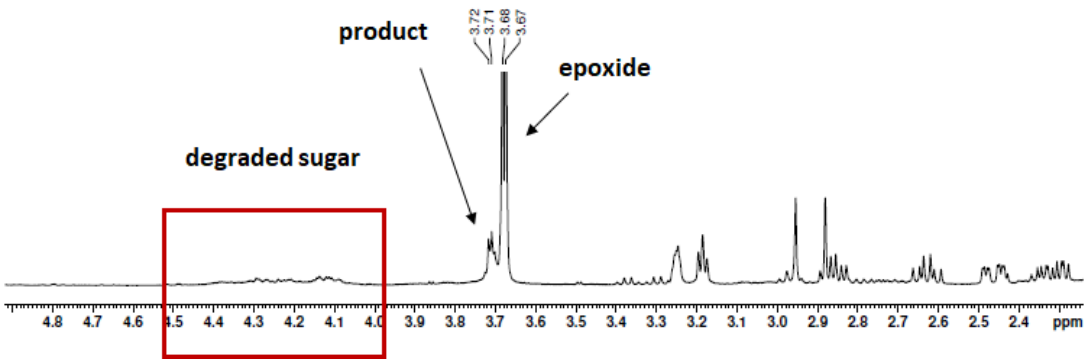

Fig. 4.12 ^{1}H-NMR spectrum of the crude of entry 2 of **Table 4.4**

The crude of each reaction was also checked by TLC: numerous spots with low R_f were found, presumably derived from the sugar. We concluded that the formation of the thiolate was very fast and it occurred immediately when the thioacetate encountered the diethylamine. Probably, in the time between the first

mixer and the inlet of the epoxide, the sugar underwent degradation and the reaction ended up with a low conversion.

The micro-reactor was then replaced with the one depicted below (**Fig. 4.13**). In the first syringe pump the thioacetate **4.8** and the epoxide **4.5** dissolved in DMF were charged (since they could not react with each other without the amine); in the second one the diethylamine in DMF. In this way, when the thiolate was formed, the epoxide was already present, ready to be opened.

Table 4.5 Conditions used in terms of final concentration of **4.5** (into the reactor) and equivalents of the other reagents

$[4.5]_f$	4.8	Et_2NH
0.3 M	1.3 eq	1.9 eq

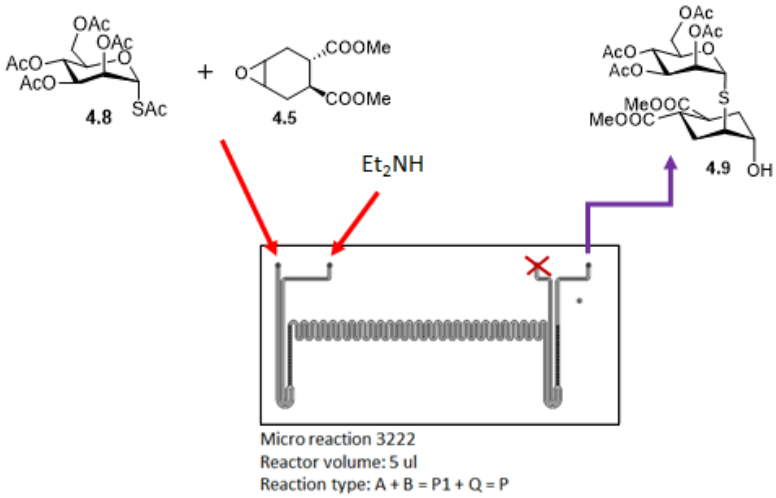

Fig. 4.13 Micro-reactor 3222 employed (on the right); the reaction conditions (**Table 4.5** on the left)

Keeping the same residence time (2 minutes) than in the previous experiments (and thus decreasing the flow rate to 2.5 µl/min), we immediately observed better results in terms of conversion, even at 40°C (**Table 4.6**, entry 1, 29% conversion). However, increasing the temperature did not lead to any improvement, neither did changing the flow rates.

Table 4.6 Optimization of the conditions for the one-pot reaction performed in micro-reactor 3222

Entry	Flow	Temperature	Residence time	Conversion
1	2.5 µl/min	40°C	2 min	29%
2	2.5 µl/min	50°C	2 min	28%
3	2.5 µl/min	60°C	2 min	not detectable
4	2.5 µl/min	70°C	2 min	/

Only when the concentration into the reactor was doubled (from 0.3 M to 0.6 M) and the residence time increased, better results were observed (**Table 4.7**, entry 1 and 2), until conversion reached 69% (**Fig. 4.14**) with 30 min of residence time (entry 4).

Table 4.7 Best results obtained for the one-pot reaction performed in the flow micro-reactor 3222

Entry	Flow	Temperature	Residence time	Conversion
1	0.5 µl/min	25°C	10 min	45%

2	0.5 µl/min	40°C	10 min	55%
3	0.25 µl/min	50°C	20 min	65%
4	0.17 µl/min	60°C	30 min	69%

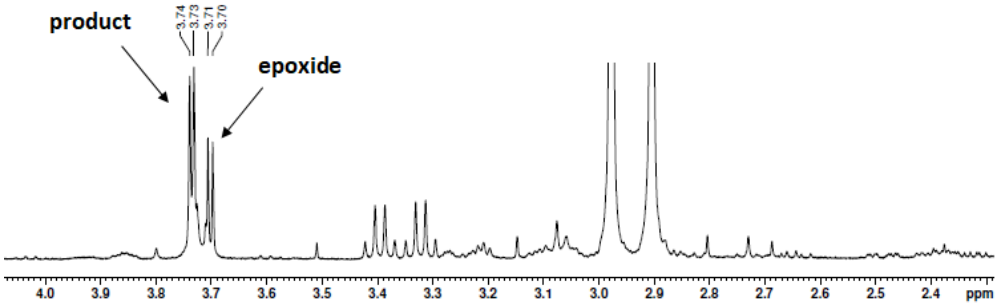

Fig. 4.14 ^{1}H-NMR spectrum of the crude of entry 4, **Table 4.7**

However, the low flow rate, required to obtain reasonable results in terms of conversion, made these conditions clearly not competitive with the batch ones and the use of this technique was not further pursued.

When the reaction was performed under micro-wave irradiation at 60°C, reproducing the optimized batch conditions, complete consumption of the starting epoxide **4.5** was observed after 1h, giving the final product **4.9** in 75% yield and allowing the scale up of the reaction from 50 mg to 200 mg, with reproducible yields. Below all the results obtained for the one-pot reaction are summarized:

- Batch conditions: room temperature, 7 h, conversion= 89%, y= 77%
- Flow conditions: 60°C, 30 min (residence time), conversion= 69% (scale up not allowed)
- MW conditions: 60°C, 1 h, conversion= 90%, y= 75% (scale up allowed)

4.1.4 Deacetylation of 4.9 and conformational analysis of 4.10

The pseudo-thiodisaccharide **4.9** underwent deacetylation in standard Zemplén conditions (methoxide solution in anhydrous methanol, at room temperature) giving quantitatively compound **4.10** after only 10 minutes (**Scheme 4.4**).

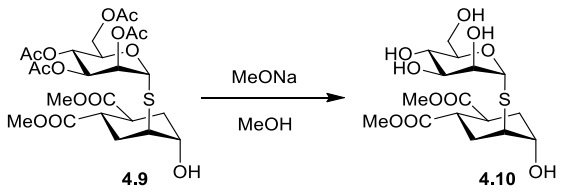

Scheme 4.4 Zemplén deacetylation of compound **4.9**

To predict the three-dimensional structure of compound **4.10**, we followed the same approach already used for the original pseudo-dimannoside **2.1**. NMR studie had revealed that **2.1** has a conformational distribution similar to the natural disaccharide Manα(1,2)Man. Two conformations, dubbed E (for Extended) and S (for

Stacked), in fast equilibrium around the (pseudo)glycosidic bond, are characterized by two mutually exclusive NOE contacts: the H_1-$H_{1'}$ contact for the S conformer, and the H_1- $H_{3'eq}$ contact for the E conformer (**Fig. 4.15**, the unconventional numbering of the cyclohexane ring was adopted for easier comparison with natural sugars).[10]

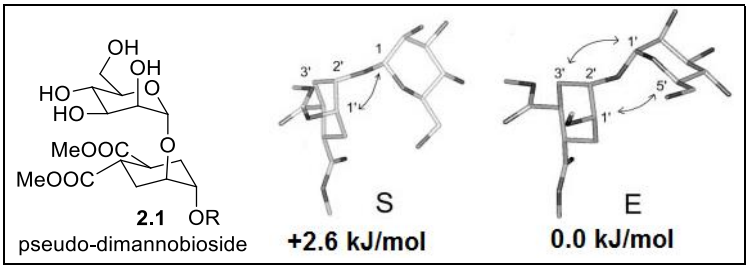

Fig. 4.15 E and S conformations found at lowest energy for the pseudo-dimannoside **2.1** and their typical NOE contacts

A qualitative analysis of the NOE data allowed deducing that the E conformer of **2.1** is the preferred conformation in solution (D_2O). Interestingly, the E conformation was also the one observed in the X-ray of the DC-SIGN:**2.1** complex.[11]

The conformation of **4.10** was investigated by NOESY experiments (in D_2O, 500 MHz) performed in collaboration with prof. Vasile and prof. Sattin. The experimental data were then compared with the results obtained for the pseudo-dimannoside **2.1**. This analysis showed an intense H_1-$H_{3'eq}$ cross-peak, while the H_1-$H_{1'}$ contact was revealed as a weak cross-peak, using 800 ms of mixing time (**Fig. 4.16**).

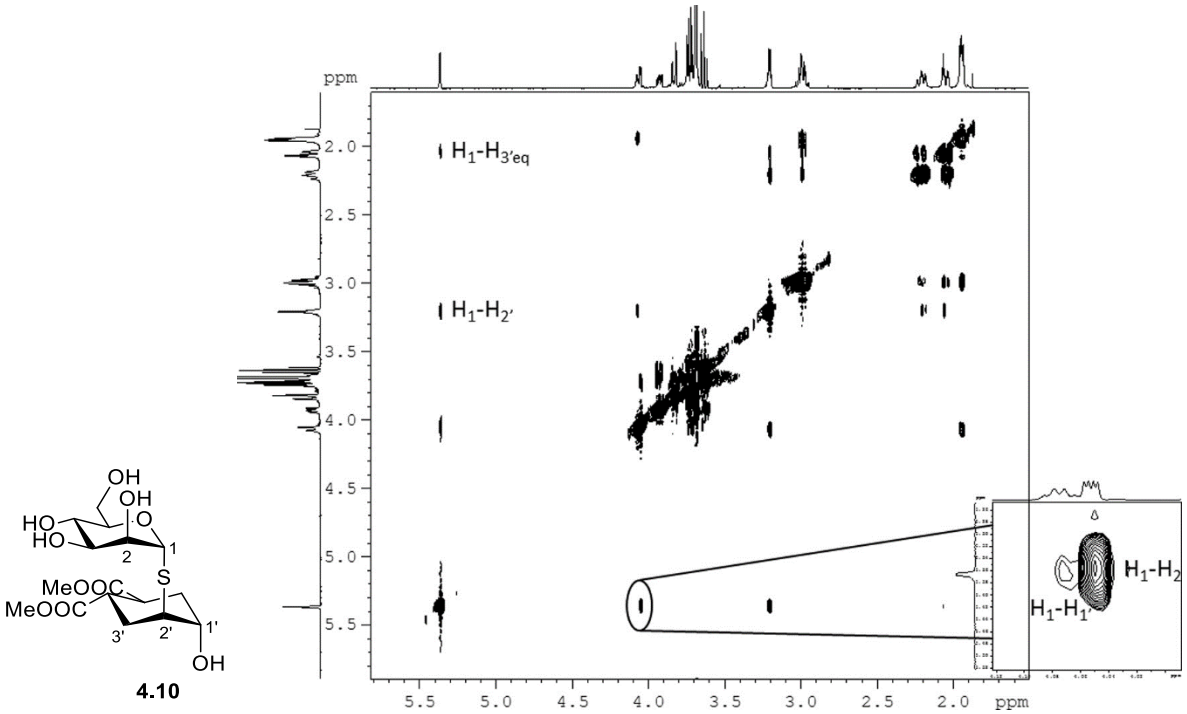

Fig. 4.16 NOESY spectrum (500 MHz, D_2O, 300 K, 800 ms of mixing time) of compound **4.10** performed with solvent suppression

These results suggested that compound **4.10** assumes preferentially an extended-like conformation (that is also the one found at the lowest energy for the pseudo-dimannoside **2.1**).

A conformational search of **4.10** (performed with the MM3* force field, by the prof. S. Sattin) supported the existence of both S and E conformers of similar strain energy (**Fig. 4.17**). However, due to the increased length of the C-S bond relative to the C-O bond, the calculated H_1-$H_{1'}$ distance in the S conformation of **4.10** is 3.1 Å, as opposed to 2.6 Å in **2.1**, in qualitative agreement with a reduced intensity of the H_1-$H_{1'}$ cross-peak.

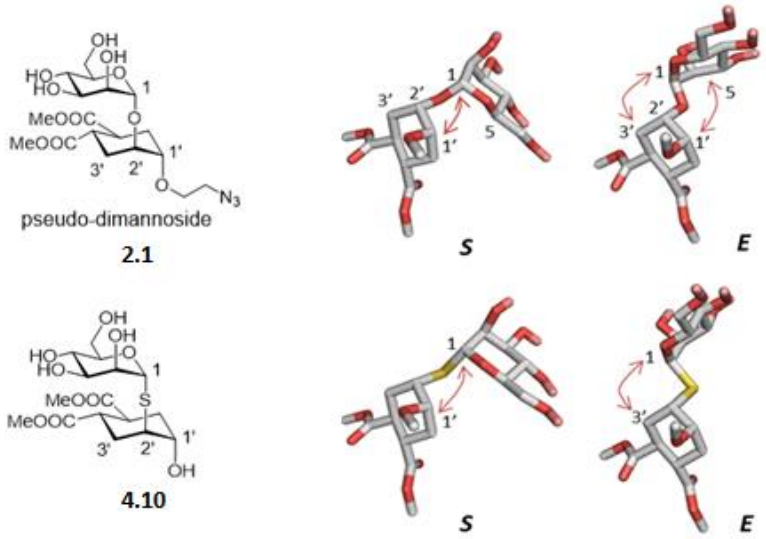

Fig. 4.17 Stacked (S) and Extended (E) conformations of the pseudo-1,2dimannoside **2.1** (on the top), and the pseudo-thio-1,2-dimannoside **4.10** (on the bottom). The mutually exclusive NOE contacts defining the conformation are indicated by arrows.

Overall, the data are consistent with both the pseudo-dimannoside **2.1** and the pseudo-thiodimannoside **4.10** populating the same conformational space and mimicking the conformational features of the native Manα(1,2)Man sugar.[12]

4.1.5 Functionalization of 4.10 with an azido-linker

To allow the synthesis of multivalent derivatives of **4.10**, we planned the functionalization of the free alcohol function of the cyclohexane moiety with an azido-terminated linker (**Fig. 4.18**).

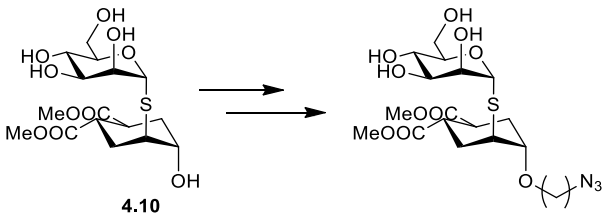

Fig. 4.18 General plan for the functionalization of **4.10** with an azido-linker

To check the ability of this molecule to undergo esterification, the coupling conditions were tested initially between the peracetylated-pseudo-thiodisaccharide **4.9** and pivaloyl chloride **4.11,** to give the pivaloate ester **4.12** in 59% yield (**Scheme 4.5**).

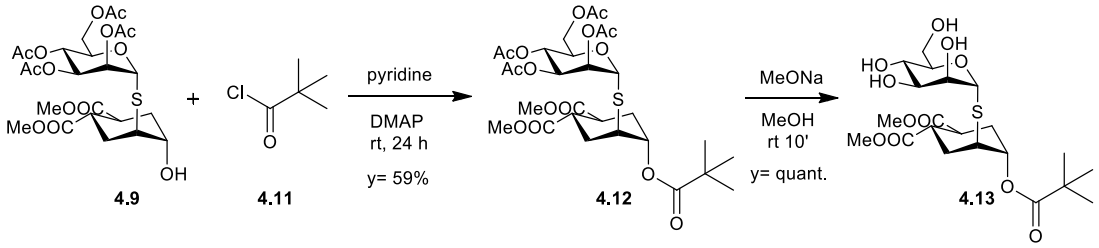

Scheme 4.5 Functionalization of **4.9** with pivaloyl chloride **4.11** and subsequent deacetylation to obtain compound **4.13**

This compound could be selectively deacetylated under Zemplén conditions (using a 0.02 M solution of MeONa in anhydrous MeOH), affording the final mimic **4.13** in quantitative yield and confirming that the pivalic framework was bulky enough to allow selective hydrolysis of the acetyl groups.

Having tested the resistance of a bulky ester, we looked for something similar: a simple molecule, possibly disubstituted in α-position, with an azide at the end of a short aliphatic chain.

In 2010 Sewald and co-workers reported the synthesis of a β-azidopivalic acid **4.15**, starting from the β-chloropivalic acid **4.14** (**Scheme 4.6**).[13]

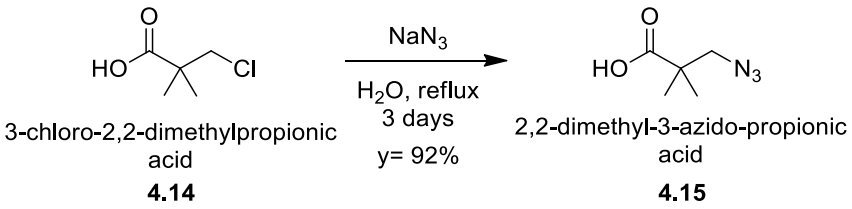

Scheme 4.6 Conditions reported by Sewald et al.[13] for the synthesis of **4.15**

The reaction is performed in refluxing water, using excess of NaN_3 and worked-up by acidifying the cooled mixture to pH 2-3 by addition of concentrated aqueous hydrochloric acid. We deemed this procedure unsafe, since highly toxic and explosive HN_3 is produced. Additionally, the product **4.15** itself is to be considered with caution, since the rule of thumb to gauge the safety of organic azides is the one reported below:

$$\frac{(N_{Carbon} + N_{Oxygen})}{N_{Nitrogen}} \geq 3$$

The sum of the total number of carbon atoms plus the total number of oxygen atoms divided by the total number of nitrogen atoms should not exceed (or be equal at least) 3. The calculated ratio for the azido pivalic acid **4.15** is 2.3, meaning that this compound must be handled very carefully.

For these reasons, the reaction conditions of the Cl→N_3 exchange reported by Sewald were modified and the work-up procedure made safer, starting from the same β-chloropivalic acid **4.14** (commercially available at low cost, 5 g/ 21,60 €). The process was performed in *N,N*-dimehtylformamide, at 60°C for 3 days (**Scheme 4.7**) and finally the crude was diluted with non-flammable dichloromethane and filtered over celite, which removed the excess sodium azide, avoiding acidification of the mixture.

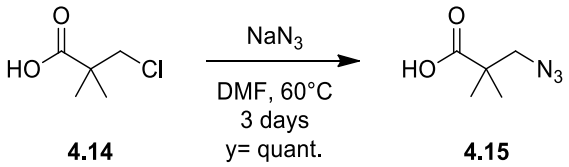

4.14 **4.15**

Scheme 4.7 Our conditions for the preparation of **4.15**

The formation of the azido compound **4.15** was confirmed by the up-field shift of the methylene group observed in the ^{1}H-NMR of the crude from 3.63 ppm in the chloride to 3.43 ppm in the azide (**Fig. 4.19**).

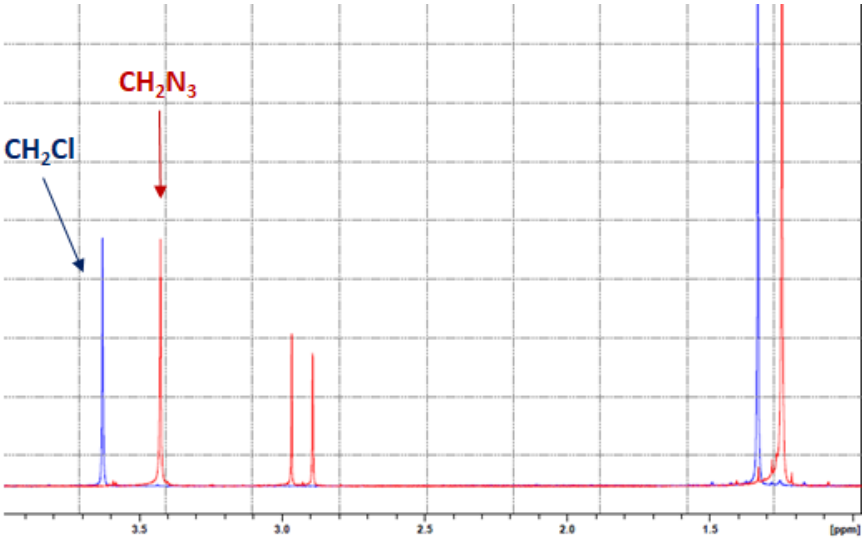

Fig. 4.19 ^{1}H-NMR ($CDCl_3$) spectra of **4.14 (**in blue) and **4.15** (in red) superimposed: see the shift of the CH_2 signal next to the Cl in **4.14** from 3.63 to 3.43 ppm.

For the coupling between **4.15** and **4.9** we took inspiration again from Sewald's work who described the esterification of a secondary alcohol with the acyl chloride of **4.15**, freshly prepared *in situ* (**Scheme 4.8**).[13]

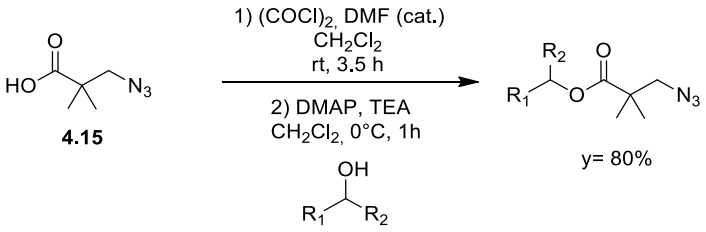

4.15

Scheme 4.8 Conditions for the esterification of the carboxylic function of **4.15** proposed by Sewald et al.[13]

These conditions were reproduced in our laboratory, increasing the temperature to 40°C (boiling point of the solvent, **Scheme 4.9**). This transformation occurred by using oxalyl chloride, a catalytic amount of DMF in dichloromethane for 3 h.

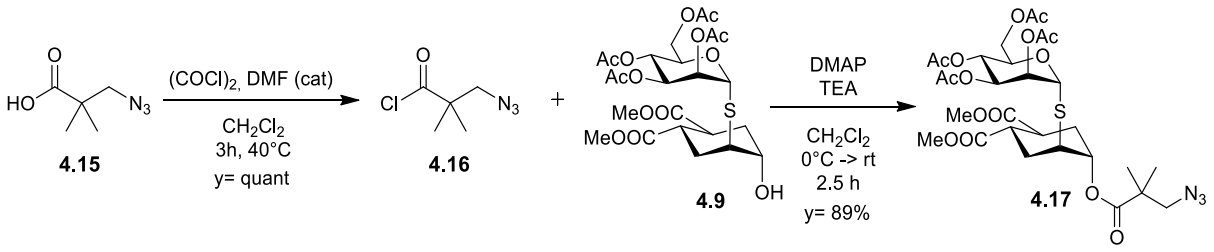

Scheme 4.9 Esterification coupling between **4.9** and the corresponding acyl chloride of **4.15** to generate **4.17**

In this process, the real chlorinating agent is the imidoyl chloride generated *in situ* from the reaction between DMF and the oxalyl chloride (**Fig. 4.20**). Then the reaction proceeds as reported below, regenerating the DMF catalyst and affording the product as the acyl chloride **4.16**.

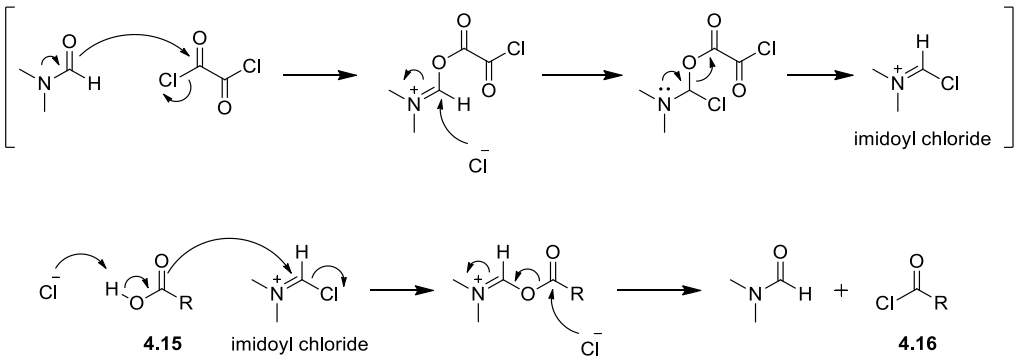

Fig. 4.20 Mechanism for the synthesis of the acyl chloride **4.16** using DMF and oxalyl chloride

In the next step (**Scheme 4.9**), after testing milder conditions for the esterification process (pyridine as solvent and dimethylaminopyridine, at different temperatures) without obtaining yields above 40%, the protocol of Sewald was followed: it involved the use of DMAP and triethylamine (equimolar to **4.16**, used in excess compared to **4.9**) for the esterification of a secondary bulky alcohol. In our case, the process occurred at room temperature (after the addition of **4.16** as last reactant at 0°C) and proceeded for 2.5 h, affording the ester **4.17** in good yield (89%, **Scheme 4.9**).

Finally, the pseudo-thiodisaccharide **4.17** underwent Zemplén deacetylation in the conditions previously tested for the pivaloate ester **4.12** (**Scheme 4.10**).

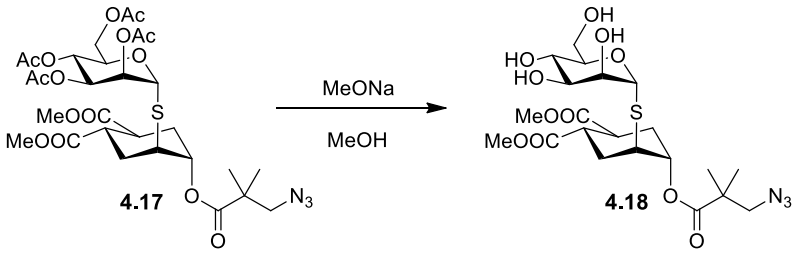

Scheme 4.10 Deacetylation of **4.17**

In the first experiment, this hydrolysis reaction was performed in a very small scale (8 mg, **Table 4.8** entry 1) and the yield of the isolated product was quantitative. However, when the reaction was scaled up to 50 mg,

50% of fully hydrolysed compound **4.10** was found in the ^{1}H-NMR of the crude (entry 2). **4.18** was anyway isolated from the mixture, confirming its stability under chromatographic conditions.

Table 4.8 Optimization of the deacetylation conditions of **4.17**

Entry	Scale	[MeONa/MeOH]	$[4.17]_f$	T	Reaction time	4.10[a]	y
1	8 mg	0.02 M	0.02 M	r.t.	10 min	not observed	quant.
2	50 mg	0.02 M	0.02 M	r.t.	10 min	50%	29 %[b]
3	50 mg	0.02 M	0.02 M	0°C	12 min	51%	/
4	30 mg	0.01 M	0.02 M	0°C	20 min	not observed	quant.
5	50 mg	0.01 M	0.02 M	0°C	25 min	27%	/

[a] (hydrolyzed product) measured by ^{1}H-NMR spectrum of the crude
[b] isolated product by chromatographic column, CH_2Cl_2:MeOH (95:5)

The process performed at 0°C did not lead to any improvements (entry 3). At this point, we came back to a smaller scale (30 mg), decreasing the concentration of the methoxide solution (to 0.01 M, entry 4) and maintaining the lower temperature. The reaction was quenched after 20 min, when the spot of the starting peracetylated sugar disappeared on the TLC (95:5 CH_2Cl_2:MeOH, cerium ammonium molibdate stain). In this case, no product of hydrolysis was observed in the crude and compound **4.18** was isolated in quantitative yield. The attempt to reproduce these conditions on a bigger scale was useless (entry 5).

In conclusion, although the pivalic azido linker was rationally selected to survive in hydrolytical conditions, the Zemplén deprotection had to be performed very carefully and in mild conditions to limit the formation of the hydrolysed compound.

Although this approach was efficient enough to allow the synthesis of multivalent compounds (see Chapter 4.1.8), the results obtained made prohibitive the scale up of the process and forced us to reconsider the synthetic strategy for the preparation of these mimetics (see Chapter 5 of Aziridines).

4.1.6 Surface Plasmon Resonance (SPR) inhibition studies with DC-SIGN

In order to investigate the biological activity of these new thio-glycomimetics and to compare their affinity towards DC-SIGN to the original pseudo-dimannoside **2.1**, compounds **4.10** and **4.13** were tested by Surface Plasmon Resonance (SPR) inhibition assays from Franck Fieschi's group, in Grenoble. In particular, through these tests, the ability of the glycomimetics to inhibit DC-SIGN ECD (Extra Cellular Domain) binding to immobilized mannosylated Bovine Serum Albumin (Man-BSA) on a SPR sensor chip was measured. The IC_{50} values (obtained from the same campaign) are reported below (**Fig. 4.21**).

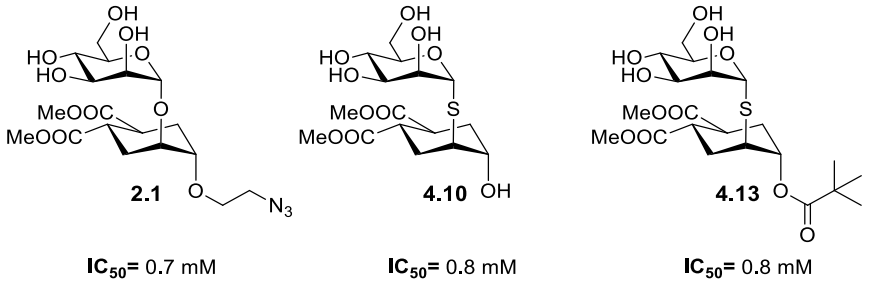

Fig. 4.21 IC_{50} values obtained through SPR inhibition assay for the final pseudo-thiodisaccharides **4.10** and **4.13**, compared to that of the pseudo-dimannoside **2.1**

The biological results revealed that, replacing the glycosidic oxygen atom of **2.1** with a sulphur, the activity remained perfectly comparable with the corresponding *O*-linked glycomimetics and also the presence of a bulky substituent connected to the cyclohexane ring did not affect the affinity for the receptor.

4.1.7 Mannosidase stability

As mentioned before, these new thio-mimetics were designed to be first of all more metabolically stable than the original pseudo-dimannoside **2.1**. The stability of **2.1** to enzymatic hydrolysis was previously investigated: the molecule is a substrate of jack-bean mannosidase, but it appeared to be significantly more resistant (8-fold) than the natural disaccharide.[10] The experiment consisted of an incubation of the glycomimetic (for 30 min at 37°C) with increasing concentrations of the enzyme (from 0.5 μg/mL to 10 μg/mL); afterwards the mixture was lyophilized and the products analyzed by GC. The extent of the hydrolysis was evaluated by integration of the peaks relative to **2.1** and to the aglycon part (found as product of the hydrolysis).

To compare the stability of the pseudo-thiodisaccharide **4.10** to the *O*-analog **2.1**, we set up a different experiment: the test was performed into an NMR tube, in a buffer solution of KH_2PO_4 in deuterium oxide (D_2O) at pH 4.5 (maximum activity pH for the α-mannosidase employed), where the substrate was added first and finally the enzyme. In these experiments the concentration of the enzyme was more than 10-fold higher (140 μg/mL) compared to the previous tests performed in 2004. The enzyme utilized for this experiment was the α-mannosidase from *Canavalia ensiformis* (Jack bean) that is commercially available as an ammonium sulfate suspension (3 M) at pH 7.5. The extent of hydrolysis was evaluated by NMR spectroscopy, by recording proton spectra over time.

In **Fig. 4.22** are reported the spectra recorded at different time for compound **2.1**. We followed the disappearance of the H_1 proton of the pseudo-dimannoside (4.95 ppm) and the appearance of the H_1 of free mannose (5.10 ppm) that is released when the glycosidic bond is cleaved by the enzyme. After only 85 min, complete hydrolysis of **2.1** was observed: indeed the last spectrum (bottom trace) revealed only the presence of the anomeric proton of the free mannose unit.

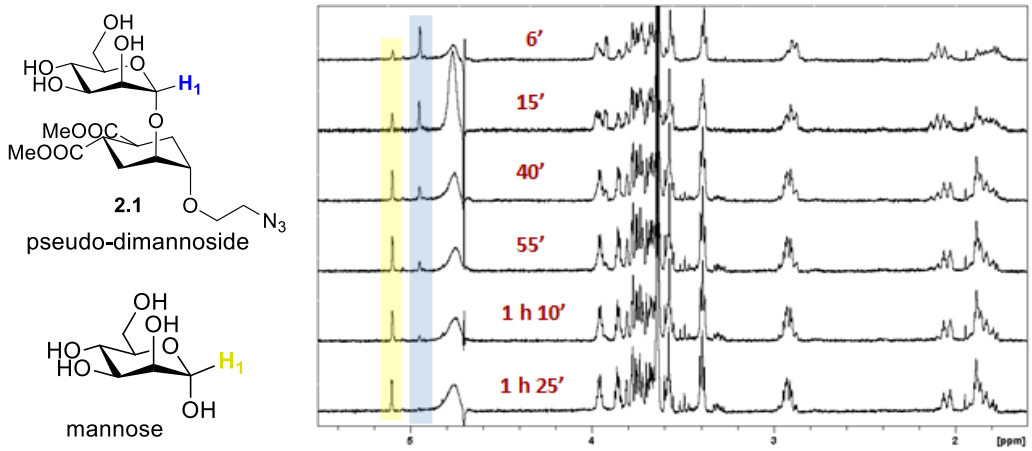

Fig. 4.22 Hydrolysis of **2.1** over the time monitored by ^{1}H-NMR spettroscopy; highlighted in blue the H_1 signal of **2.1** at 4.95 ppm, in yellow the H_1 signal of the free mannose at 5.10 ppm

The same experiment performed for the thio-glycomimetic confirmed the higher resistance of this compound towards enzymatic hydrolysis, since no degradation of **4.10** was observed, even after 24 h (see the last spectrum on the bottom where **4.10** appeared clearly intact, **Fig. 4.23**).

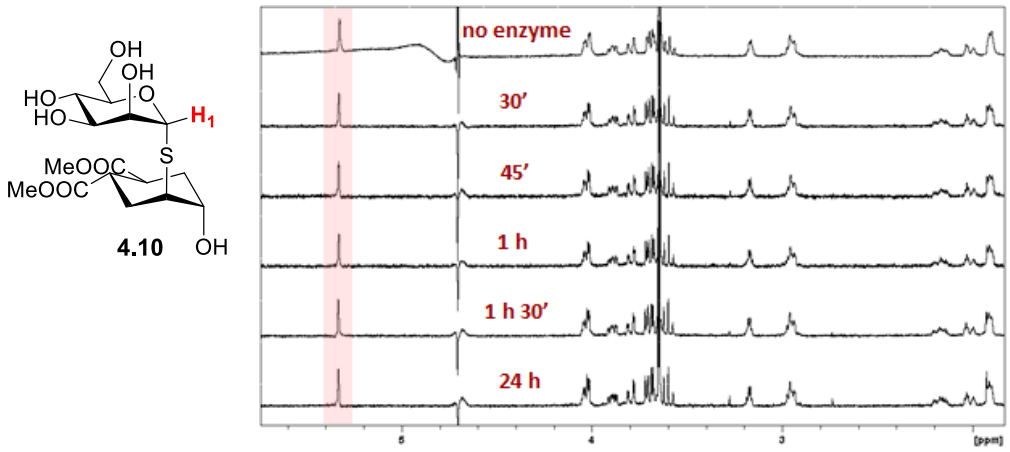

Fig. 4.23 Experiment performed for **4.10** that did not show any hydrolysis; highlighted in red the H_1 signal og **4.10** at 5.33 ppm

4.1.8 Creation of multivalent systems

As mentioned in the Introduction, multivalent carbohydrate presentations can be exploited to overcome the low affinity typical for the interaction between sugars and lectins. During my visit in Sevilla, at the "Instituto de Investigaciones Químicas-IIQ" under the supervision of Dr. F. Javier Rojo, I worked on the synthesis of multivalent scaffolds, such as dendrimers and glyconanogels, both decorated with the pseudo-thiomannoside **4.18** to be used as DC-SIGN antagonists.

4.1.8.1 As dendrimers

The dendrimer core **4.19** (**Scheme 4.11**) bearing three terminal alkyne functions had already been synthetized by Rojo's group; it was then coupled with two commercially available spacers of different length, the chloroethyl ether **4.20** and the tetraethylene glycol dichloride **4.21**.

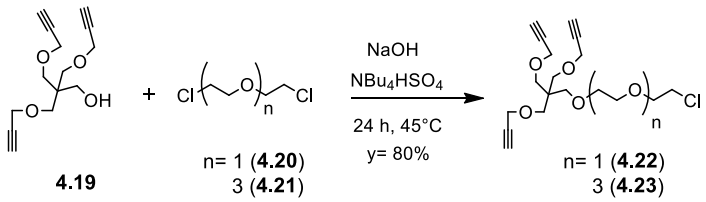

Scheme 4.11 Synthesis of the dendrimer cores **4.22** and **4.23** starting from commercially available chloroethyl ether **4.20** and tetraethylene glycol dichloride **4.21**

The processes were set up in the same conditions, using NaOH and tetrabutylammonium hydrogensulfate at 45°C for one day, employing a very large excess of the chlorinated peg chains. In both cases the final compounds (**4.22**, **4.23**) were obtained in about 80% yield of the isolated products.

Afterwards, the Cu(I)-catalyzed azido-alkyne cycloaddition (CuAAC) was performed with the azido compound **4.18** on **4.22** and **4.23** under micro-wave irradiation, at 60°C, using $CuSO_4$ as copper source, sodium ascorbate as reductant specie and TBTA as stabilizer of the active form of the metal-catalyst (**Scheme 4.12**).

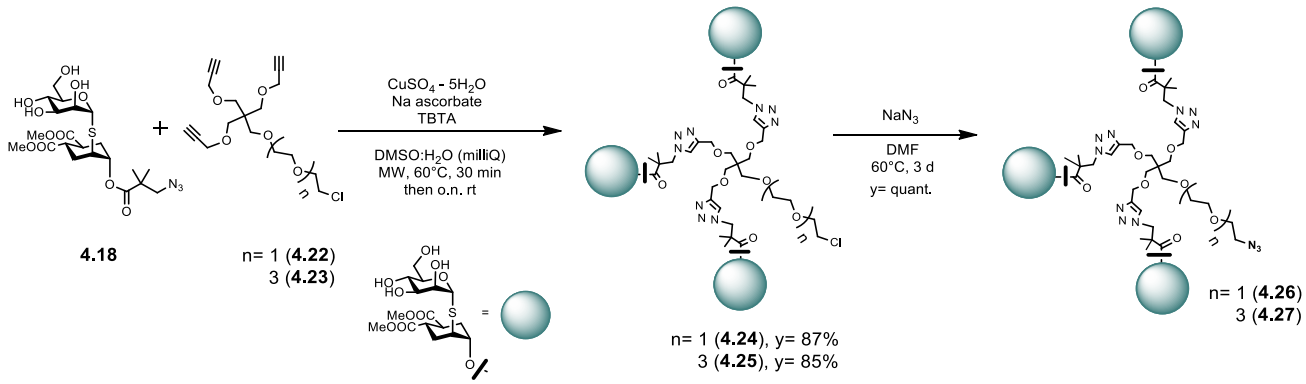

Scheme 4.12 Synthesis of dendrimers **4.26** and **4.27** decorated with thio-glycomimetic **4.18**

The trivalent systems **4.24** and **4.25** were purified through size exclusion chromatography (using a Sephadex LH-20 column in methanol) and the clean compounds, obtained in excellent yields, analyzed by ESI-MS and NMR spectroscopy. Subsequently, the chloride of **4.22** and **4.23** was replaced with an azide in standard conditions to afford the final products **4.26** and **4.27** in quantitative yield (after another purification by Sephadex).

At this point, 4.**26** and **4.27** could be exploited directly as multivalent DC-SIGN ligands or incorporated in a more complex structures (like glyconanogels) to further raise the multivalency, thanks to the presence of that terminal azides.

4.1.8.2 As glyconanogels

Nanogels (NGs) are a type of cross-linked, nanometric-sized hydrogel particles with a tunable size and an interior network that is typically used for the incorporation of therapeutics. NGs are soft, flexible and quite stable.[14-16] These structures require an easy preparation and they have been mainly employed as drug and gene delivery system. Recently (in 2011), Haag and his team highlighted the potential of these nanostructures

as antiviral agents.[17] Later on, Rojo's group developed a straightforward preparation of glycoNGs specifically designed to inhibit viral infections by multivalent interaction with the cellular receptor DC-SIGN, mimicking the virus dimension (**Fig. 4.24**). In particular, their glyconanogels have been decorated with multiple copies of mannose that are exposed on the nano-particle surface (results not published yet). The antiviral activity towards pseudo-Ebola virus of these structures are under investigations.

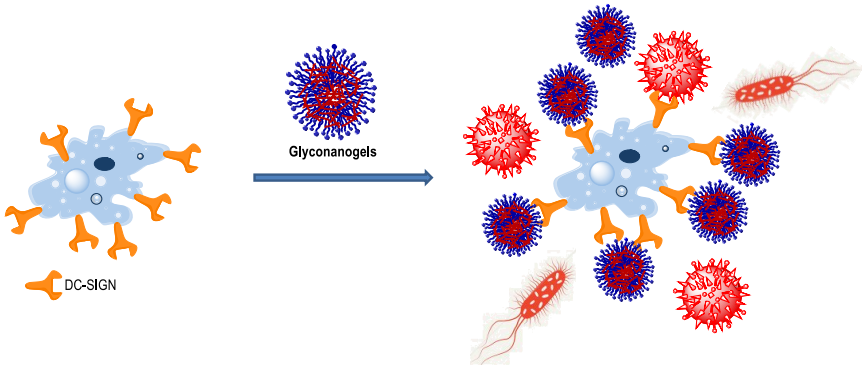

Fig. 4.24 Antiviral activity of glycoNGs by multivalent interaction with DC-SIGN receptors

With the aim to further improve the activity of these structures, we decided to prepare glycoNGs incorporating the thio-glycomimetic **4.18**.

Below the preparation of the glyconanogels is reported schematically (**Fig. 4.25**).

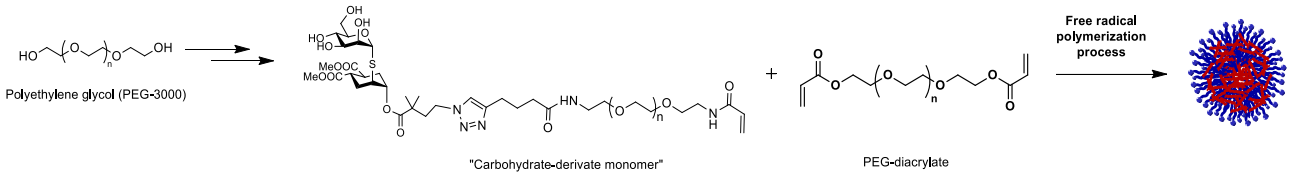

Fig. 4.25 General procedure for the preparation ofglyconanogels decorated with glycomimetic **4.18**

The preparation of the glyconanogels starts with a commercially available polyethylene glycol (PEG-3000), chosen since the presence of PEG moieties in the molecule should result in an enhanced biocompatibility and longer circulation times in the blood stream (stealth properties). This structure undergoes some modifications (synthesis developed and optimized by Noelia de la Cruz, PhD student, and Ana Sousa-Herves, Post-doc of Rojo's group; results not published yet) until the formation of the alkyne **4.28**. Personally, I performed the subsequent CuAAC coupling between **4.28** and mimetic **4.18** to generate the polymerizable building block **4.29** as "carbohydrate-derivate monomer" (**Scheme 4.13**).

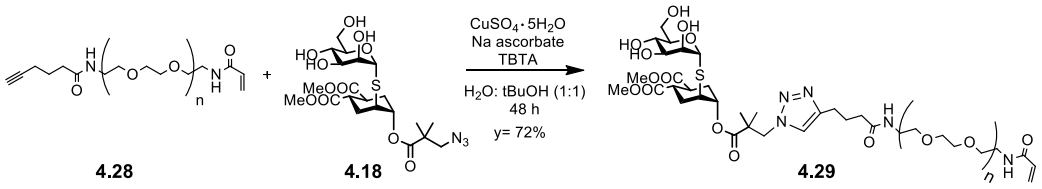

Scheme 4.13 Click reaction between **4.28** and **4.18** to generate the carbohydrate-derivative monomer **4.29**

4.29 was purified by Sephadex LH-20 column in MeOH and then analysed and characterized by NMR spectroscopy. The next step was the creation of the glyconanogels, through free-radical polymerization process, using inverse miniemulsion to template NGs formation. Miniemulsion technique allowed the creation of stable nanodroplets (typically with size range in 50-500 nm) in a continuous phase by applying ultrasonication.[18-19] The formation of the miniemulsion was followed and confirmed by Dynamic Light Scattering (DLS). The procedure was optimized by Rojo's group (results not published yet).

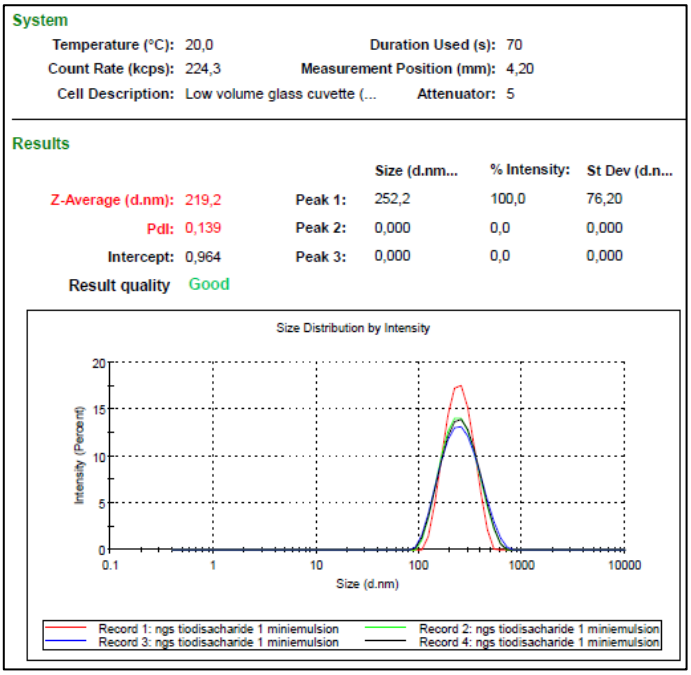

Fig. 4.26 DLS analysis of the miniemulsion that showed the presence of only one population of nanoparticles

The DLS analysis (**Fig. 4.26**) showed that the miniemulsion was composed by only one population of nanoparticles (diameter average= 200 nm), with a relatively narrow polydispersity (PdI < 0.2).

Subsequently the polymerization took place inside the nanodroplets with the addition of an initiator and finally, an extensive purification afforded the desired glycoNGs, which were characterized by DLS. The DLS analysis revealed the presence of particles with a hydrodynamic diameter around 100 nm and narrow size distribution (**Fig. 4.27**).

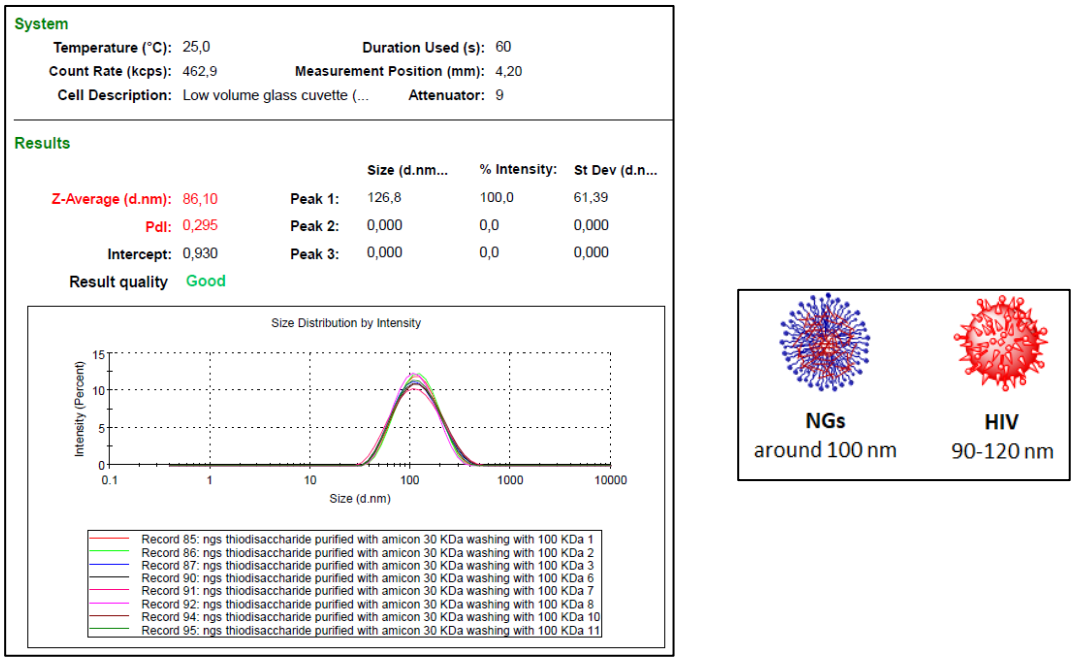

Fig. 4.27 DLS analysis of the final NGs (on the left); comparison between hydrodinamic diameters of our NGs and the HIV

The diameter of these NGs was very similar to that of HIV (90-120 nm).[20] We are currently waiting for the biological activity results obtained for these particles.

4.2 References

1) T. Belz; S. J. Williams, *Carbohydr Res* **2016**, *429*, 38-47.
2) J. J. Reina; S. Sattin; D. Invernizzi; S. Mari; L. Martinez-Prats; G. Tabarani; F. Fieschi; R. Delgado; P. M. Nieto; J. Rojo; A. Bernardi, *ChemMedChem* **2007**, *2*, 1030-6.
3) S. Dasgupta‡; V. K. Rajput‡; B. Roy; B. Mukhopadhyay, *Journal of Carbohydrate Chemistry* **2007**, *26*, 91-106.
4) P. Shu; J. Zeng; J. Tao; Y. Zhao; G. Yao; Q. Wan, *Green Chemistry* **2015**, *17*, 2545-2551.
5) Z. Pei; R. Larsson; T. Aastrup; H. Anderson; J. M. Lehn; O. Ramstrom, *Biosens Bioelectron* **2006**, *22*, 42-8.
6) R. U. Lemieux, Effects of unshared pairs of electrons and their solvation on conformational equilibria. In *Pure and Applied Chemistry*, 1971; Vol. 25, p 527.
7) Y. Hayashi, *Chem Sci* **2016**, *7*, 866-880.
8) A. Fürst; P. A. Plattner, *Helvetica Chimica Acta* **1949**, *32*, 275-283.
9) B. Brazdova; N. S. Tan; N. M. Samoshina; V. V. Samoshin, *Carbohydr Res* **2009**, *344*, 311-21.
10) S. Mari; H. Posteri; G. Marcou; D. Potenza; F. Micheli; F. J. Cañada; J. Jimenez-Barbero; A. Bernardi, *European Journal of Organic Chemistry* **2004**, *2004*, 5119-5225.
11) M. Thepaut; C. Guzzi; I. Sutkeviciute; S. Sattin; R. Ribeiro-Viana; N. Varga; E. Chabrol; J. Rojo; A. Bernardi; J. Angulo; P. M. Nieto; F. Fieschi, *J Am Chem Soc* **2013**, *135*, 2518-29.
12) A. Tamburrini; S. Achilli; F. Vasile; S. Sattin; C. Vives; C. Colombo; F. Fieschi; A. Bernardi, *Bioorg Med Chem* **2017**, *25*, 5142-5147.
13) B. Sammet; T. Bogner; M. Nahrwold; C. Weiss; N. Sewald, *J Org Chem* **2010**, *75*, 6953-60.
14) R. T. Chacko; J. Ventura; J. Zhuang; S. Thayumanavan, *Advanced Drug Delivery Reviews* **2012**, *64*, 836-851.
15) A. V. Kabanov; S. V. Vinogradov, **2009**, *48*, 5418-5429.
16) M. Asadian-Birjand; A. Sousa-Herves; D. Steinhilber; J. C. Cuggino; M. Calderon, *Current Medicinal Chemistry* **2012**, *19*, 5029-5043.
17) I. Papp; C. Sieben; A. L. Sisson; J. Kostka; C. Böttcher; K. Ludwig; A. Herrmann; R. Haag, *Chem Bio Chem* **2011**, *12*, 887-895.
18) K. Landfester, *Angew Chem Int Ed Engl.* **2009**, *48*, 4488-4507.

19) K. Landfester; A. Musyanovych, *Hydrogels in Miniemulsions*, Pich, A.; Richtering, W., Eds. Springer Berlin Heidelberg: Berlin, Heidelberg, **2011**; 39-63.
20) S. M. Dorosko; R. I. Connor, *J. Virol.* **2010**, *84*, 10533-10542.

4.3 Conclusions

A straightforward one-pot ring opening reaction between tetra-*O*-acetylmannose-1-thioacetate **4.8** and epoxide **4.5** was proposed and optimized for the synthesis of the pseudo-thiodisaccharide **4.9**, designed to mimic the pseudo-dimannoside **2.1** and thus the natural disaccharide.

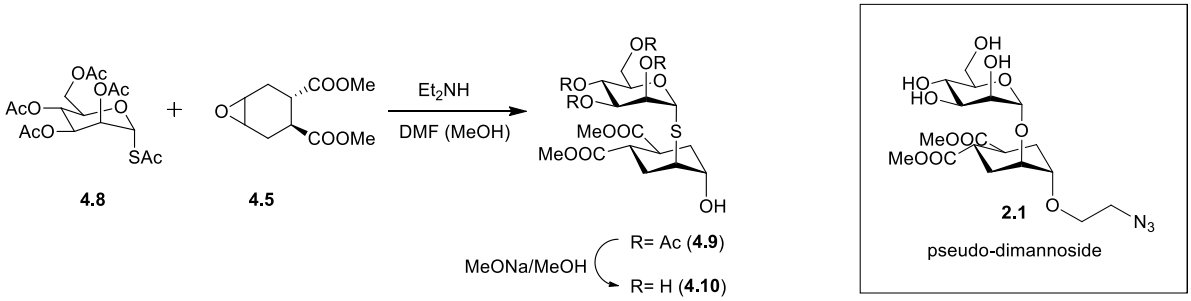

Fig. 4.28 General scheme for the preparation of the corresponding pseudo-thiodimannoside **4.10** of **2.1**

Conformational analysis of the corresponding deacetylated product **4.10** by NMR-NOESY studies, supported by molecular modelling, strongly suggested that the molecule is a mimic of the natural Mana(1,2)Man sugar and shares the conformational features of the *O*-linked analog **2.1**. Interaction studies with DC-SIGN, performed by Surface Plasmon Resonance (SPR) confirmed that the molecule acts as a DC-SIGN antagonist and has the same potency of analog **2.1**. These results were all collected and recently published.[1]

The mannosidase stability of **4.10** was tested against hydrolysis by a commercially available α-mannosidase and was found to be significantly higher than that of **2.1**.

4.10 was finally equipped with an azido-terminated ester tether (giving compound **4.18**) which survived Zemplén deprotection conditions. However, the scale-up of the deacetylation process was prohibitive for this compound that was observed to undergo hydrolysis of the ester bond.

The azido group of **4.18** allowed the creation of multivalent systems (dendrimers and glyconanogels, **Fig. 4.29**) and this work was carried out in Sevilla, under the supervision of Dr. Javier Rojo.

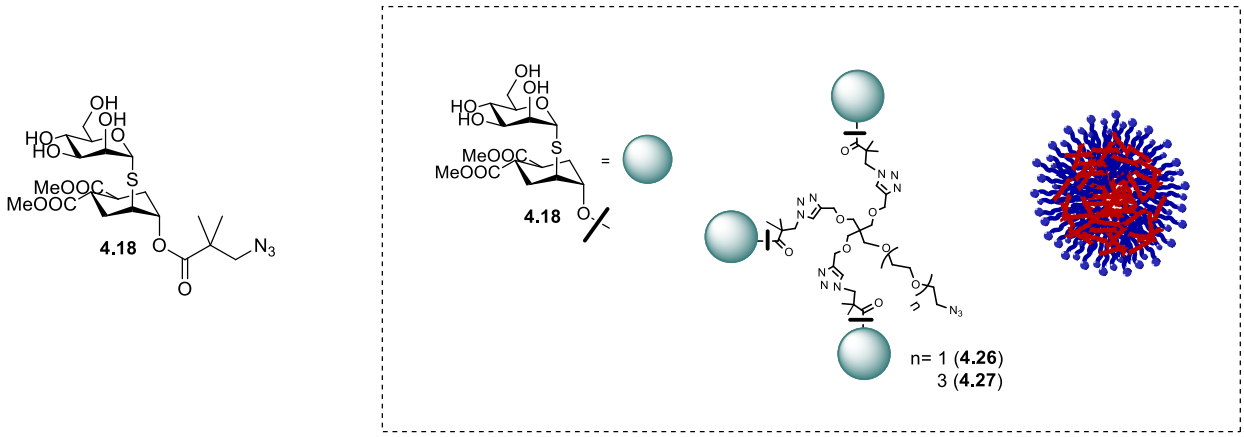

Fig. 4.29 Multivalent scaffolds decorated with the pseudo-thiodimannoside **4.18** synthesized in Sevilla

1) A. Tamburrini; S. Achilli; F. Vasile; S. Sattin; C. Vives; C. Colombo; F. Fieschi; A. Bernardi, *Bioorg Med Chem* **2017**, *25*, 5142-5147.

4.3 Experimental section

General methods and procedures for the monovalent ligands

Chemicals were purchased from commercial sources and used without further purification, unless otherwise indicated. When anhydrous conditions were required, the reactions were performed under nitrogen or argon atmosphere. Anhydrous solvents were purchased from Sigma-Aldrich® with a content of water ≤0.005%. Triethylamine (TEA), methanol and dichloromethane were dried over calcium hydride, THF was dried over sodium/benzophenone and freshly distilled. *N*,*N*-dimethylformamide (DMF) was dried over 4Å molecular sieves. Reactions were monitored by analytical thin-layer chromatography (TLC) performed on Silica Gel 60 F_{254} plates (Merck), and TLC Silica gel 60 RP-18 F_{254}s (Merck) with UV detection (254 nm and 365 nm) and/or staining with ammonium molybdate acid solution, potassium permanganate alkaline solution or ninhydrin. Flash column chromatography was performed according to the method of Still and co-workers[1] using silica gel 60 (40-63 µm, Merck). Automated flash chromatography was performed with Biotage Isolera Prime system, Biotage SNAP ULTRA cartridges were employed. Microwave irradiation was performed by a Biotage Initiator$^+$ system. The kit for the flow processes was supplied by Chemtrix (Labtrix® Start system). NMR experiments were recorded on a Bruker AVANCE-400 MHz instrument at 298 K. Chemical shifts (δ) are reported in ppm. The ^{1}H and ^{13}C NMR resonances of compounds were assigned with the assistance of COSY, HSQC and in some cases NOESY experiments. Multiplicities are assigned as s (singlet), d (doublet), t (triplet), q (quartet), quint (quintet), m (multiplet). The NOESY spectra of **4.10** were acquired using a Bruker 500 MHz instrument at 300 K. Spectra (8 scans and 256 increments) were collected using three mixing times (300, 600 and 800 ms). Water suppression was achieved by excitation−sculpting pulse sequence. Mass spectra were recorded on Apex II ICR FTMS (ESI ionization-HRMS), Waters Micromass Q-TOF (ESI ionization-HRMS) or ThermoFischer LCQ apparatus (ESI ionization. Specific optical rotation values were measured using a Perkin-Elmer 241, at 589 nm in a 1 dm cell. The following abbreviations are used: DCC (*N,N'*-dicyclohexylcarbodiimide), DCM (CH_2Cl_2 dichloromethane), m-CPBA (meta-chloroperoxybenzoic acid), DMF (*N, N'*-dimethylformamide), DMAP (4-dimethylaminopyridine), TBTA (tris[(1-benzyl-1*H*-1,2,3-triazol-4-yl)methyl]amine), TFA (trifluoroacetic acid).

SPR (Surface Plasmon Resonance) studies were carried out using a ProteOn XPR36 Protein Interaction Array Apparatus (Bio-Rad Laboratories, Hercules, CA). The instrument is characterized by six parallel flow channels that can immobilize up to six ligands on the same sensor chip.[2] Mannosylated Bovine Serum Albumin (Man-BSA, Dextra Laboratories, Reading, UK) was immobilized, as a reference, in a parallel different channel. Immobilization levels were typically 3000 and 4000 resonance units (RU, 1RU 1 pg protein/mm2), respectively.

The epoxide **4.5** was prepared as previously described[3] 2,3,4,6-Tetra-*O*-acetyl-1-*S*-acetyl-α-D-mannopyranose **4.8** was prepared from penta-*O*-acetylmannopyranose **4.7** following a reported procedure[4]

and 2,2-dimethyl-3-azido-propanoylchloride **4.16** was synthesized from commercially available 2,2-dimethyl-3-chloro-propanoic acid according to Sewald,[5] with modifications.

Synthesis of *O*-linked pseudo-thiodisaccharides

(1S,2S)-dimethyl cyclohex-4-ene-1,2-dicarboxylate 4.4

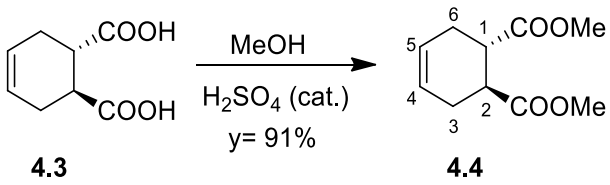

4.3 **4.4**

To a solution of diacid **4.3** (3 g, 17.6 mmol) in fresh distilled MeOH (58 mL), sulphuric acid (188 µL), was added at room temperature. The mixture was then heated to reflux (60-65°C) and stirred overnight, under nitrogen atmosphere. The reaction was monitored by TLC (Hex:EtOAc 1:1, potassium permanganate stain). The solvent was evaporated at reduced pressure to half the starting volume and then the mixture diluted with EtOAc and washed with $NaHCO_3$ and H_2O. The organic phases were dried over anhydrous Na_2SO_4 and the solvent was evaporated under *vacuum* to afford product **4.4** (3.17 g, 16 mmol) as a colourless oil in 91% yield. ^{1}H-NMR (400 MHz, $CDCl_3$): δ = 5.71-5.66 (m, 2H, H_4, H_5), 3.69 (s, 6H, 2xOCH_3), 2.91-2.81 (m, 2H, H_1, H_2), 2.47-2.36 (m, 2H, H_{3eq}, H_{6eq}), 2.24-2.12 (m, 2H, H_{3ax}, H_{6ax}).

^{1}H-NMR (400 MHz, $CDCl_3$):

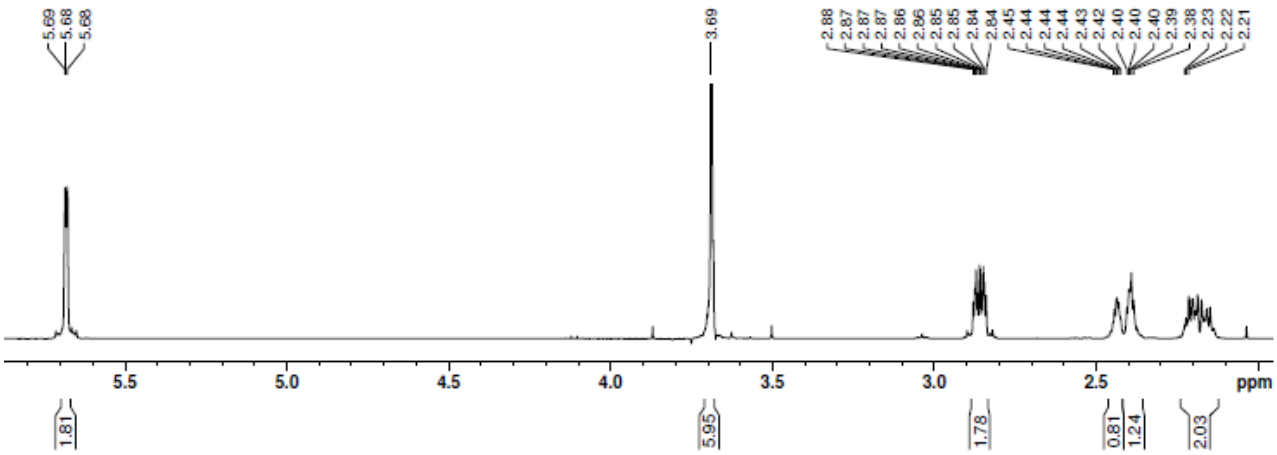

(3S-4S)-dimethyl 7-oxabicyclo[4.1.0]heptane-3,4-dicarboxylate 4.5

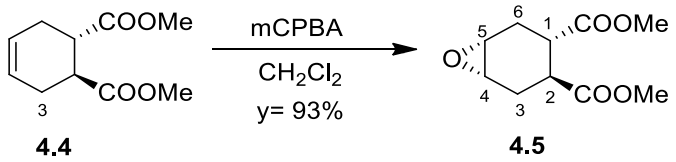

4.4 **4.5**

Compound **4.4** (180 mg, 0.91 mmol) was dissolved in fresh distilled CH_2Cl_2 (2 mL) under nitrogen atmosphere and mCPBA (225 mg, 1.27 mmol) was added. The mixture was stirred at room temperature for 2 h. The reaction was monitored by TLC (Hex:EtOAc 7:3, cerium ammonium molibdate stain). The mixture was then diluted with CH_2Cl_2 and washed with Na_2CO_3 (x2) and H_2O. The organic phase was dried over anhydrous Na_2SO_4 and the solvent was removed at reduced pressure, affording product **4.5** (181 mg, 844 mmol) in 93% yield. The spectral data of the compound corresponded to those reported[3] and no further purification was required.

^{1}H-NMR (400 MHz, $CDCl_3$): δ = 3.68 (s, 3H, OMe), 3.67 (s, 3H, OMe), 3.26-3.23 (m, 1H, H_4), 3.20-3.17 (m, 1H, H_5), 2.86 (dt, $J_{1\text{-}6eq}$= 4.8 Hz, $J_{1\text{-}2}$= $J_{1\text{-}6ax}$= 10.7 Hz, 1H, H_1), 2.62 (dt, $J_{2\text{-}3eq}$= 4.8 Hz, $J_{2\text{-}3ax}$=10.7 Hz, 1H, H_2), 2.42 (ddd, $J_{6eq\text{-}5}$= 1.8 Hz, $J_{6eq\text{-}6ax}$= 15 Hz, 1H, H_{6eq}), 2.27 (ddd, $J_{3eq\text{-}4}$= 6.7 Hz, $J_{3eq\text{-}3ax}$= 15.5 Hz, 1H, H_{3eq}), 2.06-2.02 (m, 1H, H_{3ax}), 1.90 (ddd, $J_{6ax\text{-}5}$=2.2 Hz, 1H, H_{6ax}).

^{1}H-NMR (400 MHz, $CDCl_3$):

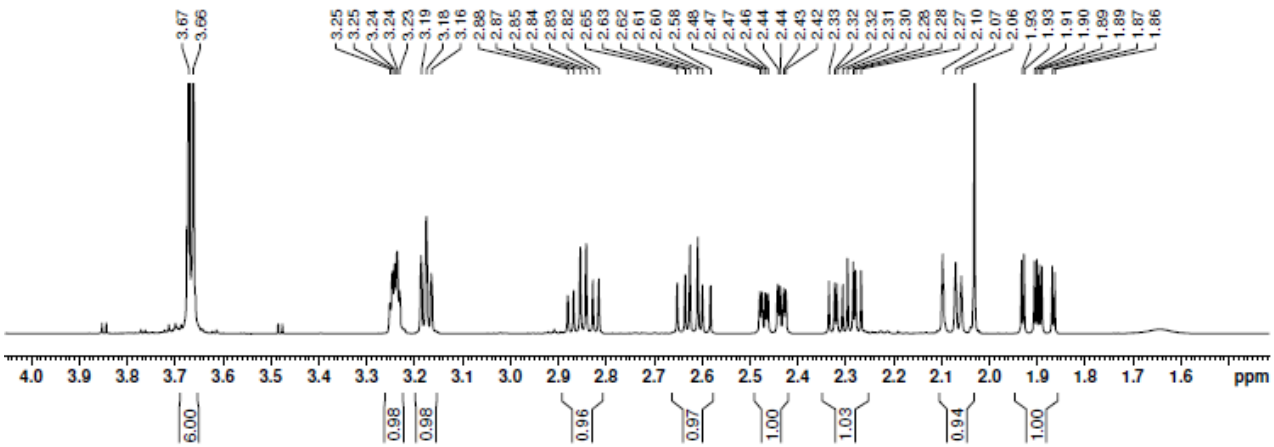

1,2,3,4,6-Tetra-O-acetyl-α-D-mannopiranose 4.7

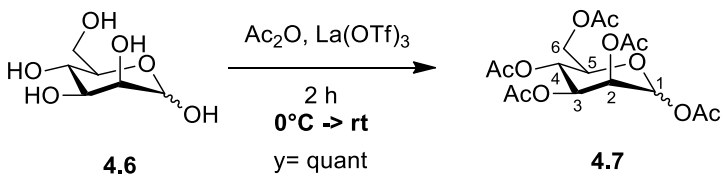

4.6 **4.7**

To a solution of mannose (5 g, 27.7 mmol) in acetic anhydride (13 mL, 138.5 mmol) under nitrogen atmosphere, $La(OTf)_3$ (49 mg, 0.083 mmol) was added at 0°C. Then the mixture was stirred at room

temperature overnight. The reaction was monitored by TLC (1:1 Hex:EtOAc, cerium ammonium molibdate stain). A saturated water solution of $NaHCO_3$ was finally added till neutral pH; the product was extracted with CH_2Cl_2 and the organic phase dried over Na_2SO_4. After removal of the solvent under reduced pressure, compound **7** (10.8 g, 27.7 mmol) was isolated in quantitative yield.

^{1}H-NMR (400 MHz, $CDCl_3$): δ = 6.08 (d, $J_{1\alpha\text{-}2\alpha}$= 1.8 Hz, 1H, $H_{1\alpha}$), 5.85 (d, $J_{1\beta\text{-}2\beta}$= 1.0 Hz, 1H, $H_{1\beta}$), 5.48 (dd, $J_{2\alpha\text{-}3\alpha}$= 3.25 Hz, $J_{2\alpha\text{-}1\alpha}$= 1.2 Hz, 1H, $H_{2\alpha}$), 5.35-5.23 (m, 4H, $H_{2\beta}$, $H_{4\beta}$, $H_{4\alpha}$, $H_{3\alpha}$), 5.12 (dd, $J_{3\beta\text{-}4\beta}$= 10.1 Hz, $J_{3\beta\text{-}2\beta}$= 3.3 Hz, 1H, $H_{3\beta}$), 4.33-4.24 (m, 2H, $H_{6\alpha}$), 4.16-4.07 (m, 2H, $H_{6\beta}$), 4.07-4.01 (m, 1H, $H_{5\alpha}$), 3.82-3.76 (m, 1H, $H_{5\beta}$), 2.21-1.99 (m, 30H, 10xOAc).

2,3,4,6-Tetra-O-acetyl-1-S-acetyl-α-D-mannopyranose 4.8

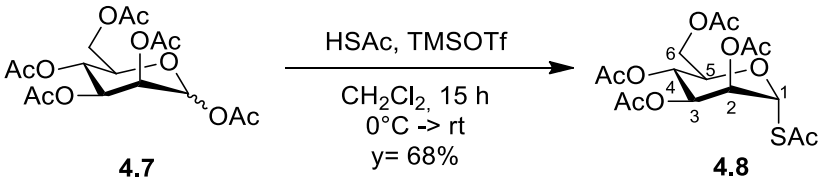

4.7 **4.8**

To a solution of penta-*O*-acetylmannopyranose **4.7** (1.021 g, 2.62 mmol) in dry CH_2Cl_2 (1.75 mL), thioacetic acid (558 µL, 7.85 mmol) was added under nitrogen atmosphere. TMSOTf (473 µL, 2.62 mmol) was added dropwise at 0 °C and the resulting mixture was stirred at room temperature overnight. After 15 h, TLC (2:8 CH_2Cl_2:iPr_2O) showed complete conversion of the starting material. The reaction mixture was diluted with CH_2Cl_2 and washed with satd aq $NaHCO_3$ and H_2O. The organic phase was dried over anhydrous Na_2SO_4, filtered and concentrated in vacuo. The crude material was purified by automated flash chromatography (Biotage, ULTRA column, HP samplet) (2:8 CH_2Cl_2:iPr_2O) to afford **4.8** (723 mg, 1.78 mmol) in 68% yield. TLC: R_f = 0.35 (CH_2Cl_2:iPr_2O 2:8); ^{1}H-NMR (400 MHz, $CDCl_3$): δ = 5.93 (d, $J_{1\text{-}2}$= 1.6 Hz, 1H, H_1), 5.35-5.27 (m, 2H, H_4, H_2), 5.08 (dd, $J_{3\text{-}4}$= 10 Hz, $J_{3\text{-}2}$= 3.2 Hz, 1H, H_3), 4.26 (dd, $J_{6a\text{-}6b}$= 12.4 Hz, $J_{6a\text{-}5}$= 4.8 Hz, 1H, H_{6a}), 4.05 (dd, $J_{6b\text{-}6a}$= 12.4 Hz, $J_{6b\text{-}5}$= 2.4 Hz, 1H, H_{6b}), 3.91 (ddd, $J_{5\text{-}4}$= 10 Hz, $J_{5\text{-}6a}$= 4.8 Hz, $J_{5\text{-}6b}$= 2.4 Hz, 1H, H_5), 2.41 (s, 3H, SAc), 2.16, 2.06, 2.02, 1.97 (4 s, 4xOAc); ^{13}C-NMR (100 MHz, $CDCl_3$): δ = 190.3 (CO), 170.5 (CO), 169.8 (CO), 169.7 (CO), 169.4 (CO), 80.1 (C_1), 72.4 (C2), 70.9 (C3), 69.8 (C4), 65.6 (C5), 62.1 (C6), 31.2 (SAc), 20.8 (OAc), 20.6 (OAc), 20.6 (OAc), 20.5 (OAc).

^{1}H-NMR (400 MHz, $CDCl_3$):

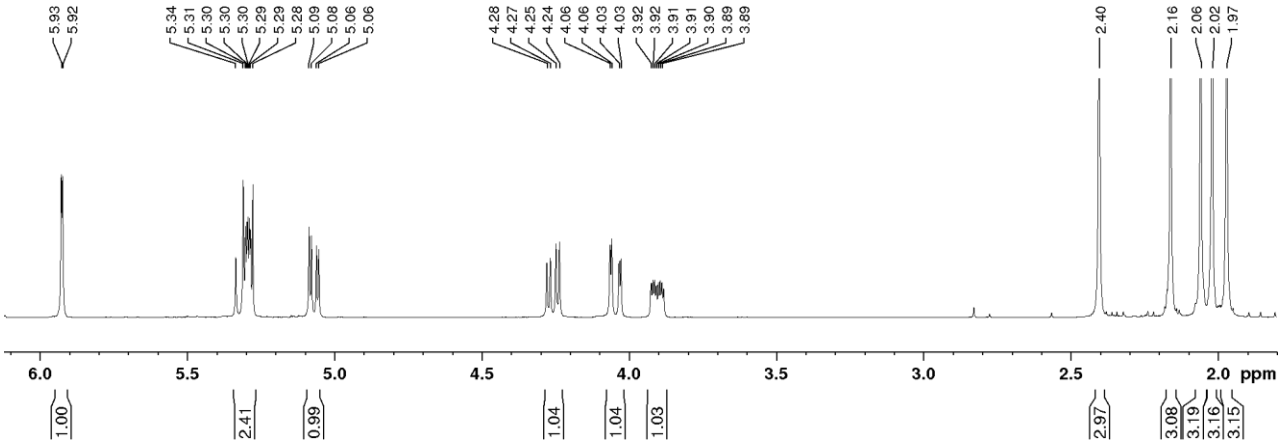

^{13}C-NMR (100 MHz, $CDCl_3$):

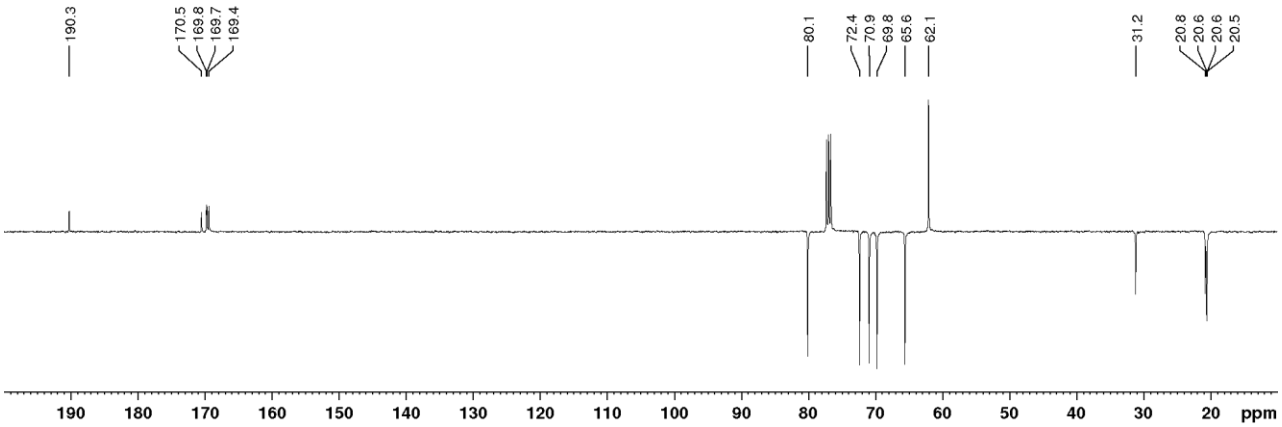

Synthesis compound 4.9

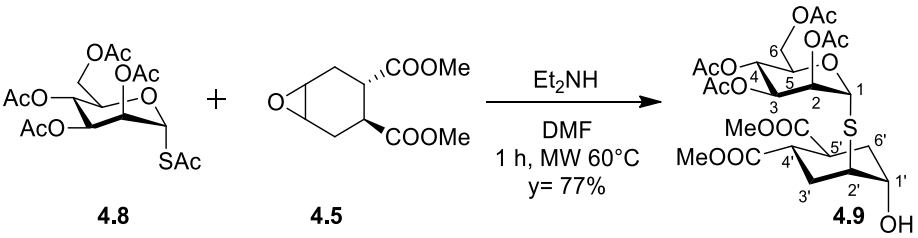

4.8 **4.5** **4.9**

Diethylamine (185 µL, 1.77 mmol) was added to a solution of thioacetate **4.8** (493 mg, 1.21 mmol) and epoxide **4.5** (200 mg, 0.93 mmol) in dry DMF (1.55 mL). The reaction mixture was stirred for 1 h, at 60°C under micro-wave irradiation, then diluted with EtOAc, washed with 1 M HCl and H_2O. The organic phase was dried over anhydrous Na_2SO_4, filtered and concentrated in vacuo. The crude material was purified by flash chromatography (4:6 Hex:EtOAc) to afford **4.9** (414 mg, 0.72 mmol) in 77% yield. TLC: R_f = 0.3 (4:6 Hex:EtOAc); $[\alpha]_D^{14}$ ($CHCl_3$, *c* 1.03)= +68; ^{1}H-NMR (400 MHz, $CDCl_3$): δ = 5.36 (dd, $J_{2\text{-}3}$ = 3.2 Hz, $J_{2\text{-}1}$= 1.5 Hz, 1H, H_2), 5.33 (d, $J_{1\text{-}2}$= 1.3 Hz, 1H, H_1), 5.26 (t, $J_{4\text{-}3}$= $J_{4\text{-}5}$= 9.9 Hz, 1H, H_4), 5.19 (dd, $J_{3\text{-}4}$= 9.9 Hz, $J_{3\text{-}2}$= 3.2 Hz, 1H, H_3), 4.40–4.34 (m, 1H, H_5), 4.24 (dd, $J_{6a\text{-}6b}$= 12 Hz, $J_{6a\text{-}5}$= 6.4 Hz, 1H, H_{6a}), 4.11 (dd, $J_{6b\text{-}6a}$= 12.3 Hz, $J_{6b\text{-}5}$= 2.6 Hz, 1H, H_{6b}), 3.86–3.78 (m, 1H, $H_{1'}$), 3.71 (s, 3H, OMe), 3.69 (s, 3H, OMe), 3.22–3.14 (m, 1H, $H_{5'}$), 3.10–2.98 (m, 2H, $H_{4'}$, $H_{2'}$), 2.40-2.30 (m, 1H, $H_{3'eq}$), 2.20–2.10 (m, 1H, $H_{6'eq}$), 2.15 (s, 3H, OAc), 2.09 (s, 3H, OAc), 2.05 (s, 3H, OAc), 1.98 (s, 3H, OAc),

1.93–1.76 (m, 2H, $H_{3'ax}$, $H_{6'ax}$); ^{1}H-NMR (400 MHz, CD_3OD): δ = 5.45 (d, $J_{1\text{-}2}$= 1.3 Hz, 1H, H_1), 5.37 (dd, $J_{2\text{-}3}$ = 3.2 Hz, $J_{2\text{-}1}$= 1.5 Hz, 1H, H_2), 5.24 (t, $J_{4\text{-}3}$= $J_{4\text{-}5}$= 9.9 Hz, 1H, H_4), 5.19 (dd, $J_{3\text{-}4}$= 9.9 Hz, $J_{3\text{-}2}$= 3.2 Hz, 1H, H_3), 4.38–4.32 (m, 1H, H_5), 4.25 (dd, $J_{6a\text{-}6b}$= 12 Hz, $J_{6a\text{-}5}$= 6.4 Hz, 1H, H_{6a}), 4.12 (dd, $J_{6b\text{-}6a}$= 12.3 Hz, $J_{6b\text{-}5}$= 2.6 Hz, 1H, H_{6b}), 4.0 (m, 1H, $H_{1'}$), 3.68 (s, 6H, 2xOMe), 3.20 (m, 1H, $H_{2'}$), 3.05 (dt, $J_{5'\text{-}4'}$= 11 Hz, $J_{5'\text{-}6'}$= 5.5 Hz, 1H, $H_{5'}$), 2.92 (dt, $J_{4'\text{-}5'}$= 11 Hz, $J_{4'\text{-}3'}$= 3.8 Hz, 1H, $H_{4'}$), 2.22–2.32 (m, 1H, $H_{3'eq}$), 2.15 (s, 3H, OAc), 2.06 (s, 3H, OAc), 2.05 (s, 3H, OAc), 2.00–2.06 (m, 1H, $H_{6'eq}$) 1.97 (s, 3H, OAc), 1.88–1.97 (m, 2H, $H_{3'ax}$, $H_{6'ax}$); ^{13}C-NMR (100 MHz, $CDCl_3$): δ = 174.1 (CO), 173.8 (CO), 170.6 (CO), 169.9 (CO), 169.7 (CO), 169.6 (CO), 82.6 (C_1), 71.1 (C_2), 69.5 (C_5), 69.3 ($C_{1'}$), 69.1 (C_3), 66.3 (C_4), 62.5 (C_6), 52.2 (OMe), 52.1 (OMe), 48.7 ($C_{2'}$), 40.3 ($C_{4'}$), 39.6 ($C_{5'}$), 31.3 ($C_{6'}$), 28.6 ($C_{3'}$), 20.8 (OAc), 20.6 (OAc), 20.6 (OAc), 20.5 (OAc); MS (ESI) calcd for $C_{24}H_{34}O_{14}S$ $[M+Na]^+$ m/z: 601.16, found 601.42; HR-MS (ESI) calcd for $C_{24}H_{34}O_{14}S$ $[M+Na]^+$ m/z: 601.15615, found 601.15571.

^{1}H NMR (400 MHz, $CDCl_3$):

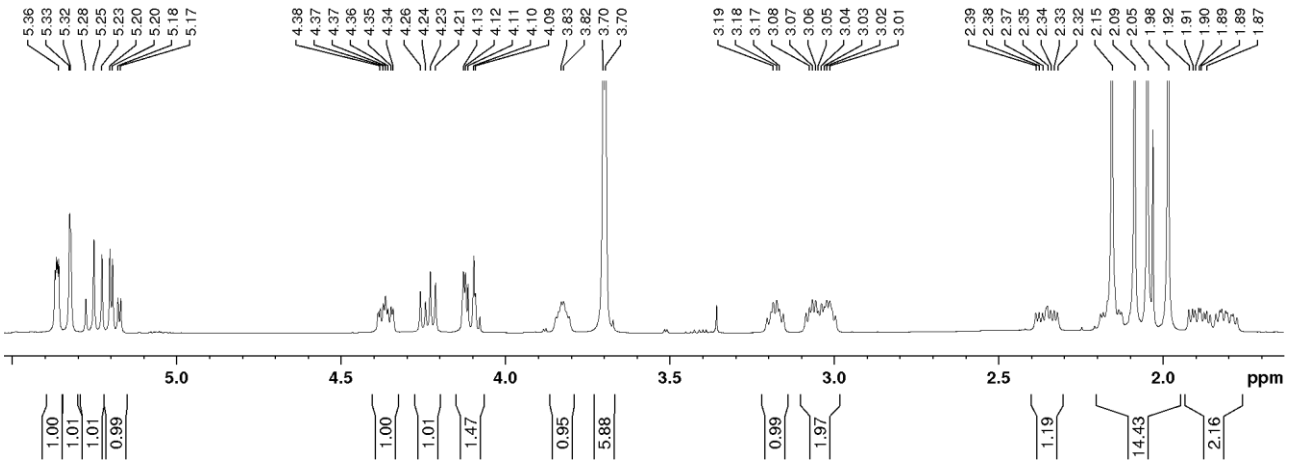

^{1}H NMR (400 MHz, CD_3OD):

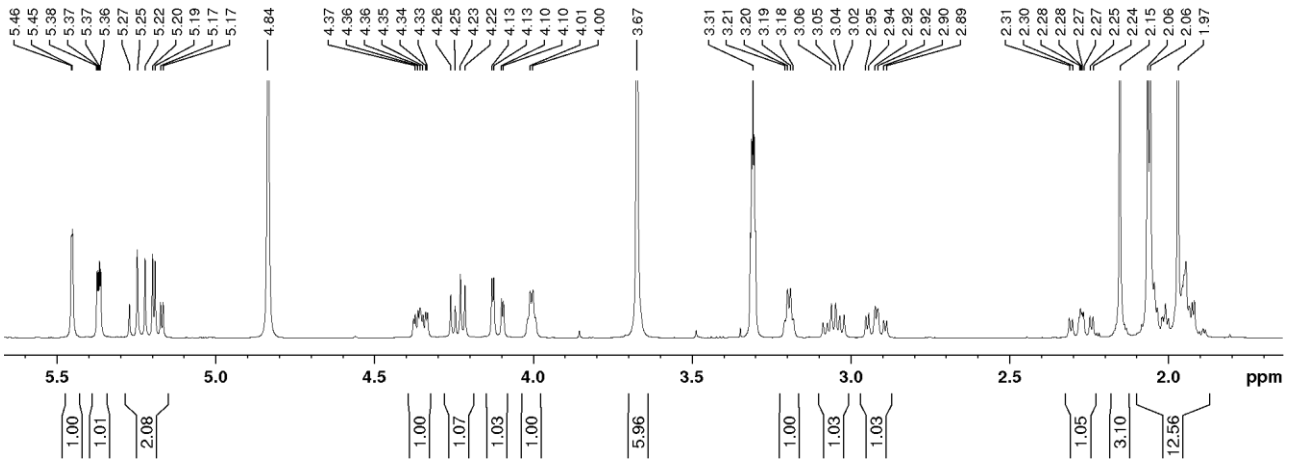

^{13}C NMR (100 MHz, $CDCl_3$):

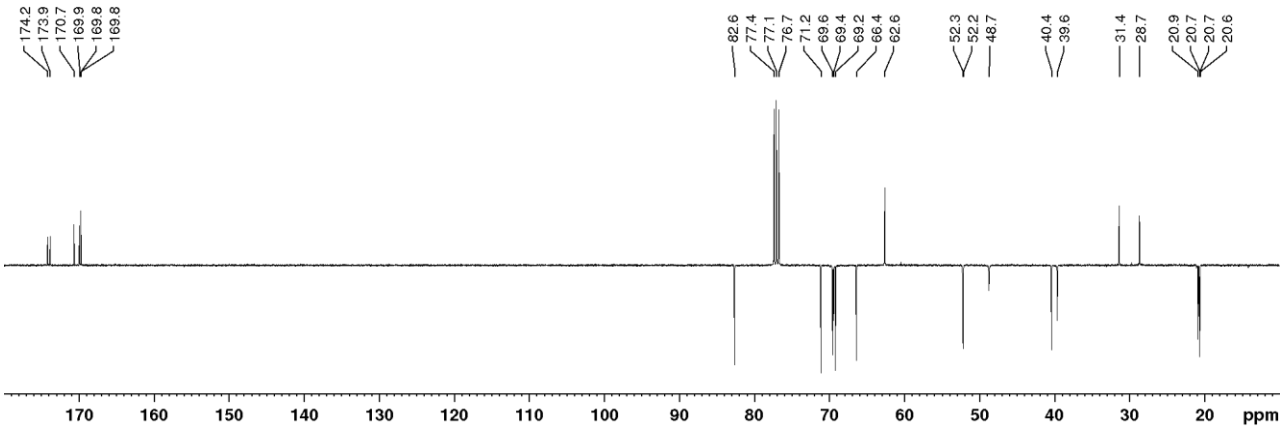

One-pot epoxide ring opening performed into a flow micro-reactor

Below, only the conditions that led to the best results are reported (see **Table 4.7**, entry 4).

175 mg (0.43 mmol, 1.3 equiv) of thioacetate **4.8** and 77 mg (0.36 mmol, 1 equiv) of the epoxide **4.5** were dissolved together in a previously sonicated dry DMF (300 µL; initial epoxide concentation 1.2 M), and charged into a gas-tight syringe of 500 µL, while the Et_2NH (71 µL, 0.68 mmol, 1.9 equiv) dissolved in a previously sonicated dry DMF (300 µL) was withdrew with the second syringe.

Micro-reactor 3222 (volume of 5 µL, depicted in the figure below) was employed: the gas-tight syringes were connected with the two inlet channels. The quench inlet was kept closed for all the process and the product **4.9** was collected outside the reactor where was analysed by ^{1}H-NMR spectroscopy, after the removal of the solvent under reduced pressure.

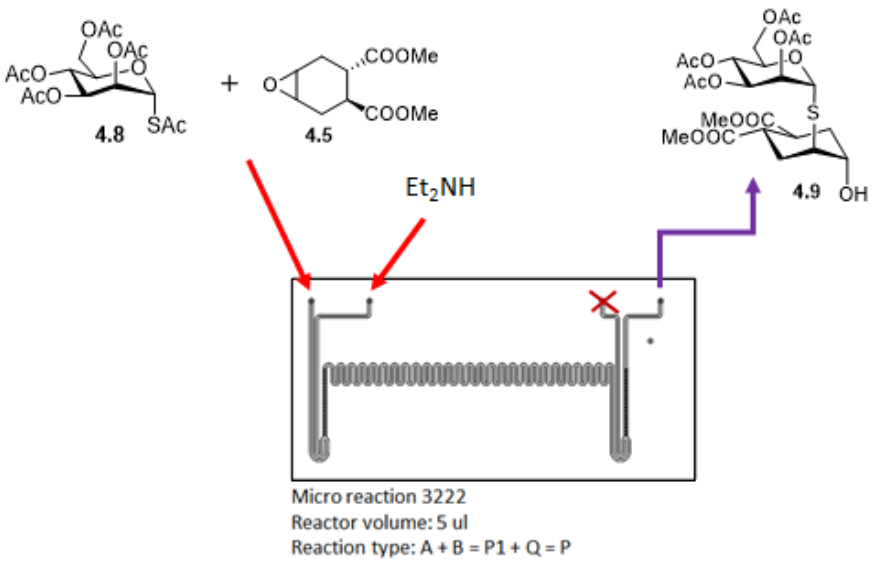

Experimental details:

concentration of the epoxide inside the micro-reactor= 0.6 M

flow of the reactants= 0.17 µl/min

temperature of the micro-reactor platform= 60°C

residence time of the reactants inside the reactor= 30 min

conversion of **4.5** into **4.9** detected by ^{1}H-NMR spectroscopy= 69%

Synthesis of compound 4.12

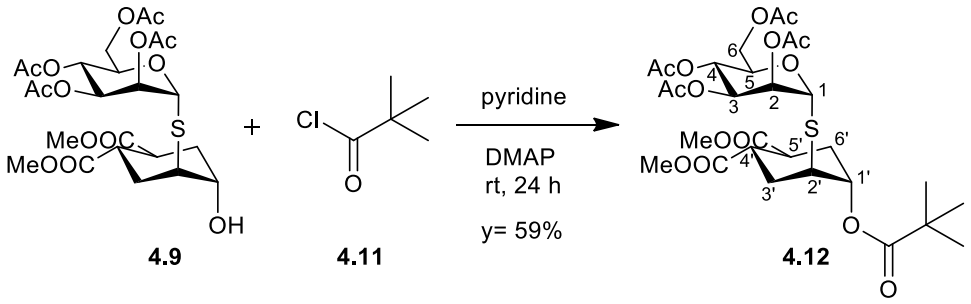

To a solution of compound **4.9** (40 mg, 0.069 mmol) in dry pyridine (150 µL), DMAP (8 mg, 0.069 mmol) and pivaloyl chloride (43 µL, 0.35 mmol) were added. The mixture was stirred at room temperature under nitrogen atmosphere. After 5 h, a second aliquot of pivaloyl chloride (25 µL, 0.21 mmol) was added. After reaction completion (24 h, monitored by TLC, 6:4 Hex:EtOAc) the mixture was diluted with EtOAc, washed with 1 M HCl, H_2O and satd aq $NaHCO_3$. The organic layer was dried over anhydrous Na_2SO_4 and concentrated under reduced pressure. Flash chromatography (6:4 Hex:EtOAc) yielded product **4.12** (27 mg, 0.041 mmol) in 59% yield. TLC= R_f 0.3 (6:4 Hex:EtOAc); $[\alpha]_D^{22}$ ($CHCl_3$, *c* 1.61)= +75; ^{1}H-NMR (400 MHz, $CDCl_3$): δ = 5.38 (d, $J_{1\text{-}2}$= 1.5 Hz, 1H, H_1), 5.35 (dd, $J_{2\text{-}3}$= 3.2 Hz, $J_{2\text{-}1}$= 1.6 Hz, 1H, H_2), 5.29 (t, $J_{4\text{-}3}$= 9.7 Hz, 1H, H_4), 5.18 (dd, $J_{3\text{-}4}$= 10.0 Hz, $J_{3\text{-}2}$= 3.3 Hz, 1H, H_3), 5.08–5.04 (m, 1H, $H_{1'}$), 4.36–4.27 (m, 2H, H5, H_{6a}), 4.16–4.07 (m, 1H, H_{6b}), 3.7 (s, 3H, OMe), 3.69 (s, 3H, OMe), 3.34–3.29 (m, 1H, $H_{2'}$), 3.01–2.87 (m, 2H, $H_{4'}$, $H_{5'}$), 2.15 (s, 3H, OAc), 2.13–2.00 (m, 10H, $H_{3'eq}$, $H_{6'eq}$, $H_{3'ax}$, $H_{6'ax}$, 2xOAc), 1.99 (s, 3H, OAc) 1.2 (s, 9H, tBu); ^{13}C-NMR (100 MHz, $CDCl_3$): δ = 177.0 (CO), 174.2 (CO), 174.1 (CO), 170.5 (CO), 169.8 (CO), 169.7 (CO), 169.5 (CO), 82.9 (C_1), 70.8 (C_2), 69.7 ($C_{1'}$), 69.6 (C_5), 69.2 (C_3), 65.9 (C_4), 62.3 (C_6), 52.0 (OMe), 52.0 (OMe), 43.6 ($C_{2'}$), 39.6 ($C_{4'}$), 39.5 ($C_{5'}$), 38.8 (C IV), 28.7 ($C_{3'}$), 27.9 ($C_{6'}$), 27.0 (3xMe, tBu), 20.8 (OAc), 20.6 (OAc), 20.5 (OAc), 20.5 (OAc); MS (ESI) calcd for $C_{29}H_{42}O_{15}S$ $[M+Na]^+$ m/z: 685.21, found 685.29.

^{1}H NMR (400 MHz, $CDCl_3$):

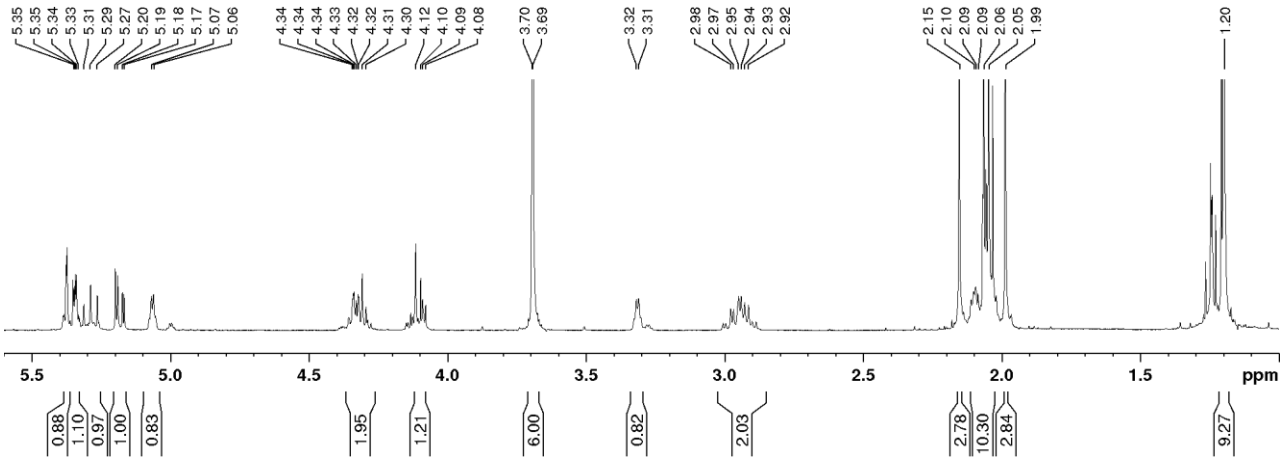

^{13}C NMR (100 MHz, $CDCl_3$):

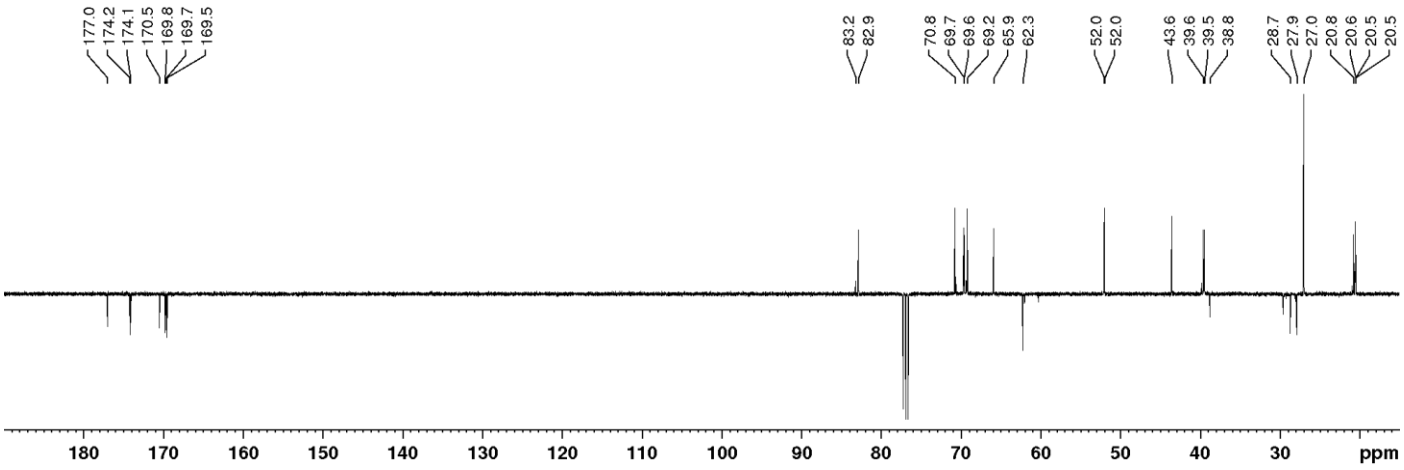

3-Azido-2,2-dimethylpropanoyl chloride 4.16

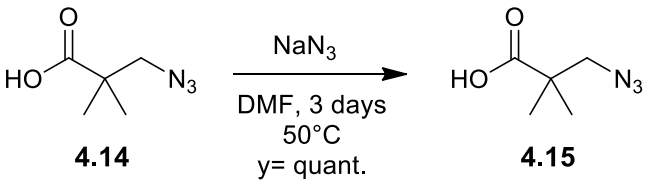

4.14 **4.15**

2,2-dimethyl-3-chloro-propanoic acid **4.14** (400 mg, 2.97 mmol) was dissolved in dry DMF (14.6 mL) and NaN_3 (990 mg, 15.2 mmol) was added. The mixture was stirred at 50°C under nitrogen atmosphere. After 3 days, the reaction was allowed to reach room temperature. The mixture was diluted with CH_2Cl_2 and filtered over a celite pad to remove unreacted NaN_3 and the generated salts (NaCl). The solvent was evaporated at reduced pressure giving 3-azido-2,2-dimethylpropanoic acid **4.15** in quantitative yield (425 mg). ^{1}H-NMR (400 MHz, $CDCl_3$): δ = 3.42 (s, 2H, CH_2), 1.25 (s, 6H, 2xCH_3).

^{1}H NMR (400 MHz, $CDCl_3$):

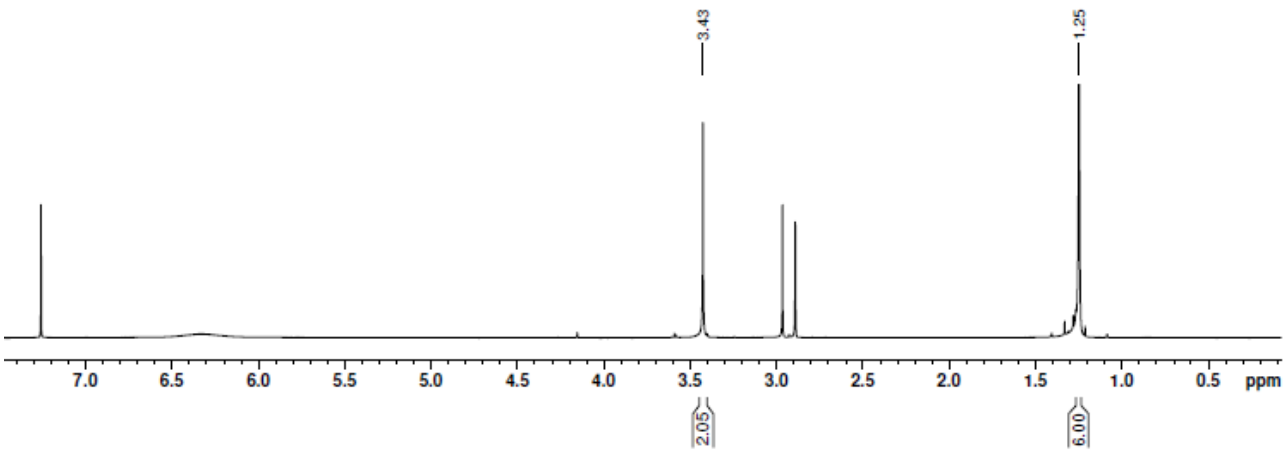

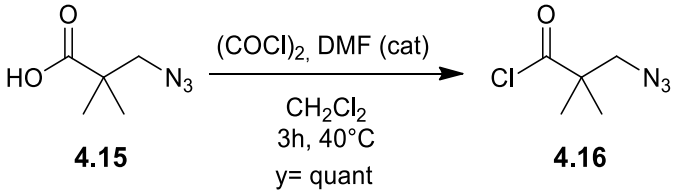

4.15 **4.16**

Acid **4.15** was used without further purification: the crude azide (143 mg, 1.00 mmol) was dissolved in fresh distilled CH_2Cl_2 (3.3 mL) and oxalyl chloride (254 µL, 2.00 mmol) was added drop wise to the solution. After the addition of one drop of dry DMF, the mixture was refluxed for 3 h. The solution was cooled to room temperature and the solvent was carefully removed in vacuo to yield 3-azido-2,2-dimethylpropanoyl chloride **4.16**. The complete conversion was confirmed by NMR analysis and the product was used in the next step without further purification. ^{1}H-NMR (400 MHz, $CDCl_3$): δ = 3.53 (s, 2H, CH_2), 1.35 (s, 6H, 2xCH_3).

^{1}H NMR (400 MHz, $CDCl_3$):

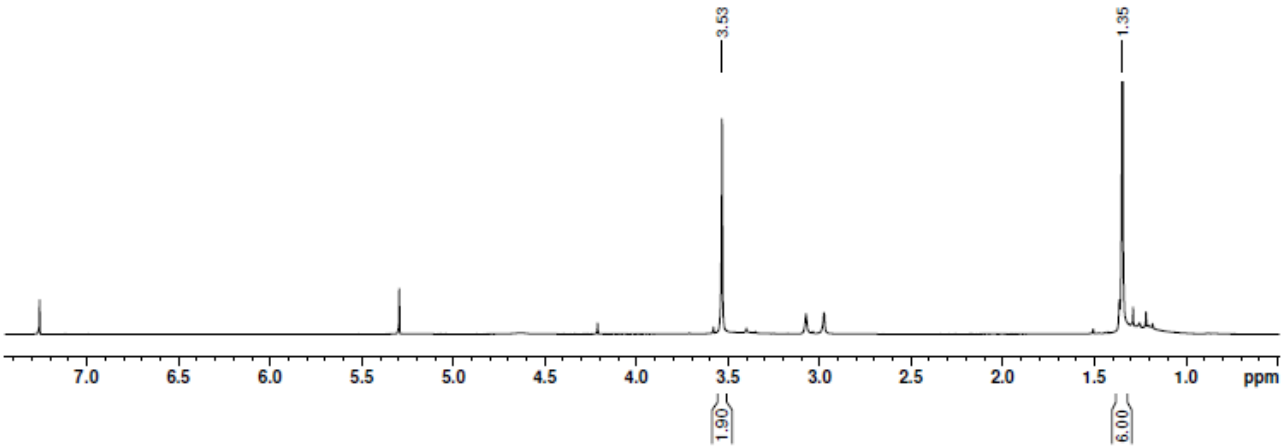

Synthesis of compound 4.17

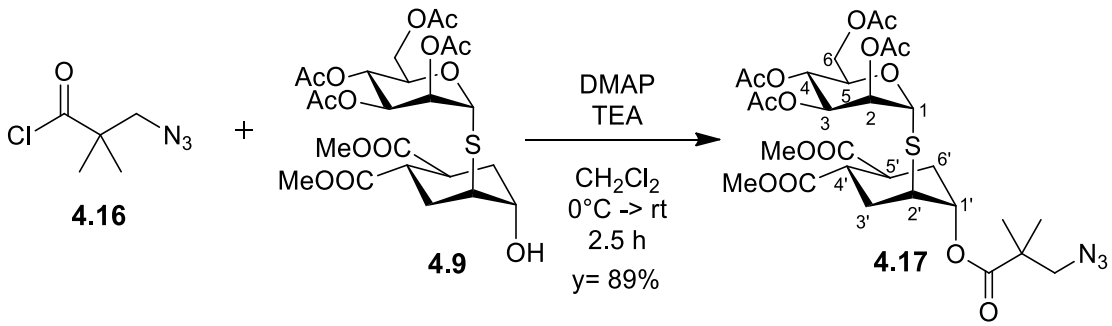

To a solution of compound **4.9** (209 mg, 0.36 mmol) in dry CH_2Cl_2 (2.7 mL) and Et_3N (112 µL, 0.81 mmol), DMAP (98 mg, 0.8 mmol) was added. The solution was cooled to 0°C and the acylchloride **4.16** (131 mg, 0.81 mmol) was added. The mixture was stirred at room temperature under nitrogen atmosphere. After reaction completion (2.5 h, monitored by TLC, 1:1 Hex:EtOAc) the mixture was diluted with CH_2Cl_2, washed with satd aq $NaHCO_3$ and 1 M HCl. The organic layer was dried over anhydrous Na_2SO_4 and concentrated under reduced pressure. Flash chromatography (6:4 Hex:EtOAc) yielded product **4.17** (226 mg, 0.32 mmol) in 89% yield. TLC: R_f 0.5 (1:1 Hex:EtOAc); $[\alpha]_D^{16}$ ($CHCl_3$, *c* 1.08)= +67; ^{1}H-NMR (400 MHz, $CDCl_3$): δ= 5.39 (m, 1H, H_1), 5.37–5.34

(m, 1H, H_2), 5.30 (t, $J_{4\text{-}3}$= 9.5 Hz, 1H, H_4), 5.19 (dd, $J_{3\text{-}4}$= 9.7 Hz, $J_{3\text{-}2}$= 3.6 Hz, 1H, H_3), 5.14–5.11 (m, 1H, $H_{1'}$), 4.37–4.30 (m, 2H, H_5, H_{6a}), 4.15– 4.07 (m, 1H, H_{6b}), 3.71 (s, 3H, OMe), 3.71 (s, 3H, OMe), 3.42 (s, 2H, CH_2N_3), 3.36–3.33 (m, 1H, $H_{2'}$), 3.03–2.89 (m, 2H, $H_{4'}$, $H_{5'}$), 2.17 (s, 3H, OAc), 2.14–2.06 (m, 4H, $H_{3'eq}$, $H_{6'eq}$, $H_{3'ax}$, $H_{6'ax}$), 2.18 (s, 3H, OAc), 2.05 (s, 3H, OAc), 2.00 (s, 3H, OAc), 1.23 (s, 3H, CH_3), 1.23 (s, 3H, CH_3); ^{13}C-NMR (100 MHz, $CDCl_3$): δ= 174.6 (CO), 174.5 (CO), 174.3 (CO), 170.8 (CO), 170.2 (CO), 170.0 (CO), 169.9 (CO), 83.3 (C_1), 71.1 (C_2), 70.9 ($C_{1'}$), 70.0 (C_5), 69.6 (C_3), 66.3 (C_4), 62.6 (C_6), 59.9 (CH_2N_3), 52.4 (2xOMe), 44.2 (C IV), 43.8 ($C_{2'}$), 40.0 ($C_{4'}$), 39.9 ($C_{5'}$), 29.1 ($C_{3'}$), 28.2 ($C_{6'}$), 23.3 (CH_3), 23.3 (CH_3), 21.1 (OAc), 20.9 (OAc), 20.9 (OAc), 20.9 (OAc); MS (ESI) calcd for $C_{29}H_{41}N_3O_{15}S$ $[M+Na]^+$ m/z: 726.2; found 726.8.

^{1}H NMR (400 MHz, $CDCl_3$):

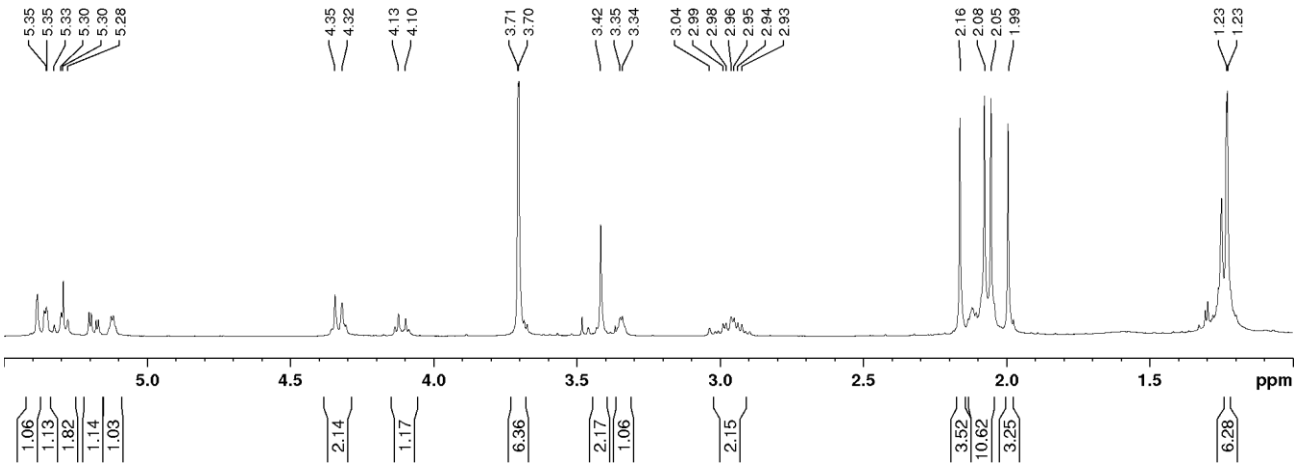

^{13}C NMR (100 MHz, $CDCl_3$):

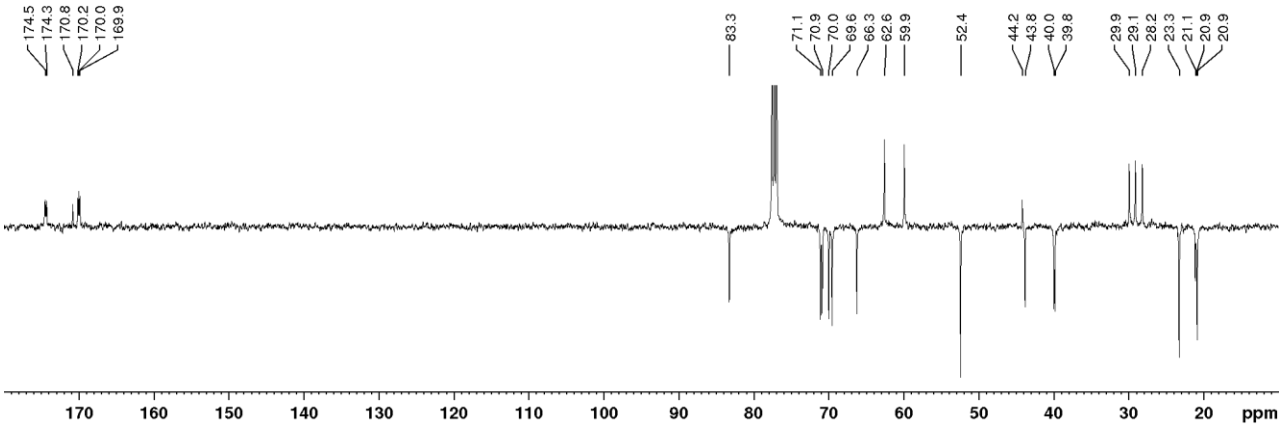

General procedure for the Zemplén deacetylation

A MeONa/MeOH solution was added to the substrate dissolved in freshly distilled MeOH under nitrogen atmosphere (substrate and MeONa final concentration 0.02 M) and the reaction mixture was stirred at room temperature. After completion, (approx. 10 min, monitored by TLC) the reaction was quenched with AMBERLITE IR-120 H+ till neutral pH, the resin was filtered off and the solvent was evaporated at reduced pressure, obtaining the pure product.

Synthesis of the pseudo-thio-1,2-dimannoside 4.10

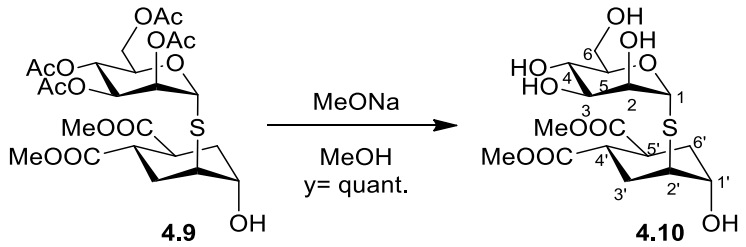

TLC: R_f 0.4 (8:2 CH_2Cl_2:MeOH); $[\alpha]_D^{19}$ (MeOH, *c* 0.51)= +155; ^{1}H-NMR (400 MHz, D_2O): δ= 5.38 (d, $J_{1\text{-}2}$= 1.5 Hz, 1H, H_1), 4.12–4.07 (m, 1H, $H_{1'}$), 4.06 (dd, $J_{2\text{-}3}$= 3.2 Hz, $J_{2\text{-}1}$= 1.5 Hz, 1H, H_2), 3.95 (ddd, $J_{5\text{-}4}$= 9.0 Hz, $J_{5\text{-}6a}$= 6.2 Hz, $J_{5\text{-}6b}$= 1.9 Hz, 1H, H_5), 3.85 (dd, $J_{6a\text{-}6b}$= 12.4 Hz, $J_{6a\text{-}5}$= 2.2 Hz, 1H, H_{6a}), 3.77–3.71 (m, 2H, H_{6b}, H_3), 3.70 (s, 3H, OMe), 3.69 (s, 3H, OMe), 3.64 (t, $J_{4\text{-}3}$= 9.8 Hz, 1H, H_4), 3.25–3.19 (m, 1H, $H_{2'}$), 3.06–2.95 (m, 2H, $H_{5'}$, $H_{4'}$), 2.27–2.16 (m, 1H, H_{3eq}), 2.11–2.03 (m, 1H, H_{3ax}), 2.00– 1.92 (m, 2H, H_{6eq}, H_{6ax}); ^{13}C-NMR (100 MHz, D_2O): δ= 177.3 (CO), 177.0 (CO), 84.9 (C_1), 73.4 (C_5), 71.7 (C_2), 71.0 (C_3), 67.7 ($C_{1'}$), 67.0 (C_4), 60.8 (C_6), 52.6 (2xOMe), 45.4 ($C_{2'}$), 40.0 ($C_{5'}$), 39.0 ($C_{4'}$), 29.9 ($C_{3'}$), 27.5 ($C_{6'}$); HR-MS (ESI) calcd for $C_{16}H_{26}O_{10}S$ $[M+Na]^+$ m/z: 433.11389; found 433.11346.

^{1}H NMR (400 MHz, D_2O):

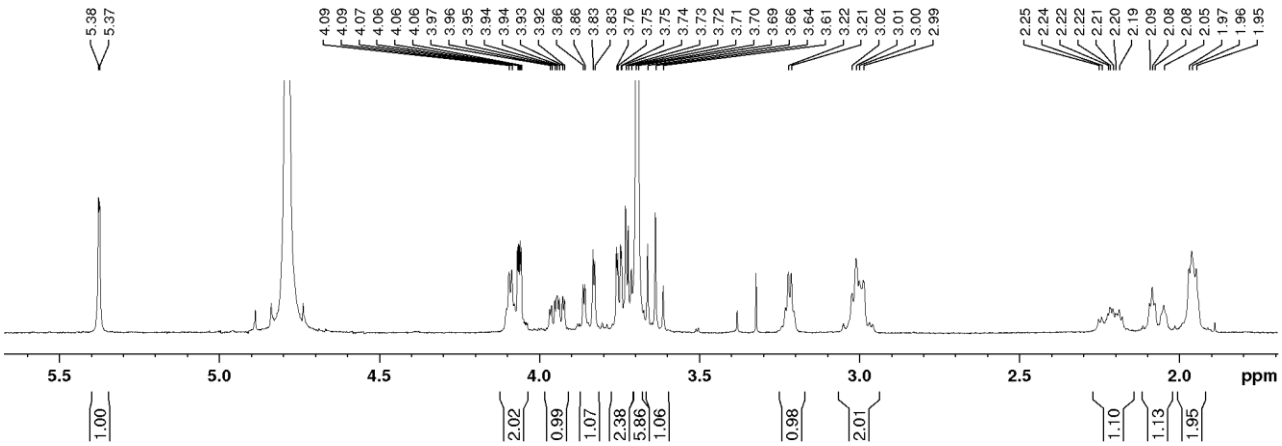

^{13}C NMR (100 MHz, D_2O):

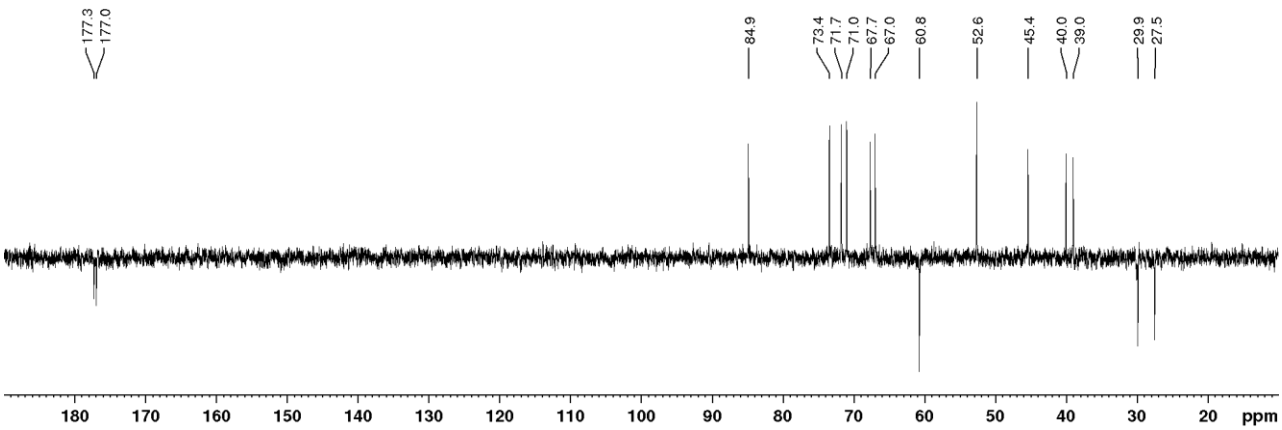

Synthesis of compound 4.13

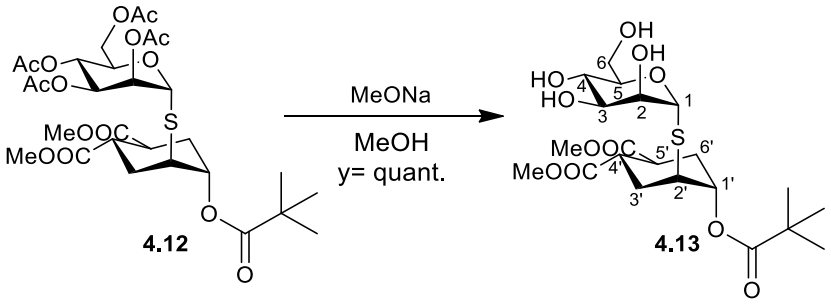

TLC: R_f 0.24 (9:1 CH_2Cl_2:MeOH); $[\alpha]_D^{20}$ (MeOH, *c* 1.01)= +128; ^{1}H-NMR (400 MHz, D_2O): δ= 5.41 (d, $J_{1\text{-}2}$= 1.1 Hz, 1H, H_1), 5.11–5.08 (m, 1H, $H_{1'}$), 4.08 (dd, $J_{2\text{-}3}$= 3.3 Hz, $J_{2\text{-}1}$= 1.5 Hz, 1H, H_2), 3.95 (ddd, $J_{5\text{-}4}$= 9.4 Hz, $J_{5\text{-}6a}$= 5.8 Hz, $J_{5\text{-}6b}$= 2.4 Hz, 1H, H_5), 3.85 (dd, $J_{6a\text{-}6b}$= 12. 5 Hz, $J_{6a\text{-}5}$= 2.4 Hz, 1H, H_{6a}), 3.79–3.72 (m, 2H, H_{6b}, H_3), 3.71 (s, 3H, OMe), 3.70 (s, 3H, OMe), 3.69– 3.63 (m, 1H, H_4), 3.42–3.38 (m, 1H, $H_{2'}$), 3.05–2.92 (m, 2H, $H_{4'}$, $H_{5'}$), 2.23–2.01 (m, 4H, $H_{3'eq}$, $H_{3'ax}$, $H_{6'eq}$, $H_{6'ax}$), 1.21 (s, 9H, tBu); ^{13}C-NMR (100 MHz, D_2O): δ= 180.3 (CO), 176.8 (CO), 176.8 (CO), 85.3 (C_1), 73.6 (C_5), 71.7 (C_2), 71.0 ($C_{1'}$), 70.6 (C_3), 66.8 (C_4), 60.6 (C_6), 52.7 (OMe), 52.7 (OMe), 42.8 ($C_{2'}$), 39.9 ($C_{4'}$), 39.6 ($C_{5'}$), 38.7 (CIV), 28.4 ($C_{3'}$), 27.3 ($C_{6'}$), 26.2 (tBu); HR-MS (ESI) calcd for $C_{21}H_{34}O_{11}S$ $[M+Na]^+$ m/z: 517.17140; found 517.17166.

^{1}H NMR (400 MHz, D_2O):

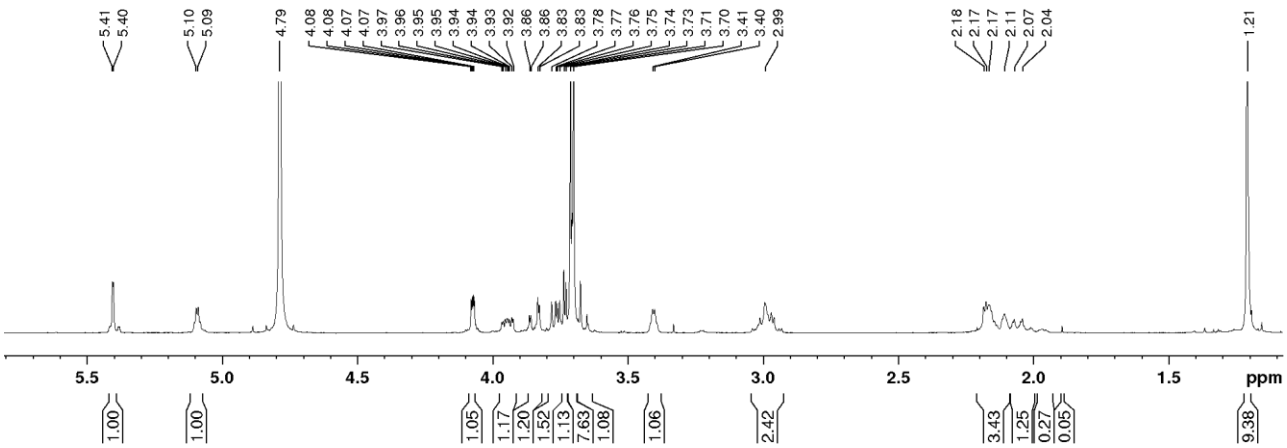

^{13}C NMR (100 MHz, D_2O):

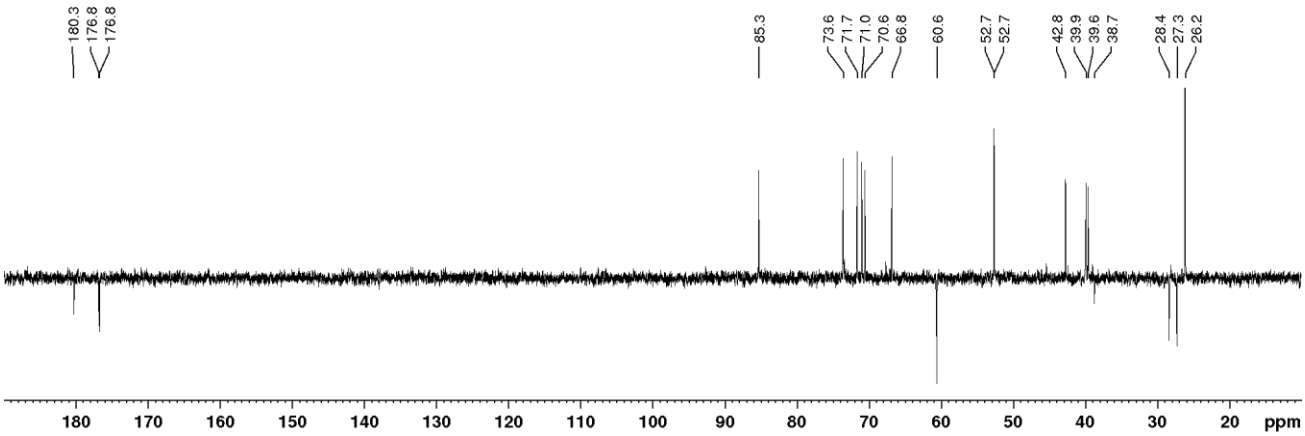
180.3
176.8
176.8
85.3
73.6
71.7
71.0
70.6
66.8
60.6
52.7
52.7
42.8
39.9
39.6
38.7
28.4
27.3
26.2
180
170
160
150
140
130
120
110
100
90
80
70
60
50
40
30
20
ppm

Synthesis of compound 4.18

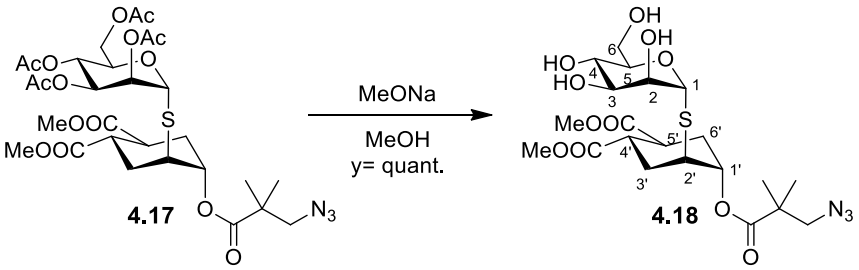

TLC: R_f 0.37 (9:1 CH_2Cl_2:MeOH); $[\alpha]_D^{20}$ (MeOH, *c* 0.81)= +112; ^{1}H-NMR (400 MHz, MeOD): δ= 5.40–5.36 (m, 1H, H_1), 5.17–5.12 (m, 1H, $H_{1'}$), 3.95 (dd, $J_{2\text{-}3}$= 3.2 Hz, $J_{2\text{-}1}$= 1.6 Hz, 1H, H_2), 3.88–3.81 (m, 2H, H_5, H_{6a}), 3.75 (dd, $J_{6b\text{-}6a}$= 12.2 Hz, $J_{6b\text{-}5}$= 6.0 Hz, 1H; H_{6b}), 3.72–3.68 (m, 1H, H_4), 3.69 (s, 3H, OMe), 3.67 (s, 3H, OMe), 3.62 (dd, $J_{3\text{-}4}$= 9.2 Hz, $J_{3\text{-}2}$= 3.2 Hz, 1H, H_3), 3.50 (s, 2H, CH_2N_3), 3.43–3.38 (m, 1H, $H_{2'}$), 3.00–2.89 (m, 2H, $H_{4'}$, $H_{5'}$), 2.19–2.02 (m, 4H, $H_{3'eq}$, $H_{6'eq}$, $H_{3'ax}$, $H_{6'ax}$), 1.24 (s, 6H, 2xCH_3); ^{13}C-NMR (100 MHz, MeOD): δ = 176.1 (CO), 176.0 (CO), 176.0 (CO), 87.1 (C_1), 75.7 (C_5), 73.6 (C_2), 73.1 (C_3), 72.4 ($C_{1'}$), 68.5 (C_4), 62.5 (C_6), 60.8 (CH_2N_3), 52.6 (OMe), 52.6 (OMe), 44.1 ($C_{2'}$), 41.1 ($C_{4'}$), 40.9 ($C_{5'}$), 30.0 ($C_{3'}$), 29.0 ($C_{6'}$), 23.3 (CH_3), 23.3 (CH_3); HR-MS (ESI) calcd for $C_{21}H_{33}N_3O_{11}S$ $[M+Na]^+$ m/z: 558.17280; found 558.17371.

^{1}H NMR (400 MHz, CD_3OD):

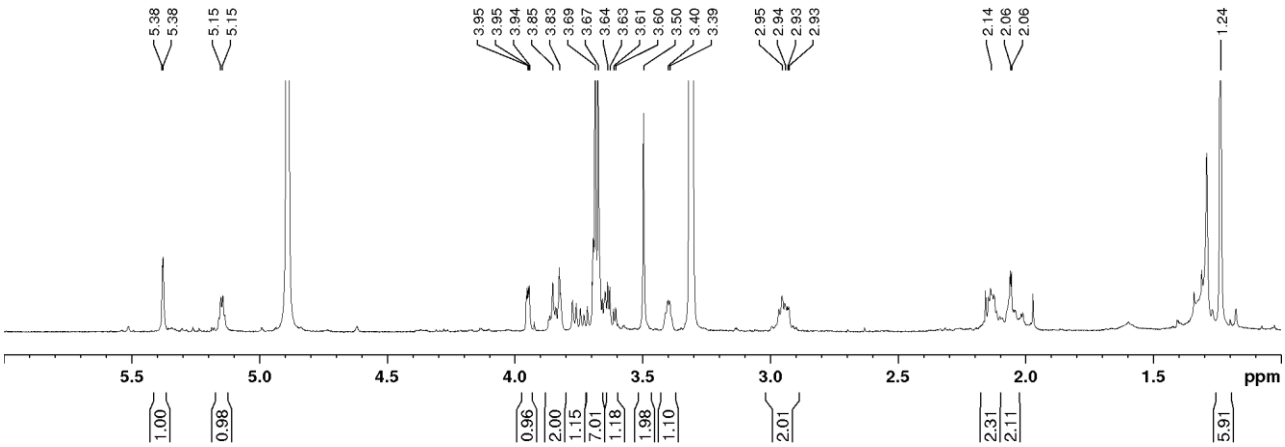

^{13}C NMR (100 MHz, CD_3OD):

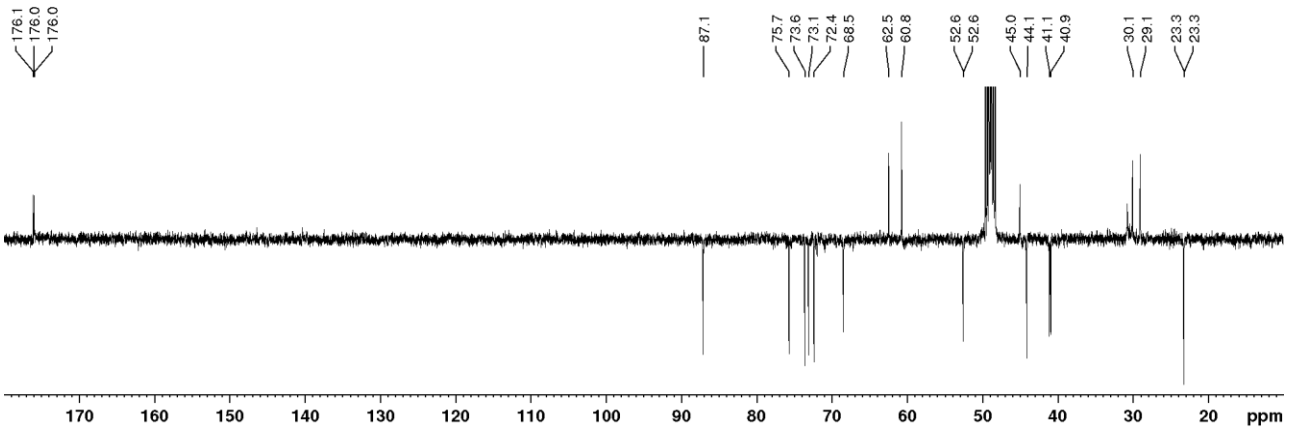

Surface Plasmon Resonance (SPR) analysis of 4.10 and 4.13

The extracellular domain (ECD) of DC-SIGN (residues 66-404) was overexpressed and purified.[6] The SPR experiments were performed on a BIAcore T200 using a CM3 sensor chip. Flow cells were activated as described.[7] Flow cell one was functionalised with BSA and blocked with ethanolamine and subsequently used as a control surface. Flow cells 2 and 3 were treated with BSA-Mana1-3[Mana1-6]Man (Dextra) (60 lg/ml) in 10 mM NaOAc pH 4 to reach different binding densities and blocked with ethanolamine. The final densities on flow cells 2 and 3 were 2579 and 2923 RU, respectively. The affinity of the various compounds for DC-SIGN ECD were evaluated via an established inhibition assay35 in which DC-SIGN ECD was injected at 20 lM alone or in the presence of increasing concentration of inhibitors (ranging from 0 to 5 mM). Injections were performed at 5 lL/min using 25 mM Tris-HCl pH 8, 150 mMNaCl, 4 mMCaCl2, 0,05% P20 surfactant as running buffer. The surface was regenerated by the injection of 50 mM EDTA.

Synthesis of multivalent systems

Materials and methods

Solvents were HPLC grade and used as received unless otherwise stated. Size exclusion chromatography was done with Sephadex LH-20 (GE Healthcare). Thin-layer chromatography (TLC) was done on silica plates. NH_2-PEG-NH_2 (*M*n 2135, *M*p 2153 [M+Na+], *M*w 2184, PDI 1.01, By MALDI-TOF), PEG di-acrylate (*M*n 575), 2-[2-(2-azidoethoxy)ethoxy]ethanol, di-*tert*-butyl dicarbonate (Boc2O), 1-[bis(dimethylamino)methylene]-1H-1,2,3-triazolo[4,5-b]pyridinium 3-oxid hexafluorophosphate (HATU), acryloyl chloride, 4-Dimethylaminopyridine (DMAP), Quadrasil® MP, Tween® 80, Span® 80, ammonium persulfate (APS) and tetramethylethylenediamine (TEMED) were purchased from Sigam-Aldrich. Amicon Ultra-15 centrifugal filters (MWCO 100 KDa) were obtained from Millipore. NMR experiments were performed in a Bruker Advance DRX 400 instrument. NMR chemical shifts (δ) are reported in ppm downfield from the CDCl3 signal or the HOD peak (D_2O). 2D experiments (COSY and HSQC) were performed when necessary. NMR spectra

were analysed with MestreNova software. Mass spectra (ESI) were recorded with an Esquire 6000 ESI-Ion Trap from Bruker Daltonics.

Synthesis of compounds 4.22 and 4.23

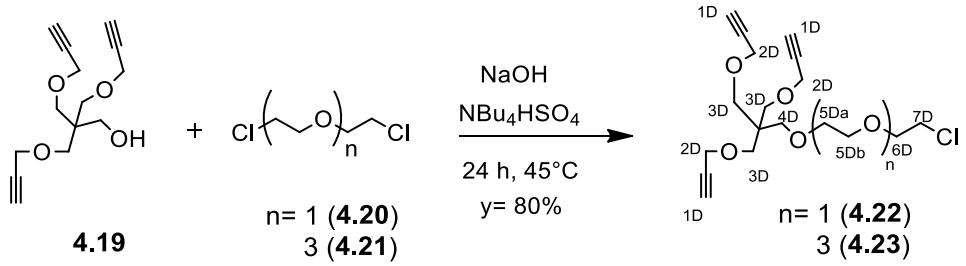

Compound **4.19** (600 mg, 2.40 mmol) was dissolved in tetraethylene glycol dichloride **4.21** (7 mL, 35.95 mmol). Then a solution of NaOH (50%) was added (7 mL) dropwise to the mixture and tetrabutylammonim hydrogensulfate (NBu_4HSO_4, 1.63 g, 4.79 mmol) under stirring. Finally the reaction was heated up to 45°C. After 24 h, the mixture was allowed to reach room temperature; afterwards it was diluted with CH_2Cl_2, washed with H_2O. The organic layer was recovered and dried over $MgSO_4$, filtered and the solvent removed under vacuo. The purification through chromatographic column (2:1 Hex/EtOAc) afforded compound **4.23** (1.065 g, 2.39 mmol) in 80% yield.

The same procedure was followed for the preparation of compound **4.22** (already synthetized by the host group), starting from alkyne **4.19** and using the chloroethyl ether **4.20**.

^{1}H NMR (400 MHz, $CDCl_3$) of compound **4.23**:

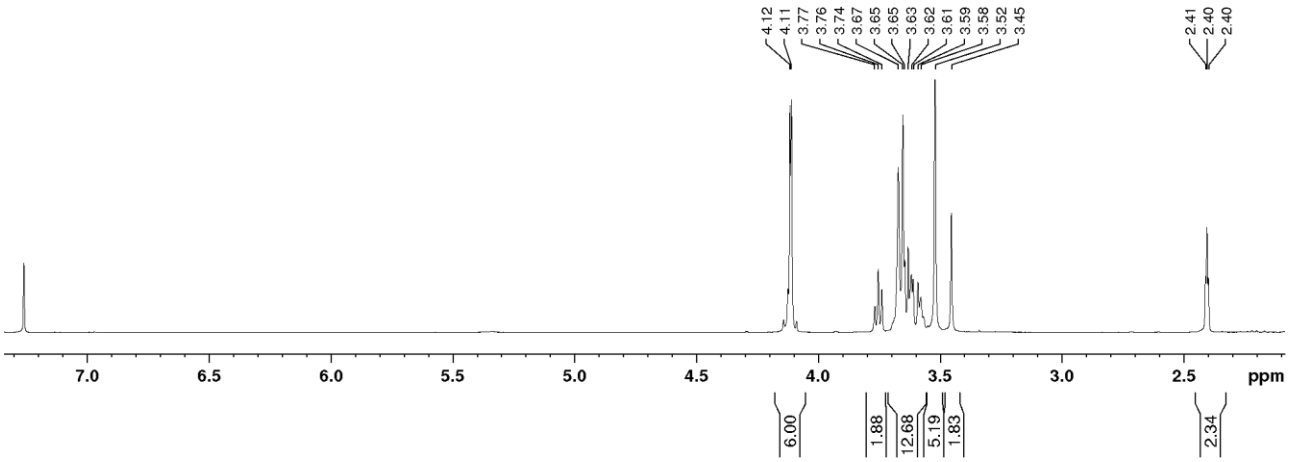

δ= 4.12 (d, $J_{2D\text{-}1D}$= 2.4 Hz, 6H, 3x2D), 3.75 (t, $J_{7D\text{-}6D}$= 5.8 Hz, 2H, 7D), 3.71-3.56 (m, 14H, 3xDa, 3x5Db, 6D), 3.52 (s, 6H, 3x3D), 3.45 (s, 2H, 4D), 2.40 (t, *J*=2.3 Hz, 3H, 3x1D).

Synthesis of compounds 4.24 and 4.25

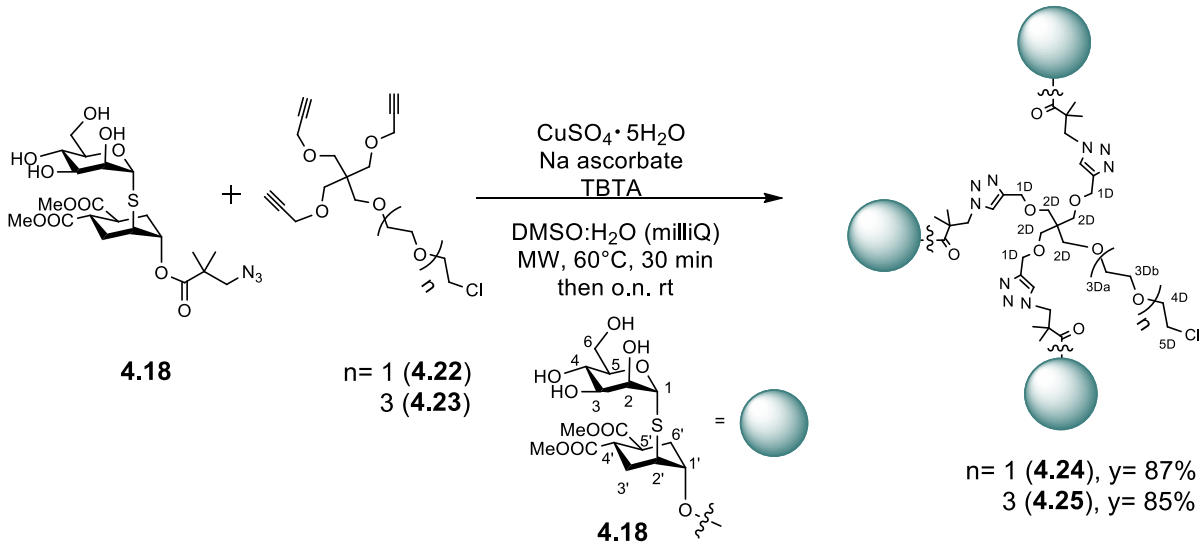

4.22 (9.5 mg, 0.027 mmol) was dissolved in 1:1 DMSO/milliQ H_2O (V_f= 1.08 mL). Then TBTA (8.6 mg, 0.0162 mmol), $CuSO_4 \cdot H_2O$ (2 mg, 0.008 mmol) and Na ascorbate (4.8 mg, 0.024 mmol) and finally the thioglycomimetic **4.18** (50 mg, 0.093 mmol) were added in this order. The reaction proceeded under MW irradiation at 50°C for 30 minutes, then at room temperature over night under nitrogen atmosphere. Quadrasil MP was added and the mixture was stirred for 20 minutes and afterwards directly charged into a Sephadex LH-20 column (in MeOH) without previous filtration. The fractions were analysed by TLC 7:3 AcCN/H_2O. Compound **4.24** (45 mg, 0.023) was isolated in 87% yield.

The same procedure was followed for the preparation of dendrimer **4.25**, isolated (35 mg, 0.017 mmol) in 85% yield.

^{1}H NMR (400 MHz, MeOD) of compound **4.24**:

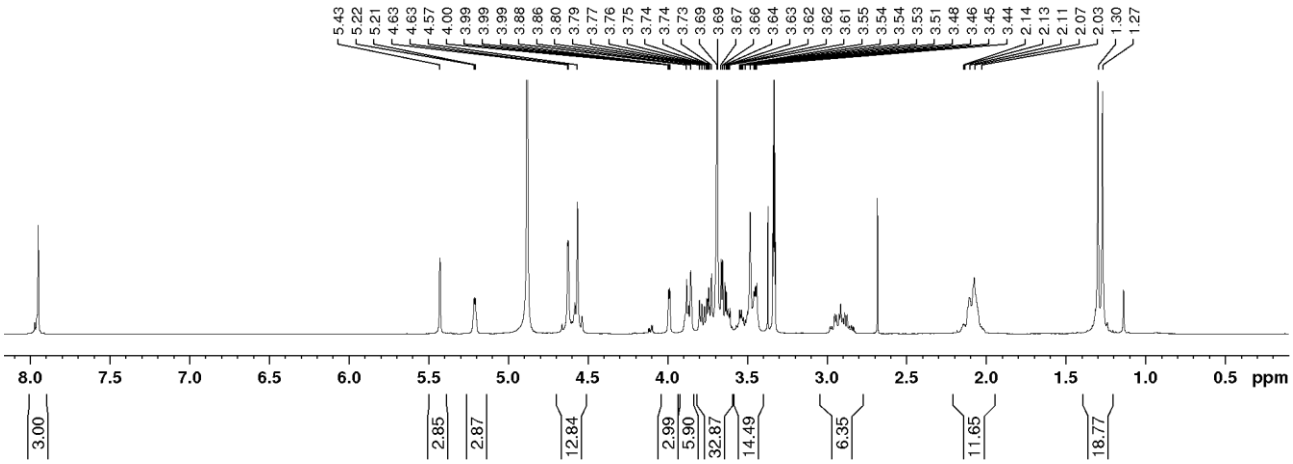

δ= 7.95 (s, 3H, triazole ring), 5.42-5.39 (m, 3H, 3xH_1), 5.22-5.18 (m, 1H, $H_{1'}$), 4.63-4.52 (m, 12H, 3x1D, 3xCH_2 linker), 4.02-3.98 (3H, 3x$H_{2'}$), 3.91-3.82 (m, 6H, 3xH_{6a}, 3xH_5), 3.81-3.41 (m, 46H, 3xH_{6b}, 3xH_4, 3x(2xOMe), 3xH_3,

3xH_2, 4x2D, 3Da, 3Db, 4D, 5D), 3.0-2.81 (m, 6H, 3x$H_{4'}$, 3x$H_{5'}$), 2.19-2.0 (m, 12H, 3x$H_{3'eq}$, 3x$H_{6'eq}$, 3x$H_{3'ax}$, 3x$H_{6'ax}$), 1.30 (s, 9H, 3xCH_3 linker), 1.27 (s, 9H, 3xCH_3 linker).

ESI-MS of compound **4.24**:

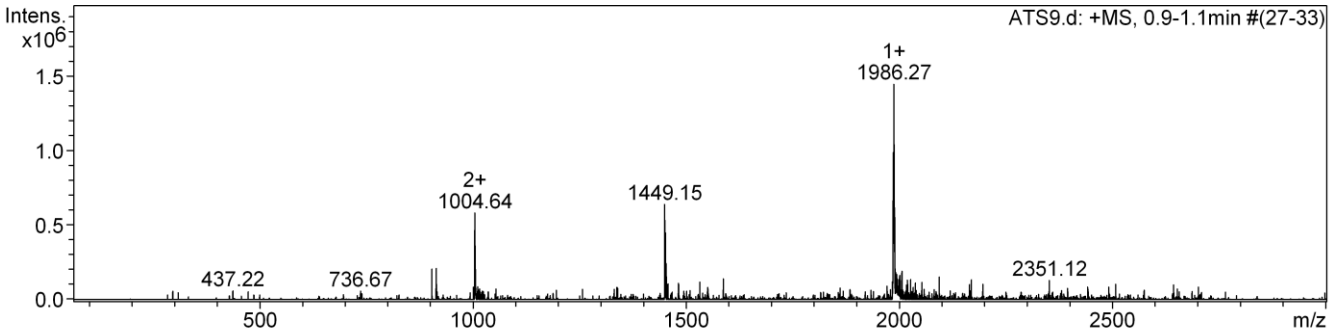

1004.64 [**4.24**+2Na]$^{2+}$; 1986.27 [**4.24**+Na]$^{+}$

^{1}H NMR (400 MHz, MeOD) of compound **4.25**:

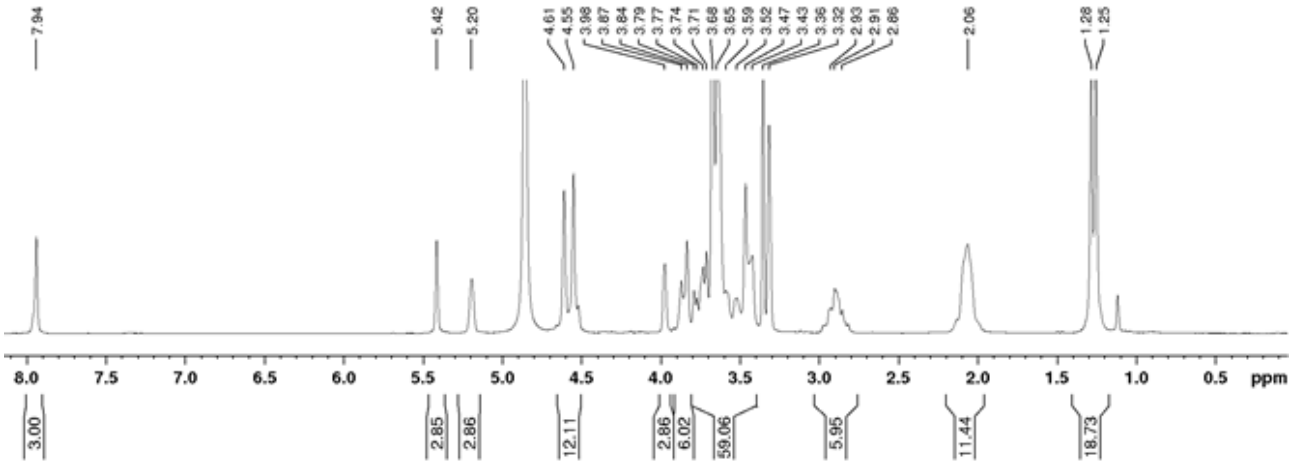

δ= 7.94 (s, 3H, triazole ring), 5.42-5.39 (m, 3H, 3xH_1), 5.22-5.18 (m, 1H, $H_{1'}$), 4.65-4.50 (m, 12H, 3x1D, 3xCH_2 linker), 4.01-3.93 (3H, 3x$H_{2'}$), 3.91-3.81 (m, 6H, 3xH_{6a}, 3xH_5), 3.81-3.39 (m, 54H, 3xH_{6b}, 3xH_4, 3x(2xOMe), 3xH_3, 3xH_2, 4x2D, 3x3Da, 3x3Db, 4D, 5D), 2.99-2.79 (m, 6H, 3x$H_{4'}$, 3x$H_{5'}$), 2.19-1.98 (m, 12H, 3x$H_{3'eq}$, 3x$H_{6'eq}$, 3x$H_{3'ax}$, 3x$H_{6'ax}$), 1.29 (s, 9H, 3xCH_3 linker), 1.25 (s, 9H, 3xCH_3 linker).

ESI-MS compound **4.25**:

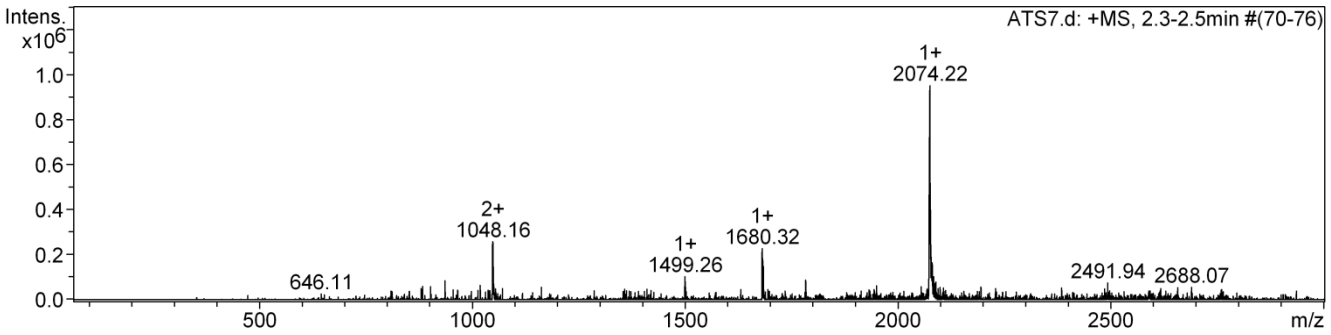

1048.16 [**4.25**+2Na]$^{2+}$; 2074.22 [**4.25**+Na]$^{+}$

Synthesis of compounds 4.26 and 4.27

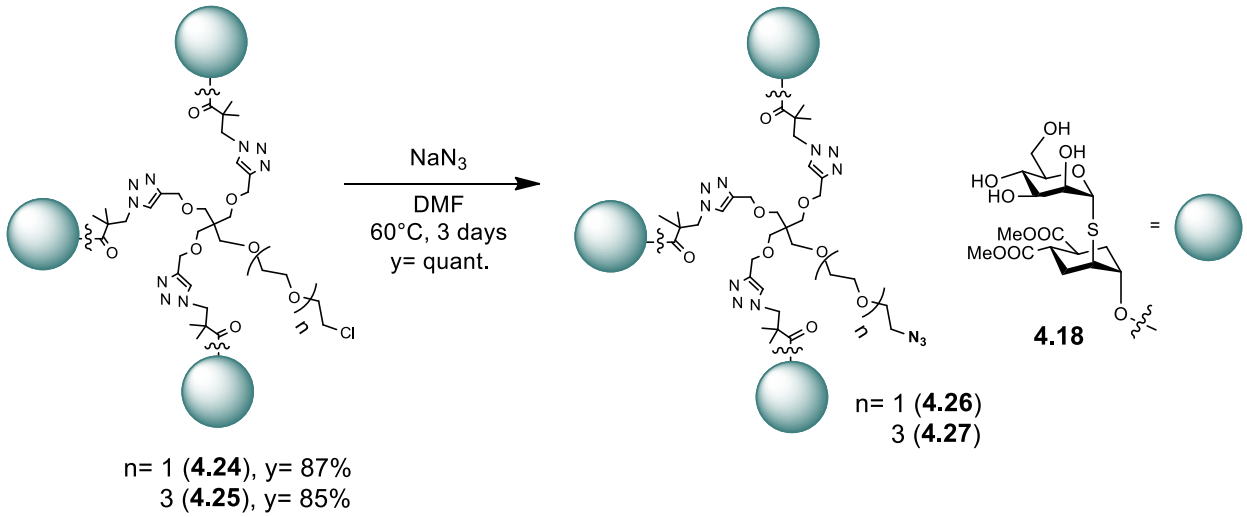

For both compounds **4.26** and **4.27** was followed the same protocol: the chlorinated molecule (scale about 60 mg) was dissolved in anhydrous DMF (0.06 M). Then the NaN_3 (10 eq) was added and mixture heated up to 60°C and stirred for 3 days. Both azido-products **4.26** and **4.27** were obtained in quantitative yield.

ESI-MS of compound **4.26**:

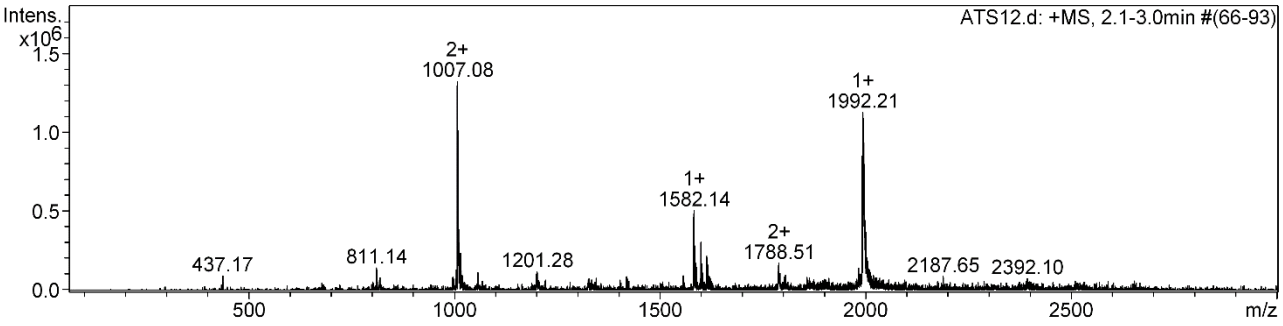

1007.8 [**4.26**+2Na]$^{2+}$; 1992.21 [**4.26**+Na]$^{+}$

ESI-MS of compound **4.27**:

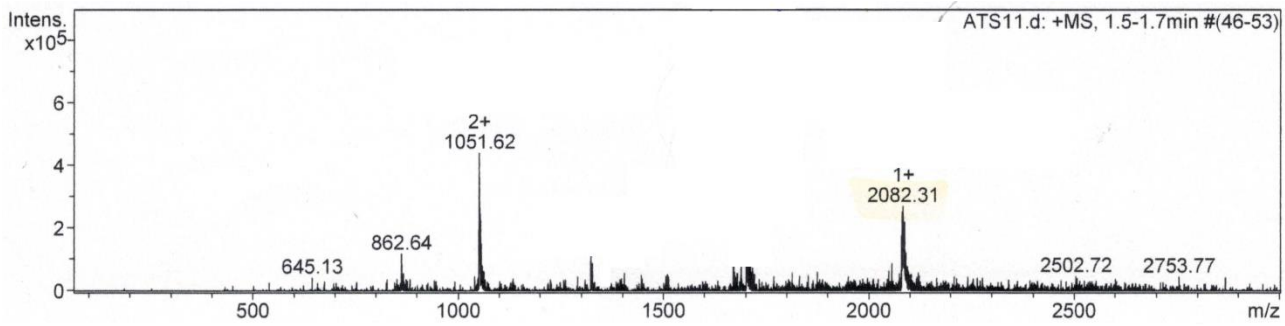

1051.62 [**4.27**+2Na]$^{2+}$; 2082.31 [**4.27**+Na]$^{+}$

Preparation of the glyconanogels

Synthesis of the "carbohydrate-derivate monomer" 4.29

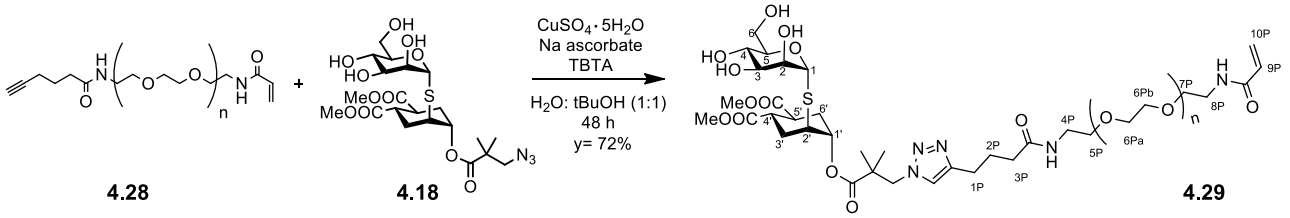

4.28 **4.18** **4.29**

To a solution of the alkyne **4.28** (70 mg, 0.022 mmol) in 1:1 milliQ H_2O:tBuOH (V_f= 440 µL), the other reactants were added in the following order: TBTA (14 mg, 0.026 mmol), $CuSO_4 \cdot H_2O$ (3.3 mg, 0.013 mmol), Na ascorbate (13 mg, 0.066 mmol) and finally the glycomimetic **4.18** (30 mg, 0.056 mmol). The reaction proceeded at room temperature for 48 h under nitrogen atmosphere. Then Quadrasil MP was added and after 20 minutes under stirring the mixture was filtered and the solvents removed in vacuo. The final product **4.29** was isolated (58 mg, 0.016 mmol) through Sephadex LH-20 column (in MeOH) in 72% yield.

^{1}H NMR (400 MHz, MeOD):

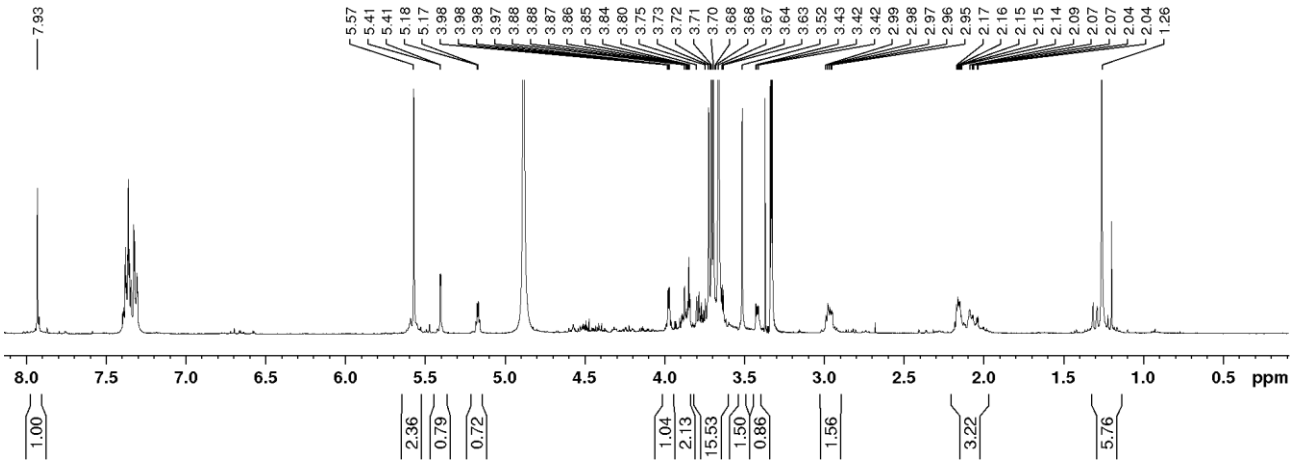

δ= 7.93 (s, 1H, triazole ring), 7.45-7.3 (signals of residual TBTA), 5.57 (s, 2H, 10P), 5.41 (d, $J_{1\text{-}2}$= 1.3 Hz,1H, H_1), 5.21-5.15 (m, 1H, $H_{1'}$), 4.0-3.95 (m, 1H, H_2), 3.92-3.81 (m, 2H, H_{6a}, H_5), 3.80-3.62 (m, H_{6b}, H_4, 2xOMe, H_3, H_2, 1P, 2P, 3P, 4P, 5P, 6Pa, 6Pb, 7P, 8P), 3-52 (s, 2H, CH_2N_3), 3.43-3.38 (m, 1H, $H_{2'}$), 3.01-2.90 (m, 2H, $H_{4'}$, $H_{5'}$), 2.19-1.98 (m, 4H, $H_{3'eq}$, $H_{6'eq}$, $H_{3'ax}$, $H_{6'ax}$), 1.26 (s, 6H, 3xCH_3 linker).

The next step was the creation of the glyconanogels, through free-radical polymerization process, using inverse miniemulsion to template NGs formation. The formation of the miniemulsion was followed and confirmed by Dynamic Light Scattering (DLS). The procedure was optimized by Rojo's group (results not published yet).

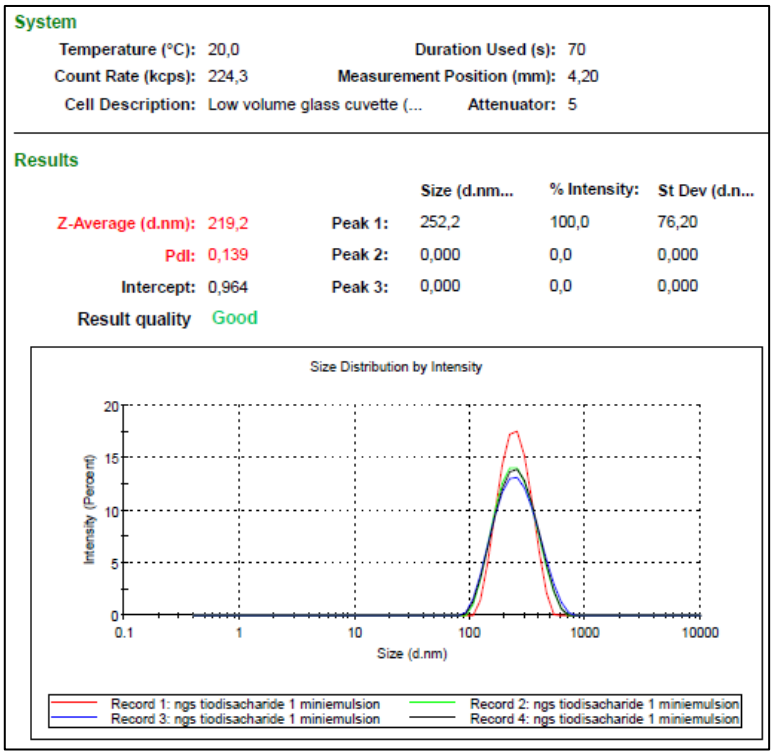

DLS analysis of the miniemulsion that showed the presence of only one population of nanoparticles

The DLS analysis showed that the miniemulsion was composed by only one population of nano-particles, with a relatively narrow polydispersity.

The polymerization took place inside the nanodroplets with the addition of an initiator and finally, an extensive purification afforded the desired glycoNGs, which were characterized by DLS. The DLS analysis revealed the presence of particles with a hydrodynamic diameter around 100 nm and narrow size distribution.

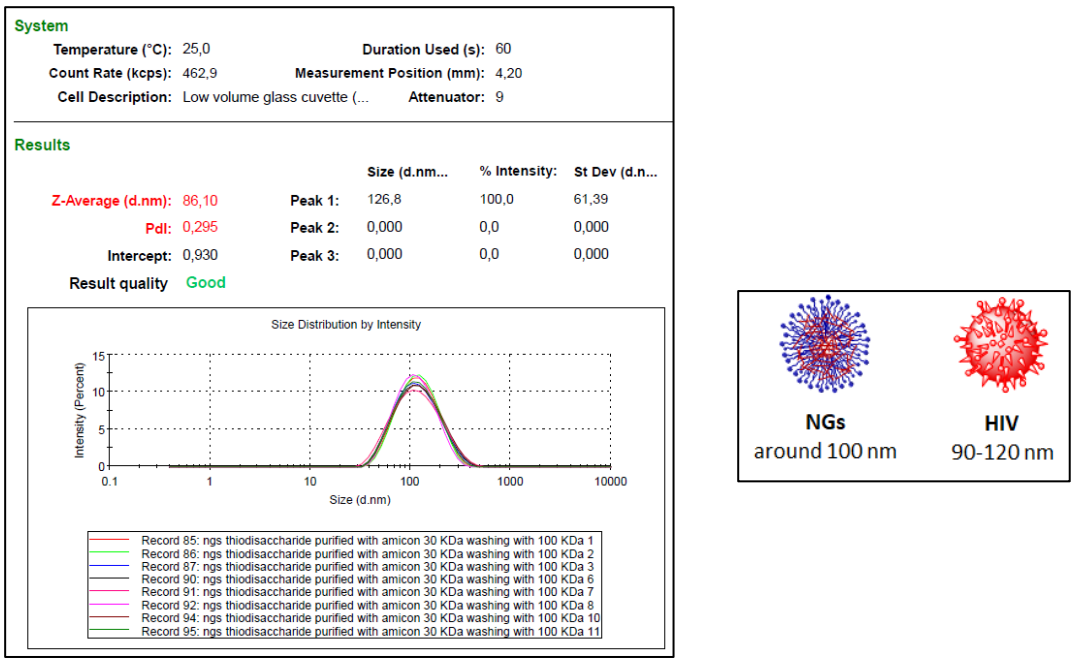

DLS analysis of the final NGs (on the left); comparison between hydrodinamic diameters of our NGs and the HIV

The diameter of these NGs was very similar to that of HIV (90-120 nm).[8] We are currently waiting for the biological activity results obtained for these particles.

1) W. C. Still; M. Kahn; A. Mitra, *The Journal of Organic Chemistry* **1978**, *43*, 2923-2925.
2) T. Bravman; V. Bronner; K. Lavie; A. Notcovich; G. A. Papalia; D. G. Myszka, *Analytical Biochemistry* **2006**, *358*, 281-288.
3) J. J. Reina; S. Sattin; D. Invernizzi; S. Mari; L. Martinez-Prats; G. Tabarani; F. Fieschi; R. Delgado; P. M. Nieto; J. Rojo; A. Bernardi, *ChemMedChem* **2007**, *2*, 1030-6.
4) P. Shu; J. Zeng; J. Tao; Y. Zhao; G. Yao; Q. Wan, *Green Chemistry* **2015**, *17*, 2545-2551.
5) B. Sammet; T. Bogner; M. Nahrwold; C. Weiss; N. Sewald, *J Org Chem* **2010**, *75*, 6953-60.
6) G. Tabarani; M. Thépaut; D. Stroebel; C. Ebel; C. Vivès; P. Vachette; D. Durand; F. Fieschi, *The Journal of biological chemistry* **2009**, *284*, 21229-21240.
7) Franck Halary; Ali Amara; Hugues Lortat-Jacob; Martin Messerle; Thierry Delaunay; Corinne Houlés; Franck Fieschi; F. Arenzana-Seisdedos, *Immunity* **2002**, *17*, 653-664.
8) S. M. Dorosko; R. I. Connor, *J. Virol.* **2010**, *84*, 10533-10542.

CHAPTER FIVE: aziridines

As discussed before (see Chapter 4.1.5), the pseudo-thiodisaccharide **4.10** was functionalized with a particularly bulky azido-linker with the aim to stabilize it against hydrolysis.[1] However, the ester linkage remains a weak point of the molecule, as demonstrated by the partial hydrolysis of the linker under Zemplén conditions. For this reason, we decided to modify our synthetic strategy and examine the ring opening reaction of an aziridine rather than an epoxide, in order to generate an *N*-linked glycomimetic much more resistant towards hydrolysis.

O-linked pseudo-thiodimannoside:

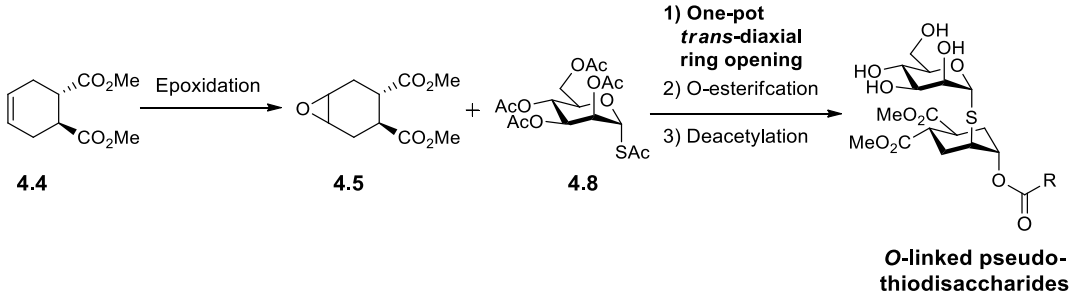

N-linked pseudo-thiodisaccharide:

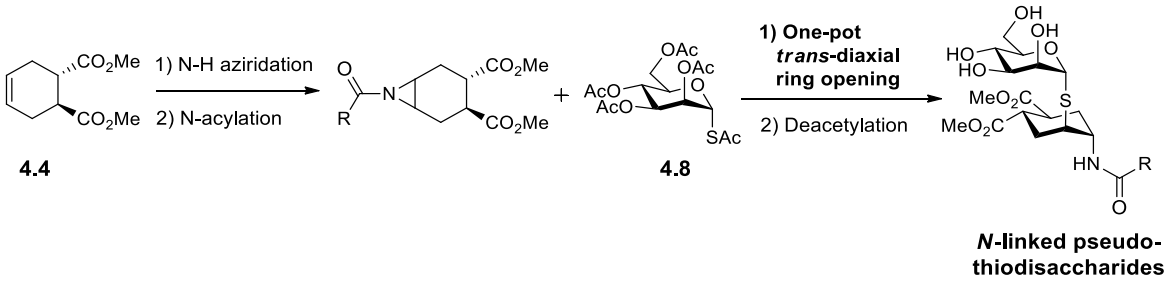

The new synthetic pathway includes the formation of a free aziridine on the double bond of **4.4**, followed by *N*-functionalization with an acylating agent. Finally, the one-pot *trans*-diaxial ring opening by α-thioacetate **4.8** can be performed to generate the final pseudo-thiodimannoside with an amide linker.

However, although aziridines are the nitrogen analogues of epoxides, the direct aziridation of olefins is more difficult and less described than the corresponding epoxidation. A key feature responsible for this situation is the comparative inertness of N-O and N-N bonds compared to the peroxide linkage. Aziridines have raised less interest amongst synthetic organic chemists than their oxygenated counterparts, because of objective difficulties faced not only in their synthesis, but also for their critical stability. Furthermore, oxiranes and aziridines show quite different reactivity and physical properties.

In the next chapter, the chemistry of aziridines will be introduced and discussed: their structural and physical features will be described, as well as their biological properties, the main synthetic methods reported in literature, their reactivity and the most important transformations in which they have been involved so far (some attractive examples will be reported).

5.1 Aziridines: the main structural and chemical features

Aziridines are the simplest structures belonging to the class of three-membered saturated nitrogen-containing heterocycles. As analogues to epoxides, they are strategic precursors for the synthesis of more complex structures, as exemplified in **Fig. 5.1**.[2-8]

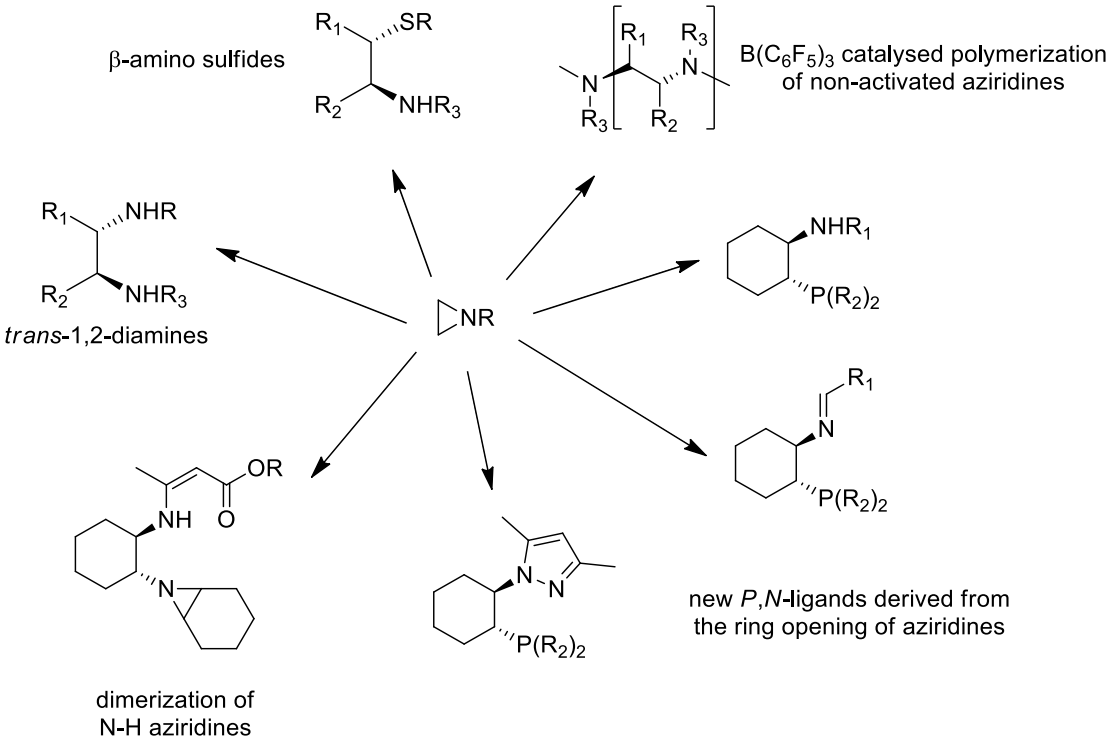

Fig. 5.1 Examples of elaborations of aziridines

Compared to acyclic aliphatic amines, the lone pair of the nitrogen of aziridines shows a greater s-character and this makes them less basic and weaker species as π-donors (**Fig. 5.2**).

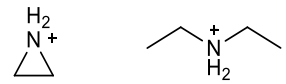

Fig. 5.2 Comparison between the pKa of a N-H aziridine and of an acyclic aliphatic amine

Furthermore, the bond strain caused by the geometric constraints of the 3-membered ring makes the barrier to inversion at nitrogen considerably higher than in acyclic analogues. Indeed, the activation enthalpy of the *N*-inversion of an N-H aziridine is approximately 70 kJ mol^{-1}, considerably greater than that of a typical secondary amine but at the same time not enough to prevent racemization at room temperature. However, when the nitrogen bears an electronegative substituent, that inversion barrier's energy increases up to 112 kJ mol^{-1} and two diastereomers, stable at room temperature, can be separated (**Fig. 5.3**).[3]

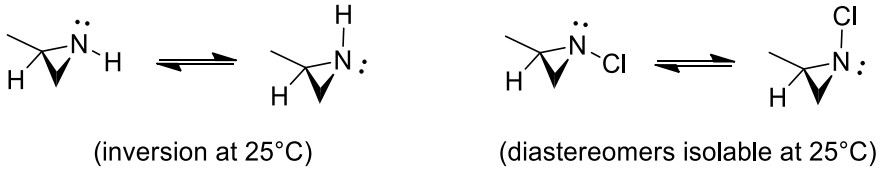

Fig. 5.3 Difference in inversion barrier's energy between N-H aziridines (on the left) and N-Cl aziridines (on the right)

Conventionally, depending on the nature of the *N*-substituent, aziridines are classified as *activated*, when the nitrogen is protected as a carbamate, a sulfonyl-amide or an amide, and *non-activated*, when the aziridine is a secondary (N-H) or a tertiary amine (*N*-alkyl) (**Fig. 5.4**).[9]

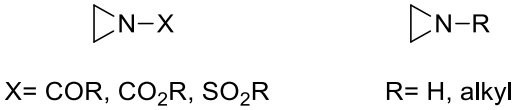

Fig. 5.4 Examples of *activated* (on the left) and *non-activated* (on the right) aziridines

5.2 Biological properties of aziridines

Aziridines were found in various biologically active natural products (**Fig. 5.5**).[10-11]

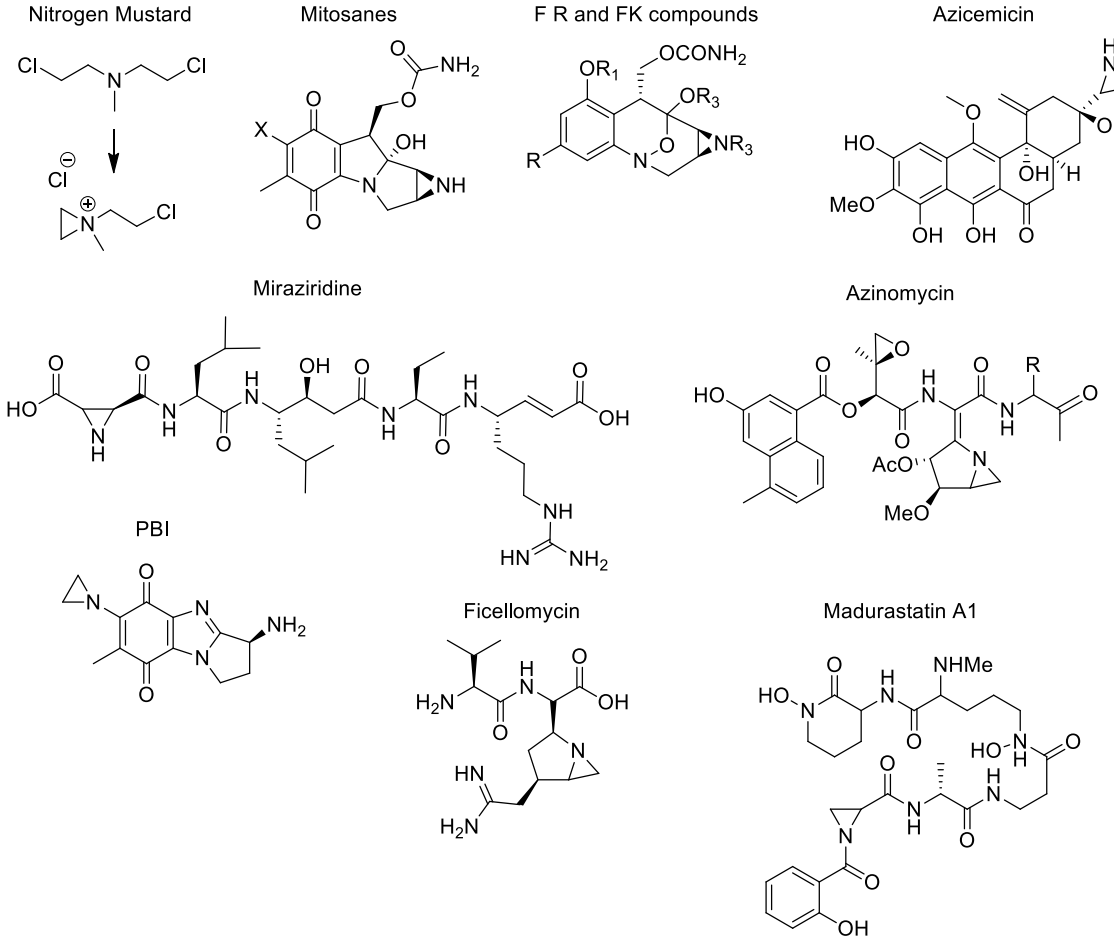

Fig. 5.5 Some biological compounds bearing aziridine ring

Their *in vivo* potency have raised in the last 25 years an increased interest for both their synthesis and chemical applications.[12]

For example, an important class of these natural products is that of Mitosanes, in which the aziridine ring was found to be essential for the anti-tumour activity (**Fig. 5.6**).[13-15]

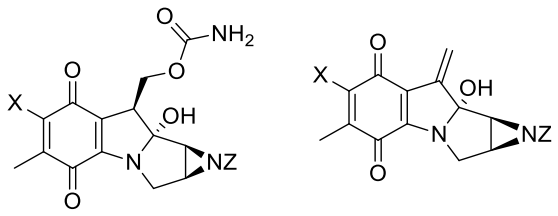

Fig. 5.6 General structure of Mitosane, where Z is H or Me

Another structure that presents a potent antitumoral and antibiotic activity is the Azinomycin (**Fig. 5.7**).[16-18] These natural products are of synthetic interest because of the unprecedented and densely functionalized aziridino-pyrrolidine ring system.

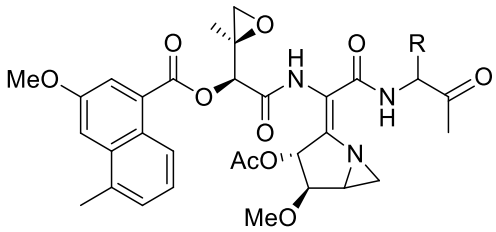

Fig. 5.7 Structure of Azinomycin

The activity of all of these compounds lies in their ability to act as DNA cross-linking agents through nucleophilic opening of the aziridine ring.

5.3 Elaborations and applications of aziridines in organic chemistry

From a synthetic point of view, aziridines have been studied widely in the last decades because of their versatility in myriad regio- and stereo-selective transformations, like ring openings, isomerizations, ring expansions, 1-3 dipolar cycloadditions, etc. …[3, 19-25]

5.3.1 Nucleophilic ring-opening of aziridines

The most widely exploited and studied elaboration of aziridines is their opening by nucleophilic species for the formation of 1,2-difunctional ring-opened products that represent common motifs in many organic molecules of interest. The reactivity of aziridines in ring opening reactions depends on both the ring strain (upon ring opening approximately 105 kJ/mol are released) and the nature of the *N*-substituent. Indeed the nitrogen atom is often modified with electron-withdrawing groups that promote ring opening through polarization of the C-N bond (**Fig. 5.8**).[3] In particular, sulphonamides stand out as the most commonly utilized aziridine protecting groups for these kind of processes.

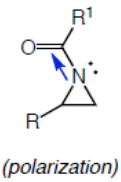

Fig. 5.8 Polarization of the C-N bond in the presence of an EWG as *N*-substituent

In 2004 Eric Hu published a very accurate summary of all the new methodologies (developed until that moment) for the nucleophilic ring opening of aziridines.[26] In this review, interesting and peculiar examples were reported, including carboanions, enamines, olefins, cyanides, alcohols, hydroxyl and carboxylate anions, sulphide anions, amines, azides as nucleophiles, concluding with some cases of halogen, hydrogen and other heteroatom nucleophilic addition of aziridines. Just to provide an idea of the huge versatility of this process, some examples described in Hu's work are reported in the figure below (**Fig. 5.9**).

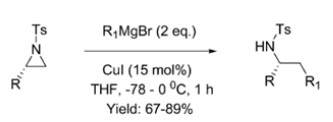

Nenajdenko, V. G., Karpov, A. S., Balenkova, E. S. *Tetrahedron*, **2001**, *12*, 2517–2527.

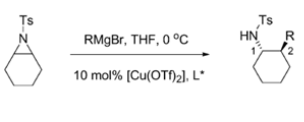

Muller P., Nury P., *Helv. Chem. Acta* **2001**, *84*, 662–677.

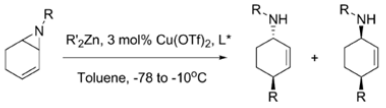

Gini F., Moro F. D., Macchia F., Pineschi M., *Tetrahedron Lett.* **2003**, *44*, 8559–8562.

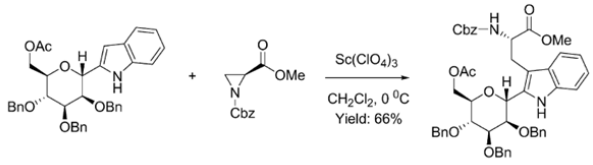

Nishikawa T., Kajii S., Wada K., Ishikawa M., Isobe M., *Synthesis* **2002**, 1658–1662.

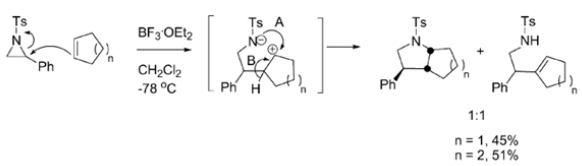

Ungureanu I., Klotz P., Mann A., *Angew. Chem. Int. Ed.* **2000**, *39*, 4615–4617.

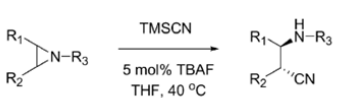

Wu J. W., Hou, X.-L., Dai L.-X., *J. Org. Chem*. **2000**, *65*, 1344–1348.

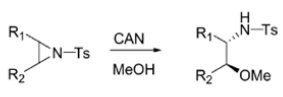

Chandrasekhar S., Narsihmulu C., Sultana S. S., *Tetrahedron Lett.* **2002**, *43*, 7361–7363.

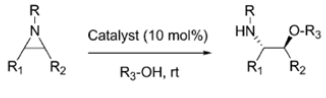

Bhanu B. A. B., Sanghi R., Singh V. K., *Tetradredron* **2002**, *58*, 7355–7363.

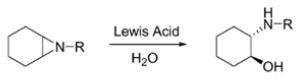

Prasad B. A. B., Sekar G., Singh V. K., *Tetrahedron Lett.* **2000**, *41*, 4677–4679.

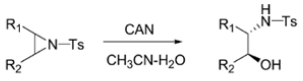

Chakraborty T. K., Ghosh A., Raju T. V., *Chem. Lett.* **2003**, *32*, 82–83.

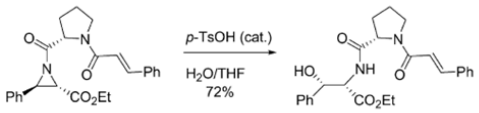

Saha B., Nandy J. P., Shukla S., Siddiqui I., Iqbal J., *J. Org. Chem.* **2002**, *67*, 7858–7860.

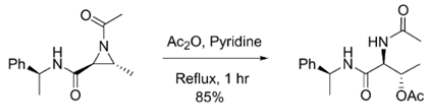

Cardillo G., Gentilucci L., Tolomelli A., Tomasini C., *J. Org. Chem.* **1998**, *63*, 3458–3462.

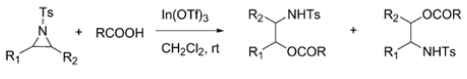

Yadav J. S., Reddy B. S. S., Sadashiv, K., Harikishan K., *Tetrahedron Lett.* **2002**, *43*, 2099–2101.

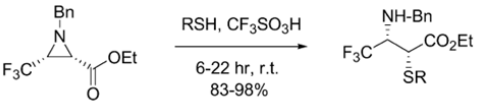

Crousse B., Narizuka S., Bonnet-Delpon D., Begue J.-P., *Synlett* **2001**, 679–681.

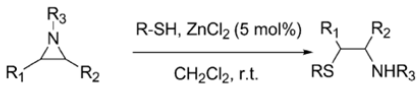

Wu J., Hou X.-L., Dai L.-X., *J. Chem. Soc.*, **2001**, 1314–1317.

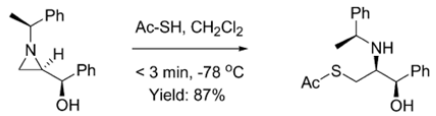

Bae J. H., Shin S.-H., Park C. S., Lee W. K., *Tetrahedron* **1999**, *55*, 10041–10046.

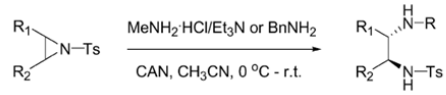

Chakraborty T. K., Ghosh A., Raju T. V., *Chem. Lett.* **2003**, *32*, 82–83.

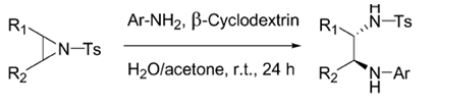

Reddy M. A., Reddy L. R., Bhanumathi N., Rao, K. R., *Chem. Lett.* **2001**, 246–247.

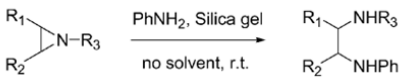

Anand R. V., Pandey G., Singh V. K., *Tetrahedron Lett.* **2002**, *43*, 3975–3976.

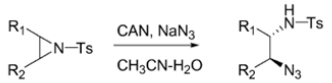

Chandrasekhar S., Narsihmulu C., Sultana S. S., *Tetrahedron Lett.* **2002**, *43*, 7361–7363.

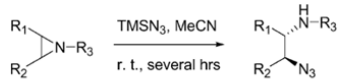

Chandrasekhar M., Sekar G., Singh V. K., *Tetrahedron Lett.*, **2000**, *41*, 10079–10083.

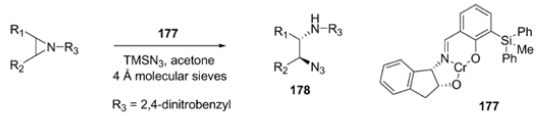

Li Z., Fernandez M., Jacobsen E. N., *Org. Lett.* **1999**, *1*, 1611–1613.

Fig. 5.9 Example of nucleophilic ring opening reactions of aziridines

In almost all the cases illustrated in Hu's review, *N*-acyl or *N*-tosyl aziridines were employed. Indeed un-activated aziridines emerged as significantly less reactive in ring opening reactions, because of their lack of substituents capable to stabilize the intermediate anion formed after the nucleophilic attack.

In 2006, Watson and co-workers reported ring opening reactions of a range of alkyl aziridines catalysed by *tris*-(pentafluorophenyl)borane (**Fig. 5.10**).[27] The procedure worked with a variety of amines and thiols, giving the corresponding *trans*-diamines and α-aminosulphides in good yields. On the contrary, the reaction with alcohols under similar conditions failed to give *trans*-1,2-aminoethers. They also observed that the activation of the substrate in the absence of nucleophiles afford adducts of polymerization.

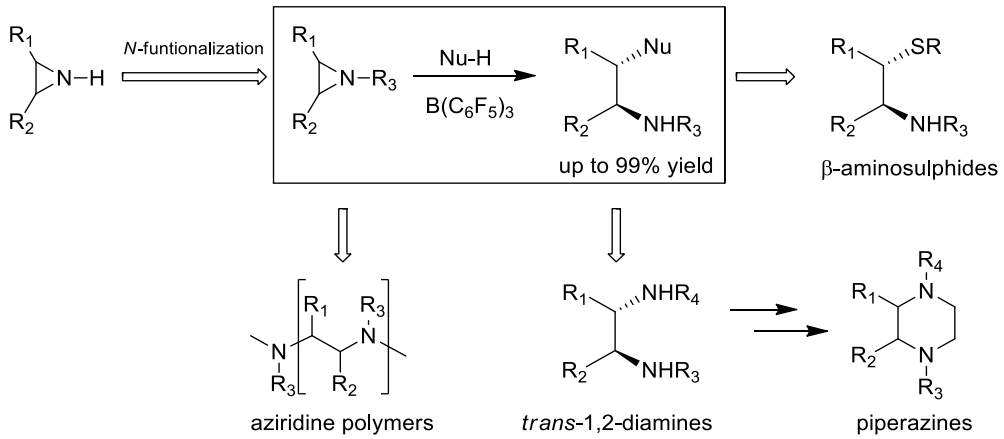

Fig. 5.10 Ring opening of un-activated aziridines catalysed by $B(C_6F_5)_3$ proposed by Watson et al.[27]

The mechanism was also investigated: the process occurs through the formation of an aziridinium adduct (confirmed by NMR analysis), due to the interaction between the nitrogen atom and the borane, finally followed by the attack of the nucleophile (**Fig. 5.11**).

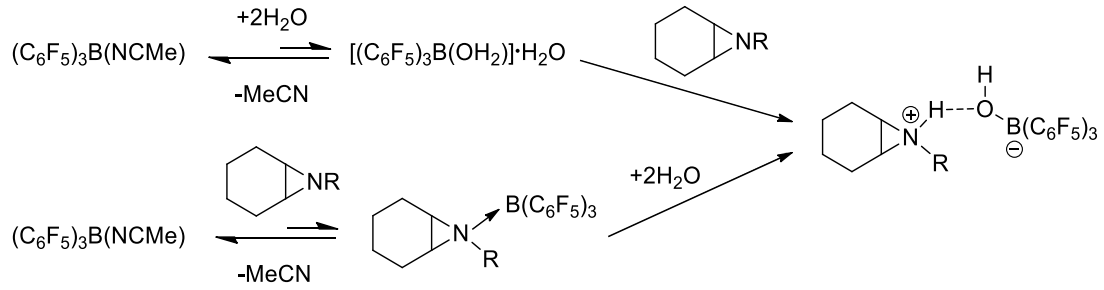

Fig. 5.11 Mechanism proposed by Watson et al.[27] for the ring opening of unactivated aziridines catalysed by $B(C_6F_5)_3$

Recently (in 2016), the regioselective aziridine opening was employed in the synthesis of β-substituted tryptamines, molecules that are known in pharmacology as important neurotransmitters and that contain an indole ring structure.[28] In particular, this work described the addition of a series of indoles to 4-nitrobenzyl carbamate (PNZ)-protected aziridines to produce a library of tryptamine derivatives (**Fig. 5.12**).

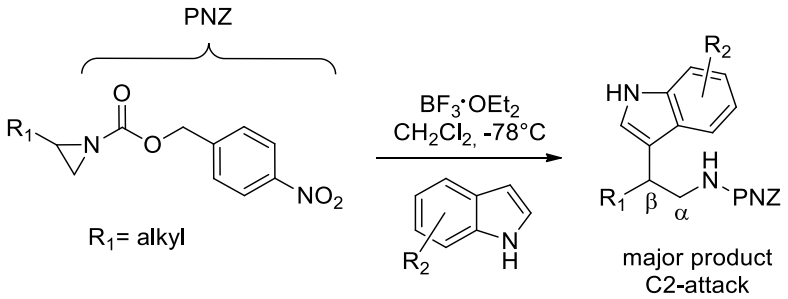

Fig. 5.12 Addition of a series of indoles to 4-nitrobenzyl carbamate (PNZ)-protected aziridines to produce a library of tryptamine derivatives

5.3.2 Possible rearrangements of the aziridine ring

5.3.2.1 Rearrangement by ring expansion: synthesis of oxazolines

Another chemical property of aziridines, recently exploited in the organic synthesis of heterocycles, is their ability to undergo rearrangement by ring expansion through an addition/elimination mechanism, producing oxazolines. In this process, known as "Heine's reaction", the attack by a nucleophilic specie on the least hindered carbon of the aziridine leads to the intermediate opened product that can undergo intramolecular ring closure generating an oxazoline (**Fig. 5.13**).

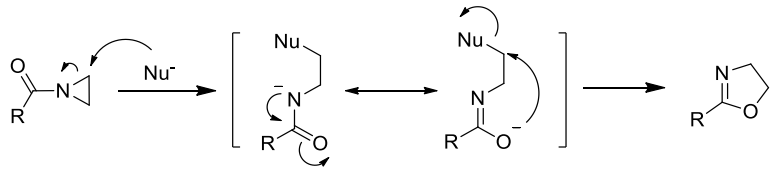

Fig. 5.13 General scheme for the Heine's rearrangement

Heine originally reported a series of intramolecular aziridine rearrangements that took place in the presence of nucleophilic inorganic salts, such as sodium iodide.[29-31] Specifically, the rearrangement of *N*-acylaziridines to oxazolines is known to occur under a range of Lewis acid and Lewis base-catalyzed conditions.[32-42] However, Heine reaction led only to a mixture of products due to the lack of regio-control during the process (**Fig. 5.14**).

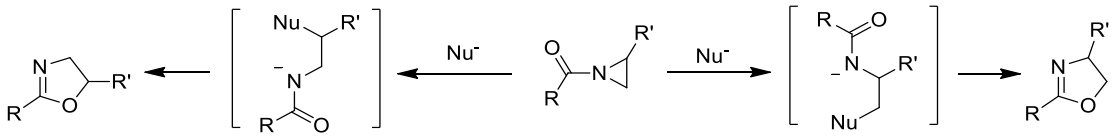

Fig. 5.14 Regio-selectivity problem of Heine reaction

In 2011 (more than 50 years later than Heine's work) Morgan and co-workers reported the regioselective rearrangement of *N*-acylaziridines to oxazolines catalysed by electron-rich phopshines (**Fig. 5.15**).[43]

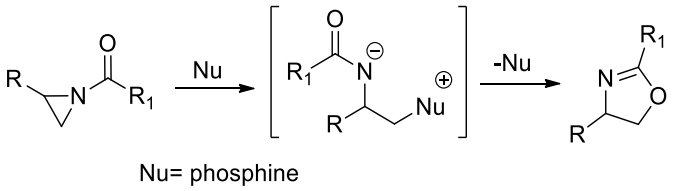

Fig. 5.15 Nucleophile-catalysed rearrangement of aziridines

The proposed mechanism for this process is reported in the figure below (**Fig. 5.16**).

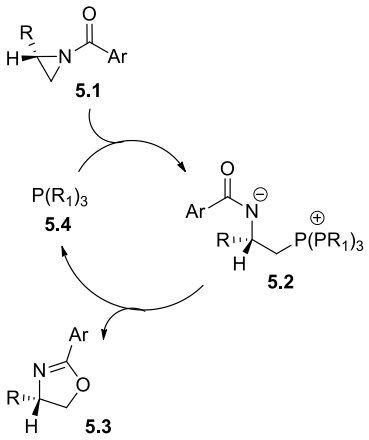

Fig. 5.16 Proposed mechanism for the nucleophile-catalysed rearrangement of aziridines

The aziridine **5.1** undergoes nucleophilic attack at the least hindered carbon by the phosphine **5.4**. The phosphine catalyst must be small enough to efficiently open the aziridine, but additional steric bulk around phosphorus may prevent non-productive decomposition of the intermediate specie **5.2**. Intramolecular displacement of the phosphine, acted by the oxygen, leads to ring closure and to the formation of the oxazoline **5.3** as a single regioisomer.

The authors of this paper demonstrated that, employing enantioenriched phosphines with the role of both the catalyst and the nucleophilic specie in the Heine reaction, it was possible to reach very high yields and levels of regioselectivity, generating a wide range of differently functionalized heterocycles (an example is reported in **Fig. 5.17**).

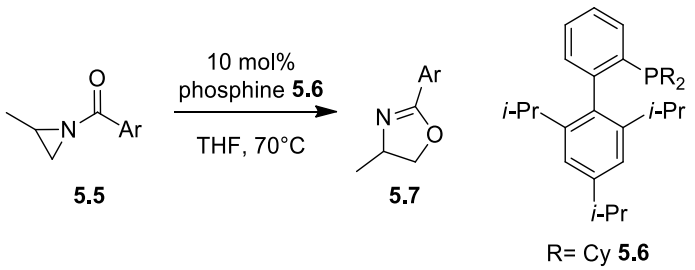

Fig. 5.17 Application of Heine reaction for the preparation of the heterocycle **5.7**

Recently, Morgan has also proposed the first example of direct catalytic, highly enantioselective Heine reaction.[44] In this work, highly enantioenriched oxazoline products were synthetized in a palladium(II)-diphosphine catalysed process (**Fig. 5.18**). Furthermore, acylisoxazoles were identified as a novel directing group to generate isoxazole-based oxazoline products.

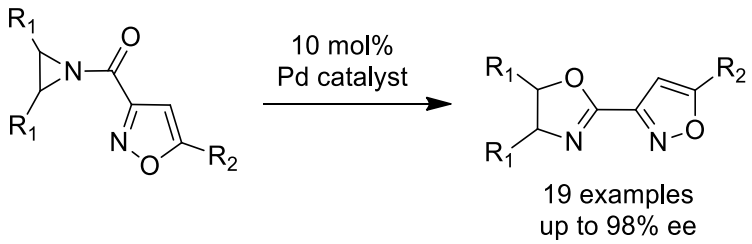

Fig. 5.18 Synthesis of highly enantioenriched oxazolines through the palladium(II)-diphosphine catalysed process proposed by Morgan et al.[44]

The isomerization of aziridines was deeply investigated also by Lectka and co-workers in the early nineties. This work took inspiration from a previous study on the effect of metal ions on the rotational barrier in amides, which explained the *cis-trans* conformational isomerization of amides catalysed by late transition metals through the coordination of the nitrogen atom (**Fig. 5.19**).[45]

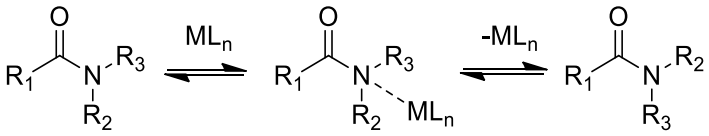

Fig. 5.19 Cis-trans conformational isomerization of amides catalysed by late transition metals through the coordination of the nitrogen atom proposed by Lectka et al.[45]

According to the literature available until the nineties, Lewis acids should raise the isomerization barrier coordinating the oxygen, which reinforces the double-bond character of the C-N bond.[46] Starting from this assumption, for Leckta and co-workers it was reasonable to believe that the coordination of the metal to the nitrogen atom instead should disrupt the amide resonance and catalyse the isomerization. To prove that, they started screening different metal salts (such as Cu(II)), taking into account that late transition metals should be less oxophilic, thus favouring coordination of the N atom.

Once this hypothesis was demonstrated, they applied the same theory to acylaziridines.[41] In particular, they demonstrated that azaphilic Lewis acids (able to coordinate the amide nitrogen) catalysed the rearrangement of aziridines to the corresponding oxazolines, whereas oxophilic Lewis acids (through the coordination of the oxygen atom) activated the substrates towards external nucleophilic attack (**Fig. 5.20**).

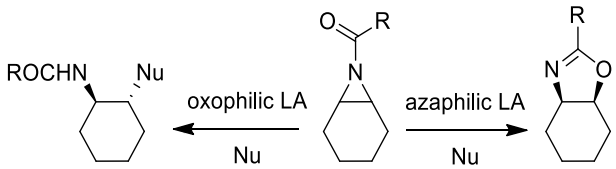

Fig. 5.20 Rearrangement of aziridine ring in the presence of azaphilic LAs; ring opening of acylaziridines promoted by oxophilic LAs

For example, they observed that the $TMSN_3$ promoted the conversion of the *N*-functionalized aziridines towards the opened product when a Lewis acid, such as oxophilic Yb(2,2'-biphenol)OTf, was present. Complexes of Zr and Ti were also found to catalyse the nucleophilic attack of $TMSN_3$. When metals that are usually classified as more azaphilic, such as Zn, Cu and Sn were investigated, addition of the nucleophile was not observed, but rearrangement of acylaziridines to 2-aryloxazolines occurred. In particular, the authors

observed that this process proceeded smoothly at room temperature and that electron-donating *N*-substituents increased the rate of reaction.

A few years later, the same approach was employed in the synthesis of a biologically active compound by Tolomelli and co-workers.[47] In particular, they exploited the aziridine rearrangement to build a crucial framework for the synthesis of the antibiotic Lysobactin. In agreement with the observations of Lectka's team, the azaphilic Lewis acid BF_3 led to the spontaneous ring expansion of the aziridine of **5.8** to the corresponding oxazoline **5.9** in almost quantitative yield (**Fig. 5.21**).

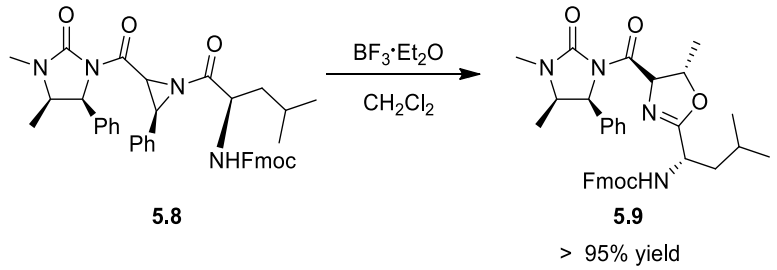

Fig. 5.21 Spontaneous ring expansion of the aziridine of **5.8** to the corresponding oxazoline **5.9** in the presence of an azaphilic LA

5.3.2.2 Thermal rearrangement of aziridines

N-acylaziridines can undergo thermal rearrangement to allylamides at high temperatures (usually around 80-90°C).[48-49] The thermal behaviour of these structures was also investigated by Stogryn and Brois.[50] In particular, they reported that divinylaziridines can be thermally ring-expanded to generate the azepine structure in high yields (**Fig. 5.22**).

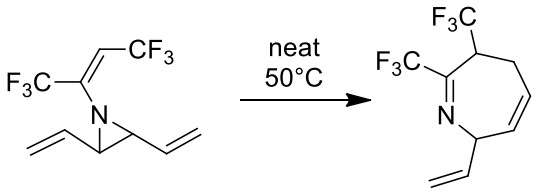

Fig. 5.22 Stogryn's work (1965)[50]

Stogryn noted that, upon exposure to thermal/basic conditions, the corresponding *trans*-divinylaziridine was unreactive. Explorations of thermal vinylaziridine ring expansions revealed that the nature of the nitrogen substituent was critical for this process. Rees[51] and Lwowski[52] reported that the thermolysis of *N*-substituted vinylaziridines at high temperatures yielded pyrroline products (**Fig. 5.23**).

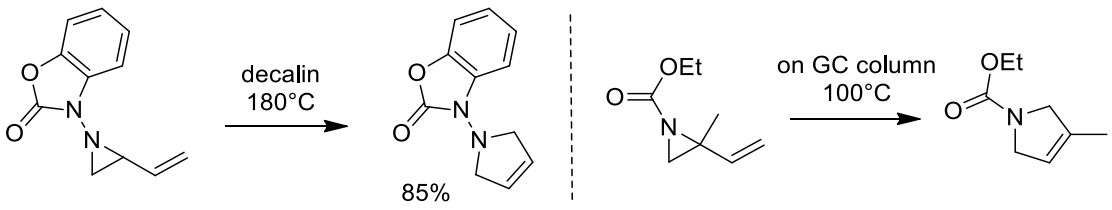

Fig. 5.23 Rees'work (1967, on the left)[51]; Lwowski's (1968, on the right)[52]

Heine demonstrated that a *p*-nitrobenzyl carbamate substituted aziridine afforded a 2-pyrroline product, presumably proceeding through an ylide intermediate.[53] Heine also observed that alternate acyl groups

(benzoyl and thiourea) resulted in strain-assisted aza-Claisen rearrangements to form seven membered ring products (**Fig. 5.24**).[54]

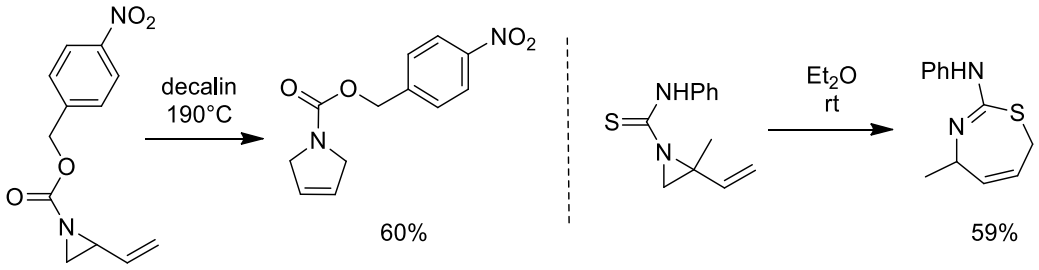

Fig. 5.24 Heine's work[53-54]

Finally, also Scheiner[55] revealed that *N*-aryl- and *N*-vinyl-substituted aziridines both undergo thermal Claisen rearrangement to form azepine structures (**Fig. 5.25**).

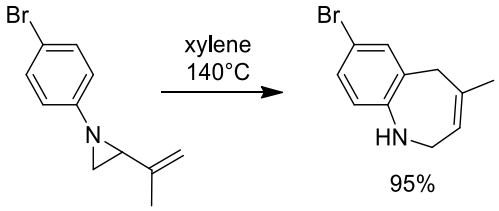

Fig. 5.25 Scheiner's work (1967)[55]

5.3.2.3 The base-promoted isomerization of aziridines to allyl amines

In 2001 Müller and co-workers described the base-promoted desymmetrization of *meso*-sulfonyl aziridines (**5.10**) to generate allyl amines (**5.12**).[56]

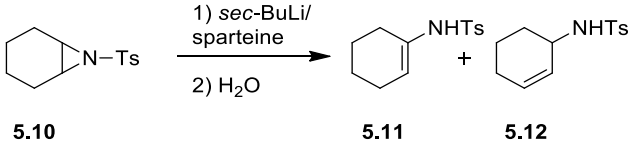

Fig. 5.26 Example of base-promoted isomerization of aziridines to allyl amines and enamines

However, in those conditions the isomerization was not regioselective, giving a mixture of the desired allyl amine **5.12** and the enamine **5.11**, due to an α-deprotonation (**Fig. 5.26**).

Mordini and co-workers investigated the same process one year later.[57] They treated a series of *N*-substituted aziridines (**5.13**) with superbasic mixtures (butyllithium/potassium tert-butoxide, LICKOR or lithium diisopropylamide/potassium tert-butoxide, LIDAKOR; **Fig.5.27**).

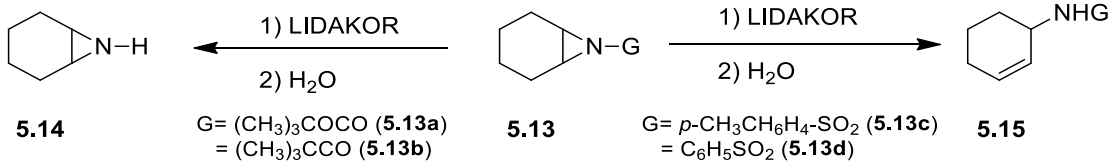

Fig. 5.27 Different behaviour of *N*-substituted aziridines under treatment with superbasic mixtures

While the two sulfonyl aziridines **5.13c** and **5.13d** underwent a regioselective rearrangement to the corresponding allylic sulfonyl amide **5.15c** and **5.15d** by treatment with LIDAKOR, the Boc- and pivaloyl

aziridines **5.13a** and **5.13b** were simply deprotected to N-H compound. After this screening, the tosyl group revealed to be certainly the best *N*-substituent in promoting the base-induced rearrangement.

5.4 Synthesis of aziridines

Despite all the advantages of working with aziridines, from their important role in biological processes to their versatility as building blocks, they have received limited application in synthesis due to several difficulties in their preparation and handling.

The first example of synthesis of aziridines was reported by Wenker in 1935: he described the cyclization of amino alcohols to generate the three-membered ring. However his procedure afforded the free aziridine in low yields (**Fig. 5.28**).[58]

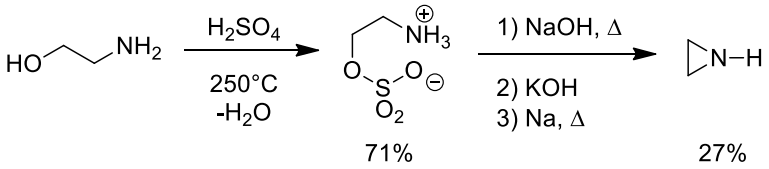

Fig. 5.28 Wenker's synthesis (1935)[58]

Afterwards, other chemists proposed different procedures, like Hoch and Campbell with their study about the conversion of oximes to free-aziridines (**Fig. 5.29**).[59-60]

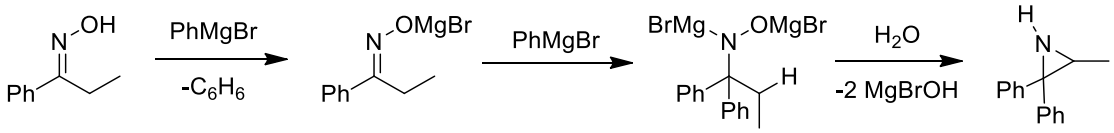

Fig. 5.29 Hoch-Campbell synthesis [59, 61]

In subsequent years, various synthetic pathways were reported in the literature for the formation of aziridines.

The main available routes involve transfer of a nitrogen atom from an aminating agent to an olefin, carbene and ylid addition to imines, or cyclization of 1,2-aminohalides and 1,2-azidoalcohols (**Fig. 5.30**).[58, 61-64]

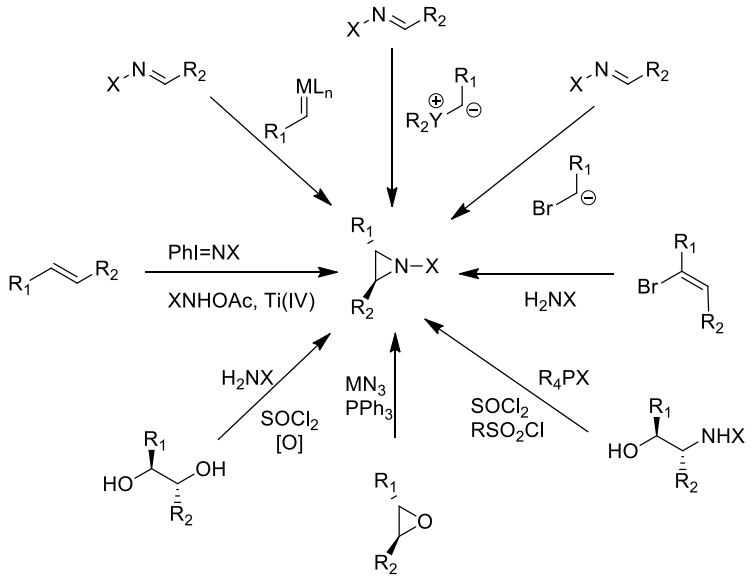

Fig. 5.30 Various synthetic pathways for the preparation of aziridines

So far, the most studied process is the aziridination of olefins, that is typically accomplished via metal-mediated transfer of nitrene fragments or by 1,4-addition of nitrogen transfer reagents to electron-deficient olefins followed by elimination.[65-71]

Nitrenes are those intermediates whose reactivity is comparable to carbenes. The nitrogen atom can present two free electron lone pairs (singlet electrophilic state), or the four electrons in three different orbitals, one filled and two semi-filled (triplet state) showing a diradical behaviour.[72]

One of the most widely used nitrene source are iminoiodinanes (e.g. PhI=NTs) for the synthesis of *N*-sulfonyl aziridines. However, the main problem correlated to this reagent is the need to isolate the nitrene precursor.[12] To overcome this issue, novel *in situ* procedures for the generation of the metal-nitrene active species have emerged, also changing the nitrogen donor with sulphonamides, sulfonimidamides and sulfamates in a metal-catalyzed aziridination of olefins in the presence of an oxidant (**Fig. 5.31**).

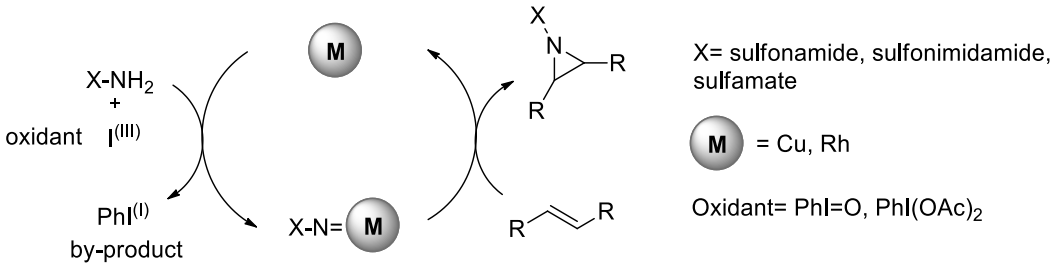

Fig. 5.31 Metal-catalysed aziridination of olefins in the presence of an oxidant

Recently, several tricks to make this process stereoselective have been also proposed, involving the use of external controller such as a catalyst, or a ligand or a simple chiral agent.[12]

The *N*-protecting tosyl moiety has sometimes even an active role in some stereoselective aziridination reactions: with a bulky *N*-substituent, minimization of the steric repulsion could be the driving force of the

process, when the **metal-nitrene**, the ligand and the olefin are very close to each other, and thus the discrimination of one face/site of the olefin from the other for the formation of the aziridine can be possible. However, all of these procedures showed various drawbacks, such as the need for new nitrene sources to improve the versatility of the method and the often problematic removal of the *N*-substituent (usually *N*-sulfonyl groups) at the end of the synthesis. In addition, the mechanisms of most of these processes are not completely clear yet.

Another organic source of nitrogen are azido compounds. They can be synthetized from the corresponding amines and they are tolerant to a wide range of functional groups. Azides can afford the required nitrenoid species by simply dissociating, releasing molecular nitrogen. The only drawbacks of these compounds are in their preparation, that could involve several synthetic steps, and in their often low reactivity, overcome by using high temperatures or UV irradiation in some cases. An example of this chemistry is reported below in **Fig. 5.32**:[73-75]

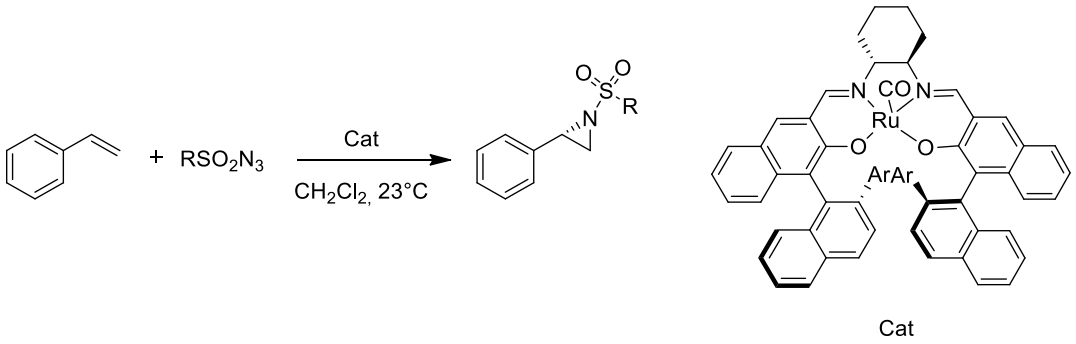

Fig. 5.32 Synthesis of aziridines by using azides as nitrogen sources

Recently, a metal-free visible-light induced decarboxylative aza-Darzens reaction between *N*-aryl glycines and diazo compounds was reported, to generate a series of mono-substituted aziridines (**Fig. 5.33**).[76]

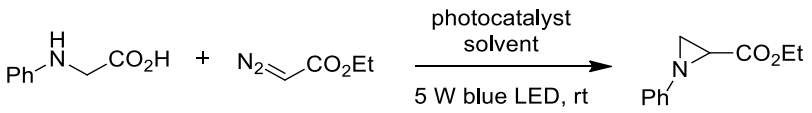

Fig. 5.33 Metal-free visible-light inducing decarboxylative aza-Darzen reaction; the photocatalyst is the Rose Bengal (RB), the solvent is MeOH

The aziridine-2-carboxylate generated represents a very interesting electrophilic scaffold for the design of cysteine protease inhibitors.[77-83]

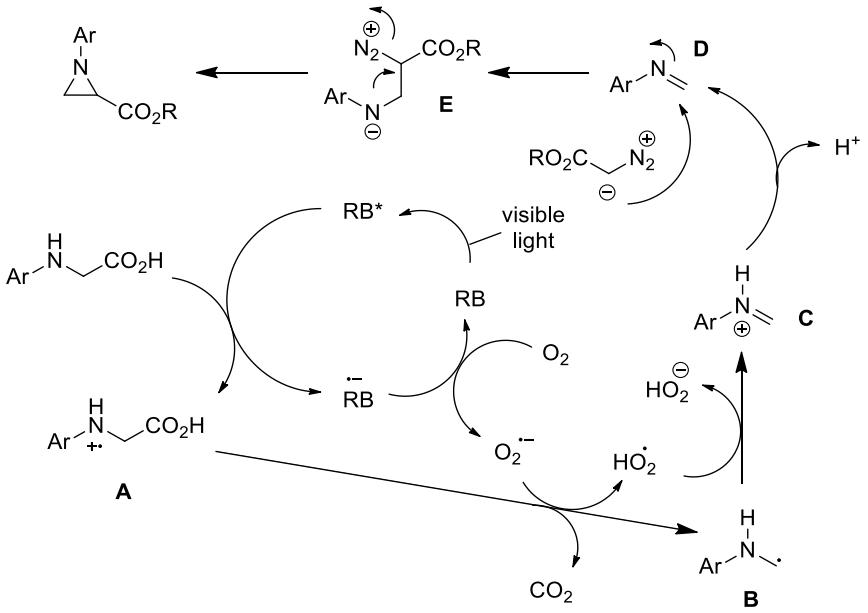

Fig. 5.34 Mechanism for the aza-Darzen process, where RB is the Rose Bengal photocatalyst

A mechanism for the aza-Darzen process was proposed (**Fig. 5.34**): the photoexcitacion of the rose bengal (**RB**) by visible light generates excited **RB*** that is quenched by *N*-aryl glycine to afford the cation radical intermediate **A**. The decarboxylation of **A** leads to the α-amino alkyl radical **B** which is further oxidized to give the iminium ion **C**. Deprotonation of **C** affords the active imine **D** and finally the nucleophilic addition of the diazo specie on the C=N bond, followed by an intramolecular nucleophilic attack (**E**), leads to the final aziridine product.

The authors of this work investigated also the versatility and the functional group tolerance of this procedure, that was found to be significantly sensitive to the *N*-aryl glycine substituent: while EDGs, such as methoxy, and EWGs, such as fluoro, chloro and bromo were well tolerated (even located in different positions on the ring), other EWGs such as NO_2 or Boc, Ts and Ac resulted not compatible with this transformation.

5.4.1 Synthesis of *N*-acylaziridines

In activated aziridines, such as *N*-tosyl and N-acyl aziridines, the electron-withdrawing group on the nitrogen facilitates the ring opening reaction, increasing the electrophilicity of the two adjacent carbons and stabilizing the negatively charged intermediate, generated after the nucleophilic attack.

N-acylaziridines are considered strategic organic intermediates, deserving many efforts for the discovery and the optimization of new synthetic methodologies for their production. Indeed, the traditional methods present several drawbacks, like all the challenges associated to the possible thermal rearrangement of these molecules (see Chapter 5.3.2.2),[84] but also the formation of by-products due to the undesired ring-opening processes that complicates the purification step.

In 2013, Morgan and co-workers published a procedure that allows the gram scale synthesis of *N*-acylaziridines by deprotection of *N*-tosylaziridines and reprotection with *N*-hydroxysuccinimide derivatives

(**Fig. 5.35**).[85] They also demonstrated the advantage of having an electro-deficient aziridine (bearing the 3,5-dinitrobenzoyl (DNB) as nitrogen protecting group, for example) in order to favour the ring opening by a wide range of nucleophiles.

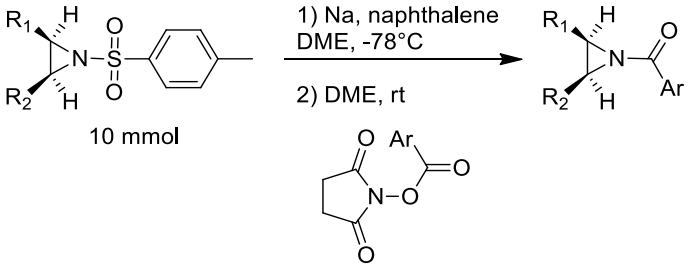

Fig. 5.35 Gram scale synthesis of *N*-acylaziridines by deprotection of *N*-tosylaziridines and reprotection with *N*-hydroxysuccinimide derivatives proposed by Morgan et al.[85]

As described above, most of the procedures reported so far in literature have described the synthesis of *N*-tosylaziridine and for this reason Morgan's method revealed to be so efficient and useful. Furthermore, it allows to functionalize *N*-tosylaziridines directly, avoiding the isolation of the intermediate free-aziridine, whose stability is quite variable and thus not predictable.

In summary…

All of these examples demonstrate the recent efforts and the interest in the preparation of aziridines. Most of these methods are still limited to the synthesis of *N*-activated aziridines that usually bear strongly electron-withdrawing groups on the nitrogen atom. In particular, without question *N*-sulfonyl activated aziridines are the most widely-employed class used in organic chemistry because of their relatively easy preparation and because of their significantly greater stability compared to the corresponding N-H compounds. The only significant drawback to the use of such aziridines as synthetic intermediates is the reluctance of the *N*-substituent bond (sulfonammide or carbamate) to undergo cleavage using mild conditions: strongly acidic or reductive conditions must often be employed to liberate the amine product, which is inevitably the desired target of the synthetic sequence. The harsh conditions usually necessary for the deprotection could lead to a loss of valuable material or to the disruption of the sensitive three-membered ring. In addition to this additional step with all its risks and complications correlated, most of the synthetic methodologies in literature involves nitrogen sources generated by using strong oxidants.

For all of these reasons, the development of new methodologies for the direct synthesis of N-H aziridines remains a very attractive and challenging task.

5.4.2 Synthesis of N-H aziridines

Unprotected aziridines are important compounds due to their presence in various pharmacologically active natural products and other pharmaceutical agents with antitumor activity. [27, 86-88] They are also important intermediates in organic chemistry thanks for their reactivity and versatility. However, as already mentioned, until 2014 there were no examples available for the direct synthesis of N-H aziridines. There were instead some methods that describe the preparation of these compounds in more than one step.

In 2010, Lebel and co-workers proposed a method for the stereoselective synthesis of N-H aziridines through copper catalysis using a chiral bis-oxazoline as the ligand.[89-92] This procedure requires an electron deficient styrene as the starting olefin, used in large excess, and it involves tosyloxycarbamate as a cheap and stable nitrogen source, avoiding the use of additional oxidant (**Fig. 5.36**). The *N*-protecting group can be removed at the end in mild conditions (by using 5 equivalents of LiOH).

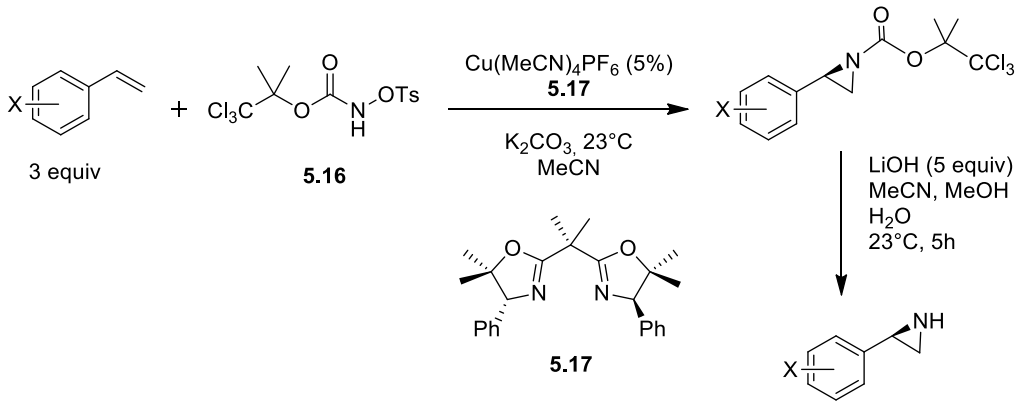

Fig. 5.36 Stereoselective synthesis of N-H aziridines through copper catalysis using a chiral bis-oxazoline **5.17** as the ligand

The carbamoyl moiety used as a protecting group could also be useful to promote nucleophilic opening of the aziridine ring upon *N*-deprotection, giving an amino-alcohol as final product (**Fig. 5.37**).

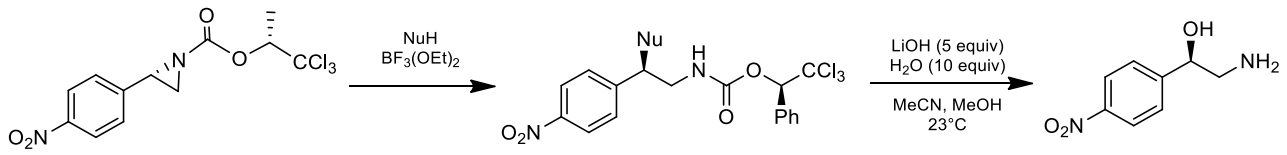

Fig. 5.37 Nucleophilic opening of aziridine ring upon *N*-deprotection to give an amino-alcohol

Katsuki and co-workers demonstrated that $SESN_3$ is an ideal as nitrogen source, due to the easy removal of the corresponding SES moiety nitrogen protective group (by simple treatment with the tris(dimethylamino)sulfonium difluorotrimethylsilicate, TASF) (**Fig. 5.38**).[73-75]**Errore. Il segnalibro non è definito.**

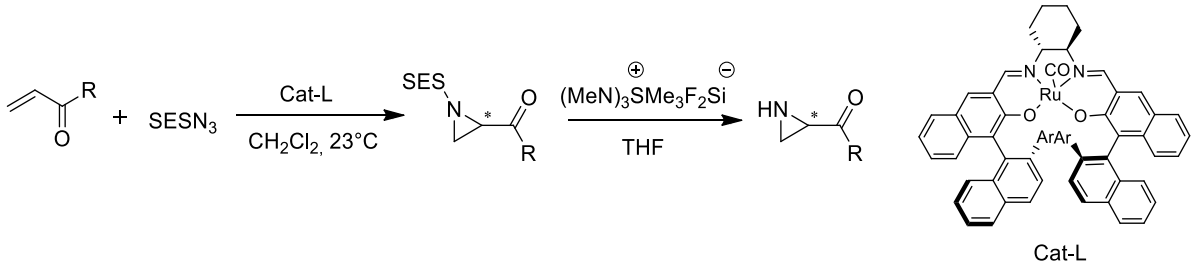

Fig. 5.38 $SESN_3$ used as nitrogen source in the aziridine synthesis; follows the removal of SES nitrogen protective group to give the free-aziridine

Another quite old procedure is the three-step sequence proposed initially by Sweeney and by Tanner later, which leads to N-H aziridines from alkenes through epoxidation, ring opening with an azide and reductive ring closure with triphenylphosphine (**Fig. 5.39**).[93-95]

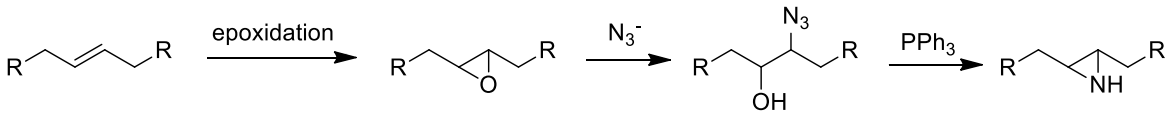

Fig. 5.39 Three-step synthesis of N-H aziridines proposed by Sweeney and Tanner[93-95]

Although this methodology usually provided high yields, the multi-step pathway was long and tedious.
Only in 2014 the first procedure was published for the direct aziridination of diverse mono-, di-, tri- and tetra-substituted olefins, through homogeneous rhodium catalysis.[96] This method does not require external oxidants and involves the use of an hydroxylamine (the *O*-(2,4-dinitrophenyl)hydroxylamine, DPH) as aminating agent that is commercially available and quite stable when exposed to air.[97] Furthermore, for this process the authors proposed the Du Bois' catalyst ($Rh_2(esp)_2$), which is a dimeric rhodium dicarboxylate complex that can be handled in air without any special precautions and is not so expensive (100 mg/63.90 €) considering the low loadings required in the procedure. After screening different reaction media (like MeCN, MeOH, etc. …) they selected 2,2,2-trifluoroethanol (TFE) as highly polar, hydroxylic and non-nucleophilic solvent (**Fig. 5.40**).

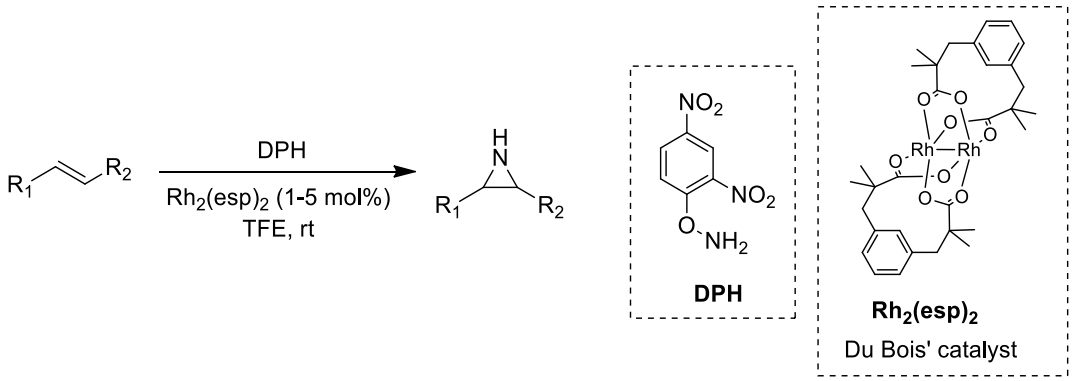

Fig. 5.40 N-H aziridation process catalysed by Du Bois' catalyst proposed by Falck et al.[96]

In order to demonstrate the efficiency of the method, the authors explored the versatility of the N-H aziridation conditions and its tolerance for many functional groups located in different regions in the starting

materials. The procedure was found to be suitable for aliphatic substrates, bearing terminal or less accessible unfunctionalized double bonds, and for cyclic olefins like cyclohexene, with good yields (60-90%).

They also examined the possible mechanisms of the process, with quantum mechanical density-functional theory (DFT) calculations: the most plausible pathway goes through the formation of a metal-nitrene species as intermediate (**Fig. 5.41**). Indeed, in the first step the hydroxylamine (DPH) coordinates the metal centre of the catalyst loosing dinitrophenol (ArO-H), giving the nitrene in a triplet-spin state (which calculations evaluated at 8 kcal/mol lower in energy than the open-shell singlet). However, since the catalyst and the final aziridine product have singlet-spin ground states, a spin interconversion is necessary after the formation of the first C-N bond with the alkene, generating a diradical intermediate. Afterwards, the second C-N bond is formed by coupling of the two free electrons without energy barriers and leading directly to the final N-H aziridine.

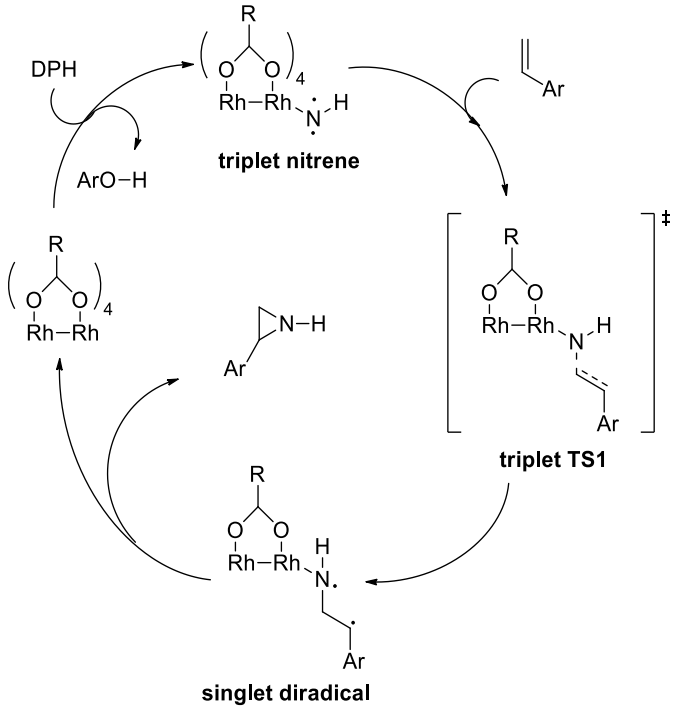

Fig. 5.41 The most plausible pathway for the N-H aziridation catalysed by Du Bois' catalyst, using DPH as aminating agent

Although the method revealed to be really versatile, operationally simple, scalable and involving mild conditions and low catalyst loading, a drawback remains the nitrogen source: although DPH is air stable and not so expensive (1g/34 €), it is required in stoichiometric amount and its commercial sources are still limited. Other problems are related to its relatively short shelf life, reason why DPH has to be stored in the fridge, and to the toxicity of both DPH and the by-product (the 2,4-dinitrophenol released during the process) that could be a serious issue from an industrial application point of view.

In 2017, Kürti (one of the authors of the above mentioned work[96]) and co-workers proposed an alternative aminating agent: hydroxylamine-*O*-sulfonic acid HOSA (**Fig. 5.42**).[98]

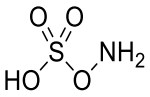

Fig. 5.42 Hydroxylamine-*O*-sulfonic acid HOSA

This reagent presents a robust thermal stability, it is widely available and is even cheaper than DPH (5g/47 €). Moreover, the only by-product derived from HOSA is an inorganic sulphate produced during the work-up that can be easily removed through aqueous extraction. Besides having solved the problems correlated to DPH, compared to the previous procedure this method provides shorter reaction times and a wider substrate scope, including cyclic and acyclic olefins that bear various functional groups, like esters, silyl ethers and alcohols.

5.5 References

1) A. Tamburrini; S. Achilli; F. Vasile; S. Sattin; C. Vives; C. Colombo; F. Fieschi; A. Bernardi, *Bioorg Med Chem* **2017**, *25*, 5142-5147.
2) A. Padwa; C. Murphree, *Chapter 4.1 Three-membered ring systems*, Elsevier: **2003**; *15*.
3) J. B. Sweeney, *Chem. Soc. Rev.* **2002**, *31*, 247-258.
4) U. M. Lindström; P. Somfai, *Synthesis* **1998**, *1998*, 109-117.
5) J. B. Sweeney, Georg Thieme Verlag: Stuttgart: Germany, **2008**; *40*.
6) B. Zwanenburg; P. ten Holte, *Curr. Chem.* **2001**, *216*, 93.
7) P. Somfai; J. Ahman, *Targets Heterocycl. Syst.* **1999**, *3*, 341.
8) A. Padwa, *Aziridines and Azirines: Monocyclic*, Elsevier: Oxford, **2008**.
9) G. E. Ham, *The Journal of Organic Chemistry* **1964**, *29*, 3052-3055.
10) F. M. D. Ismail; D. O. Levitsky; V. M. Dembitsky, *European Journal of Medicinal Chemistry* **2009**, *44*, 3373-3387.
11) C. J. Thibodeaux; W.-c. Chang; H.-w. Liu, *Chemical Reviews* **2012**, *112*, 1681-1709.
12) L. Degennaro; P. Trinchera; R. Luisi, *Chem Rev* **2014**, *114*, 7881-929.
13) M. Kasai; M. Kono, *Synlett* **1992**, *1992*, 778-790.
14) W. A. Remers, *The Chemistry of Antitumor Antibiotics, Vol. 1*, Wiley-Interscience: **1979**; *1*, 242.
15) W. A. Remers; R. T. Dorr, *Alkaloids: Chemical and Biological prespectives*, Wiley: New York, **1988**; *6*, 1.
16) T. J. Hodgkinson; M. Shipman, *Tetrahedron* **2001**, *57*, 4467-4488.
17) R. S. Coleman; J.-S. Kong; T. E. Richardson, *Journal of the American Chemical Society* **1999**, *121*, 9088-9095.
18) R. S. Coleman; J. Li; A. Navarro, *Angew Chem Int Ed Engl* **2001**, *40*, 1736-1739.
19) W. McCoull; F. A. Davis, *Synthesis* **2000**, *2000*, 1347-1365.
20) W. Hao; X. Wu; J. Z. Sun; J. C. Siu; S. N. MacMillan; S. Lin, *J Am Chem Soc* **2017**, *139*, 12141-12144.
21) R. Chawla; A. K. Singh; L. D. S. Yadav, *RSC Advances* **2013**, *3*, 11385-11403.
22) J. T. Njardarson, *Synlett* **2013**, *24*, 787-803.
23) P. Dauban; G. Malik, *Angew Chem Int Ed Engl* **2009**, *48*, 9026-9.
24) C. Botuha; F. Chemla; F. Ferreira; A. Perez-Luna, *Aziridines in natural product synthesis*, Wiley-VCH: Weinheim, Germany, **2011**; 3-39.
25) S. Kobayashi; C. Ogawa, *Science of Synthesis, Water in Organic Synthesis*, Thieme, Stuttgart: **2012**; 579-599.
26) X. E. Hu, *Tetrahedron* **2004**, *60*, 2701-2743.
27) I. D. Watson; L. Yu; A. K. Yudin, *Acc Chem Res* **2006**, *39*, 194-206.
28) J. Kidd; K. Maiden; J. B. Morgan, *Tetrahedron* **2016**, *72*, 3802-3807.
29) H. W. Heine; M. E. Fetter; E. M. Nicholson, *Journal of the American Chemical Society* **1959**, *81*, 2202-2204.
30) H. Heine; H. Bender, *The Journal of Organic Chemistry* **1960**, *25*, 461-463.
31) H. W. Heine; D. C. King; L. A. Portland, *The Journal of Organic Chemistry* **1966**, *31*, 2662-2665.
32) P. Thyrum; A. R. Day, *Journal of Medicinal Chemistry* **1965**, *8*, 107-111.

33) H. W. Heine; M. S. Kaplan, *The Journal of Organic Chemistry* **1967**, *32*, 3069-3074.
34) J. W. Lown; T. Itoh; N. Ono, *Canadian Journal of Chemistry* **1973**, *51*, 856-869.
35) F. W. Eastwood; P. Perlmutter; Q. Yang, *Journal of the Chemical Society, Perkin Transactions 1* **1997**, 35-42.
36) B. F. Bonini; M. Fochi; M. Comes-Franchini; A. Ricci; L. Thijs; B. Zwanenburg, *Tetrahedron: Asymmetry* **2003**, *14*, 3321-3327.
37) H. Heine; Z. Proctor, *The Journal of Organic Chemistry* **1958**, *23*, 1554-1556.
38) T. Nishiguchi; H. Tochio; A. Nabeya; Y. Iwakura, *Journal of the American Chemical Society* **1969**, *91*, 5835-5841.
39) T. Nishiguchi; H. Tochio; A. Nabeya; Y. Iwakura, *Journal of the American Chemical Society* **1969**, *91*, 5841-5846.
40) K. Hori; T. Nishiguchi; A. Nabeya, *The Journal of Organic Chemistry* **1997**, *62*, 3081-3088.
41) D. Ferraris; W. J. Drury; C. Cox; T. Lectka, *The Journal of Organic Chemistry* **1998**, *63*, 4568-4569.
42) G. Cardillo; L. Gentilucci; M. Gianotti; A. Tolomelli, *Tetrahedron* **2001**, *57*, 2807-2812.
43) A. Martin; K. Casto; W. Morris; J. B. Morgan, *Organic Letters* **2011**, *13*, 5444-5447.
44) M. Punk; C. Merkley; K. Kennedy; J. B. Morgan, *ACS Catal* **2016**, *6*, 4694-4698.
45) C. Cox; D. Ferraris; N. N. Murthy; T. Lectka, *Journal of the American Chemical Society* **1996**, *118*, 5332-5333.
46) R. Fussenegger; B. M. Rode, *Chemical Physics Letters* **1976**, *44*, 95-99.
47) Giuliana Cardillo; Luca Gentilucci; Massimo Gianotti; A. Tolomelli, *Eur J Org Chem* **2000**, 2489.
48) P. E. Fanta; E. N. Walsh, *The Journal of Organic Chemistry* **1966**, *31*, 59-62.
49) G. Szeimies; K. Mannhardt; M. Junius, *Chemische Berichte* **1977**, *110*, 1792-1803.
50) E. L. Stogryn; S. J. Brois, *The Journal of Organic Chemistry* **1965**, *30*, 88-91.
51) R. S. Atkinson; C. W. Rees, *Chemical Communications (London)* **1967**, 1232a-1232a.
52) A. Mishra; S. N. Rice; W. Lwowski, *The Journal of Organic Chemistry* **1968**, *33*, 481-486.
53) H. W. Heine; P. G. Mente, *The Journal of Organic Chemistry* **1971**, *36*, 3076-3078.
54) P. G. Mente; H. W. Heine; G. R. Scharoubim, *The Journal of Organic Chemistry* **1968**, *33*, 4547-4548.
55) P. Scheiner, *The Journal of Organic Chemistry* **1967**, *32*, 2628-2630.
56) P. Müller; C. Boléa, *Helvetica Chimica Acta* **2002**, *85*, 483-494.
57) A. Mordini; F. Russo; M. Valacchi; L. Zani; A. Degl'Innocenti; G. Reginato, *Tetrahedron* **2002**, *58*, 7153-7163.
58) H. Wenker, *Journal of the American Chemical Society* **1935**, *57*, 2328-2328.
59) J. Hoch, *Compt. Rend.* **1934**, *198*, 1865.
60) K. N. Campbell; B. K. Campbell; J. F. McKenna; E. P. Chaput, *J. Org. Chem.* **1943**, *8*, 103.
61) K. N. Campbell; B. K. Campbell; E. P. Chaput, *The Journal of Organic Chemistry* **1943**, *08*, 99-102.
62) J. Jiang; H. Liu; C. D. Lu; Y. J. Xu, *J Org Chem* **2017**, *82*, 811-818.
63) K. N. Campbell; J. F. McKenna, *The Journal of Organic Chemistry* **1939**, *04*, 198-205.
64) Gabriel, *Ber. deut. Chem. Ges.* **1888**, *21*, 1049.
65) Z. Li; K. R. Conser; E. N. Jacobsen, *Journal of the American Chemical Society* **1993**, *115*, 5326-5327.
66) D. A. Evans; M. T. Bilodeau; M. M. Faul, *Journal of the American Chemical Society* **1994**, *116*, 2742-2753.
67) P. Müller; C. Baud; Y. Jacquier, *Tetrahedron* **1996**, *52*, 1543-1548.
68) L. A. Carpino; R. K. Kirkley, *Journal of the American Chemical Society* **1970**, *92*, 1784-1786.
69) R. S. Atkinson; M. J. Grimshire; B. J. Kelly, *Tetrahedron* **1989**, *45*, 2875-2886.
70) R. S. Atkinson; G. Tughan, *Journal of the Chemical Society, Perkin Transactions 1* **1987**, 2797-2802.
71) R. S. Atkinson; J. R. Malpass; K. L. Skinner; K. L. Woodthorpe, *Journal of the Chemical Society, Perkin Transactions 1* **1984**, 1905-1912.
72) S. Fantauzzi; A. Caselli; E. Gallo, *Dalton Trans* **2009**, 5434-43.
73) K. Omura; M. Murakami; T. Uchida; R. Irie; T. Katsuki, *Chemistry Letters* **2003**, *32*, 354-355.
74) K. Omura; T. Uchida; R. Irie; T. Katsuki, *Chemical Communications* **2004**, 2060-2061.
75) H. Kawabata; K. Omura; T. Katsuki, *Tetrahedron Letters* **2006**, *47*, 1571-1574.
76) Y. Liu; X. Dong; G. Deng; L. Zhou, *Science China Chemistry* **2016**, *59*, 199-202.
77) G. Callebaut; T. Meiresonne; N. De Kimpe; S. Mangelinckx, *Chem Rev* **2014**, *114*, 7954-8015.

78) L. Morodor; H. J. Musiol; R. Scharf, *FEBS Letters* **1992**, *299*, 51-53.
79) D. P. Galonić; N. D. Ide; W. A. van der Donk; D. Y. Gin, *Journal of the American Chemical Society* **2005**, *127*, 7359-7369.
80) H. Helten; T. Schirmeister; B. Engels, *The Journal of Physical Chemistry A* **2004**, *108*, 7691-7701.
81) T. Ishikawa, *Heterocycles* **2012**, *85*, 2837.
82) G. Cardillo; L. Gentilucci; A. Tolomelli, *Aldrichimica Acta* **2003**, *36*, 39.
83) W. K. Lee; H.-J. Ha, *Aldrichimica Acta* **2003**, *36*, 57.
84) H. Heine, *Mech. Mol. Migr.* **1971**, *3*, 145-176.
85) H. Rubin; J. Cockrell; J. B. Morgan, *J Org Chem* **2013**, *78*, 8865-71.
86) M. Sasaki; A. K. Yudin, *Journal of the American Chemical Society* **2003**, *125*, 14242-14243.
87) P. A. S. Lowden, *Aziridine natural products - discovery, biological activity and biosynthesis*, Wiley-VCH: WEinheim, **2006**; 399-442.
88) V. H. Dahanukar; L. A. Zavialov, *Curr. Opin. Drugs. Dis. Dev.* **2002**, *5*, 918-927.
89) H. Lebel; M. Parmentier, Copper-catalyzed enantioselective aziridination of styrenes. In *Pure and Applied Chemistry*, 2010; Vol. 82, p 1827.
90) H. Lebel; K. Huard; S. Lectard, *Journal of the American Chemical Society* **2005**, *127*, 14198-14199.
91) H. Lebel; M. Parmentier; O. Leogane; K. Ross; C. Spitz, *Tetrahedron* **2012**, *68*, 3396-3409.
92) H. Lebel; S. Lectard; M. Parmentier, *Organic Letters* **2007**, *9*, 4797-4800.
93) H. M. I. Osborn; J. Sweeney, *Tetrahedron: Asymmetry* **1997**, *8*, 1693-1715.
94) D. Tanner, *Angewandte Chemie International Edition in English* **1994**, *33*, 599-619.
95) D. Tanner; P. Somfai, *Tetrahedron* **1988**, *44*, 619-624.
96) J. L. Jat; M. P. Paudyal; H. Gao; Q. L. Xu; M. Yousufuddin; D. Devarajan; D. H. Ess; L. Kurti; J. R. Falck, *Science* **2014**, *343*, 61-5.
97) Z. Yang, *Synlett* **2014**, *25*, 1186-1187.
98) Z. Ma; Z. Zhou; L. Kurti, *Angew Chem Int Ed Engl* **2017**, *56*, 9886-9890.

CHAPTER SIX: synthesis of *N*-linked pseudo-thiodisaccharides

6.1 Results and discussion

The first step of the new synthetic pathway developed to generate more hydrolytically stable thio-glycomimetics (**Fig. 6.1**) consists in the N-H aziridation of the double bond of **4.4**.

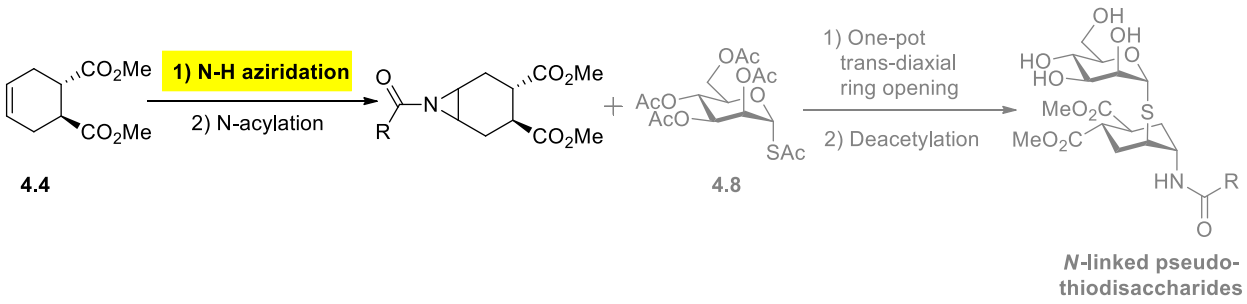

Fig. 6.1 General approach to synthesize *N*-linked pseudo-thiodisaccharides: highlighted in yellow the first step of the N-H aziridiation of **4.4**

The method published in 2014 by Falck and co-workers was applied and optimized for olefin **4.4**. Because of structural similarities, the procedure for cyclohexene **6.1** reported in the substrate scope of this work represented our starting point (**Scheme 6.1**).[1]

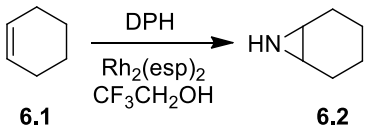

Scheme 6.1 N-H aziridation of cyclohexene **6.1** performed by Falck et al.[1]

In particular, the authors obtained aziridine **6.2** in 71% yield, after 3 hours at room temperature (25°C). No traces of allylic C-H amination, that would lead to the formation of 1-amino-2-cyclohexene, were detected by ^{1}H-NMR analysis, in contrast with other examples reported in the literature about metal nitrene-based aziridiation methods.[2]

6.1.1 N-H aziridation reaction of **4.4**

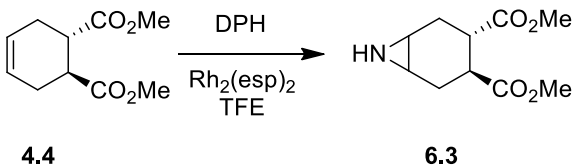

Scheme 6.2 N-H aziridation of **4.4**

Table 6.1 Optimization of the N-H aziridation conditions

Entry	[4.4]	DPH	$Rh_2(esp)_2$	T (C°)	t	SM:Dimer:Product (ratio)	y[a]	Notes
1	0.1 M	1.2 eq	1 mol%	30 (rt)[b]	2 h	1: 1: 3.5	(36 %)	

2	0.1 M	1.2 eq	1 mol%	25	4 h	1: 1: 6	39 %	
3	0.1 M	1.2 eq	1 mol%	20	8 h	1: 15: 51	58 %	
4	0.1 M	1.2 eq	2 mol%	24	6h 30'	1: 12.5: 36.5	54 %	
5	0.1 M	1.2 eq	5 mol%	10-13	8 h	1: 4.5: 19.5	60 %	
6	0.1 M	1.2 eq	1 mol%	20	8 h	/	36%	scale up (entry 3x4)
7	0.1 M	1.2 eq	1 mol%	10-13	8 h	/	68%	scale up (entry 5x4)

[a] measured on the isolated product **6.3** by chromatographic column 95:5 CH_2Cl_2:MeOH
[b] experiment performed in July (temperature not really measured)

In the first experiment with our substrate **4.4** (entry 1), Falck's procedure was faithfully reproduced: since olefin **4.4** was no more detected on the TLC plate (ninhydrin stain) after only 2 hours, the work up was done and the crude analysed by NMR spectroscopy. Although the main product was the desired aziridine **6.3** (as shown by the ^{1}H-NMR spectrum and confirmed by MS spectroscopy) the starting material was still present (recognized through the identification of its diagnostic doublet of the olefinic hydrogens at 5.7 ppm). Furthermore, other signals associated to an unexpected side product were found and the presence of this impurity was also confirmed by TLC analysis (a spot of a more polar compound appeared clearly after the work-up). The purification step by chromatography on silica gel in 95:5 CH_2Cl_2: MeOH was not trivial: despite the slow gradient, the product was isolated as a mixture with the side product, as the NMR spectrum reported below (**Fig. 6.2**) confirmed (so the yield reported in **Table 6.1**, entry 1 refers to a mixture and not to the perfectly clean product).

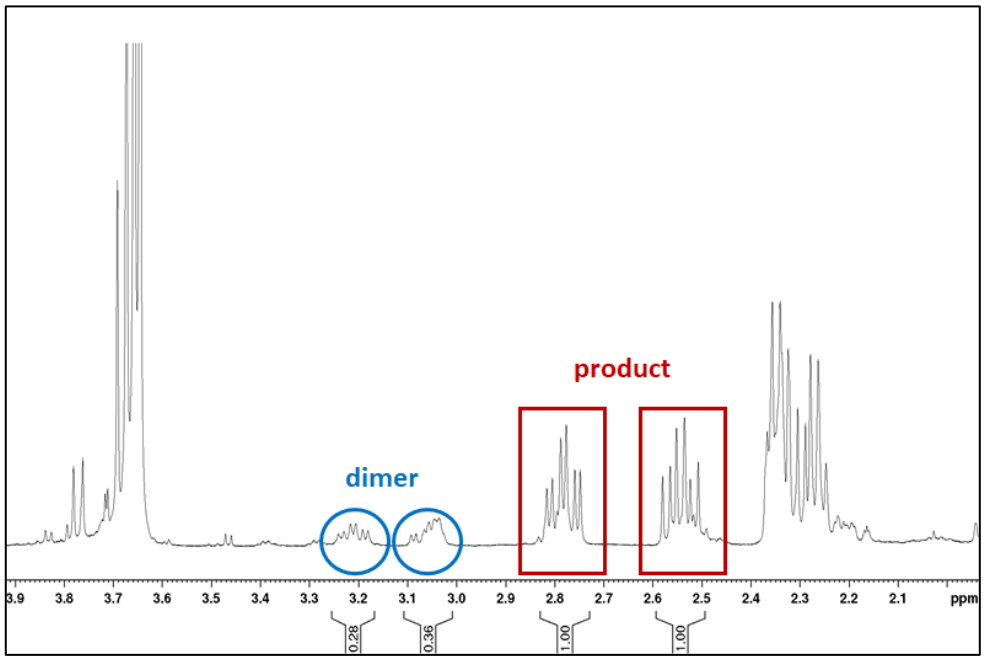

Fig. 6.2 ^{1}H-NMR spectrum of entry 1; highlighted in blue the diagnostic signals of the dimer (dt at 3.21 ppm and the m at 3.08 ppm), in red the diagnostic signals of the product (dt at 2.8 ppm and dt at 2.6 ppm)

After analysis of the ESI-MS data, it was hypothesized that the second specie could be the dimeric form **6.4**, generated upon opening of the aziridine ring by a second molecule of aziridine, working as a nucleophile (**Fig. 6.3**). This hypothesis could also explain the greater polarity of the new by-product spot observed on the TLC plate, as due to the presence of a free amine function.

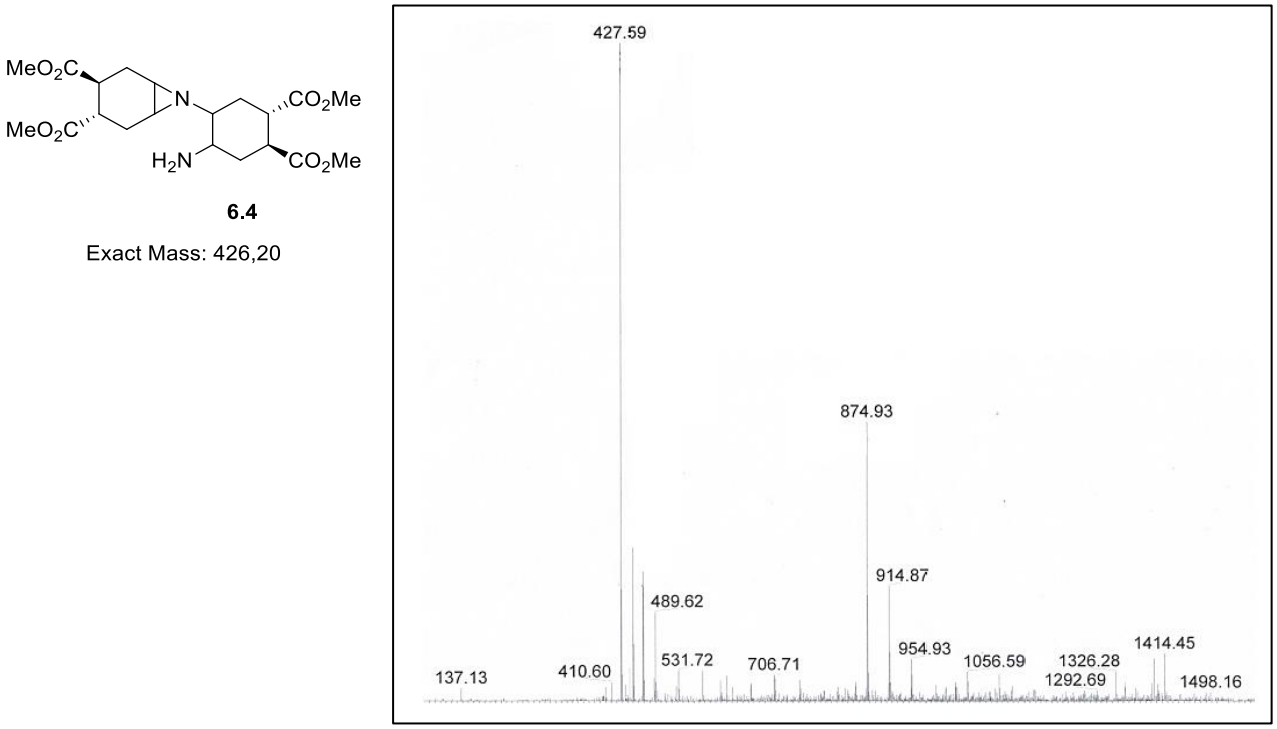

Fig. 6.3 ESI-MS spectrum of **6.4**; peak at m/z= 427.59 [**6.4**+ H]$^+$; peak at m/z= 874.93 [2x**6.4**+Na]$^+$

The hypothesis was later confirmed by isolation and characterization of **6.4** using NMR spectroscopy (see below).

In the original article, the authors did mention the formation of dimerization side products only as a possibility, without reporting any issues faced during the work-up procedure or the purification step.

In summary, three main problems were highlighted by this first trial: the difficulty in following the consumption of the starting olefin, that can not be detected by TLC when its concentration becomes low. As a consequence (second issue), it becomes difficult to judge the reaction end point and to avoid misleading interpretations of the monitoring data, such as the assumption that the conversion is complete while starting material is still available. Finally, the third problem is in the formation of the dimer that has to be limited, keeping temperature, concentration and reaction time under careful control. In the second experiment (**Table 6.1**, entry 2), the temperature was maintained at 25°C and monitored until the end of the reaction. Furthermore, the reaction time was increased to 4 hours, trying to achieve a better conversion of the starting material. In this case, the consumption of the olefin was larger than before, but not complete yet. Instead, formation of the dimer was considerably reduced, even if in small amount (17%) it appeared again in the NMR of the crude. A more careful and slow chromatographic separation (95:5 CH_2Cl_2:MeOH) allowed the

isolation of both the product **6.3** (with 39% yield, **Fig. 6.4**) and the dimeric compound **6.4** (**Fig.6.5**), which, at this point, was fully characterized (see Experimental Section).

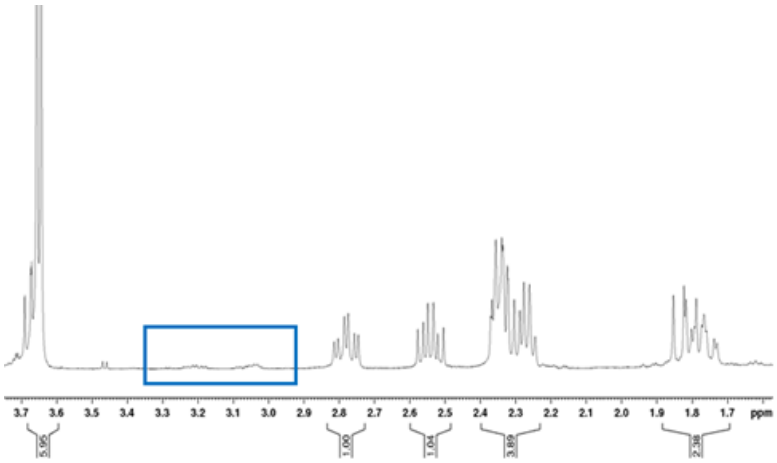

Fig. 6.4 ^{1}H-NMR of the isolated product **6.3**

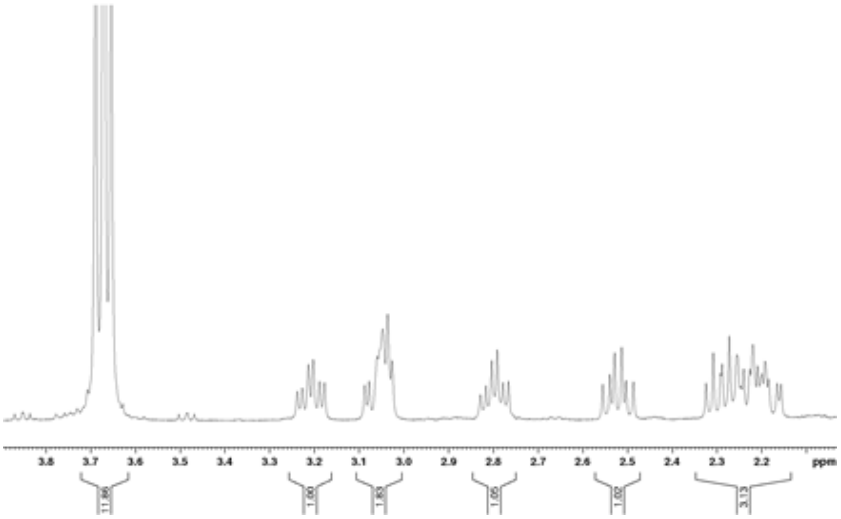

Fig. 6. 5 ^{1}H-NMR of the isolated dimer **6.4**

In the subsequent experiment (entry 3), working at lower temperature (20°C, kept with a cold-water bath) and leaving the reaction under stirring for 8 hours (rather than 4 h), we finally observed complete consumption of the olefin **4.4** (disappearance of the doublet at 5.7 ppm), while the dimer continued to be present, even if in a further decreased amount (15%) compared to the previous trial. However, when these conditions were applied in a larger scale process (entry 6, scale-up by 4-fold) the yield of aziridine **6.3** dropped again to 36%, while the ^{1}H-NMR spectrum revealed the presence of the starting material and the dimer in 1:1 ratio, besides the product.

We went back to the small scale (about 50 mg of **4.4**, 0.25 mmol), looking for reproducible conditions for this reaction. In entries 4 and 5, the amount of the catalyst was increased up to 2 and 5 mol% respectively, because the authors of this procedure, exploring the substrate scope, had noticed that a small increment of

the catalyst loading led to more rapid conversions at room temperature of some olefins. Taking into account this consideration, we tried also to decrease the reaction time (entry 4), without noticeable improvements. However, using 5 mol% of the catalyst, maintaining the temperature at 10-13°C (by using a bath of dry ice in dioxane) and quenching the reaction after 8 hours (time found to be necessary for the total conversion of the olefin **4.4**, see entry 3), a promising yield was obtained (60%, see entry 5).

Finally, with entry 7 we proved that the key factor affording good yields of aziridine **6.3** and avoiding product dimerization **6.4** is the reaction temperature, which must be kept at 10°C for 8h to achieve full conversion, while an increment of catalyst loading does not influence the process. Furthermore, because of the evident instability of the final aziridine toward dimerization, a fast and carefully work up was adopted, avoiding NMR analysis of the crude and performing directly the chromatographic purification. In this case, the best yield of the isolated product was achieved (68%) and the scale up was allowed (by 3-fold) with reproducible yields.

6.1.2 *N*-acylation of the free aziridine 6.3

One of the main advantages of working with free aziridines is their versatility, because the N atom can be functionalized with a wide range of organic frameworks and finally, of course, the three-membered ring can be opened by a variety of nucleophiles (as already described in Chapter five).

The second step of the synthetic pathway that we developed consists in an *N*-acylation reaction of **6.3** (**Fig. 6.6**).

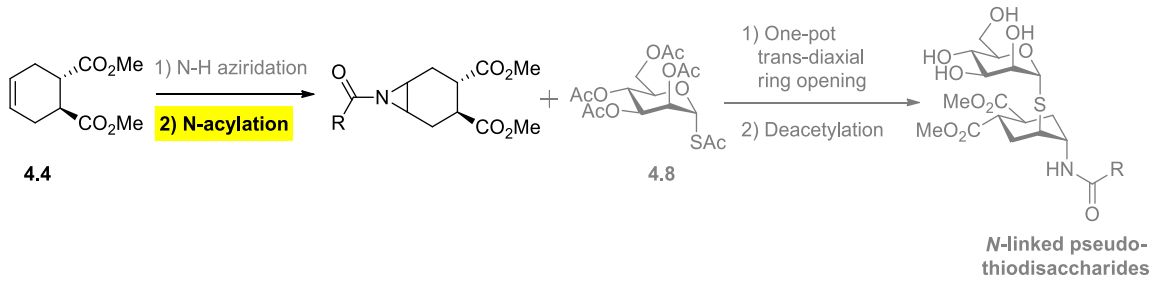

Fig. 6.6 General approach to synthesize *N*-linked pseudo-thiodisaccharides: highlighted in yellow the second step of the *N*-acylation of the free aziridine **6.3**

First of all, we tried the Boc-protection of the free nitrogen of **6.3**, following the procedure reported by Mordini and co-workers for a similar substrate (Boc_2O, TEA, DMAP at room temperature in CH_2Cl_2; **Scheme 6.3**).[3] However, in their conditions, the formation of product **6.5** was not observed.

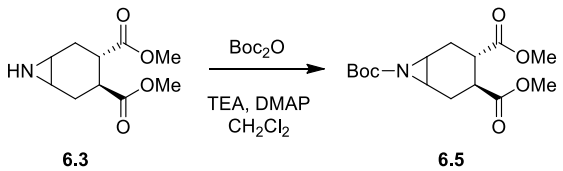

Scheme 6.3 Boc-protection of the free aziridine **6.3**

Instead, the spectrum of the crude revealed the almost complete decomposition of the starting aziridine (evident also on TLC), while the ESI-MS analysis suggested the presence of the dimeric form **6.6** depicted in **Fig. 6.7**.

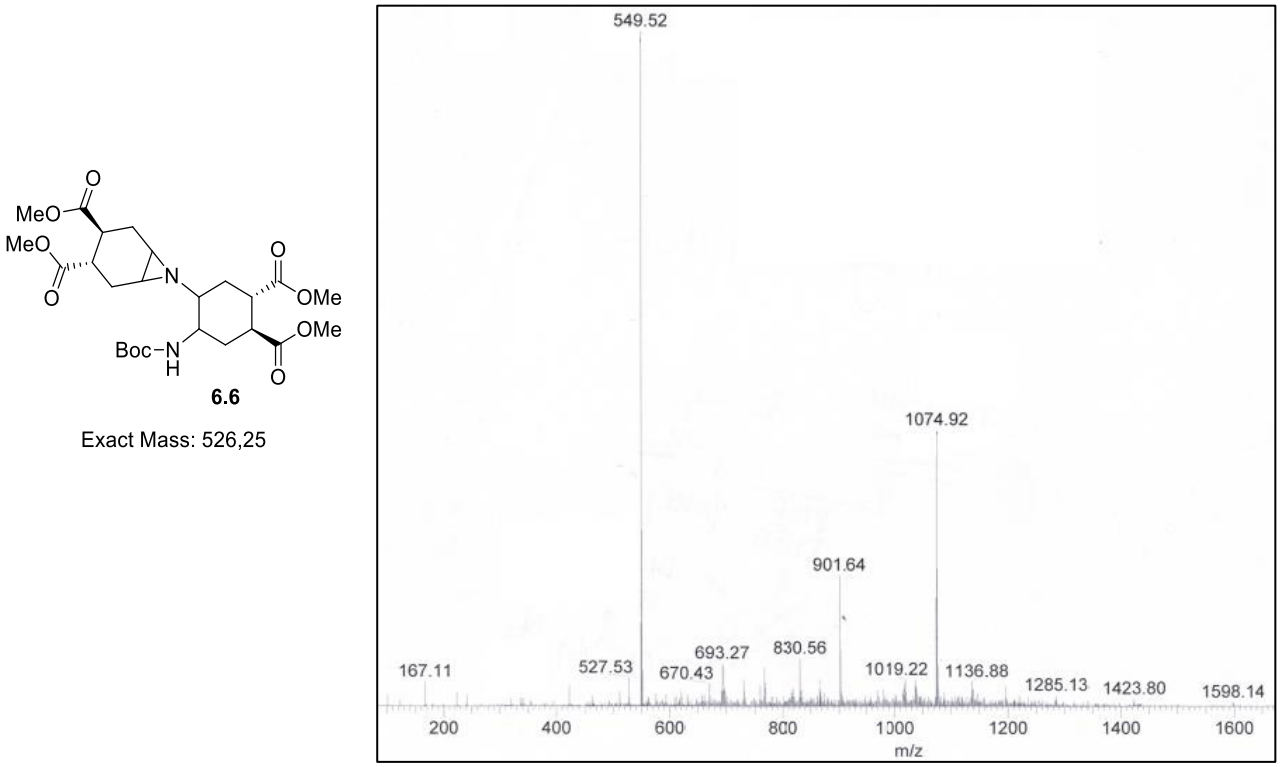

Fig. 6.7 ESI-MS spectrum of the Boc-protection reaction's crude: peak at 549.52 [**6.6**+Na]$^+$; at 1074.92 [2x**6.6**+Na]$^+$

The procedure was optimized by halving the substrate concentration (from 0.7 M to 0.35 M), decreasing the reaction time (from 3 to only 1 hour) and keeping the temperature at 0°C for the all process. In this way, the N-Boc aziridine **6.5** was obtained in 68% yield.

To introduce an azido linker, which could allow the creation of multivalent systems, we tried acylation of **6.3** with a commercially available acyl chloride, the 5-chlorovaleryl chloride **6.7**, bearing a terminal chlorine that could be converted into an azide later on. The reaction was performed in standard conditions for the synthesis of amides, using pyridine as solvent (**Scheme 6.4**).

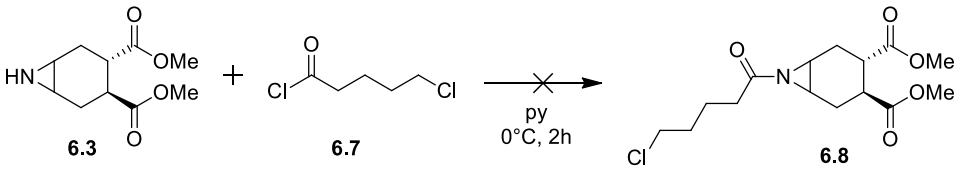

Scheme 6.4 N-acylation of **6.3** with acyl chloride **6.7**

However, the desired amide product **6.8** was not observed in the crude mixture, but ESI-MS analysis allowed to identify the presence of compound **6.9** (**Fig. 6.8**) resulting from opening of the aziridine by nucleophilic attack of the chloride ions released during the acylation process.

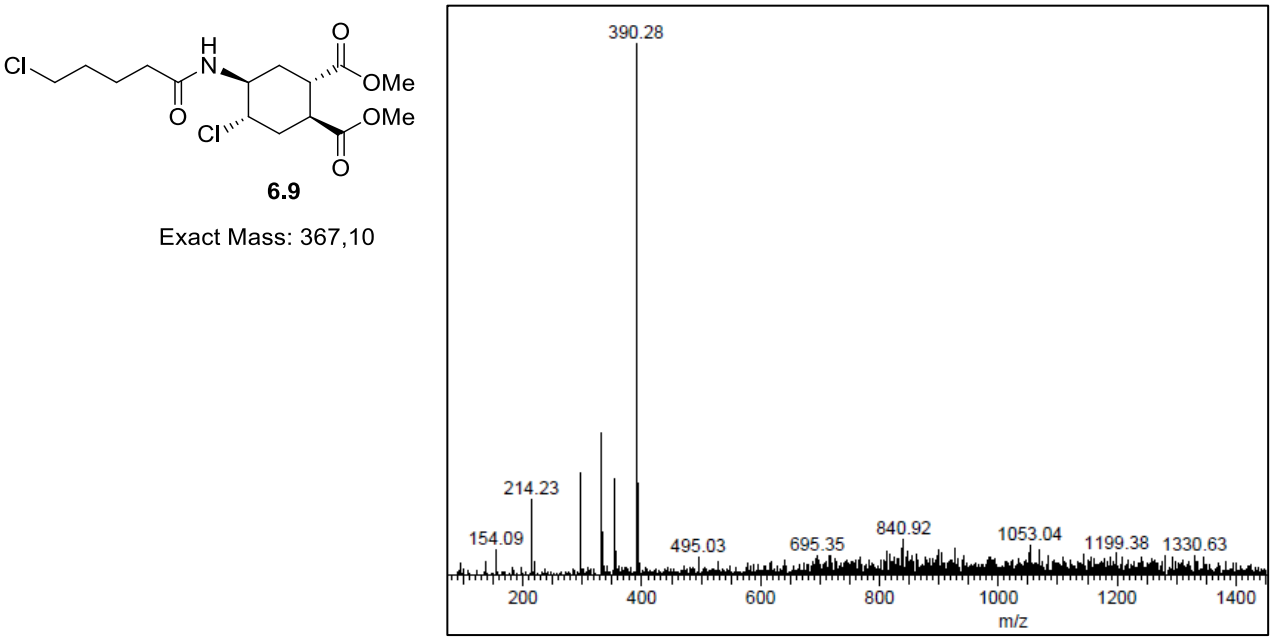

Fig. 6.8 ESI-MS spectrum of the *N*-acylation of **6.3** with **6.7**: peak at 390.28 [**6.9**+Na]$^+$

The formation of similar side-products was previously reported in various literature examples (**Fig. 6.9**).[4-6]

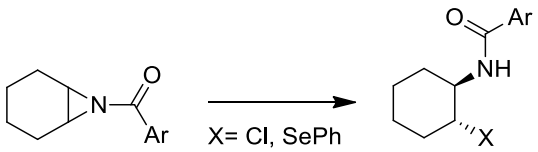

Fig. 6.9 Side opening reaction of *N*-acylated aziridine by nucleophilic species present in solution

To avoid this unwanted reaction, we changed acylating agent, employing carboxylic acid **6.10** in standard coupling conditions (**Scheme 6.5**), using dicyclohexylcarbodiimide (DCC) as condensing agent.

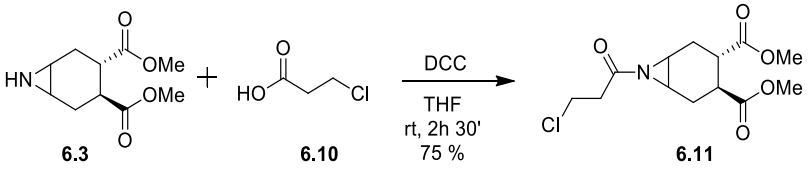

Scheme 6.5 Coupling reaction between free aziridine **6.3** and carboxylic acid **6.10**

The acylated aziridine **6.11** was isolated in 75% yield and then employed in the subsequent opening reaction (see below).

To prove the validity of the method and to optimize the coupling conditions, the *N*-acylation reaction was also performed using propionic acid **6.12** (**Scheme 6.6**). This compound turned out to be less reactive than **6.10** and full consumption of the starting material **6.3** required 4 h at room temperature. However, yields could not be established, since the *N*-propanoyl-aziridine **6.13** could not be fully purified by flash chromatography from diclyclohexylurea (DCU) that is formed in stoichiometric amount during the process.

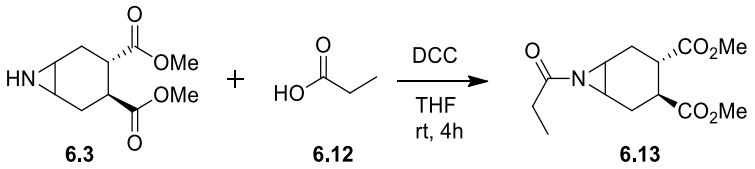

Scheme 6.6 Coupling reaction between free aziridine **6.3** and carboxylic acid **6.12**

The same acylation conditions were also adopted for the reaction between **6.3** and **6.14** (**Scheme 6.7**), which is the same linker used in the synthesis of the *O*-linked pseudo-thiodisaccharide **4.17** (see chapter 4.2.5). Cl-N_3 exchange at the end of the synthesis would afford the required linker.

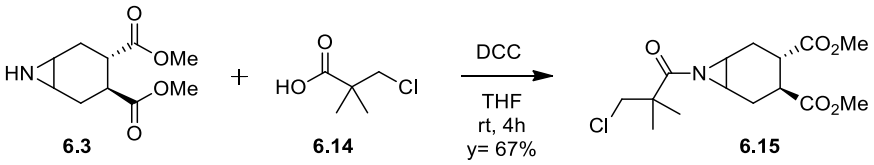

Scheme 6.7 Coupling reaction between free aziridine **6.3** and carboxylic acid **6.14**

Also in this case, the reaction led smoothly to the corresponding *N*-acylaziridine **6.15**, that was isolated through flash chromatography on silica gel (1:1 Hex:EtOAc) in 67% yields.

The olefin aziridination and acylation reactions could also be performed in "telescoped" way[7], starting from **4.4** and avoiding the isolation of the free-aziridine **6.3**, but performing the acylation with **6.14** directly on the crude. This multistep approach limited the decomposition of the free aziridine **6.3** (**Scheme 6.8**) and resulted in a satisfactory 52% yield over the two steps, as opposed to 40% obtained upon isolation of **6.3**.

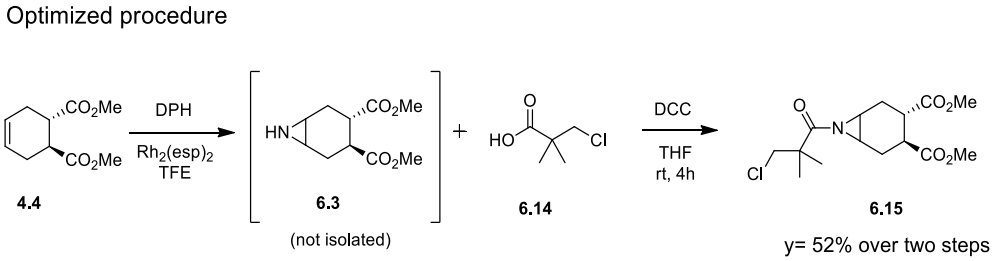

Scheme 6.8 Telescoped approach for the N-H aziridation of **4.4** and the *N*-acylation reaction of **6.3**

This procedure allowed to scale up the transformation to 200 mg of starting alkene (by 4-fold).

To improve the convergence of the synthetic approach, we also performed the chlorine-azide exchange at the beginning directly on carboxylic acid **6.14,** as described in the previous chapter 4.2.5 (**Scheme 6.9**).

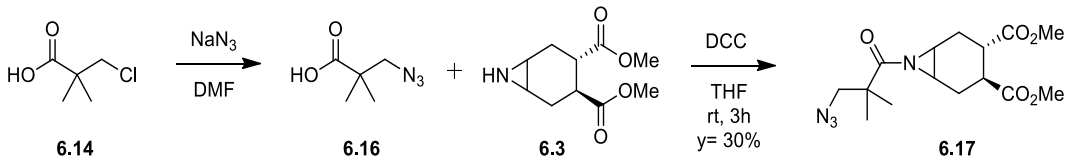

Scheme 6.9 Chlorine-azide exchange on **6.14**; follows the *N*-acylation of **6.3** through the coupling with carboxylic acid **6.16**

The resulting β-azido-acid **6.16** was then employed in the *N*-acylation of aziridine **6.3** using the same conditions developed for **6.14.** DCC-coupling of **6.16** with **6.3** was sluggish, possibly because the absence of the strongly electronegative chlorine atom in the acylating compound reduces its reactivity. The slower

reaction rate also favoured the ring-opening side reaction and the presence of the dimeric form of **6.17** was detected by ESI-MS.

We tried to improve the acylation process increasing the reactivity of **6.16** through activation of the carboxylic function as *p*-nitrophenyl ester **6.19** (**Scheme 6.10**).

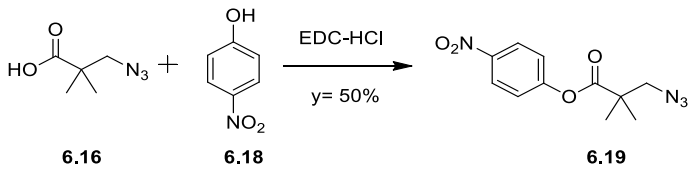

Scheme 6.10 Synthesis of the activated ester **6.19**

Reaction of **6.16** with *p*-nitrophenol **6.18** using EDC·HCl as condensing agent afforded the activated ester **6.19** only in 50% yield; however **6.19** was obtained in 76% yield by reaction of **6.16** with the 4-nitrophenyl trifluoroacetate **6.20** (**Scheme 6.11**).

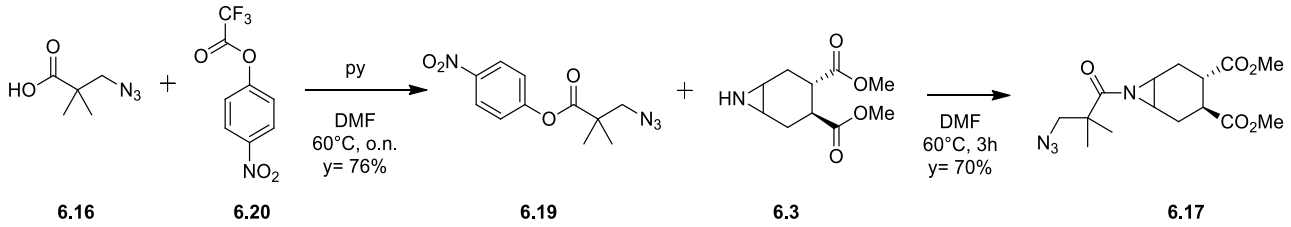

Scheme 6.11 Optimization of the activated ester **6.19** synthesis; follows the *N*-acylation of **6.3** with **6.19**

Acylation of **6.3** with **6.20** afforded amide **6.17** in 60% yield with a considerable improvement compared to the previous experiment (**Scheme 6.9**).

6.1.3 One-pot ring opening reactions

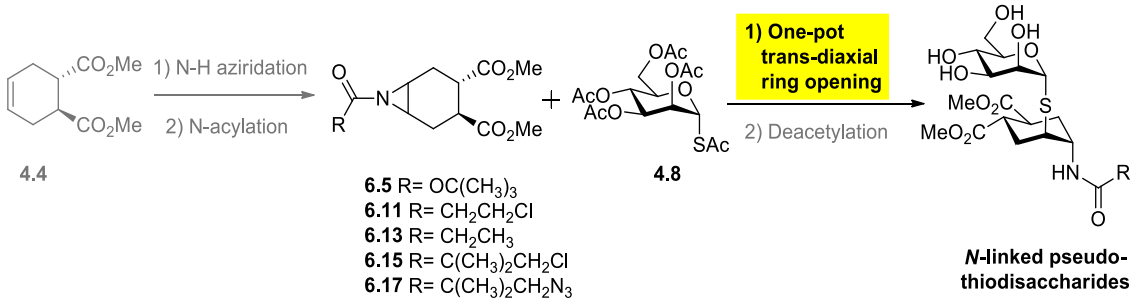

Fig. 6.10 General approach to synthesize *N*-linked pseudo-thiodisaccharides: highlighted in yellow the one-pot ring opening of the *N*-acylated aziridines by α-hioacetate **4.8**

Opening of the *N*-acylaziridines **6.5**, **6.11**, **6.13**, **6.15** and **6.17** with the mannosyl α-thioacetate **4.8** (**Fig. 6.10**) was examined using the one-pot conditions optimized for the epoxide ring opening reaction described in the previous chapter (4.1.3).

The reaction performed with the N-Boc-aziridine **6.5** in DMF using an excess of Et_2NH led smoothly to the pseudo-thiodisaccharide **6.21**, isolated in excellent yield (**Scheme 6.12**).

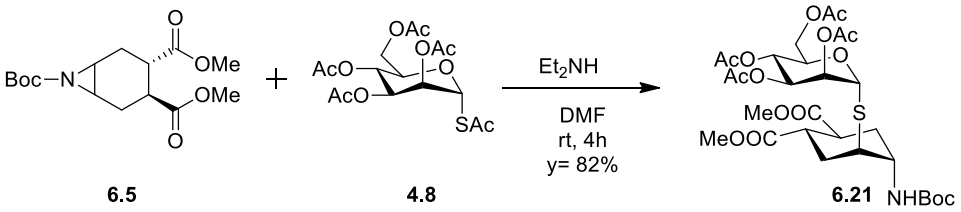

Scheme 6.12 One-pot ring opening of aziridine **6.5** by the α-hioacetate **4.8**

On the contrary, reaction of aziridine **6.11** with **4.8** in the same conditions did not afford the expected glycomimetic **6.22** (**Scheme 6.13**).

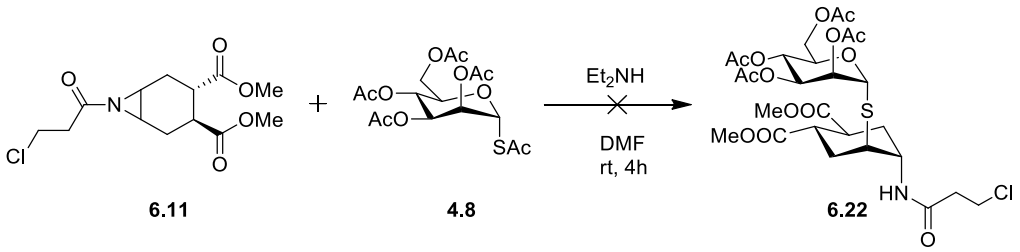

Scheme 6.13 One-pot ring opening of aziridine **6.11** by the α-hioacetate **4.8**

Rather, another specie was identified by NMR spectroscopy and with the help of the ESI-MS analysis product, deriving from nucleophilic displacement of the terminal chloride of **6.11** by the thiolate anion generated in situ from **4.8** (compound **6.23**, **Fig. 6.11**).

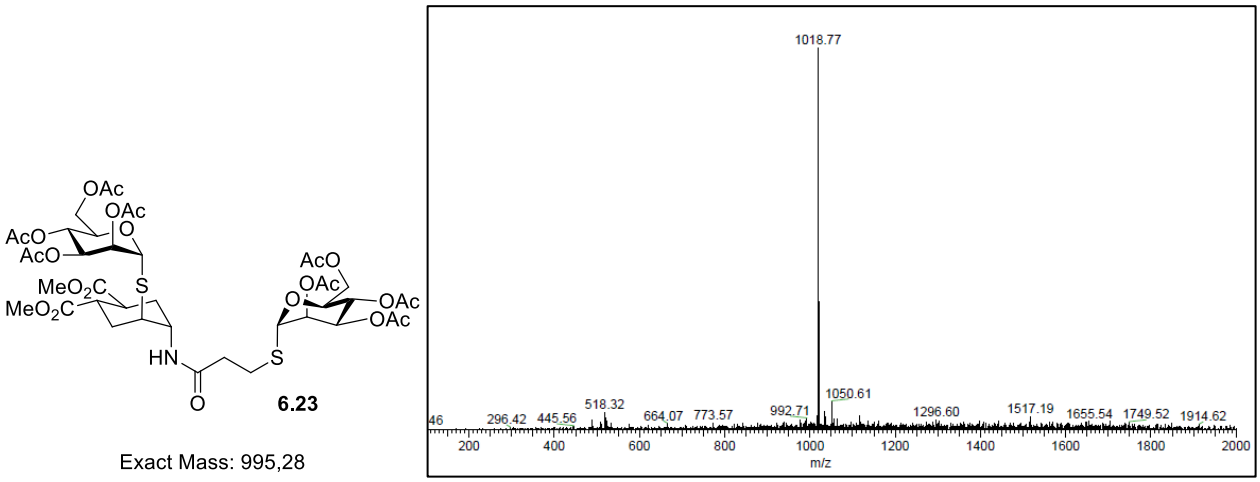

Fig. 6.11 ESI-MS of the crude of the ring opening reaction depicted in **Scheme 6.13**; peak at 1018.77 [**6.23**+ Na]$^+$

Indeed, reaction of glycosyl thioacetates with Et_2NH in DMF was used in the literature to conduct an S_N2 reaction between the thiolate anion deriving from **4.8** and primary alkyl bromides and iodides (**Fig. 6.12**).[8]

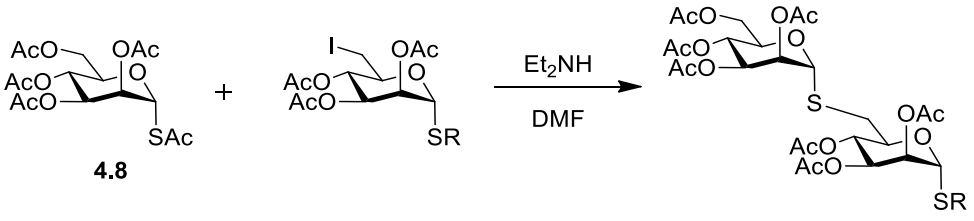

Fig. 6.12 S_N2 reaction between the thiolate anion deriving from **4.8** and primary alkyl iodides reported by Belz et al.[8]

As reported before, the *N*-propanoyl aziridine **6.13** was not completely purified from dicyclohexylurea (DCU) formed during the acylation process (**Scheme 6.6**). However, aziridine **6.13** was successfully submitted to ring opening reaction with **4.8**. The process allowed the formation and isolation of the thio-glycomimetic **6.24** in 36% yield over two steps (acylation and ring opening; **Scheme 6.14**).

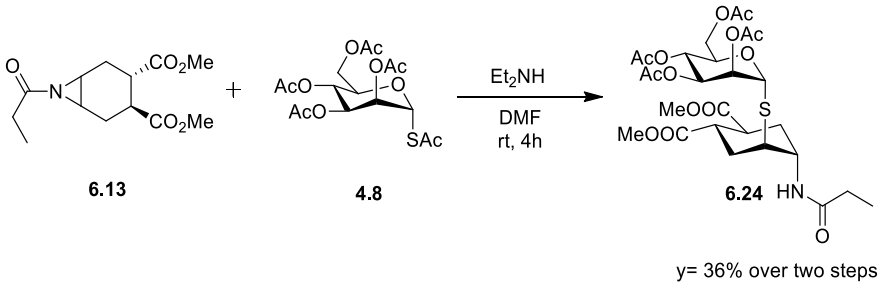

Scheme 6.14 One-pot ring opening of aziridine **6.13** by the α-hioacetate **4.8**

The ring opening of **6.15** with **4.8** afforded the corresponding pseudo-thiodisaccharide **6.25** in almost quantitative yield (**Scheme 6.15**).

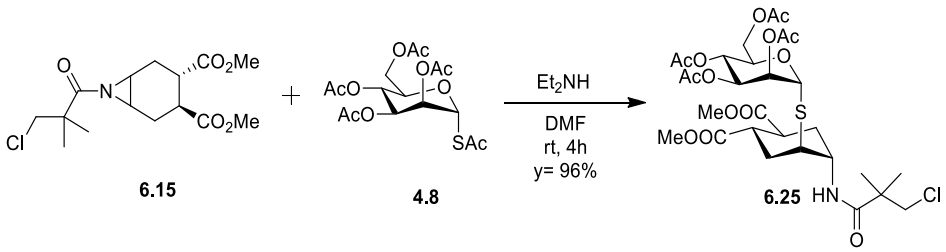

Scheme 6.15 One-pot ring opening of aziridine **6.15** by the α-hioacetate **4.8**

This excellent result confirmed that the presence of a strong EWG, such as the terminal chlorine on the N-substituent of **6.15**, has a beneficial effect on the reactivity of the acylated aziridine toward the nucleophilic attack. However, treatment of thio-glycomimetic **6.25** with sodium azide in DMF, in order to replace the chlorine atom with the azido function, was unsuccessful and the starting material was completely recovered (**Scheme 6.16**).

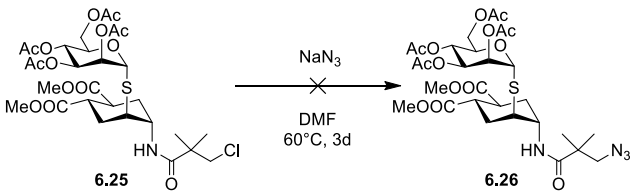

Scheme 6.16 Cl -> N_3 exchange reaction on **6.25**

The same reaction was attempted upon deacetylation of **6.25** to afford **6.28**, but neither in this case the formation of the desired azide was observed (**Scheme 6.17**).

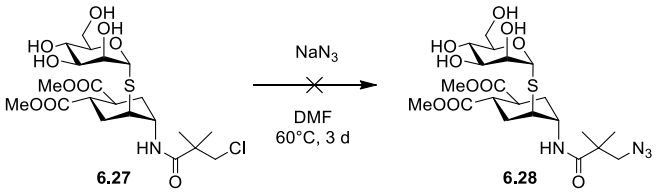

Scheme 6.17 Cl -> N_3 exchange reaction on **6.27**

However, after work-up and reverse phase chromatography (1:1 H_2O:MeOH) a stable new product was isolated in 38% yield along with unreacted starting material. The reaction product was identified by NMR and MS analysis as the β-lactam **6.29** (**Fig. 6.13**), presumably formed upon deprotonation of the amide nitrogen of **6.27** by NaN_3 followed by intramolecular displacement of the chlorine, leading to the four-membered ring formation.

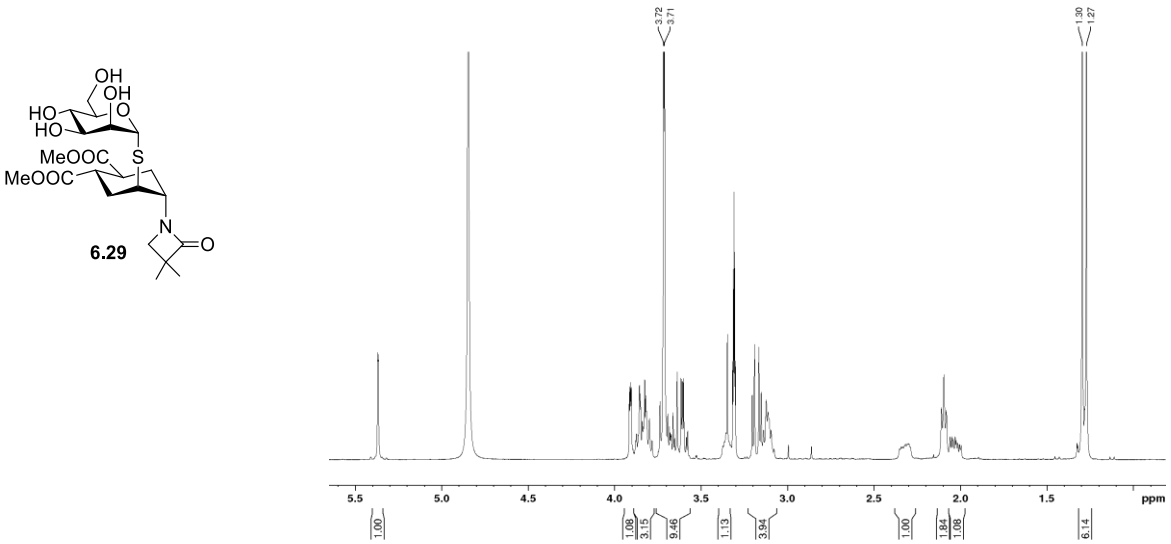

Fig. 6.13 ^{1}H-NMR spectrum in MeOD of the β-lactam **6.29**

Performing the reaction in water, rather than DMF, the basicity of the azide anion should be dampened. However, also in these conditions, nucleophilic displacement of the chlorine by sodium azide did not take place and again the presence of the β-lactam **6.29** was observed in the ESI-MS analysis of the crude.

Since the Cl->N_3 exchange on both compounds **6.25** and **6.27** turned out not to be feasible, aziridine **6.17**, which already carried the azido group, was employed in the one-pot reaction with thioacetate **4.8**.

Compared to the excellent reactivity observed in the same process of the corresponding chlorinated compound (**6.15**), aziridine **6.17** revealed to be much less reactive. Indeed the conversion was not complete (even increasing the time from 4 up to 7 hours) and the yield of the isolated product **6.26** was lower than 50%. Furthermore, the slower reaction rate allowed the formation of the dimeric form of **6.17** that was identified through ESI-MS analysis of the crude mixture.

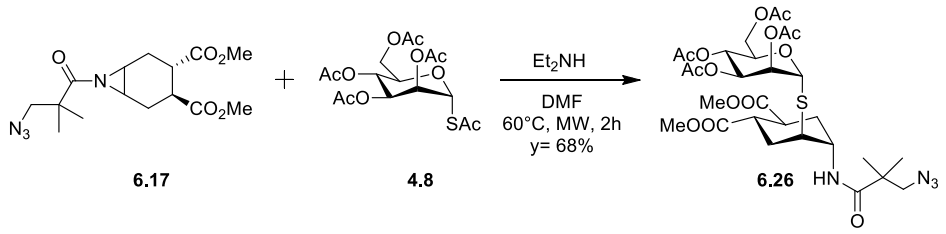

Scheme 6.18 One-pot ring opening of aziridine **6.17** by the α-hioacetate **4.8** performed under MW irradiation

An improvement of the ring opening yield was observed only when the same reaction was performed under MW irradiation for 2 hours (68% yield, **Scheme 6.18**).

Finally, an alternative pathway to exploit the versatility of these compounds was developed: indeed deprotection of the N-Boc thio-glycomimetic **6.21** leads to free amine **6.30** that can be functionalized with a wide range of different frameworks. Coupling with the activated ester **6.19** was performed and is reported in **Scheme 6.19** as an example.

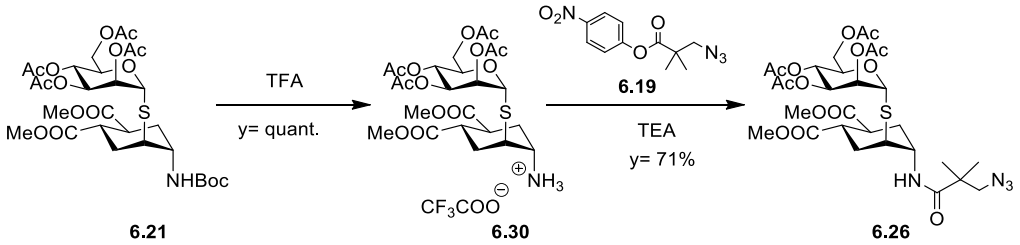

Scheme 6.19 Deprotection of **6.21** by treatment with TFA and subsequent coupling with the activated ester **6.19**

Compound **6.30** could represents an interesting building block in the construction of glyco-peptido mimetics.

6.1.4 Deacetylation of the sugar moiety and isolation of the final thioglycomimetics

The last step of the synthesis consists in the deacetylation of the sugar moiety (**Fig. 6.14**).

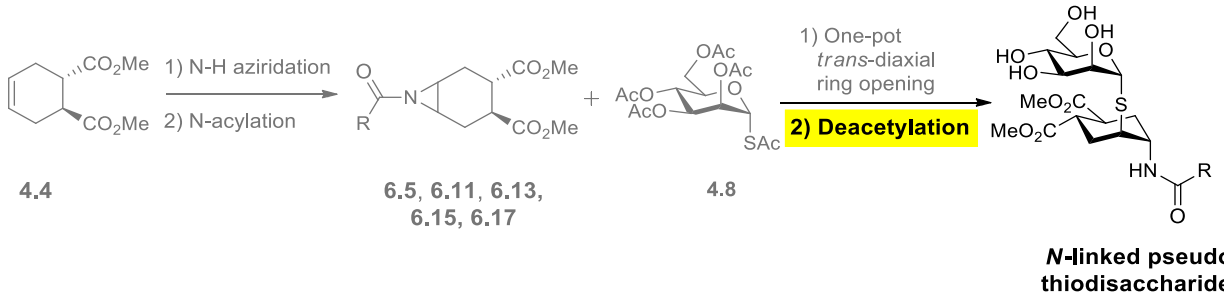

Fig. 6.14 General approach to synthesize *N*-linked pseudo-thiodisaccharides: highlighted in yellow the last step of selective deacetylation

In the first experiment, Zemplén conditions ([**6.25**]$_f$= 0.12 M, MeONa/MeOH 0.2 M) were reproduced for deacetylation of **6.25** (**Scheme 6.20**). However, this trial led to complete decomposition of the starting compound. ESI-MS analysis of the crude allowed to identify among the products the same β-lactam obtained in the azide/chlorine exchange reaction described above (**Scheme 6.17**). Likely this degradation was due to the basicity of the solution (pH range= 8.5-9.5)[9] and to the proximity in pKa values between MeOH (about

16) and the amide function (about 15), that could lead to detrimental equilibria in solution and activate intramolecular nucleophilic substitution of the primary chloride.

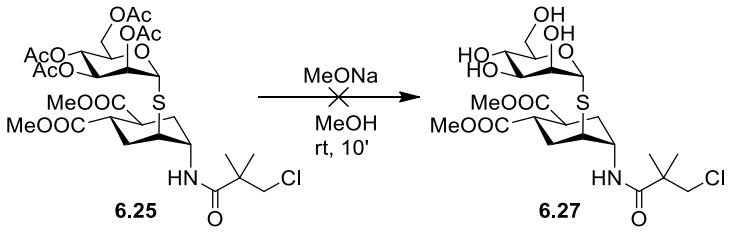

Scheme 6.20 Zemplén deacetylation of **6.25**

Base-promoted side reactions under Zemplén conditions have been frequently reported for glycopeptides[10] and milder conditions have been developed for sugar deacetylation in these situations. In particular, we found that treatment with a 4M $MeNH_2$ solution in EtOH[11] allowed smooth deacetylation of **6.21**, **6.24**, **6.25** and **6.26** affording the final deprotected compounds **6.31**, **6.32**, **6.27** and **6.28** in acceptable yields (to be optimized; **Fig. 6.15**).

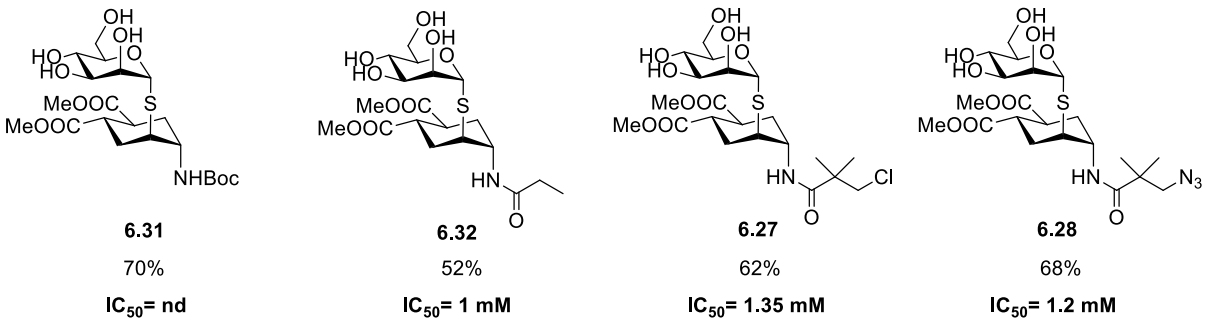

Fig. 6.15 SPR results obtained for the final deprotected *N*-linked pseudo-thiodisaccharides (nd= not detectable, **6.31** completely insoluble)

The DC-SIGN affinity of the final thio-glycomimetics **6.31**, **6.32**, **6.27** and **6.28** was tested through SPR inhibition assay in the same laboratory that performed the previous tests (see Chapter 4.2.6). The results revealed that all of these structures share very similar IC_{50} values compared to the analogues obtained through epoxide ring opening and compared also to the original pseudo-dimannoside **2.1**.

6.2 Conclusions and outlook

A new synthetic approach was devised for the synthesis of *N*-linked pseudo-thiodimannnoside mimics designed to be stable against enzymatic and chemical hydrolysis. The general structure is shown in **Fig. 6.16**: a mannose residue is linked through a thioglycosidic bond to an aglycon, mimicking the 3D structure and conformation of a second mannose residue; the pseudo-anomeric position of the aglycon is functionalized with a nitrogen atom, which allows to tether the glycomimetic structure to linkers/scaffolds/peptide residues using a non-labile amide linkage.

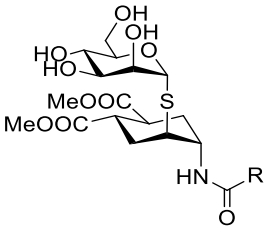

Fig. 6.16 General structure of *N*-linked pseudo-thiodisaccharides

The molecule was synthesized in a simple and effective way making use of an N-H aziridine substrate, as more reactive and versatile compounds, compared to the corresponding epoxides.

The N-H aziridiation process through homogeneous rhodium catalysis was optimized for olefin **4.4**. Afterwards, different solutions for the *N*-acylation of the free aziridine were proposed and discussed.

The one-pot ring opening reaction of the *N*-acylaziridines with mannosyl α-thioacetate **4.8** was optimized, obtaining the corresponding pseudo-thiodisaccharides in good yields. An optimized procedure was necessary for the deacetylation of the sugar moiety of the all the glycomimetics to afford the final compounds ready for the biological tests.

SPR inhibition assays measuring the ability of compounds **6.31**, **6.32**, **6.27** and **6.28** differing for the nature of the amide linker, to inhibit binding of DC-SIGN to immobilized Man-BSA, revealed that all of them share a similar DC-SIGN affinity than the previous *O*-linked pseudo-dimannosides reported by our laboratory.

An attractive application for this class of molecules will be the synthesis of glicopeptido mimetics. Possible strategies are reported below (**Fig. 6.17**), where the peptide coupling can be performed at different stages in the synthesis: at the beginning, on the free aziridine **6.3** (there are some example in literature of this process, like the work of Garner and co-workers[12]) or in the last step on the free amine function of **6.30**.

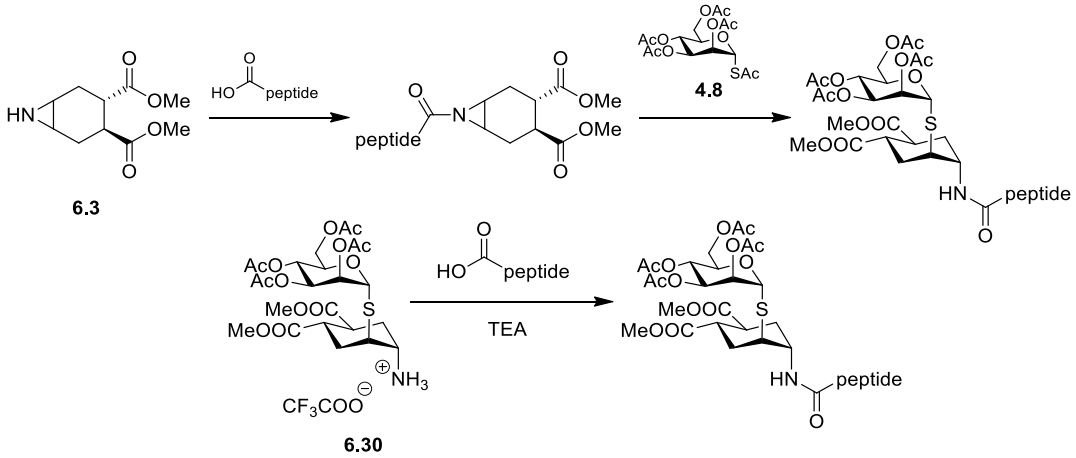

Fig. 6.17 Possible alternative applications of this strategy

Furthermore, the versatility of this methodology will be investigated, changing the sugar portion and possibly also the cyclohexene moiety, to generate a library of thio-glycomimetics resistant towards enzymatic activity and chemical hydrolysis, with the possibility of targeting other lectins than DC-SIGN.

6.3 References

1) J. L. Jat; M. P. Paudyal; H. Gao; Q. L. Xu; M. Yousufuddin; D. Devarajan; D. H. Ess; L. Kurti; J. R. Falck, *Science* **2014**, *343*, 61-5.
2) H. Lebel; K. Huard; S. Lectard, *Journal of the American Chemical Society* **2005**, *127*, 14198-14199.
3) A. Mordini; F. Russo; M. Valacchi; L. Zani; A. Degl'Innocenti; G. Reginato, *Tetrahedron* **2002**, *58*, 7153-7163.
4) M. Punk; C. Merkley; K. Kennedy; J. B. Morgan, *ACS Catal* **2016**, *6*, 4694-4698.
5) T. Mita; E. N. Jacobsen, *Synlett* **2009**, *2009*, 1680-1684.
6) M. Senatore; A. Lattanzi; S. Santoro; C. Santi; G. D. Sala, *Organic & Biomolecular Chemistry* **2011**, *9*, 6205-6207.
7) Y. Hayashi, *Chem Sci* **2016**, *7*, 866-880.
8) T. Belz; S. J. Williams, *Carbohydr Res* **2016**, *429*, 38-47.
9) C. Filser; D. Kowalczyk; C. Jones; M. K. Wild; U. Ipe; D. Vestweber; H. Kunz, *Angew Chem Int Ed Engl* **2007**, *46*, 2108-11.
10) C. Colombo. *Synthesis of unnatural a-N-linked glycopeptides*. PhD, **2011**.
11) S. Mikhailov; M. Drenichev; I. Kulikova; G. Bobkov; V. Tararov, *Synthesis* **2010**, *2010*, 3827-3834.
12) F. B. Dyer; C. M. Park; R. Joseph; P. Garner, *J Am Chem Soc* **2011**, *133*, 20033-5.

6.4 Experimental section

General methods

Chemicals were purchased from commercial sources and used without further purification, unless otherwise indicated. When anhydrous conditions were required, the reactions were performed under nitrogen or argon atmosphere. Anhydrous solvents were purchased from Sigma-Aldrich® with a content of water ≤0.005%. Triethylamine (TEA), methanol and dichloromethane were dried over calcium hydride, THF was dried over sodium/benzophenone and freshly distilled. *N*,*N*-dimethylformamide (DMF) was dried over 4Å molecular sieves. Reactions were monitored by analytical thin-layer chromatography (TLC) performed on Silica Gel 60 F_{254} plates (Merck), and TLC Silica gel 60 RP-18 F_{254}s (Merck) with UV detection (254 nm and 365 nm) and/or staining with ammonium molybdate acid solution, potassium permanganate alkaline solution or ninhydrin. Flash column chromatography was performed according to the method of Still and co-workers[1] using silica gel 60 (40-63 μm, Merck). Automated flash chromatography was performed with Biotage Isolera Prime system, Biotage SNAP ULTRA cartridges were employed. Microwave irradiation was performed by a Biotage Initiator$^+$ system. NMR experiments were recorded on a Bruker AVANCE-400 MHz instrument at 298 K. Chemical shifts (δ) are reported in ppm. The ^{1}H and ^{13}C NMR resonances of compounds were assigned with the assistance of COSY, HSQC and in some cases NOESY experiments. Multiplicities are assigned as s (singlet), d (doublet), t (triplet), q (quartet), quint (quintet), m (multiplet). Mass spectra were recorded on Apex II ICR FTMS (ESI ionization-HRMS), Waters Micromass Q-TOF (ESI ionization-HRMS) or ThermoFischer LCQ apparatus (ESI ionization. Specific optical rotation values were measured using a Perkin-Elmer 241, at 589 nm in a 1 dm cell. The following abbreviations are used: DCC (*N,N'*-dicyclohexylcarbodiimide), DCM (CH_2Cl_2 dichloromethane), m-CPBA (meta-chloroperoxybenzoic acid), DMF (*N, N'*-dimethylformamide), DMAP (4-dimethylaminopyridine), TBTA (tris[(1-benzyl-1*H*-1,2,3-triazol-4-yl)methyl]amine), TFA (trifluoroacetic acid), DPH (2,4-dinitrophenylhydroxylamine), $Rh_2(esp)_2$ (Du Boi's catalyst).

SPR (Surface Plasmon Resonance) studies were carried out using a ProteOn XPR36 Protein Interaction Array Apparatus (Bio-Rad Laboratories, Hercules, CA). The instrument is characterized by six parallel flow channels that can immobilize up to six ligands on the same sensor chip.[2] Mannosylated Bovine Serum Albumin (Man-BSA, Dextra Laboratories, Reading, UK) was immobilized, as a reference, in a parallel different channel. Immobilization levels were typically 3000 and 4000 resonance units (RU, 1RU 1 pg protein/mm2), respectively.

Synthesis of aziridine 6.3

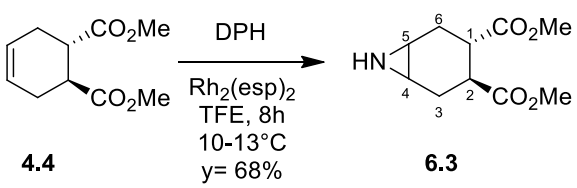

4.4 **6.3**

The reaction was performed in a previously well-dried glassware after flushing with Ar. Olefin **4.4** (150 mg, 0.76 mmol) was dissolved in CF_3CH_2OH (7.6 ml, 0.1 M) and transferred to the flask under Ar. Then the catalyst (5.8 mg, 1 mol%) and finally the DPH (181 mg, 1.2 mmol) were added to the solution at 10-13°C. This temperature was kept using a dioxane-dry ice bath for all the reaction time (8 h). Afterwards, the mixture was diluted with CH_2Cl_2 (10 mL) and then washed with a 15% $NaHCO_3$ solution (10 mL). After two extraction with CH_2Cl_2 the organic phase was collected, washed with brine and finally dried over Na_2SO_4, filtered and concentrated under reduced pressure. Chromatographic purification (95:5 CH_2Cl_2:MeOH) afforded aziridine **6.3** (110 mg, 0.52 mmol) in 68% yield. TLC: R_f 0.2 (95:5 CH_2Cl_2:MeOH, ninhydrin stain). MS (ESI) calcd for $C_{10}H_{15}NO_4$ $[M + H]^+$ m/z: 214.11; found: 214.11.

^{1}H NMR (400 MHz, $CDCl_3$): δ = 3.66 (s, 3H, OMe), 3.64 (s, 3H, OMe), 2.78 (dt, $J_{1\text{-}6ax}$= $J_{1\text{-}2}$= 11.6 Hz, $J_{1\text{-}6eq}$= 4.6 Hz, 1H, H_1), 2.54 (dt, $J_{2\text{-}3ax}$= 11.4 Hz, $J_{2\text{-}3eq}$= 6.5 Hz, 1H, H_2), 2.39-2.33 (m, 4H, H_{3eq}, H_{6eq}, H_4, H_5), 1.86-1.72 (m, 2H, H_{3ax}, H_{6ax}); ^{13}C NMR (100 MHz, $CDCl_3$): δ = 175.9 (C=O), 175.0 (C=O), 51.9 (OMe), 51.9 (OMe), 41.3 (C_2), 38.2 (C_1), 29.7 (C_4), 28.0 (C_6), 27.5 (C_3), 27.2 (C_5).

^{1}H NMR (400 MHz, $CDCl_3$):

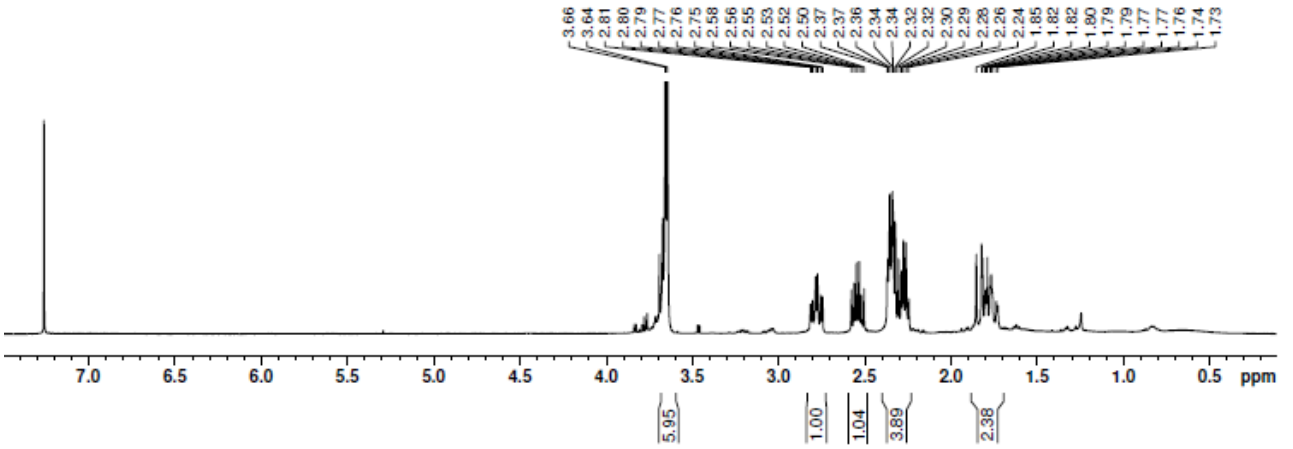

^{13}C NMR (100 MHz, $CDCl_3$):

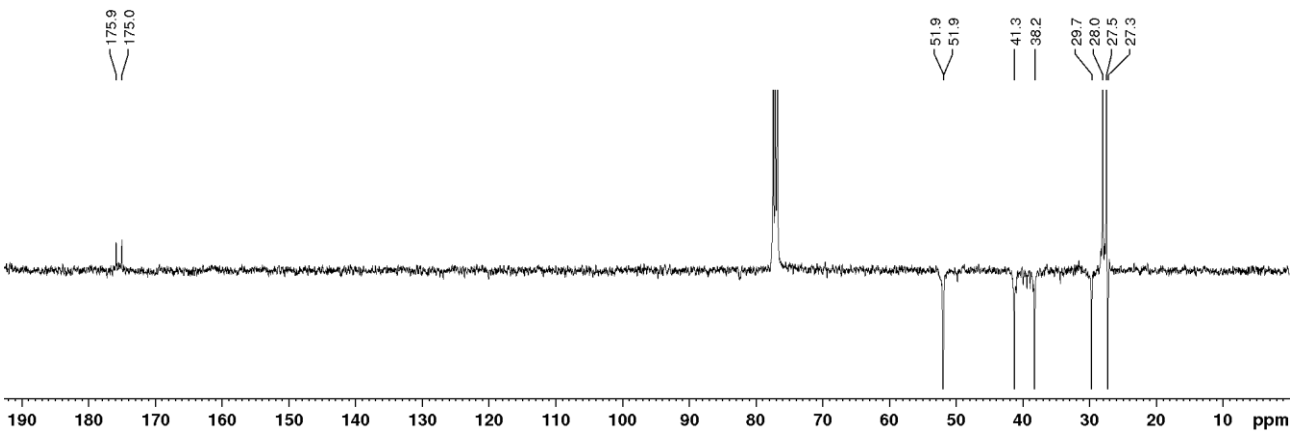

Characterization of the dimer 6.4

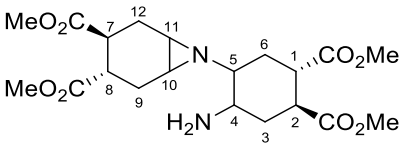

6.4

Table 6.1, entry 2 (Chapter 6.1.1): **6.4** was isolated by chromatographic column (9:1 CH_2Cl_2:MeOH; TLC: R_f 0.4, ninhydrin stain).

^{1}H NMR (400 MHz, $CDCl_3$): δ = 3.71-3.64 (m, 12H, OMe), 3.21 (dt, $J_{1\text{-}6ax}$= $J_{1\text{-}2}$= 9.9 Hz, $J_{1\text{-}6eq}$= 4.4 Hz, 1H, H_1), 3.10-3.01 (m, 2H, H_2, H_4), 2.80 (dt, $J_{10\text{-}9ax}$= $J_{10\text{-}11}$= 10.3 Hz, $J_{10\text{-}9eq}$= 5 Hz, 1H, H_{10}), 2.52 (dt, $J_{11\text{-}12ax}$= $J_{11\text{-}12}$= 10.3 Hz, $J_{11\text{-}12eq}$= 6.3 Hz, 1H), 2.34-2.14 (m, 3H, H_{12eq}, H_{9eq}, H_{3eq}), 1.96-1.66 (m, 3H, H_{12ax}, H_{6eq}, H_{6ax}, H_{9ax}, H_{3ax}), 1.66-1.60 (m, 1H, H_7), 1.37-1.31 (m, 1H, H_5); ^{13}C NMR (100 MHz, $CDCl_3$): δ = 175.9 (CO), 175.70 (CO), 175.3 (CO), 174.9 (CO), 69.4 (C_5), 52.2 (2xOMe), 52.1 (2xOMe), 50.0 (C_4), 41.1 (C_1), 40.1 (C_{10}), 39.5 (C_2), 39.0 (C_{11}), 38.6 (C_7), 34.5 (C_8), 31.7 (C_6), 28.4 (C_3), 27.9 (C_9), 27.2 (C_{12}). TLC: R_f 0.39 (9:1 CH_2Cl_2:MeOH, permanganate stain); MS (ESI) calcd for $C_{20}H_{30}N_2O_8$ $[M + H]^+$ m/z: 427.21; found: 427.59.

^{1}H NMR (400 MHz, $CDCl_3$):

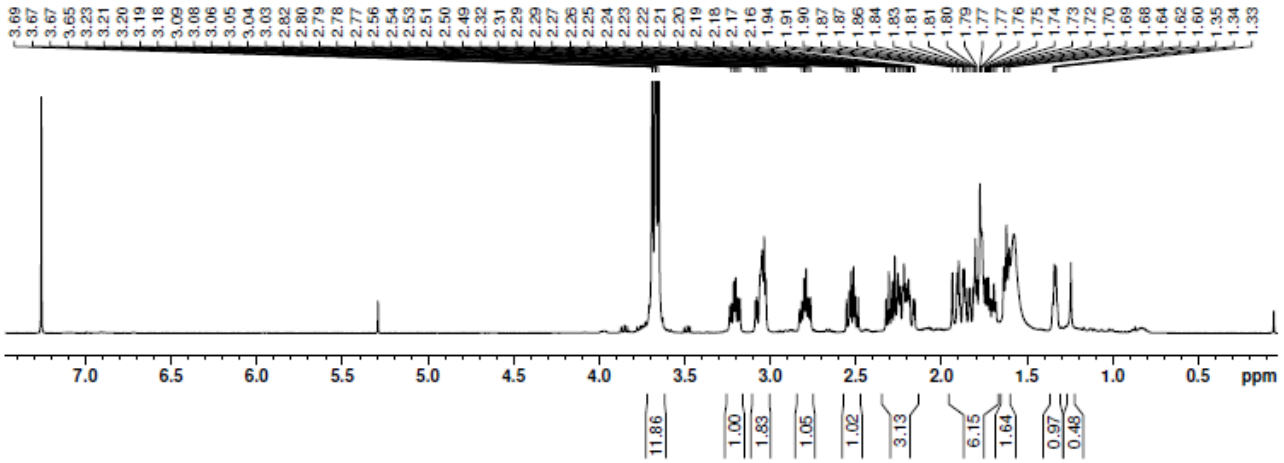

^{13}C NMR (100 MHz, $CDCl_3$):

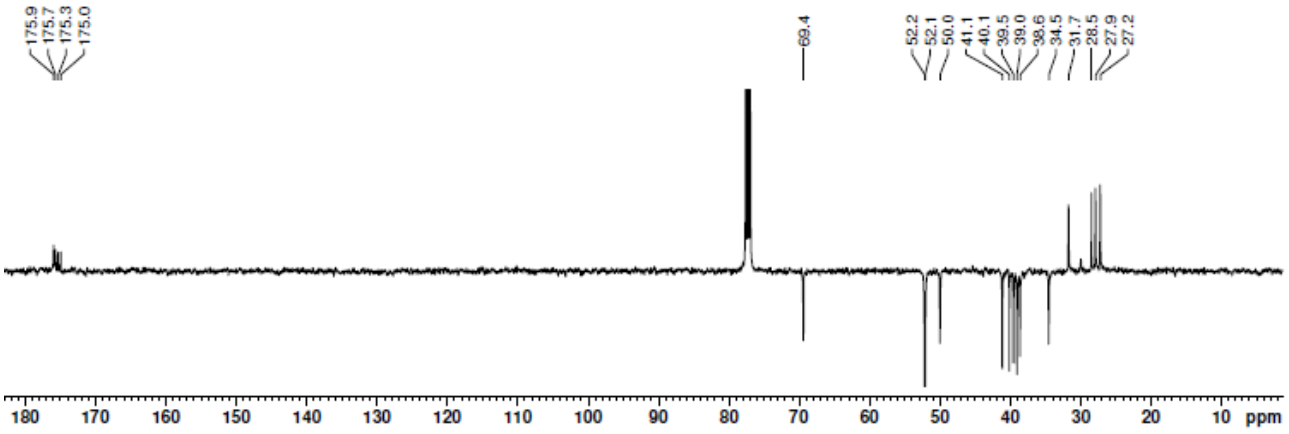

Synthesis of the Boc-aziridine 6.5

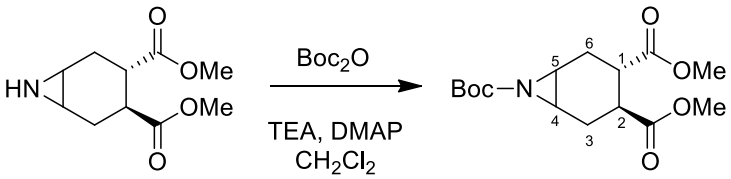

6.3 **6.5**

To a solution of the free aziridine **6.3** (22 mg, 0.1 mmol) dissolved in freshly distilled CH_2Cl_2 under N_2 atmosphere, DMAP (a few crystals) was added. The mixture was cooled to 0°C and Et_3N (freshly distilled, 85 µl, 0.62 mmol) and Boc_2O (118 µL, 0.516 mmol) were added. After 1 h under stirring at 0°C, the reaction was allowed to reach room temperature, then quenched with H_2O. The resulting mixture was diluted with a saturated solution of NH_4Cl; the aqueous phase extracted twice with Et_2O. The organic layers were washed with saturated solutions of $KHSO_4$, Na_2CO_3 and NaCl in this order and finally dried over Na_2SO_4, filtered and concentrated in *vacuum*. Purification by flash chromatography (7:3 Hex:EtOAc) afforded the *t*-butylcarbamate **6.5** (22 mg, 0.07 mmol) as a yellow liquid in 68% yield. TLC: R_f 0.33 (7:3 Hex:EtOAc, permanganate stain). MS (ESI) calcd for $C_{15}H_{23}NO_6$ $[M + Na]^+$ m/z: 336.14; found: 336.18.

^{1}H NMR (400 MHz, $CDCl_3$): δ = 3.66 (s, 3H, OMe), 3.65 (s, 3H, OMe), 2.82 (dt, $J_{1\text{-}6ax}$= $J_{1\text{-}2}$= 11.2 Hz, $J_{1\text{-}6eq}$= 4.5 Hz, 1H, H_1), 2.71-2.67 (m, 1H, H_5), 2.64-2.59 (m, 1H, H_4), 2.54 (dt, $J_{2\text{-}3ax}$= 11.6 Hz, $J_{2\text{-}3eq}$= 6.5 Hz, 1H, H_2), 2.45 (ddd, $J_{6eq\text{-}6ax}$= 14.2 Hz, $J_{6eq\text{-}1}$= 4.6 Hz, $J_{6eq\text{-}5}$= 1.6 Hz, 1H, H_{6eq}), 2.35 (dt, $J_{3eq\text{-}3ax}$= 14.9 Hz, $J_{3eq\text{-}2}$= 6.7 Hz, 1H, H_{3eq}), 1.95 (ddd, $J_{3ax\text{-}3eq}$= 15 Hz, $J_{3ax\text{-}4}$= 11.8 Hz, $J_{3ax\text{-}2}$= 0.6 Hz, 1H, H_{3ax}), 1.74 (ddd, $J_{6ax\text{-}6eq}$= 14.5 Hz, $J_{6ax\text{-}5}$= 11.4 Hz, $J_{6ax\text{-}1}$= 2.9 Hz, 1H, H_{6ax}), 1.43 (s, 9H, H_7); ^{13}C NMR (100 MHz, $CDCl_3$): δ = 175.4 (CO), 174.5 (CO), 162.3 (CO, carbamate), 52.0 (2xOMe), 40.8 (C_2), 38.3 (C_1), 37.0 (C_5), 34.5 (C_4), 28.0 (tBu), 27.5 (C_6), 26.3 (C_3).

^{1}H NMR (400 MHz, $CDCl_3$):

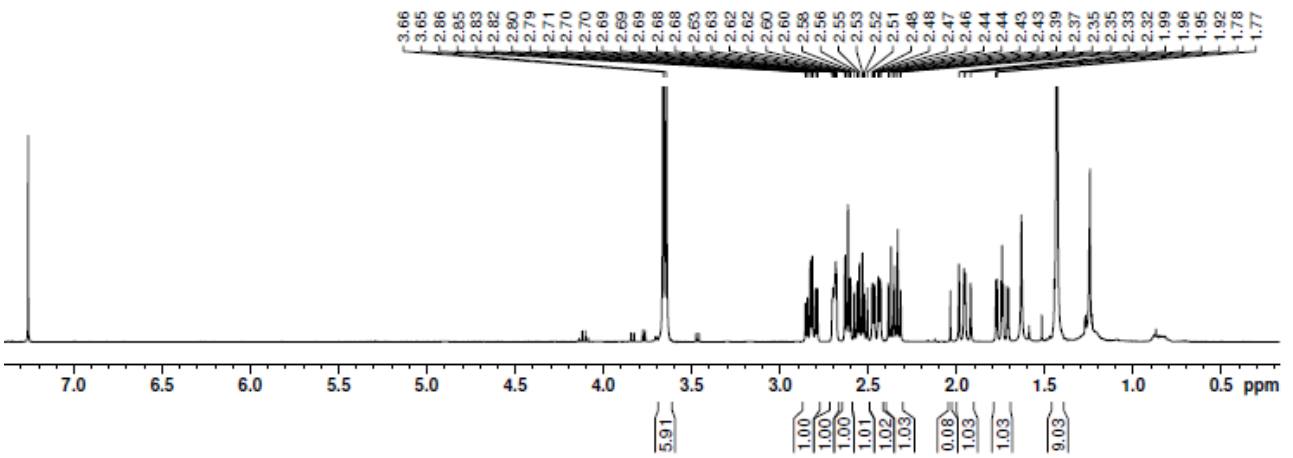

^{13}C NMR (100 MHz, $CDCl_3$):

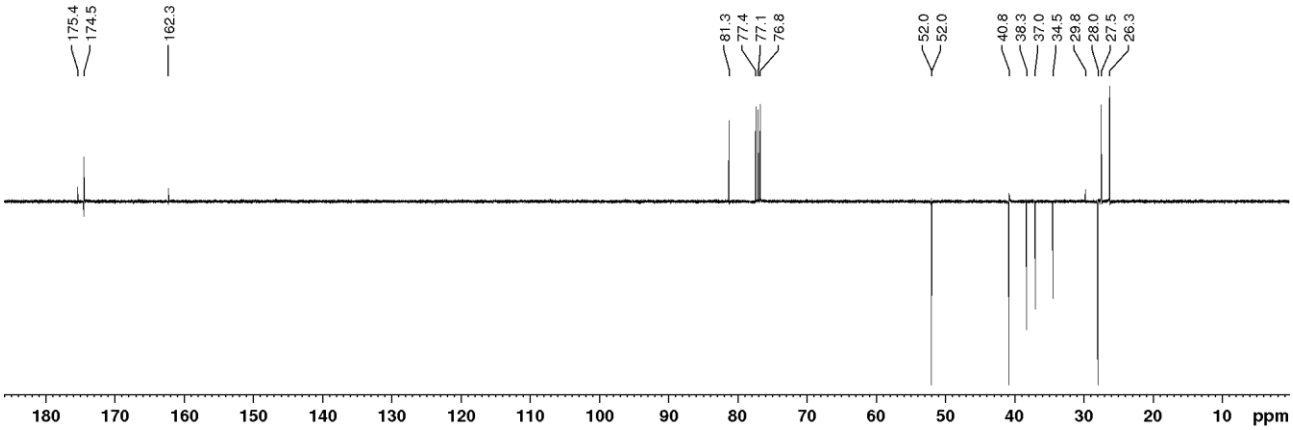

Synthesis of acyl-aziridine 6.11

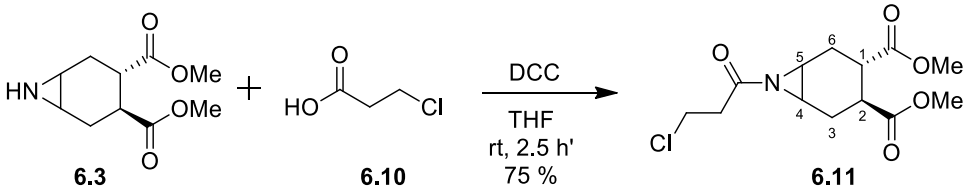

6.3 **6.10** **6.11**

To a solution of the free aziridine **6.3** (32 mg, 0.15 mmol) in dry THF (750 µl, 0.2 M), 3-chloropropionic acid (19.5 mg, 0.18 mmol) and DCC (37 mg, 0.18 mmol) were added at room temperature. After 2.5 h, the white precipitate was filtered over celite, washing with CH_2Cl_2 and finally the solvents were removed under reduced pressure. Amide **6.11** (34 mg, 0.11 mmol) was isolated through a chromatographic column 1:1 (Hex:EtOAc) in 75% yield. TLC: R_f 0.3 (1:1 Hex:EtOAc, permanganate stain); MS (ESI) calcd for $C_{13}H_{18}ClNO_5$ $[M + Na]^+$ m/z: 326.09 (100%), 328.07 (32%); found: 326.38, 328.37.

^1H NMR (400 MHz, $CDCl_3$): δ = 3.77 (t, $J_{8\text{-}7}$= 6.4 Hz, 2H, CH_2Cl), 3.68 (s, 3H, OMe), 3.67 (s, 3H, OMe), 2.91-2.78 (m, 5H, H_4, H_5, H_1, CH_2-linker), 2.64 (ddd, $J_{2\text{-}3ax}$= $J_{2\text{-}1}$= 11.1 Hz, $J_{2\text{-}3eq}$= 6.6 Hz, 1H, H_2), 2.44 (ddd, $J_{6eq\text{-}6ax}$= 14.3 Hz, $J_{6eq\text{-}5}$= 4.2 Hz, $J_{6eq\text{-}1}$= 1.3 Hz, 1H, H_{6eq}), 2.36 (dt, $J_{3eq\text{-}3ax}$= 14.8 Hz, $J_{3eq\text{-}2}$= $J_{3eq\text{-}4}$= 6.4 Hz, 1H, H_{3eq}), 2.03 (ddd, $J_{3ax\text{-}}$

$_{3eq}$= 15.1 Hz, J_{3ax-4}= 10.8 Hz, J_{3ax-2}= 0.7 Hz, 1H, H_{3ax}), 1.88 (ddd, $J_{6ax-6eq}$= 14 Hz, J_{6ax-5}= 10.2 Hz, J_{6ax-1}= 0.9 Hz, 1H, H_{6ax}).

^{1}H NMR (400 MHz, $CDCl_3$):

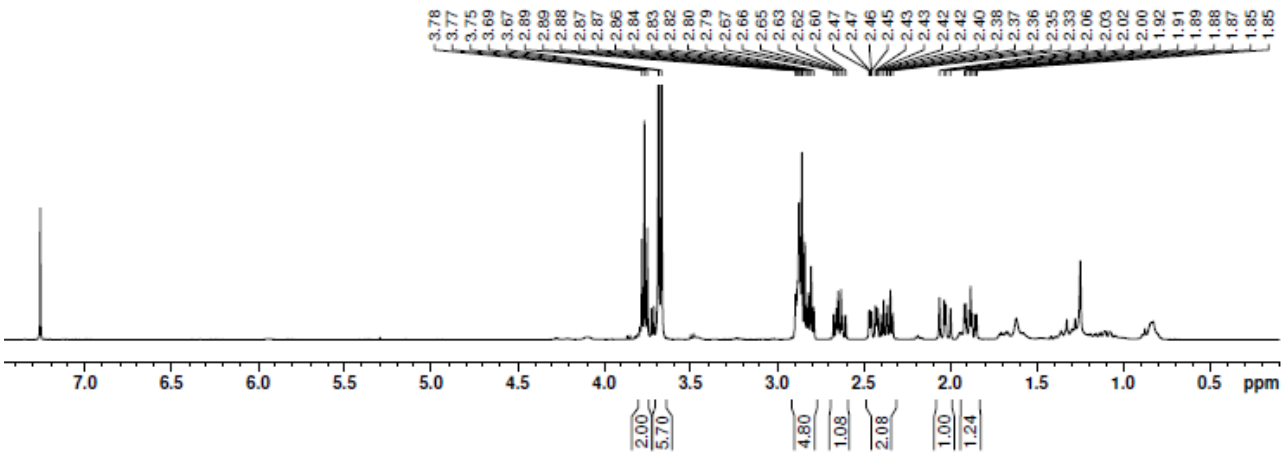

Synthesis of acyl-aziridine 6.13

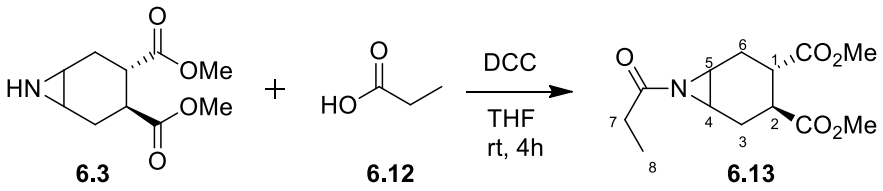

The free aziridine **6.3** (23 mg, 0.11 mmol) was dissolved in dry THF (550 µl, 0.2 M). Then propionic acid (9 µl, 0.12 mmol) and DCC (27 mg, 0.13 mmol) were added in this order at room temperature under stirring. After 4 h, DCU was filtered over celite, washing with CH_2Cl_2 and finally the solvents were evaporated under reduced pressure. Purification by flash chromatography (1:1 Hex:EtOAc) afforded compound **6.13** contaminated by residual DCU. TLC: R_f 0.38 (1:1 Hex:EtOAc, ninhydrin stain); MS (ESI) calcd for $C_{13}H_{19}NO_5$ $[M + H]^+$ m/z: 270.13; found: 270.25.

Although compound **6.13** was not perfectly clean, assignment of the proton signals was possible and it is reported below. The N-acylaziridine **6.13** was employed in the next step without further purification.

^{1}H NMR (400 MHz, $CDCl_3$): δ= 3.67 (s, 3H, OMe), 3.66 (s, 3H, OMe), 2.85 (dt, J_{1-6ax}= J_{1-2}= 10.7 Hz, J_{1-6eq}= 4.9 Hz, 1H, H_1), 2.77-2.72 (m, 1H, H_4), 2.7-2.64 (m, 1H, H_5), 2.64-2.57 (m, 1H, H_2), 2.47-2.30 (m, 2H, H_{6eq}, H_{3eq}), 2.40 (dd, J_{7a-7b}= 15 Hz, J_{7a-8}= J_{7b-8}= 7.6 Hz, 2H, CH_2 linker), 2.00 (ddd, $J_{3ax-3eq}$= 14.6 Hz, J_{3ax-4}= 11 Hz, J_{3ax-2}= 0.9 Hz, 1H, H_{3ax}), 1.85 (ddd, $J_{6ax-6eq}$= 14 Hz, J_{6ax-5}= 11 Hz, J_{6ax-1}= 3.2 Hz, 1H, H_{6ax}), 1.14 (t, J_{8-7a}= J_{8-7b}= 7.7 Hz, CH_3 linker).

^{1}H NMR (400 MHz, $CDCl_3$):

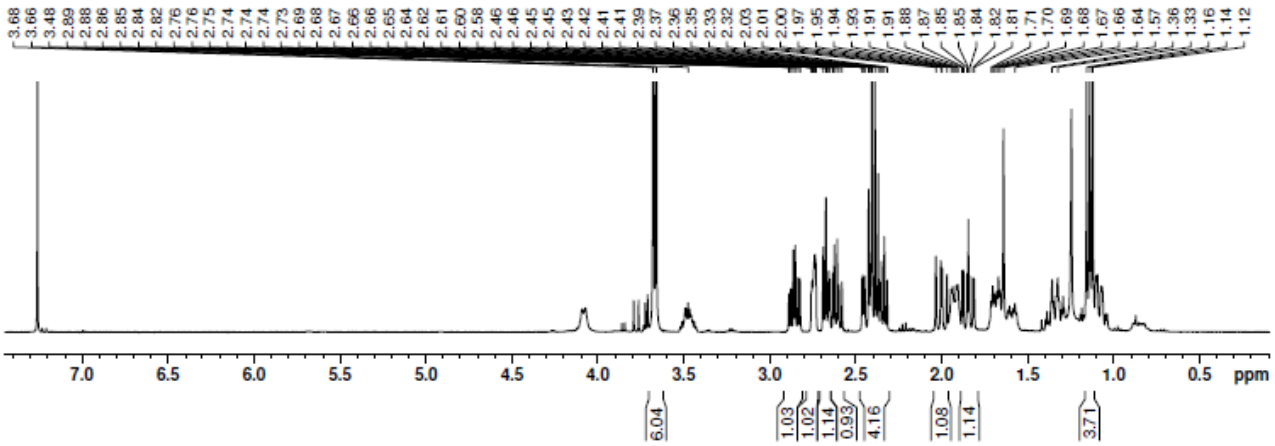

Below: on the top (in red) ^{1}H spectrum of DCU, on the bottom (in blue) fractions isolated with compound **6.13**.

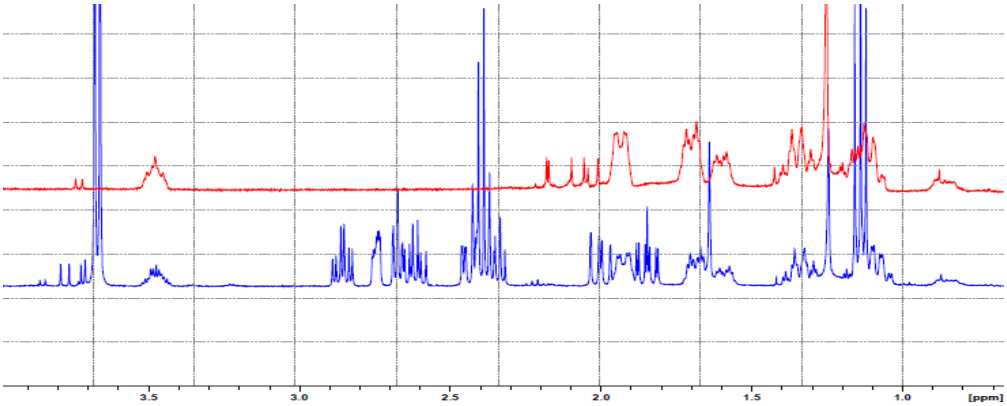

Synthesis of acyl-aziridine 6.15

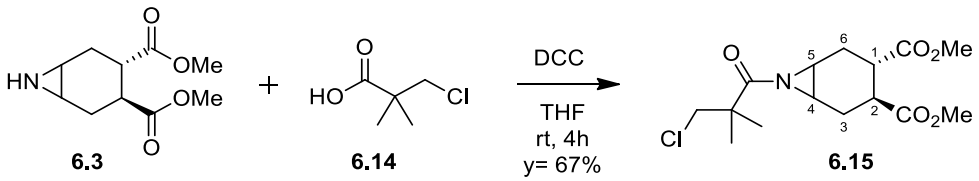

The free aziridine **6.3** (28 mg, 0.13 mmol) was dissolved in freshly distilled THF (650 µl). 3-Chloro-2,2-dimethylpropionic acid **6.14** (21 mg, 0.157 mmol) and DCC (32 mg, 0.157 mmol) were added in this order at room temperature and under nitrogen. After 4 h under stirring, the mixture was filtered over celite and washed with CH_2Cl_2. Flash chromatography (1:1 Hex:EtOAc) afforded the amide **6.15** (29 mg, 0.087 mmol) in 67% yield. TLC: R_f 0.4 (1:1 Hex:EtOAc, permanganate stain); MS (ESI) calcd for $C_{15}H_{22}ClNO_5$ $[M + Na]^+$ m/z: 354.12 (100%), 356.11 (33%); found: 354.43, 356.41.

^{1}H NMR (400 MHz, $CDCl_3$): δ = 3.69 (s, 3H, OMe), 3.67 (s, 3H, OMe), 3.61 (AB system, J_{app}= 14.7 Hz, 2H, CH_2Cl), 2.93-2.82 (m, 3H, H_4, H_5, H_1), 2.67 (dt, $J_{2\text{-}3ax}$= $J_{2\text{-}1}$= 10.1 Hz, $J_{2\text{-}3eq}$= 6.6 Hz, 1H, H_2), 2.44 (ddd, $J_{6eq\text{-}6ax}$= 14.5 Hz, $J_{6eq\text{-}1}$= 4.8 Hz, $J_{6eq\text{-}5}$= 1.3 Hz, 1H, H_{6eq}), 2.48-2.31 (m, 1H, H_{3eq}), 2.02 (ddd, $J_{3ax\text{-}3eq}$= 14.5 Hz, $J_{3ax\text{-}2}$= 10.4 Hz, $J_{3ax\text{-}4}$= 1 Hz, 1H, H_{3ax}), 1.9 (ddd, $J_{6ax\text{-}6eq}$= 14 Hz, $J_{6ax\text{-}5}$= 11 Hz, $J_{6ax\text{-}1}$= 3.3 Hz, 1H, H_{6ax}), 1.34 (s, 6H, 2xCH_3 linker); ^{13}C NMR

(100 MHz, $CDCl_3$): δ = 188.7 (CO amide), 174.9 (CO), 174.3 (CO), 52.0 (CH_2Cl), 52.0 (2xOMe), 40.4 (C_2), 38.1 (C_4), 36.7 (C_5), 34.0 (C_1), 29.6 (CMe_2)26.4 (C_6), 25.5 (C_3), 24.1, 23.9 (2xCH_3 linker).

^{1}H NMR (400 MHz, $CDCl_3$):

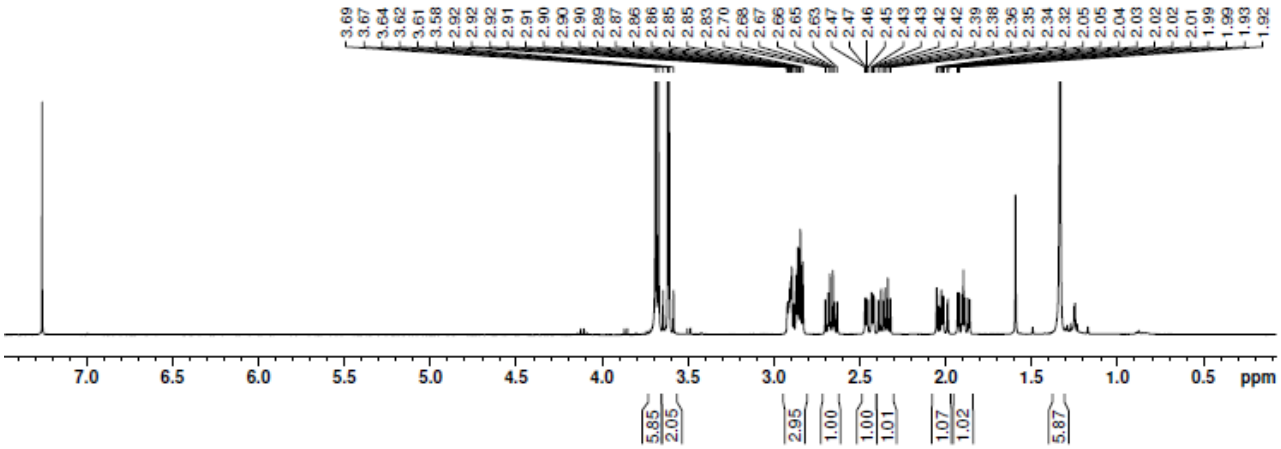

^{13}C NMR (100 MHz, $CDCl_3$):

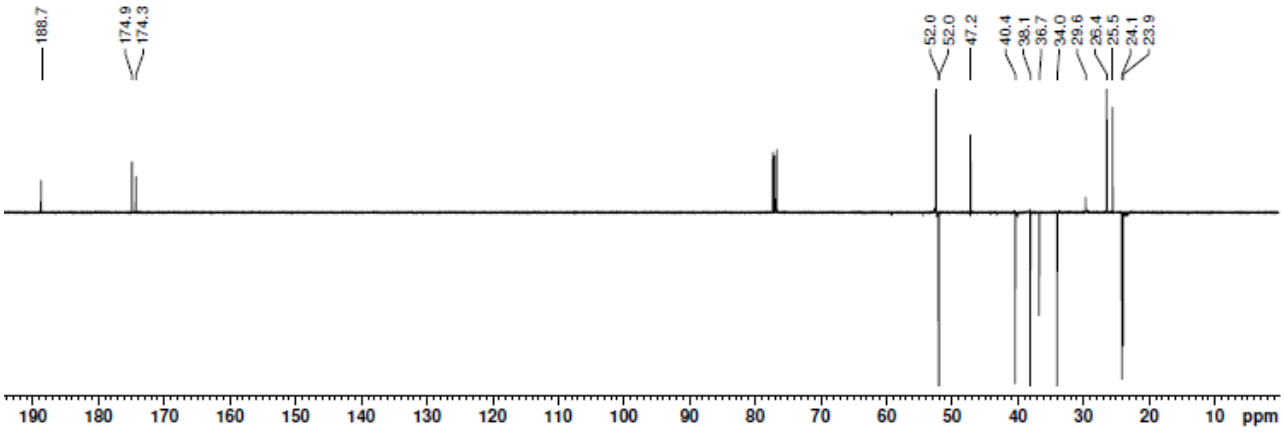

Synthesis of acyl-aziridine 6.17

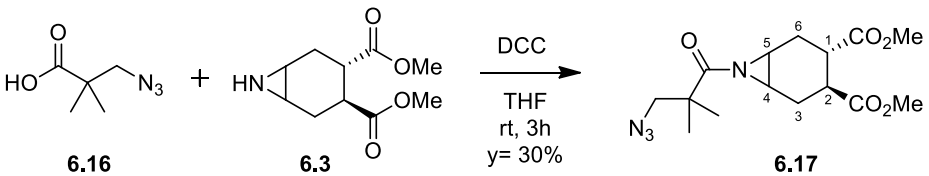

<u>Using DCC:</u>

To a solution of **6.3** (38 mg, 0.178 mmol) in dry THF (890 µl, 0.2 M) carboxylic acid **6.16** (31 mg, 0.213 mmol) was added and then the DCC (44 mg, 0.213 mmol). After 3 hours under stirring, the mixture was filtered over celite and washed with CH_2Cl_2. The chromatographic column afforded compound **6.17** (18 mg, 0.053 mmol) in 30% yield.

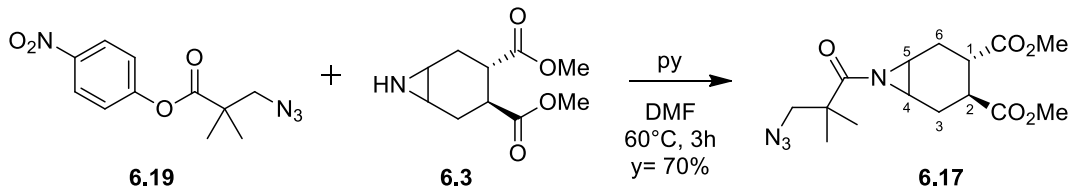

6.19 **6.3** **6.17**

Using the activated ester **6.19**:

to a solution of aziridine **6.3** (39 mg, 0.18 mmol) in dry DMF (720 µL, 0.25 M) and pyridine (18 µL) the activated ester **6.19** (63 mg, 0.24 mmol) was added. The reaction proceeded at 60°C under stirring for 3 h. The mixture was cooled to room temperature and then solvent and pyridine were removed under reduced pressure. Flash chromatography (1:1 Hex:EtOAc) allowed to isolate compound **6.17** (36 mg, 0.11 mmol) in 70% yield.

TLC: R_f 0.38 (1:1 Hex:EtOAc, permanganate stain); MS (ESI) calcd for $C_{15}H_{22}N_4O_5$ $[M + Na]^+$ m/z: 361.15; found: 361.61.

^{1}H NMR (400 MHz, $CDCl_3$): δ = 3.69 (s, 3H, OMe), 3.67 (s, 3H, OMe), 3.43 (AB system, J_{app}= 14.7 Hz, 2H, CH_2N_3), 2.90-2.79 (m, 3H, H_1, H_5, H_4), 2.66 (dt, $J_{1\text{-}6ax}$= $J_{1\text{-}2}$= 10.6 Hz, $J_{1\text{-}6eq}$= 6.7 Hz, 1H, H_2), 2.44 (ddd, $J_{6eq\text{-}6ax}$= 14.3 Hz, $J_{6eq\text{-}1}$= 4.8 Hz, $J_{6eq\text{-}5}$= 1.3 Hz, 1H, H_{6eq}), 2.36 (ddd, $J_{3eq\text{-}3ax}$= 15 Hz, $J_{3eq\text{-}2}$= 6.9 Hz, $J_{3eq\text{-}4}$= 6.4 Hz, 1H, H_{3eq}), 2.01 (ddd, $J_{3ax\text{-}3eq}$= 14.9 Hz, $J_{3ax\text{-}2}$= 10.7 Hz, $J_{3ax\text{-}4}$= 0.6 Hz, 1H, H_{3ax}), 1.26 (s, 6H, 2 CH_3 linker); ^{13}C NMR (100 MHz, $CDCl_3$): δ = 189.5 (CO amide), 175.1 (CO), 174.4 (CO), 60.3 (CH_2N_3), 52.2 (OMe), 52.1 (OMe), 40.5 (C_2), 38.3 (C_1), 36.9 (C_5), 34.2 (C_4), 29.8 ($C(CH_3)_2$ linker), 26.6 (C_6), 25.7 (C_3), 23.9 (CH_3 linker), 23.7 (CH_3 linker).

^{1}H NMR (400 MHz, $CDCl_3$):

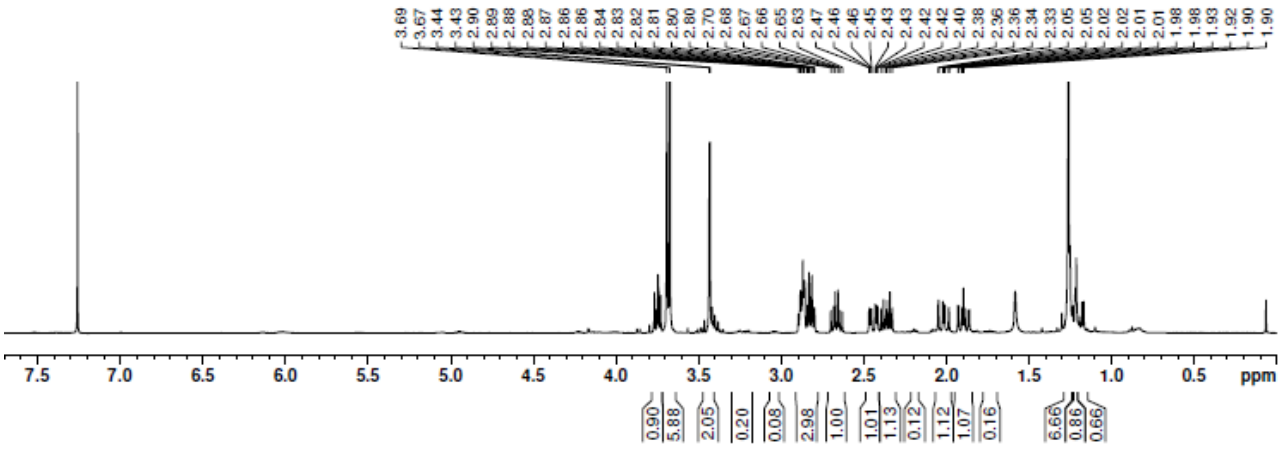

^{13}C NMR (100 MHz, $CDCl_3$):

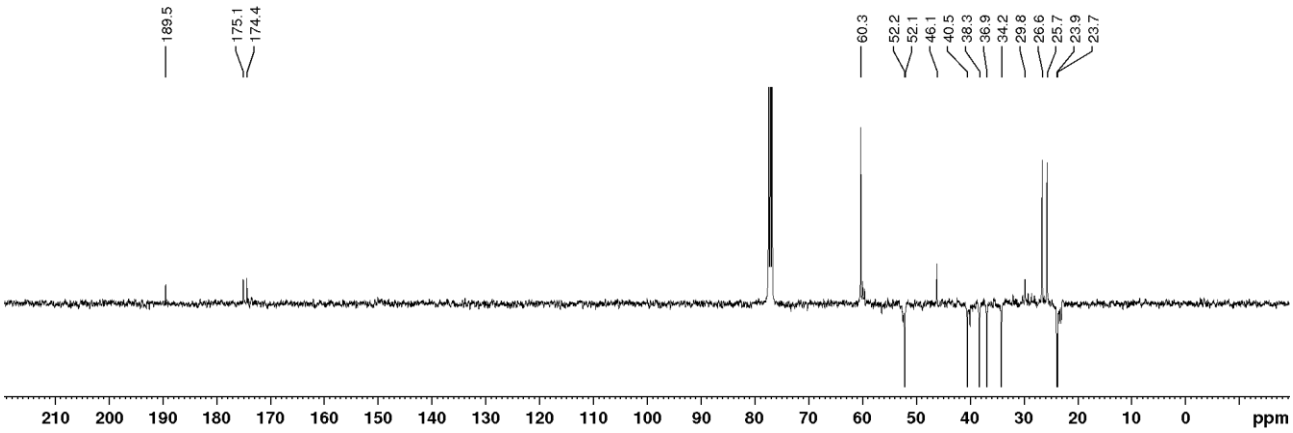

Synthesis of the activated ester 6.19

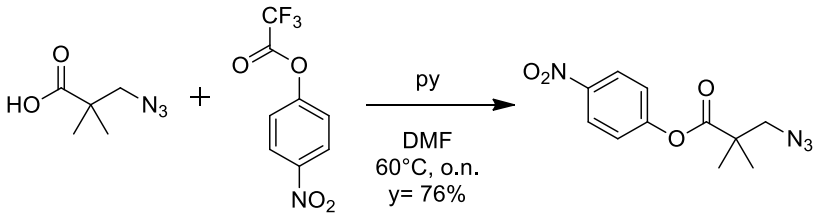

6.16 **6.20** **6.19**

To a solution of the carboxylic acid **6.16** (311 mg, 2.17 mmol) in dry DMF (7.2 ml, 0.3 M) the p-nitro trifluoacetate **6.20** (766 mg, 3.25 mmol) was added and finally the dry pyridine (350 µl). The mixture was then warmed up to 60°C and left under stirring over night. The day after, the reaction was allowed to reach room temperature and then solvent and pyridine were removed under *vacuum*. Compound **6.19** (435 mg, 1.65 mmol) was isolated in 76% yield through a chromatographic column. TLC: R_f 0.4 (8:2 Hex:EtOAc, permanganate stain, UV light).

^{1}H NMR (400 MHz, $CDCl_3$): δ = 8.28 (d, *J*= 8.9 Hz, 2H, H_{ar}), 7.27 (d, *J*= 9.2 Hz, 2H, H_{ar}), 3.57 (s, 2H, CH_2N_3), 1.4 (s, 6H, 2xCH_3); ^{13}C NMR (100 MHz, $CDCl_3$): δ = 173.5 (CO), 155.5 (C_{ar}), 145.6 (C_{ar}), 125.3 (2xCH_{ar}), 122.5 (2xCH_{ar}), 59.59 (CH_2), 44.4 ($C(CH_3)_2$), 23.03 (2xCH_3).

^{1}H NMR (400 MHz, $CDCl_3$):

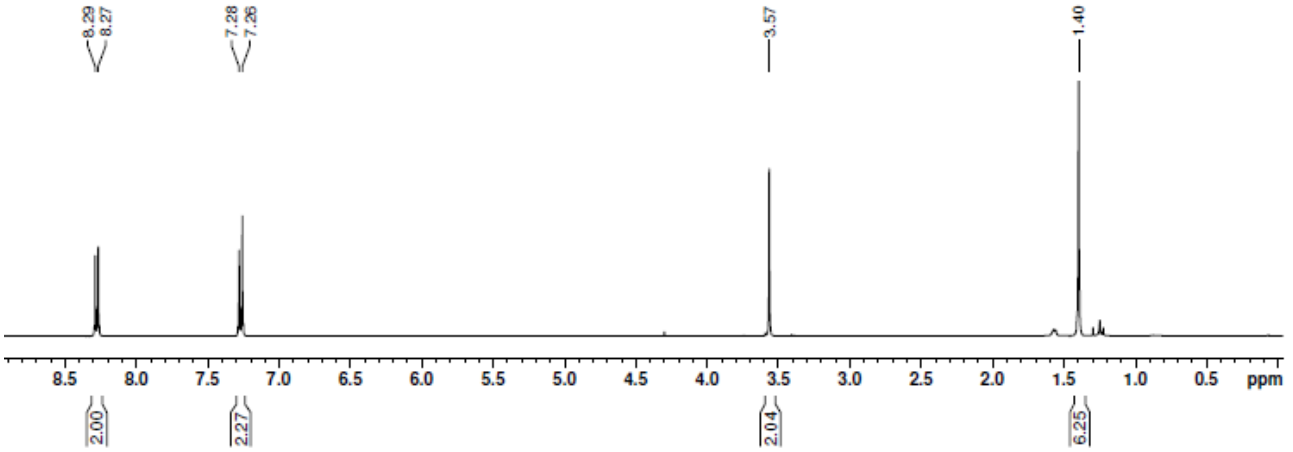

^{13}C NMR (100 MHz, $CDCl_3$):

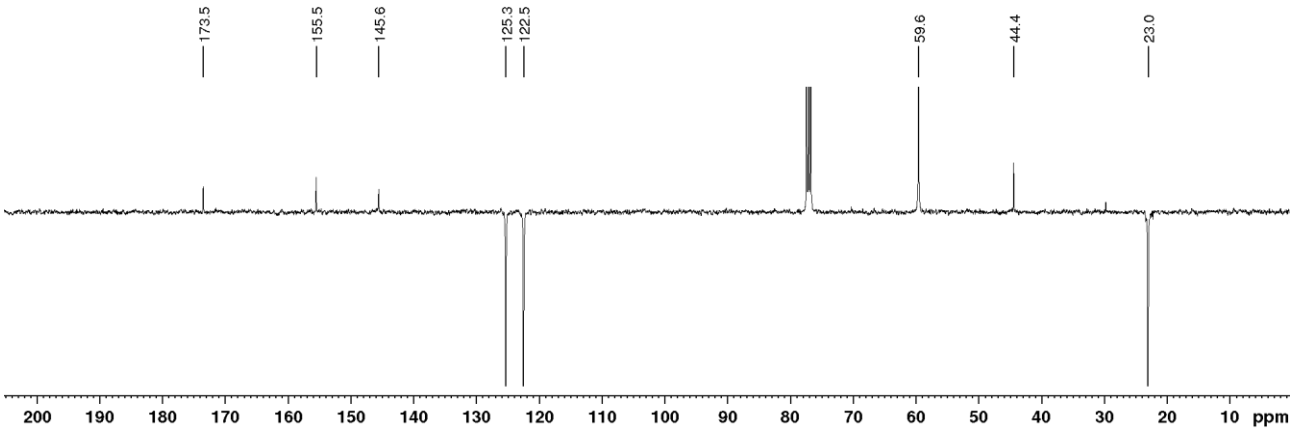

Synthesis of the pseudo-disaccharide 6.21

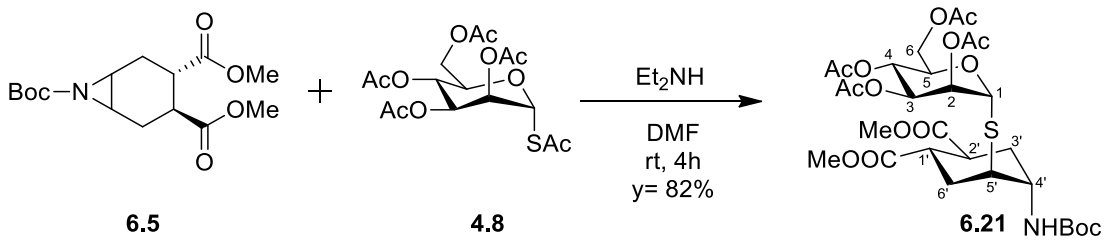

Thioacetate **4.8** (37 mg, 0.09 mmol) and the N-Boc aziridine **6.5** (22 mg, 0.07 mmol) were dissolved in dry DMF (108 µl, 0.65M) under nitrogen atmosphere. Et_2NH (14 µl, 0.13 mmol) was added to the mixture and the reaction was left stirring at room temperature for 4 h. The mixture was diluted with EtOAc and washed with HCl solution (1 M). The aqueous phase was extracted twice with EtOAc and finally the organic layers were collected, dried over Na_2SO_4, filtered and concentrated in *vacuum*. Falsh chromatography (1:1 Hex:EtOAc) led to the isolation of compound **6.21** (39 mg, 0.06 mmol) in 82% yield. TLC: R_f 0.33 (1:1 Hex:EtOAc, cerium ammonium molibdate stain); $[\alpha]_D^{19}$ ($CHCl_3$, *c* 1.95): + 59; MS (ESI) calcd for $C_{29}H_{43}NO_{15}S$ [M + Na]$^+$ m/z: 700.24; found: 701.01.

^{1}H NMR (400 MHz, $CDCl_3$): δ = 5.4-5.34 (m, 2H, H_1, H_2), 5.3 (dd, $J_{4\text{-}5}$= 10.2 Hz, $J_{4\text{-}3}$= 9.75 Hz, 1H, H_4), 5.21 (dd, $J_{3\text{-}4}$= 9.75 Hz, $J_{3\text{-}2}$= 2.9 Hz ,1H, H_3), 4.8-4.7(m, 1H, NH), 4.44-4.29 (m, 2H, H_5, H_{6a}), 4.17-4.07 (m, 1H, H_{6b}), 3.95-3.83 (m, 1H, $H_{4'}$), 3.71 (s, 3H, OMe), 3.70, (s, 3H, OMe), 3.31-3.21 (m, 1H, $H_{1'}$), 3.09-3.00 (m, 1H, $H_{5'}$), 2.88-2.77 (m, 1H, $H_{2'}$), 2.21-1.95 (m, 3H, $H_{6'eq}$, $H_{3'eq}$, $H_{6'ax}$), 2.16 (s, 3H, OAc), 2.08 (s, 3H, OAc), 2.04 (s, 3H, OAc), 1.98 (s, 3H, OAc), 1.91-1.80 (m, 1H, $H_{3'ax}$), 1.43 (s, 9H, tBu); ^{13}C NMR (100 MHz, $CDCl_3$): δ = 173.7 (CO), 173.7 (CO), 170.6 (CO), 169.9 (CO), 169.9 (CO), 169.7 (CO), 169.6 (CO, carbammate), 82.1 (C_1), 80.0 (C_{IV} Boc), 70.9 (C_2), 69.4 (C_3), 69.3 (C_5), 66.1 (C_4), 62.5 (C_6), 52.3 (OMe), 52.2 (OMe), 49.0 ($C_{4'}$), 44.5 ($C_{1'}$), 39.9 ($C_{5'}$, $C_{2'}$),29.7 ($C_{6'}$), 29.1 ($C_{3'}$), 28.3 (tBu), 20.9 (OAc), 20.7 (OAc), 20.7 (OAc), 20.6 (OAc).

^{1}H NMR (400 MHz, $CDCl_3$):

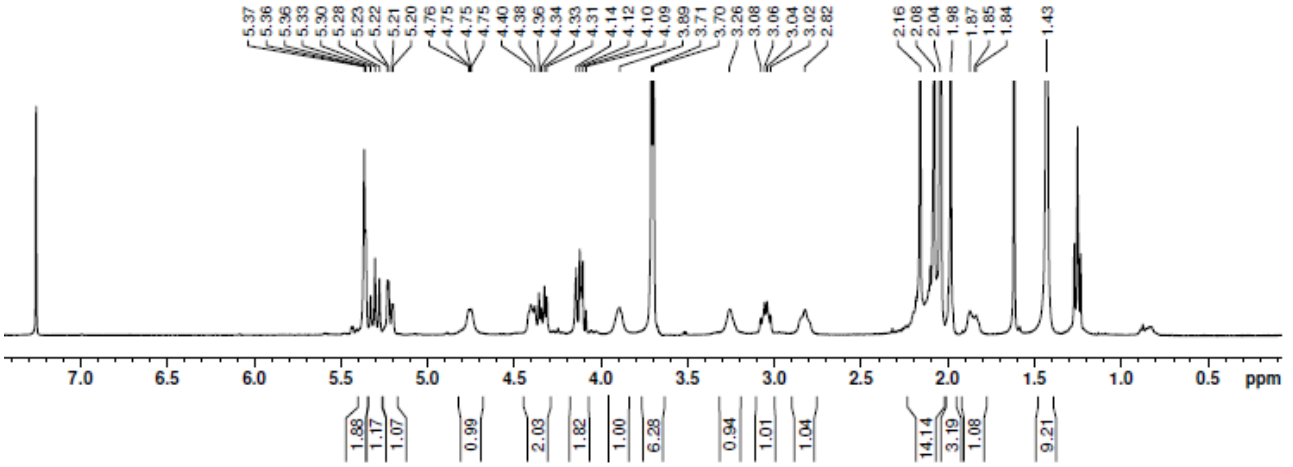

^{13}C NMR (100 MHz, $CDCl_3$):

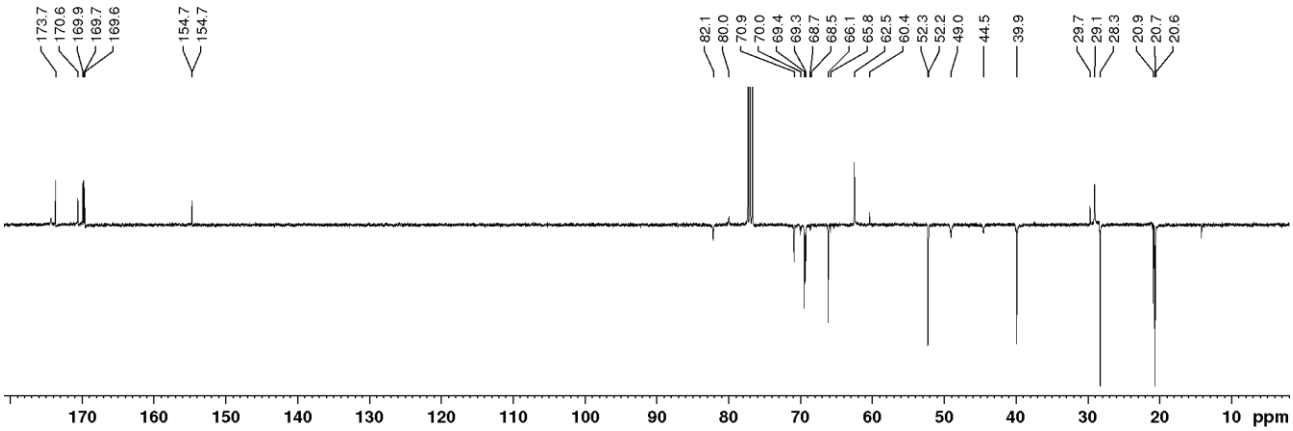

Synthesis of the pseudo-disaccharide 6.24

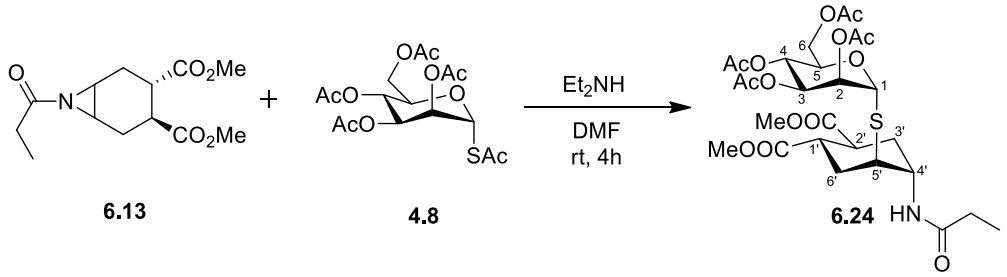

6.13 **4.8** **6.24**

y= 36% over two steps

To a solution of the thioacetate **4.8** (29 mg, 0.072 mmol) and the aziridine **6.13** (15 mg, 0.056 mmol; sample contaminated by DCU) in dry DMF (85 µl), $EtNH_2$ (11 µl, 0.106 mmol) was added. After 4 hstirring at room temperature, the reaction mixture was diluted with EtOAc and then washed with HCl solution (1 M). The aqueous layers were extracted twice with EtOAc and finally the organic phase was collected, dried over Na_2SO_4, filtered and concentrated under *vacuum*. Compound **6.24** (25 mg, 0.039 mmol) was isolated by flash chromatography (4:6 Hex:EtOAc) (36% yield over two steps). $[\alpha]_D^{16}$ ($CHCl_3$, *c* 1.05): + 59; TLC: R_f 0.14 (4:6 Hex:EtOAc, cerium ammonium molibdate stain); MS (ESI) calcd for $C_{27}H_{39}NO_{14}S$ $[M + Na]^+$ m/z: 656.20; found: 656.60.

^{1}H NMR (400 MHz, $CDCl_3$): δ = 5.82-5.74 (m, 1H, NH), 5.39 (d, $J_{1\text{-}2}$= 1.3 Hz, 1H, H_1), 5.34 (dd, $J_{2\text{-}3}$= 3.5 Hz, $J_{2\text{-}1}$= 1.3 Hz, 1H, H_2), 5.29 (t, $J_{4\text{-}3}$= $J_{4\text{-}5}$= 9.7 Hz ,1H, H_4), 5.20 (dd, $J_{3\text{-}4}$= 9.7 Hz, $J_{3\text{-}2}$= 3.5, 1H, H_3), 4.41-4.29 (m, 2H, H_5, H_{6a}), 4.22-4.07 (m, 2H, $H_{4'}$, H_{6b}),3.71 (s, 3H, OMe), 3.69, (s, 3H, OMe), 3.40-3.25 (m, 1H, $H_{5'}$), 3.1-3.02 (m, 1H, $H_{1'}$), 2.88-2.79 (m, 1H, $H_{2'}$), 2.23-1.95 (m, 5H, $CH_{2\text{-linker}}$,$H_{3'eq}$, $H_{6'eq}$, $H_{6'ax}$), 2.15 (s, 3H, OAc), 2.07 (s, 3H, OAc), 2.04 (s, 3H, OAc), 1.98 (s, 3H, OAc), 1.92-1.82 (m, 1H, H_{3ax}), 1.13 (t, $J_{CH3\text{-}CH2}$= 7.9 Hz, 3H, $CH_{3\text{-linker}}$); ^{13}C NMR (100 MHz, $CDCl_3$): δ = 174.5 (CO), 173.7 (CO), 173.3 (CO), 170.8 (CO), 170.0 (CO), 169.9 (CO), 169.7 (CO), 82.0 (C_1), 71.0 (C_2), 69.5 (C_3), 69.5 (C_5), 66.3 (C_4), 62.6 (C_6), 52.4 (OMe), 52.3 (OMe), 48.0 ($C_{4'}$), 43.9 ($C_{5'}$), 40.1 ($C_{1'}$), 39.9 ($C_{2'}$), 29.8 (CH_2 linker), 29.1 ($C_{6'}$), 28.7 ($C_{3'}$), 21.0 (OAc), 20.8 (OAc), 20.7 (OAc), 20.7 (OAc), 9.7 (CH_3 linker).

^{1}H NMR (400 MHz, $CDCl_3$):

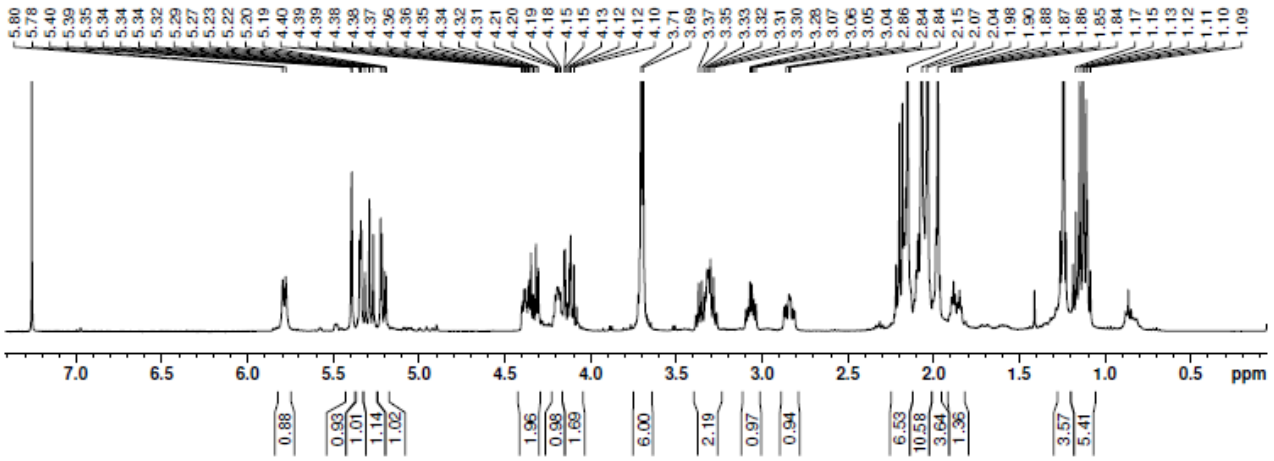

^{13}C NMR (100 MHz, $CDCl_3$):

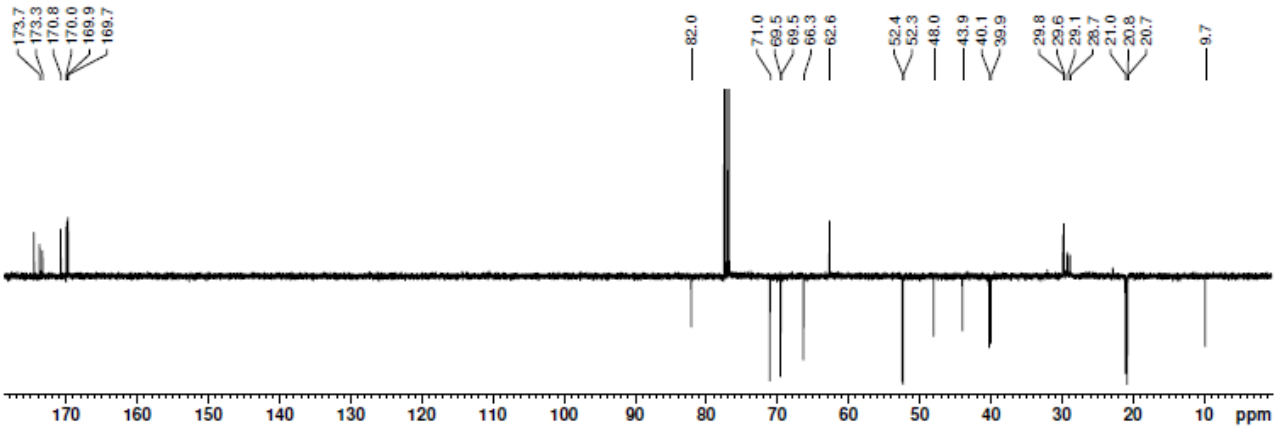

Synthesis of the pseudo-thiodisaccharide 6.25

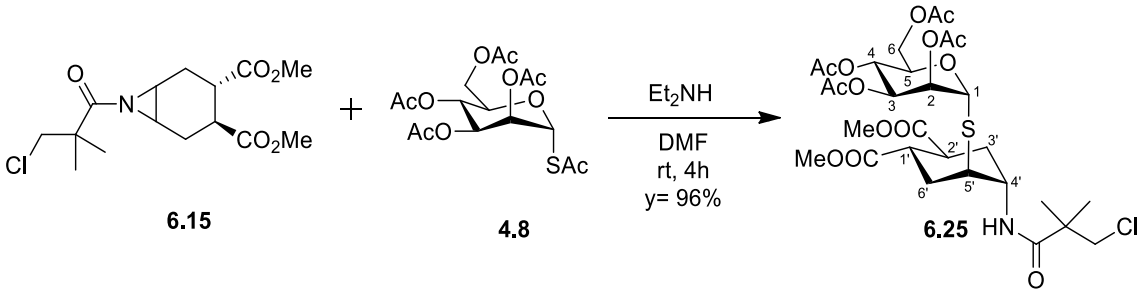

To a solution of thioacetate **4.8** (46 mg, 0.11 mmol) and aziridine **6.15** (29 mg, 0.09 mmol) in dry DMF (138 µl, 0.65 M), $EtNH_2$ (18 µl, 0.17 mmol) was added. After 4 h stirring at room temperature, the reaction mixture was diluted with EtOAc and washed with a solution of HCl (1 M); the aqueous phase extracted twice with EtOAc; finally the organic layer was collected, dried over Na_2SO_4, filtered and concentrated under reduced pressure. Flash chromatography (ELUANT) allowed to isolate compound **6.25** (60 mg, 0.086 mmol) in 96% yield. $[\alpha]_D^{19}$ ($CHCl_3$, *c* 1.22): + 55; TLC: R_f 0.2 (Hex/EtOAc 1:1, cerium ammonium molibdate stain); MS (ESI) calcd for $C_{29}H_{42}ClNO_{14}S$ $[M + Na]^+$ m/z: 718.19; found: 718.66.

^{1}H NMR (400 MHz, $CDCl_3$): δ = 5.96-5.89 (m, 1H, NH), 5.41 (d, $J_{1\text{-}2}$= 0.9 Hz, 1H, H_1), 5.34 (dd, $J_{2\text{-}3}$= 3.5 Hz, $J_{2\text{-}1}$= 1.6 Hz, 1H, H_2), 5.29 (t, $J_{4\text{-}3}$= $J_{4\text{-}5}$= 9.7 Hz ,1H, H_4), 5.20 (dd, $J_{3\text{-}4}$= 9.9 Hz, $J_{3\text{-}2}$= 3.3, 1H, H_3), 4.42-4.30 (m, 2H, H_5, H_{6a}), 4.21-4.07 (m, 2H, $H_{4'}$, H_{6b}),3.72 (s, 3H, OMe), 3.70, (s, 3H, OMe), 3.58 (AB system, J_{app}= 10.7 Hz, 2H, CH_2Cl), 3.33-3.27 (m, 1H, $H_{5'}$), 3.08 (ddd, $J_{1'\text{-}2'}$= 13.5 Hz, $J_{1'\text{-}6'ax}$= 8.8 Hz, $J_{1'\text{-}6'eq}$= 5.34 Hz, 1H, $H_{1'}$), 2.87-2.78 (m, 1H, $H_{2'}$), 2.23 (ddd, $J_{3'eq\text{-}3'ax}$= 14.1 Hz, $J_{3'eq\text{-}2'}$= 10 Hz, $J_{3'eq\text{-}4'}$= 4.4 Hz, 1H, $H_{3'eq}$), 2.18-1.94 (m, 2H, $H_{6'eq}$, $H_{6'ax}$), 2.15 (s, 3H, OAc), 2.07 (s, 3H, OAc), 2.04 (s, 3H, OAc), 1.97 (s, 3H, OAc), 1.92-1.82 (m, 1H, $H_{3'ax}$), 1.28 (s, 3H, CH_3 linker), 1.27 (s, 3H, CH_3 linker); ^{13}C NMR (100 MHz, $CDCl_3$): δ = 174.34 (CO), 174.22 (CO), 173.56 (CO), 170.76 (CO), 169.94 (CO), 169.83 (CO), 169.72 (CO), 81.80 (C_1), 70.95 (C_2), 69.52 (C_3), 69.44 (C_5), 66.26 (C_4), 62.59 (C_6), 60.4 ($C(CH_3)_2$ linker), 52.82 (CH_2 linker), 52.42 (OMe), 52.29 (OMe), 48.16 ($C_{4'}$), 43.67 ($C_{5'}$), 40.21 ($C_{1'}$), 40.03 ($C_{2'}$), 29.35 ($C_{6'}$), 28.76 ($C_{3'}$), 23.63 (CH_3 linker), 23.37 (CH_3 linker), 20.96 (OAc), 20.77 (OAc), 20.73 (OAc), 20.66 (OAc).

^{1}H NMR (400 MHz, $CDCl_3$):

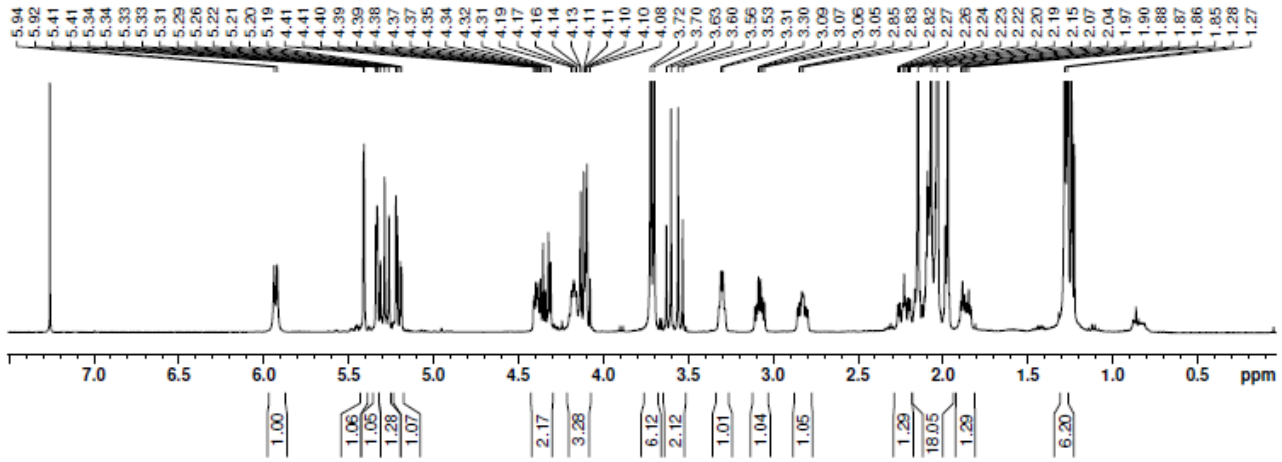

^{13}C NMR (100 MHz, $CDCl_3$):

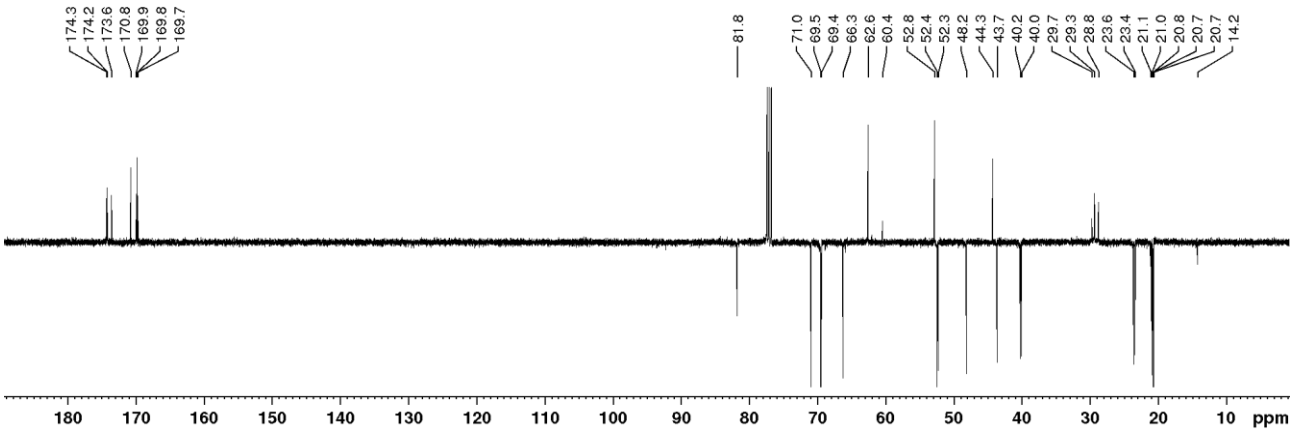

Synthesis of the pseudo-thiodisaccharide 6.26

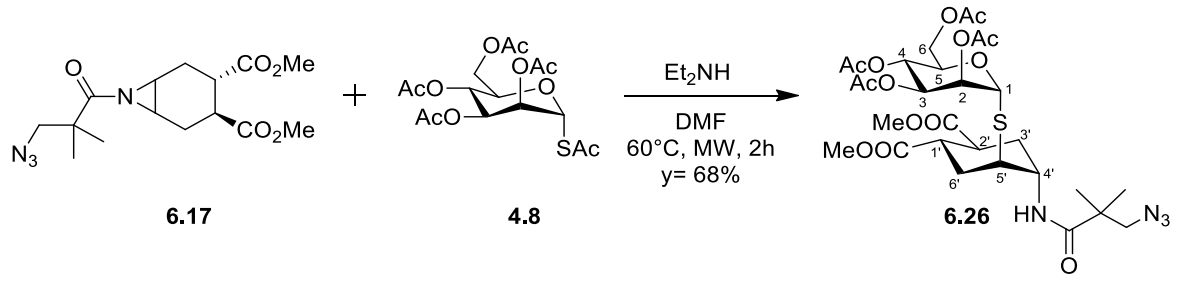

6.17 **4.8** **6.26**

Thioacetate **4.8** (78 mg, 0.19 mmol) and aziridine **6.17** (50 mg, 0.15 mmol) were dissolved in dry DMF (250 µl, 0.6 M) into a MW-reactor. After addition of $EtNH_2$ (30µl, 0.28 mmol), the reaction was stirred at 60°C under MW irradiation for 2 h. After that, the mixture was diluted with EtOAc and washed with a HCl solution (1 M). The aqueous phase was extracted twice with EtOAc and finally the organic layers collected were dried over Na_2SO_4, filtered and the solvents removed under *vacuum*. Compound **6.26** (72 mg, 0.10 mmol) was isolated through flash chromatography (1:1 Hex:EtOAc) in 68% yield. $[\alpha]_D^{18}$ ($CHCl_3$, *c* 1.55): + 69; TLC: R_f 0.27 (1:1 Hex:EtOAc, cerium ammonium molibdate stain); MS (ESI) calcd for $C_{29}H_{42}N_4O_{14}$ $[M + Na]^+$ m/z: 725.23; found: 725.66.

^{1}H NMR (400 MHz, $CDCl_3$): δ = 6.09-5.99 (m, 1H, NH), 5.41 (d, $J_{1\text{-}2}$= 1.1 Hz, 1H, H_1), 5.33 (dd, $J_{2\text{-}3}$= 3.3 Hz, $J_{2\text{-}1}$= 1.1 Hz, 1H, H_2), 5.29 (t, $J_{4\text{-}3}$= 10.0 Hz ,1H, H_4), 5.20 (dd, $J_{3\text{-}4}$= 10.0 Hz, $J_{3\text{-}2}$= 3.3, 1H, H_3), 4.42-4.29 (m, 2H, H_5, H_{6a}), 4.18-4.08 (m, 2H, $H_{4'}$, H_{6b}), 3.72 (s, 3H, OMe), 3.71 (s, 3H, OMe), 3.40 (AB system, J_{app}= 15.0 Hz, 2H, CH_2N_3), 3.29-3.23 (m, 1H, $H_{5'}$), 3.08 (ddd, $J_{1'\text{-}2'}$= 12.6 Hz, $J_{1'\text{-}6'ax}$= 8.8 Hz, $J_{1'\text{-}6'eq}$= 4.21 Hz, 1H, $H_{1'}$), 2.90-2.80 (m, 1H, $H_{2'}$), 2.28-2.18 (m, $H_{3'eq}$), 2.18-2.00 (m, 2H, $H_{6'eq}$, $H_{6'ax}$), 2.15 (s, 3H, OAc), 2.07 (s, 3H, OAc), 2.04 (s, 3H, OAc), 1.97 (s, 3H, OAc), 1.92-1.80 (m, 1H, $H_{3'ax}$), 1.20 (2xs, 6H, 2xCH_3 linker); ^{13}C NMR (100 MHz, $CDCl_3$): δ = 175.0 (CO), 174.2 (CO), 173.5 (CO), 170.7 (CO), 169.9 (CO), 169.8 (CO), 169.7 (CO), 81.8 (C_1), 71.0 (C_2), 69.5 (C_3), 69.5 (C_5), 66.3 (C_4), 62.6 (C_6), 60.0 (CH_2N_3), 52.4 (OMe), 52.3 (OMe), 48.0 ($C_{4'}$), 43.9 ($C_{5'}$), 40.2 ($C_{1'}$), 40.1 ($C_{2'}$), 29.5 ($C_{6'}$), 28.9 ($C_{3'}$), 23.4 (CH_3 linker), 23.4 (CH_3 linker), 20.1 (OAc), 20.7 (OAc), 20.7 (OAc), 20.7 (OAc).

^{1}H NMR (400 MHz, $CDCl_3$):

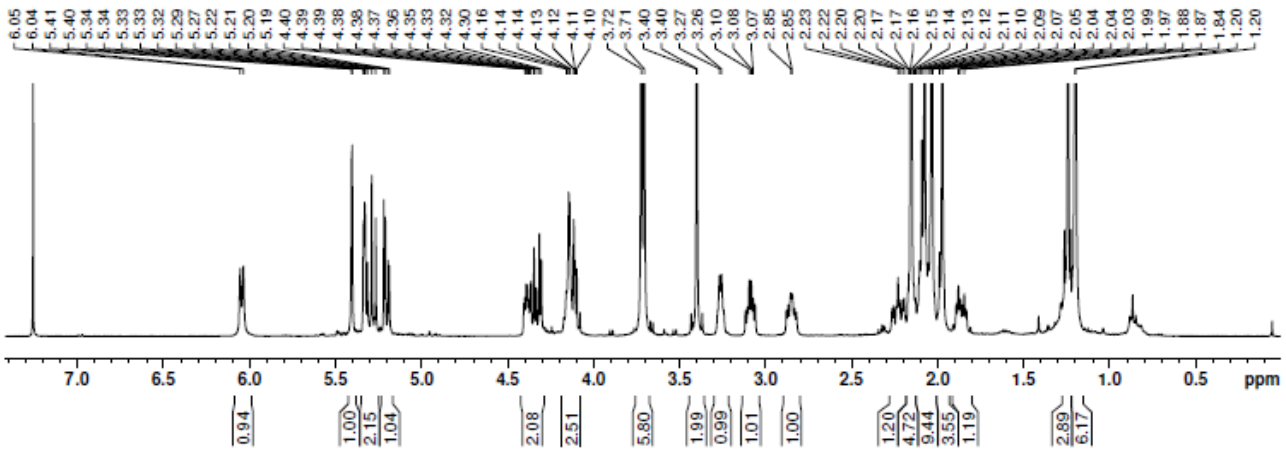

^{13}C NMR (100 MHz, $CDCl_3$):

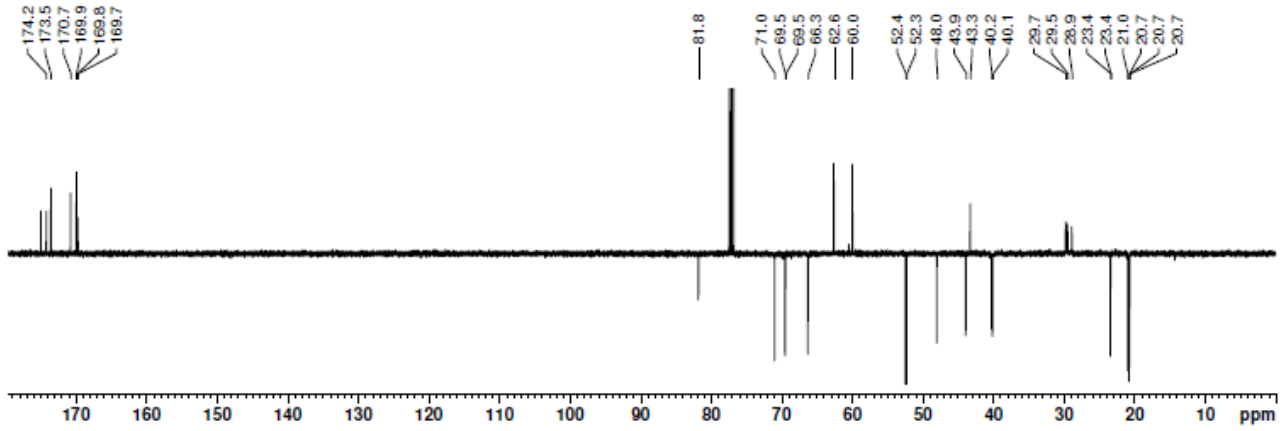

General method for the deacetylation of the sugar moiety

The substrates were dissolved in a $MeNH_2$/EtOH solution (4 M) in order to have a final solution 0.05 M of the substrate, at room temperature and under stirring. After 4 h, the solvent and the unreacted $MeNH_2$ were removed under reduced pressure. The reactions were monitored by reverse-phase TLC (eluents based on different ratios of H_2O/MeOH, see below for individual compounds). The products were isolated from the *N*-methylacetamide (MeNHCOMe) generated during the process using automated flash chromatography (Biotage Isolera Prime, SNAP Ultra HP-Sphere C18 cartridges) in reverse phase (isocratic elution, 1:1 H_2O:MeOH).

Synthesis of the pseudo-thiodisaccharide 6.31

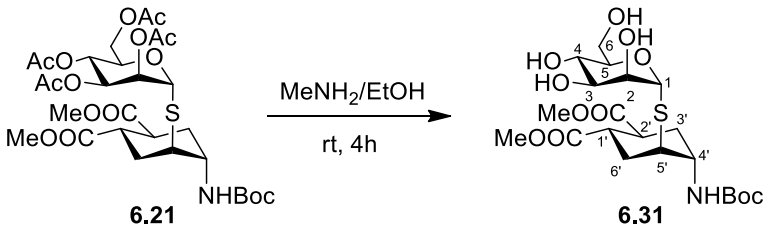

Scale: 19 mg of **6.21**, 0.028 mmol.

Reaction time: 4 h.

Isolated product (**6.31**): 10 mg, 0.02 mmol. y= 70%

$[\alpha]_D^{18}$ (MeOH, *c* 0.5): + 113; RP TLC: R_f 0.24 (1:1 H_2O:MeOH, cerium ammonium molibdate stain); MS (ESI) calcd for $C_{21}H_{35}NO_{11}S$ $[M + Na]^+$ m/z: 532.18; found: 532.51; HR-MS (ESI) calcd for $C_{21}H_{35}NO_{11}S$ $[M+Na]^+$ m/z: 532.1829; found 532.1835.

^{1}H NMR (400 MHz, CD_3OD): δ = 5.34 (d, $J_{1\text{-}2}$= 1 Hz, 1H, H_1), 3.96-3.81 (m, 4H, H_2, H_5, $H_{4'}$, H_{6a}), 3.78-3.71 (dd, $J_{6a\text{-}6b}$= 12.5 Hz, $J_{6b\text{-}5}$= 5.8 Hz, 1H, H_{6b}), 3.68 (s, 3H, OMe), 3.68 (s, 3H, OMe), 3.66-3.59 (m, 2H, H_4, H_3), 3.24-3.17 (m, 1H, $H_{5'}$), 3.06-2.94 (m, 2H, $H_{1'}$, $H_{2'}$), 2.25-2.11 (m, 1H, $H_{6'eq}$), 2.11-1.97 (m, 2H, $H_{6'ax}$, $H_{3'eq}$), 1.9-1.8 (m, 1H,

$H_{3'ax}$), 1.45 (s, 9H, tBu); ^{13}C NMR (100 MHz, CD_3OD): δ = 176.1 (CO), 176.0 (CO), 157.2 (CO, carbammate), 86.4 (C_1), 80.4 (C_{IV} Boc),75.4 (C_5), 73.8 (C_2), 73.2 (C_3), 68.8 (C_4), 62.9 (C_6), 52.5 (2xOMe), 50.7 ($C_{4'}$), 46.0 ($C_{5'}$), 41.5 ($C_{1'}$), 41.0 ($C_{2'}$), 30.3 ($C_{6'}$), 30.3 ($C_{3'}$), 28.8 (Me_3).

^{1}H NMR (400 MHz, CD_3OD):

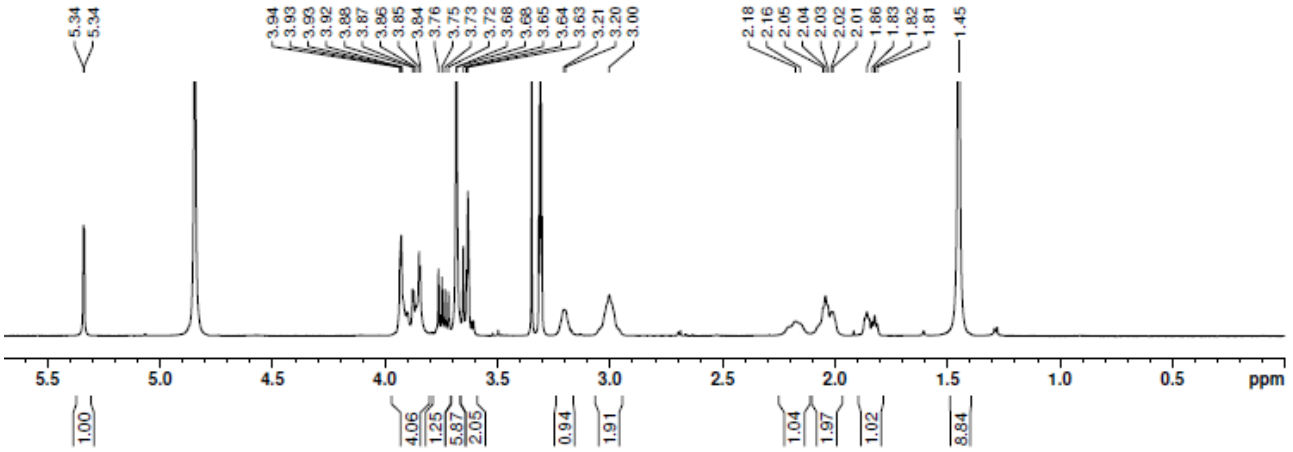

^{13}C NMR (100 MHz, CD_3OD):

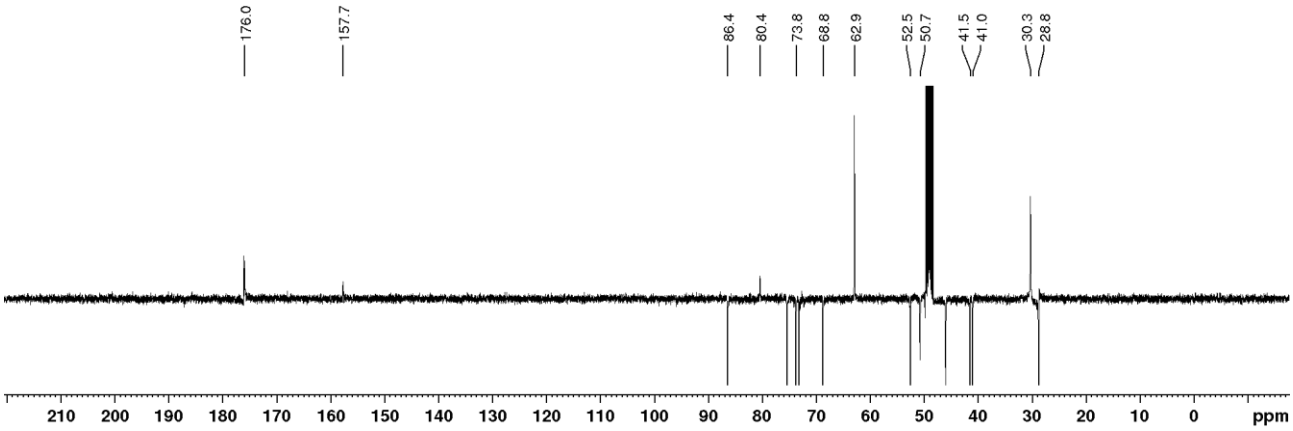

Synthesis of the pseudo-thiodisaccharide 6.32

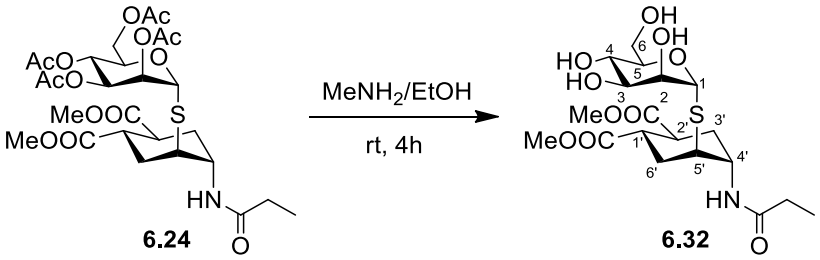

Scale: 21 mg (**6.24**), 0.033 mmol.

Reaction time: 4 h.

Isolated product (**6.32**): 7.9 mg, 0.017 mmol. y= 52%

$[\alpha]_D^{20}$ (MeOH, *c* 0.4): + 128; TLC: R_f 0.43 (85:15 CH_2Cl_2:MeOH, cerium ammonium molibdate stain); HR-MS (ESI) calcd for $C_{19}H_{31}NO_{10}S$ $[M + Na]^+$ m/z: 488.1566; found: 488.1564.

^{1}H NMR (400 MHz, CD_3OD): δ = 5.35 (d, $J_{1\text{-}2}$= 1.1 Hz, 1H, H_1), 4.19-4.12 (m, 1H, $H_{4'}$), 3.95-3.82 (m, 3H, H_2, H_5, H_{6a}), 3.73 (dd, $J_{6a\text{-}6b}$= 11.8 Hz, $J_{6b\text{-}5}$= 6.3 Hz, 1H, H_{6b}), 3.69 (s, 3H, OMe), 3.69 (s, 3H, OMe), 3.70-3.59 (m, 2H, H_4, H_3), 3.24-3.18 (m, 1H, $H_{5'}$), 3.11-2.97 (m, 2H, $H_{1'}$, $H_{2'}$), 2.24 (q, *J*= 7.7 Hz, 2H, $\underline{CH_2}CH_3$), 2.19-2.01 (m, 3H, $H_{6'eq}$, $H_{6'ax}$, $H_{3'eq}$), 1.89-1.80 (m, 1H, $H_{3'ax}$), 1.12 (t, *J*= 8 Hz, 3H, $CH_2\underline{CH_3}$-); ^{13}C NMR (100 MHz, CD_3OD): δ = 176.7 (CO), 175.9 (CO), 175.9 (CO), 86.4 (C_1), 75.5 (C_5), 73.7 (C_2), 73.1 (C_4), 68.8 (C_3), 62.9 (C_6), 52.5 (OMe), 52.5 (OMe), 49.4 ($C_{4'}$), 45.4 ($C_{5'}$), 41.5 ($C_{1'}$), 41.0 ($C_{2'}$), 30.4 ($C_{6'}$), 29.9 ($C_{3'}$), 29.9 ($\underline{CH_2}CH_3$), 10.4 ($CH_2\underline{CH_3}$).

^{1}H NMR (400 MHz, CD_3OD):

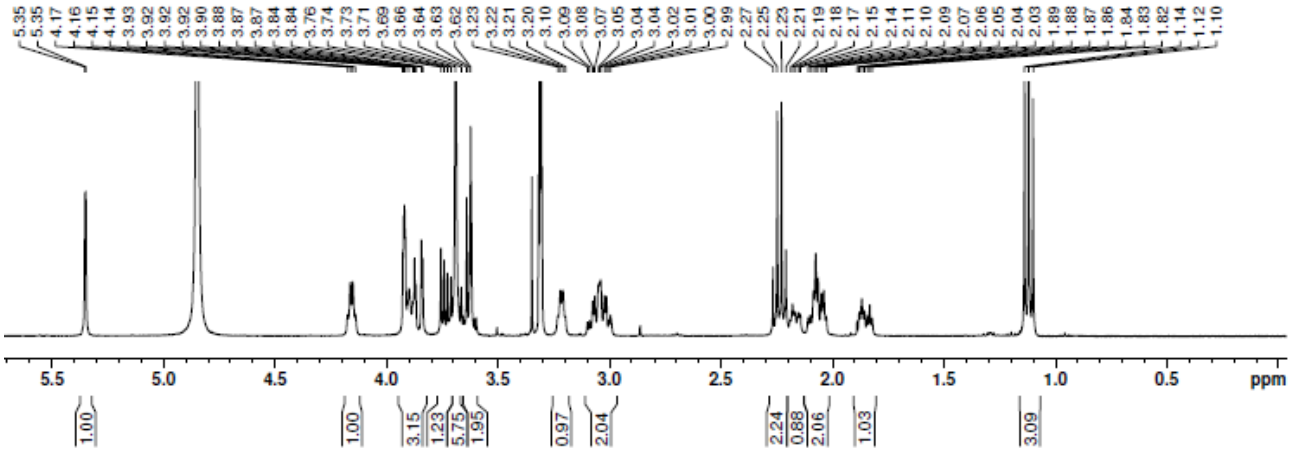

^{13}C NMR (100 MHz, CD_3OD):

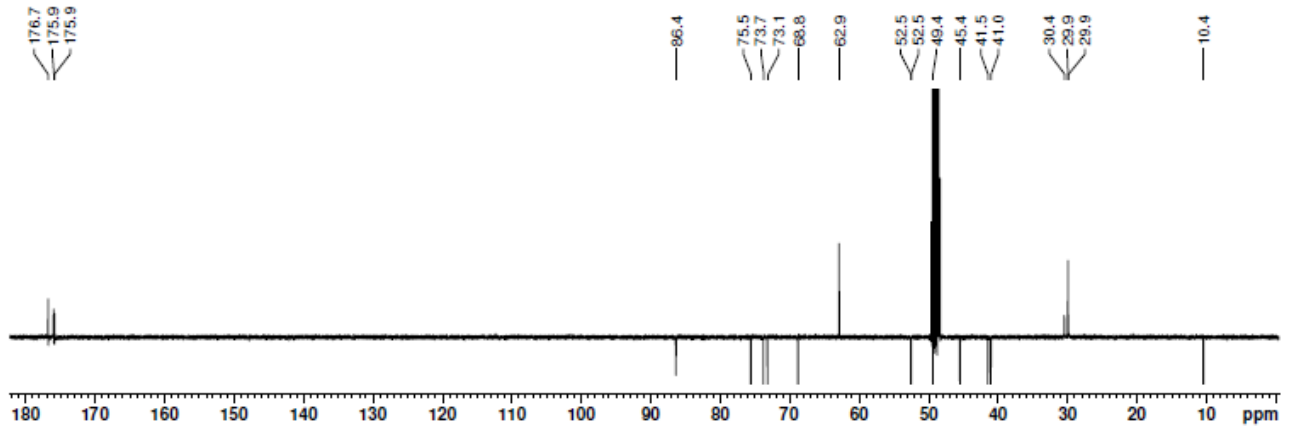

Synthesis of the pseudo-thiodisaccharide 6.27

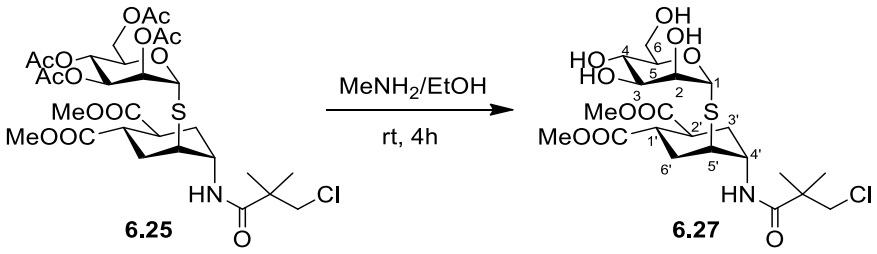

Scale: 22 mg (**6.25**), 0.032 mmol.

Reaction time: 3 h.

Isolated product (**6.27**): 10.5 mg, 0.02 mmol. y= 62%

$[\alpha]_D^{20}$ (MeOH, *c* 0.47): + 110; RP TLC: R_f 0.31 (1:1 H_2O:MeOH, cerium ammonium molibdate stain); HR-MS (ESI) calcd for $C_{21}H_{34}ClNO_{10}S$ $[M + Na]^+$ m/z: 550.1490; found: 550.1495.

^{1}H NMR (400 MHz, CD_3OD): δ = 5.34 (d, $J_{1\text{-}2}$= 1.2 Hz, 1H, H_1), 4.1 (ddd, $J_{4'\text{-}3'ax}$= 8.2 Hz, $J_{4'\text{-}3'eq}$= 7.3 Hz, $J_{4'\text{-}5'}$= 4.2 Hz, 1H, $H_{4'}$), 3.93-3.82 (m, 3H, H_5, H_2, H_{6a}), 3.77-3.56 (m, 5H, H_{6b}, H_4, H_3, CH_2Cl), 3.72 (s, 3H, OMe), 3.71 (s, 3H, OMe), 3.22-3.15 (m, 2H, $H_{5'}$, $H_{2'}$), 3.15-3.09 (m, 1H, $H_{1'}$), 2.34 (ddd, $J_{6'eq\text{-}6'ax}$= 14.4 Hz, $J_{6'eq\text{-}1'}$= 7.7 Hz, $J_{6'eq\text{-}5'}$= 3.6 Hz, 1H, $H_{6'eq}$), 2.19-2.10 (m, 1H, $H_{3'eq}$), 2.02 (ddd, $J_{6'ax\text{-}6'eq}$= 14.2 Hz, $J_{6'ax\text{-}5'}$= 8.1 Hz, $J_{6'ax\text{-}1'}$= 4.3 Hz, 1H, $H_{6'ax}$), 1.88 (ddd, $J_{3'ax\text{-}3'eq}$= 14.2 Hz, $J_{3'ax\text{-}4'}$= 7.7 Hz, $J_{3'ax\text{-}2'}$= 4.7 Hz, 1H, $H_{3'ax}$), 1.28 (s, 6H, 2x CH_3 linker); ^{13}C NMR (100 MHz, CD3OD): δ = 177.2 (CO), 175.7 (CO), 175.6 (CO), 85.3 (C_1), 75.5 (C_5), 73.9 (C_2), 73.3 (C_3), 68.9 (C_4), 63.0 (C_6), 53.5 (CH_2Cl), 52.8 (OMe), 52.7 (OMe), 49.9 ($C_{4'}$), 45.1 ($C_{5'}$), 42.0 ($C_{1'}$), 41.6 ($C_{2'}$), 31.4 ($C_{6'}$), 30.5 ($C_{3'}$), 24.0 (CH_3 linker), 23.8 (CH_3 linker).

^{1}H NMR (400 MHz, CD_3OD):

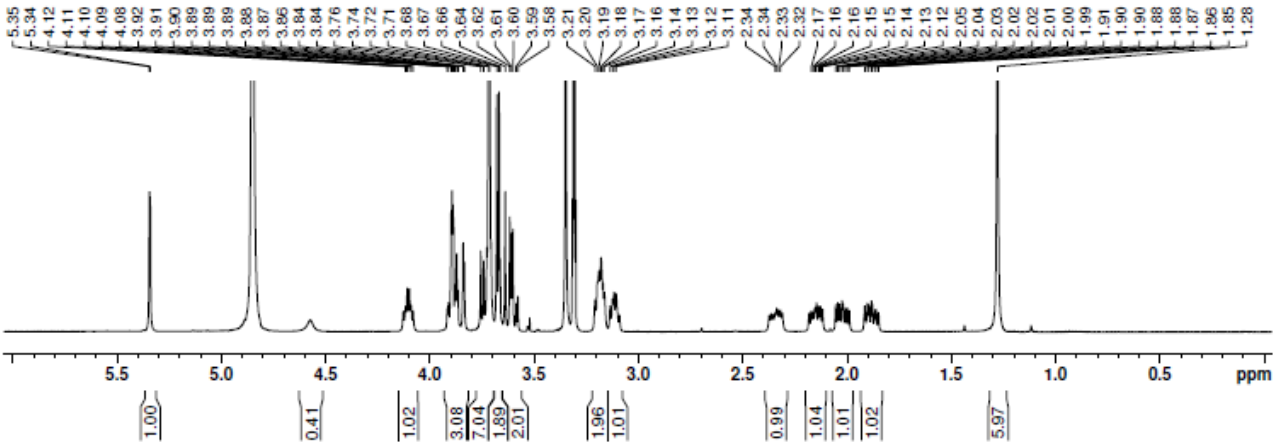

^{13}C NMR (100 MHz, CD_3OD):

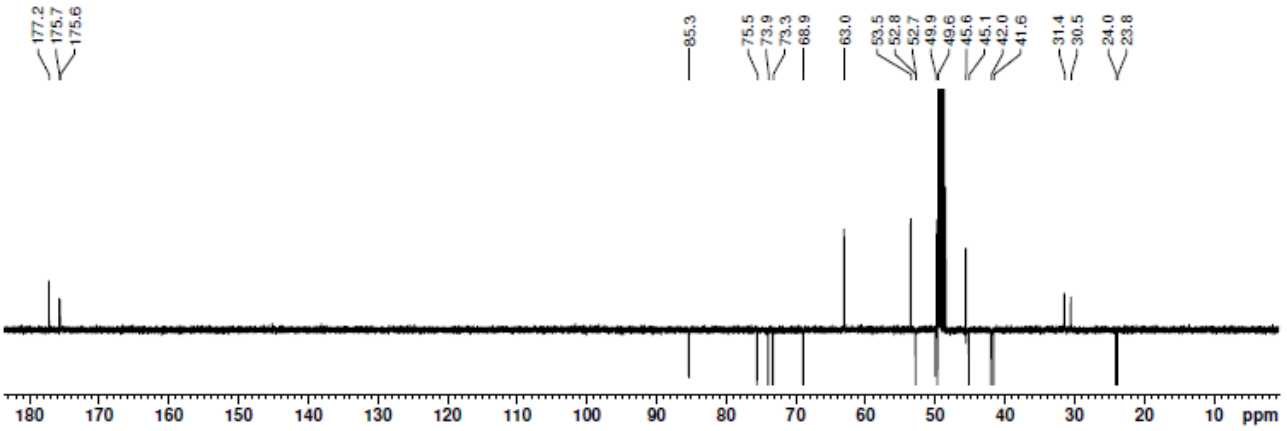

Characterization of the ß-lactam side product 6.29

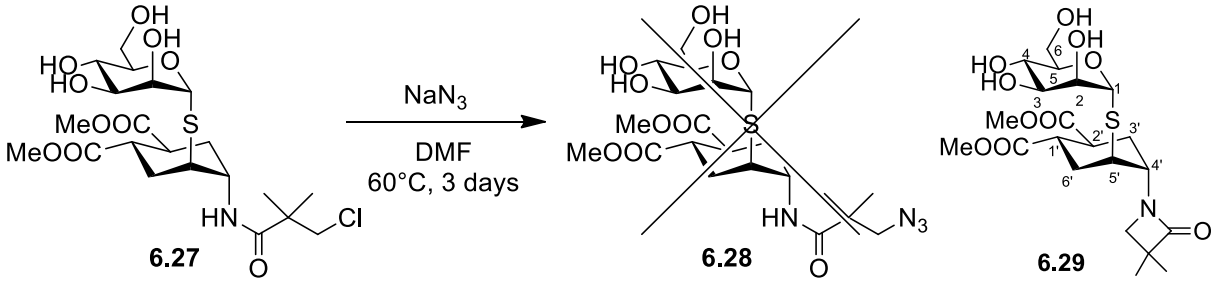

^{1}H NMR (400 MHz, CD_3OD): δ = 5.37 (d, $J_{1\text{-}2}$= 1.3 Hz, 1H, H_1), 3.91 (dd, $J_{2\text{-}3}$= 3 Hz, $J_{2\text{-}1}$= 1.3 Hz, 1H, H_2), 3.89-3.77 (m, 2H, H_5, $H_{4'}$, H_{6a}), 3.76-3.56 (m, 3H, H_{6b}, H_3, H_4), 3.72 (s, 3H, OMe), 3.71 (s, 3H, OMe), 3.39-3.32 (m, 1H, $H_{5'}$), 3.18 (AB system, J_{app}= 15.7 Hz,2H, CH_2 ß–lactam), 3.15-3.06 (m, 2H, $H_{1'}$, $H_{2'}$), 2.38-2.26 (m, 1H, $H_{6'eq}$), 2.13-2.07 (m, 2H, $H_{3'eq}$, $H_{3'ax}$), 2.03 (ddd, $J_{6'ax\text{-}6'eq}$= 14.2 Hz, $J_{6'ax\text{-}5'}$= 7.6 Hz, $J_{6'ax\text{-}1'}$= 4 Hz, 1H, $H_{6'ax}$), 1.3 (s, 3H, CH_3 ß–lactam), 1.27 (s, 3H, CH_3 ß–lactam); ^{13}C NMR (100 MHz, CD_3OD): δ = 176.5 (CO), 175.4 (CO), 175.4 (CO), 85.4 (C_1), 75.7 (C_5), 73.7 (C_2), 73.1 (C_3), 68.7 (C_4), 62.8 (C_6), 53.7 (CH_2 ß–lactam), 52.7 (OMe), 52.7 (OMe), 50.3 ($C_{4'}$), 43.7 ($C_{5'}$), 41.6 ($C_{1'}$), 41.6 ($C_{2'}$), 31.5 ($C_{6'}$), 28.7 ($C_{3'}$), 21.3 (CH_3 ß–lactam), 21.3 (CH_3 ß–lactam). MS (ESI) calcd for $C_{21}H_{33}NO_{10}S$ $[M + Na]^+$ m/z: 514.17; found: 514.91.

^{1}H NMR (400 MHz, CD_3OD):

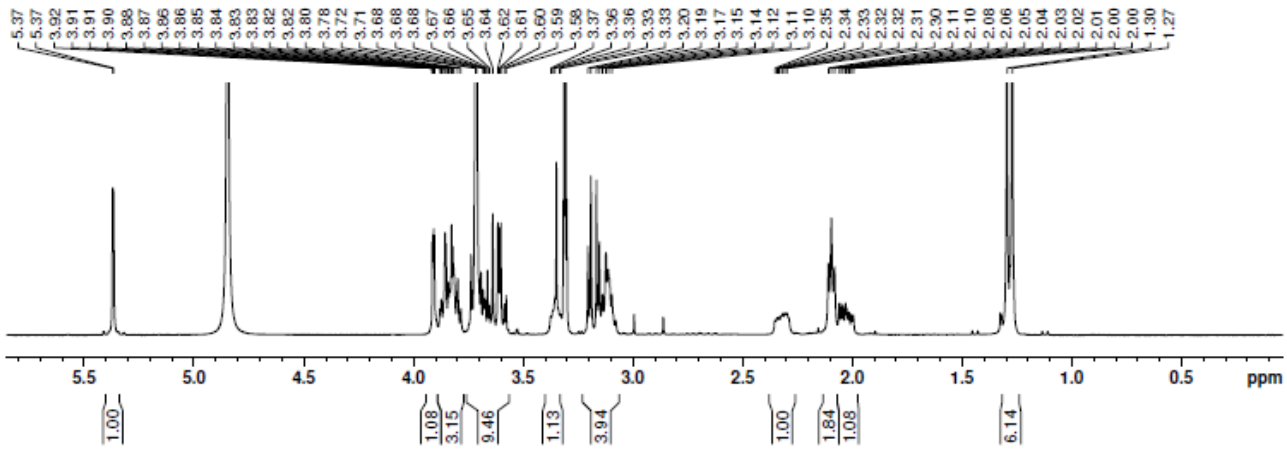

^{13}C NMR (100 MHz, CD_3OD):

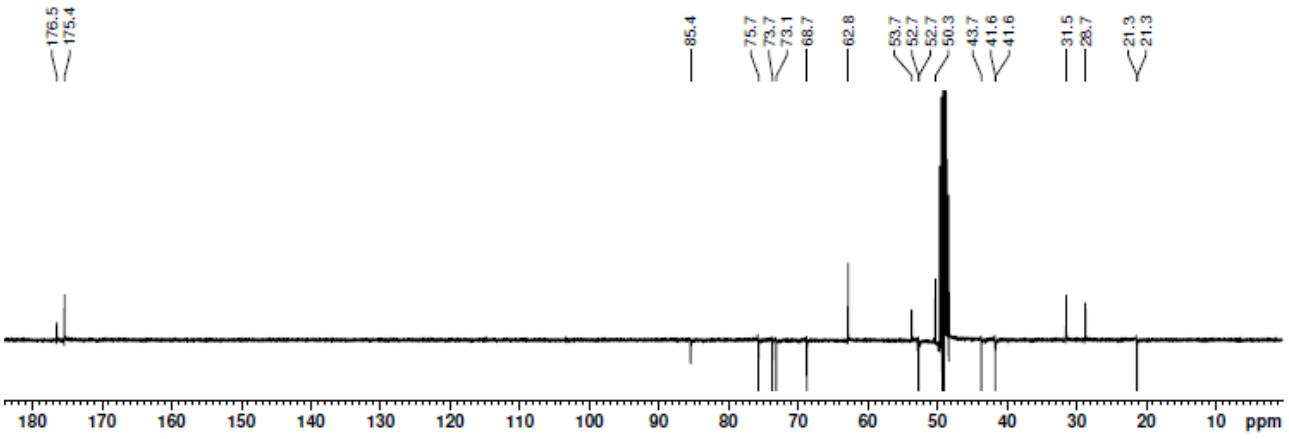

Synthesis of the pseudo-thiodisaccharide 6.28

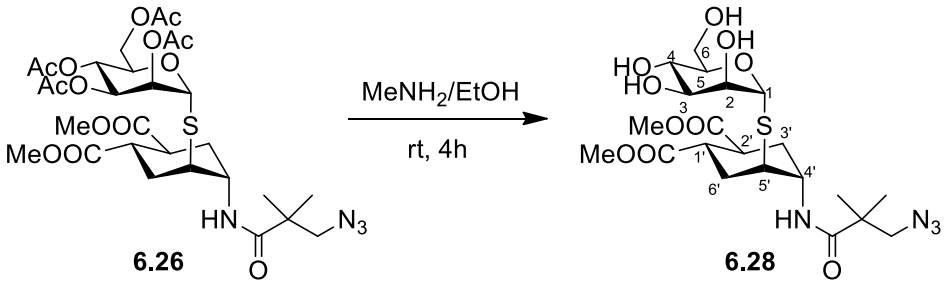

Scale: 31 mg (**6.26**), 0.044 mmol.

Reaction time: 3 h.

Isolated product (**6.28**): 16 mg, 0.03 mmol. y= 68%

$[\alpha]_D^{16}$ (MeOH, *c* 0.55): + 105; TLC: R_f 0.21 (9:1 CH_2Cl_2:MeOH, cerium ammonium molibdate stain); HR-MS (ESI) calcd for $C_{21}H_{34}N_4O_{10}S$ $[M + Na]^+$ m/z: 557.1893; found: 557.1899.

^{1}H NMR (400 MHz, CD_3OD): δ = 5.34 (d, $J_{1\text{-}2}$= 1.2 Hz, 1H, H_1), 4.1 (ddd, $J_{4'\text{-}3'ax}$= 8.1 Hz, $J_{4'\text{-}3'eq}$= 7.7 Hz, $J_{4'\text{-}5'}$= 4.1 Hz, 1H, $H_{4'}$), 3.93-3.82 (m, 3H, H_5, H_2, H_{6a}), 3.78-3.67 (m, 1H, H_{6b}), 3.72 (s, 3H, OMe), 3.72 (s, 3H, OMe), 3.67-3.57 (m, 2H, H_4, H_3), 3.44 (AB system, J_{app}= 15.7 Hz, 2H, CH_2N_3), 3.22-3.08 (m, 3H, $H_{5'}$, $H_{1'}$, $H_{2'}$), 2.34 (ddd, $J_{6'eq\text{-}6'ax}$= 14.3 Hz, $J_{6'eq\text{-}1'}$= 7.7 Hz, $J_{6'eq\text{-}5'}$= 3.8 Hz, 1H, $H_{6'eq}$), 2.15 (ddd, $J_{3'eq\text{-}3'ax}$= 14 Hz, $J_{3'eq\text{-}2'}$= 7 Hz, $J_{3'eq\text{-}4'}$= 4 Hz, 1H, $H_{3'eq}$), 2.02 (ddd, $J_{6'ax\text{-}6'eq}$= 14.3 Hz, $J_{6'ax\text{-}5'}$= 7.9 Hz, $J_{6'ax\text{-}1'}$= 4.4 Hz, 1H, $H_{6'ax}$), 1.88 (ddd, $J_{3'ax\text{-}3'eq}$= 14.1 Hz, $J_{3'ax\text{-}4'}$= 7.8 Hz, $J_{3'ax\text{-}2'}$= 4.6 Hz, 1H, $H_{3'ax}$), 1.21 (s, 6H, 2x CH_3 linker); ^{13}C NMR (100 MHz, CD_3OD): δ = 177.9 (CO), 175.6 (CO), 175.6 (CO), 85.3 (C_1), 75.5 (C_5), 73.9 (C_2), 73.3 (C_3), 68.9 (C_4), 63.0 (C_6), 61.1 (CH_2N_3), 52.7 (2xOMe), 49.5 ($C_{4'}$), 45.2 ($C_{5'}$), 42.0 ($C_{1'}$), 41.6 ($C_{2'}$), 31.4 ($C_{6'}$), 30.5 ($C_{3'}$), 23.8 (CH_3 linker), 23.5 (CH_3 linker).

^{1}H NMR (400 MHz, CD_3OD):

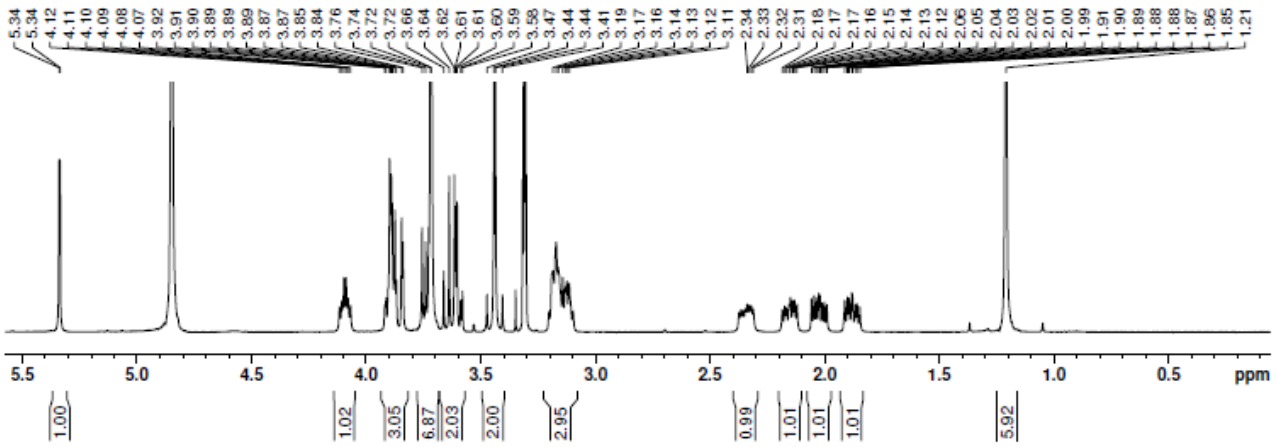

^{13}C NMR (100 MHz, CD_3OD):

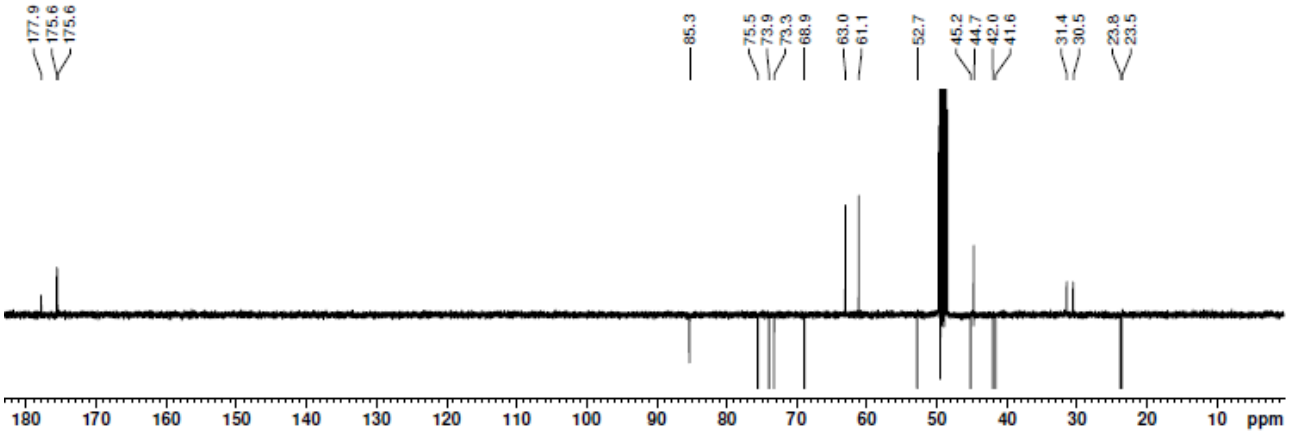

Synthesis of the pseudo-thiodisaccharide 6.30

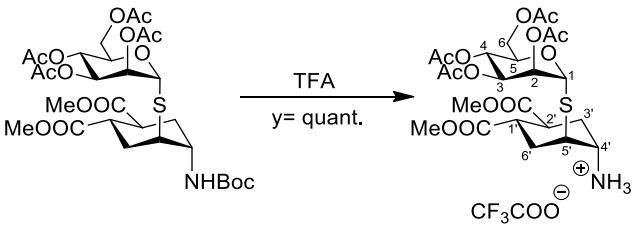

6.21 **6.30**

^1H NMR (400 MHz, $CDCl_3$): δ = 5.45-5.5.20 (m, 3H, H_1, H_2, H_4), 5.12-5.07 (m, 1H, H_3), 4.33-4.09 (m, 3H, H_5, H_{6a}, H_{6b}), 3.73 (s, 3H, OMe), 3.71 (s, 3H, OMe), 3.58-3.42 (m, 1H, $H_{4'}$), 3.4-3.25 (m, 2H, $H_{1'}$, $H_{5'}$), 3.22-3.14 (m, 1H, $H_{2'}$), 2.6-2.48 (m, 2H, $H_{6'eq}$, $H_{3'eq}$), 2.2-1.88 (m, 14H, 4xOAc, $H_{6'ax}$, $H_{3'ax}$); ^{13}C NMR (100 MHz, $CDCl_3$): δ = 172.9 (CO), 172.6 (CO), 171.2 (CO), 170.1 (CO), 170.0 (CO), 169.7 (CO), 81.8 (C_1), 70.8 (C_2), 70.0 (C_5), 69.3 (C_3), 6.9 (C_4), 62.5 (C_6), 52.6 (2xOMe), 51.35 ($C_{4'}$), 44.3 ($C_{5'}$), 40.6 ($C_{2'}$), 39.6 ($C_{1'}$), 29.8 ($C_{6'}$), 29.6 ($C_{3'}$), 20.8 (OAc), 20.7 (OAc), 20.6 (OAc), 20.5 (OAc).

MS (ESI) calcd for $C_{24}H_{35}NO_{13}S$ $[M + H]^+$ m/z: 578.19; found: 578.10 (1154= $[2M+H]^+$)

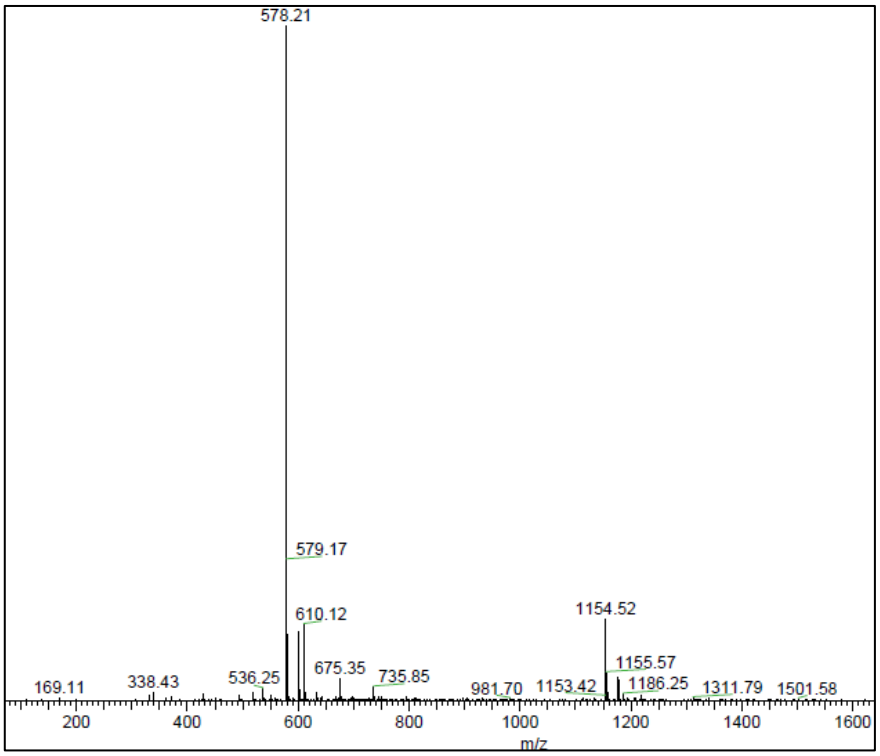

^{1}H NMR (400 MHz, $CDCl_3$):

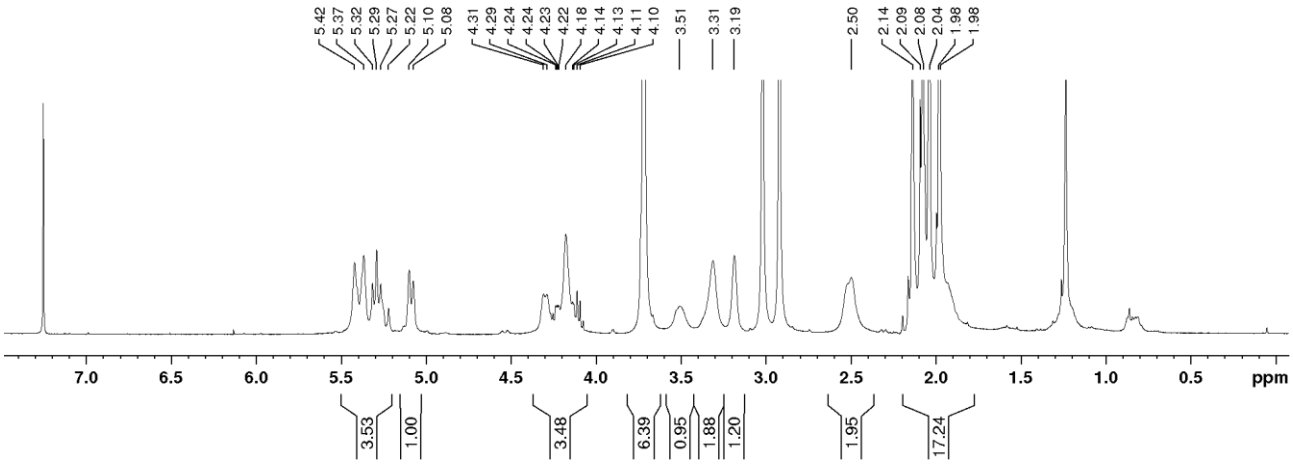

^{13}C NMR (100 MHz, $CDCl_3$):

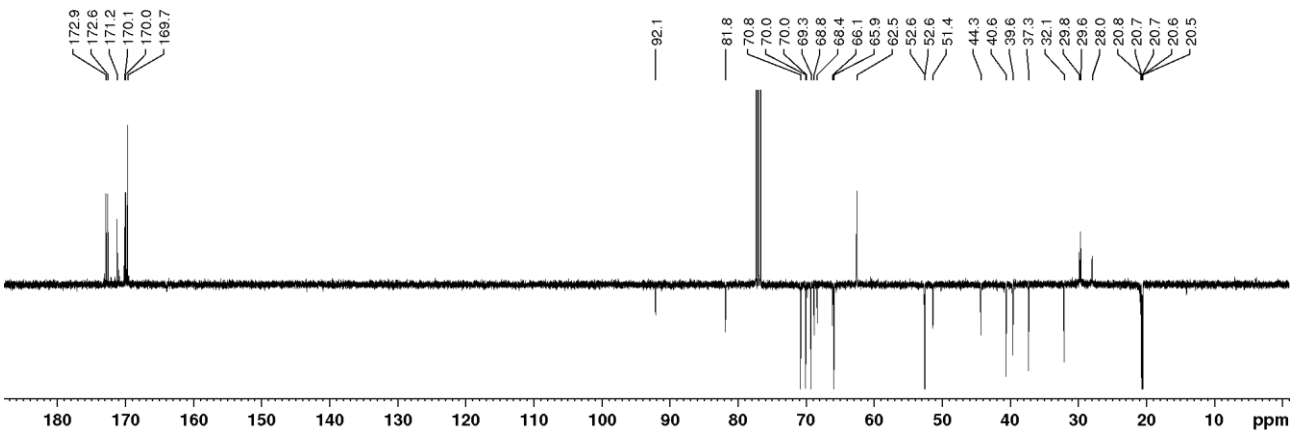

1) W. C. Still; M. Kahn; A. Mitra, *The Journal of Organic Chemistry* **1978**, *43*, 2923-2925.
2) T. Bravman; V. Bronner; K. Lavie; A. Notcovich; G. A. Papalia; D. G. Myszka, *Analytical Biochemistry* **2006**, *358*, 281-288.